RADIOTRACER STUDIES OF HETEROGENEOUS LEWIS ACID-BASE REACTIONS

A THESIS PRESENTED TO THE UNIVERSITY OF GLASGOW FOR THE DEGREE OF DOCTOR OF PHILOSOPHY

BY

KIM WHITFIELD DIXON BSc

Department of Chemistry
University of Glasgow

APRIL 1986

ProQuest LLC.
789 East Eisenhower Parkway
P.O. Box 1346
Ann Arbor, MI 48106 – 1346

DEDICATION

To my wife and my parents without whose help I could not have completed this work.

ACKNOWLEDGEMENTS

It is with pleasure that I would like to thank the following:

Dr. J M Winfield, my supervisor for his help and guidance.

The staff of the Scottish Universities Research and Reactor Centre, East Kilbride for reactor facilities.

Mr R R Spence for technical assistance.

My colleagues in the Fluorine Chemistry Group for many useful discussions.

My wife Sheila for her help and encouragement.

The other members of my family for their support over the last three years.

Mrs A Lauder for typing this thesis.

The award of a University demonstratorship by the University of Glasgow is gratefully acknowledged.

ooOoo

INDEX

ooOoo

S U M M A R Y

SUMMARY

Caesium fluoride has been widely used as a catalyst in a whole range of synthetic reactions. Mechanisms for these and related reactions are usually considered to involve intermediates related to complex fluoro-anions.

The aim of this work was to study the reactions between CsF, a solid Lewis base and several gaseous Lewis acids together with the reactions between the solid Lewis acids AlF_3, NbF_5 and β-UF_5 with SF_4, a Lewis base. This was done in an attempt to determine whether or not molecular analogies are useful in understanding the reactions which occur at metal halide surfaces.

Lewis acid base reactions between the above noted fluorides have been studied under heterogeneous conditions at room temperature, using the radiotracers ^{14}C, ^{18}F and ^{35}S. Surface adsorption of volatile acids or bases is always observed and in many systems additional bulk reactions occur.

Treatment of CsF with $(CF_3)_2CO$ in the presence of MeCN followed by thermal decomposition of the 1:1 adduct formed is one of the methods used to activate CsF for use as a heterogeneous catalyst or reagent. In this work ^{85}Kr adsorption at activated and untreated CsF has been used together with the reactions of both types of CsF with radiochemically labelled Lewis acids in order to quantify the activation effect.

Activated CsF has a B.E.T. surface area in the range 3.01 - 2.08 $m^2 g^{-1}$ (95% confidence limits), compared with 0.31 - 0.19 m^2

g^{-1} (95% confidence limits) for untreated CsF. Chemical analyses of the CsF after activation shows that a small amount of the $^{-}OCF(CF_3)_2$ anion is retained. Reaction results also suggest that activation of CsF produces a porous solid.

Room temperature ^{18}F exchange between activated CsF and $BF_2{}^{18}F$ or $AsF_4{}^{18}F$ is not observed, but reaction to give $BF_3{}^{18}F^-$ or $AsF_4{}^{18}F^-$ is rapid, and, in the case of $BF_3{}^{18}F$, complete. Uptake of $AsF_4{}^{18}F$ by CsF is smaller due to sintering and due to the constraints upon adsorption of gas imposed by the pore structure. $CsBF_4$ prepared by this means undergoes no observable room temperature ^{18}F exchange with $BF_2{}^{18}F$, but ^{18}F exchange between BF_3 and BF_4^- in MeCN is rapid and complete.

^{18}F exchange is observed between $F^{18}FCO$ and activated CsF, together with the formation of $F_2{}^{18}F\ CO^-$. Experiments carried out using $F_2{}^{14}CO$ show that there is more than one adsorbed species present both on the surface of the CsF and in the bulk of the solid.

No ^{18}F exchange is observed between $BF_2{}^{18}F$ or $AsF_4{}^{18}F$ and untreated CsF. The uptakes of gas are far smaller reflecting the smaller surface area. The extent of these reactions is comparable to that between activated CsF and the weaker Lewis acid $SF_3{}^{18}F$. No room temperature ^{18}F exchange is observed but ^{18}F and ^{35}S experiments enable surface adsorption and bulk reaction to be differentiated. 15% of the surface species are strongly adsorbed SF_5^- anions. The remainder are weakly adsorbed SF_4 molecules.

Similar Lewis acid base reactions occur between untreated CsF and SF_4, but due to the smaller surface area only the bulk reactions can be conveniently followed. ^{18}F exchange is observed when $SF_3{}^{18}F$ interacts with NbF_5 or AlF_3 although experiments with $^{35}SF_4$ show that adsorption is weak. Surface species are only observed in the presence of a pressure of $^{35}SF_4$, with all surface activity being removed on removal of the gas. The reaction of $^{35}SF_4$ with β -UF_5 results in strong adsorption. Previous work has shown that ^{18}F exchange is observed between $SF_3{}^{18}F$ and β - UF_5 at room temperature.

The reaction between CO_2 and CsF has been the subject of much debate in the literature. In an effort to clarify the situation a radiotracer study was undertaken.

The reaction between CO_2 and activated CsF is barely detectable but experiments carried out using $^{14}CO_2$ confirm that uptake of gas occurs and that more than one adsorbed species is present on the surface of the CsF.

The results obtained in this work show that molecular analogies can be very useful in describing the reactions which occur at metal halide surfaces.

ooOoo

CHAPTER ONE

INTRODUCTION

In catalysis by supported metals analogies have been made with the chemistry of metal atom clusters and with organometallic compounds in general.

The aim of this work was to examine the usefulness of molecular behaviour in explaining the reactions which occur at metal halide surfaces, in an attempt to determine to what extent molecular analogies are useful in understanding catalysis by metal halide surfaces.

Metal halides can behave as Lewis bases, that is halide ion donors or as Lewis acids, that is halide ion acceptors. Complete transfer of the halide ion is not always observed, resulting in complexes with bridging halides. A brief discussion of some of the chemistry of the fluorides studied in this work is given in sections 1.2 - 1.4. Section 1.1 reviews the various acid-base definitions and includes a more detailed discussion of the proposals of G.N. Lewis.

1.1 ACID-BASE DEFINITIONS

The earliest studies of acids and bases were restricted to aqueous solutions and were made with an inadequate understanding of the peculiarities of water. Arrhenius[1] defined acids as substances which dissociated in water to give hydrogen ions and bases as substances which dissociated to give hydroxide ions. This definition does not hold for solutions in other solvents and does not even give a true representation of the situation in

aqueous solution. Thermodynamic studies have shown that hydration of a free proton is a highly exothermic reaction and hence free H^+ ions are unlikely to exist in any appreciable concentration in water[2]. The dissociation of an acid in water is therefore presumed to lead to a hydrated proton $H^+(aq)$, usually represented by H_3O^+ and referred to as the hydroxonium ion. When an acid dissociates in anhydrous ethyl alcohol it gives the $C_2H_5OH_2^+$ cation and in liquid ammonia it gives the NH_4^+ cation.

Similarly with bases. Sodium hydroxide is a strong base in water giving the hydroxide ion, OH^-, but in anhydrous alcohol the anion present is $C_2H_5O^-$. This anion is also present in solutions of amines in ethyl alcohol. In liquid ammonia the anion present is NH_2^-.

These examples clearly show that acids and bases cannot be defined simply as substances which dissociate in water to give the ions H^+ and OH^- respectively.

1.1.1 LOWRY - BRÖNSTED THEORY OF ACIDS AND BASES

In 1923 Lowry[3] and Brönsted[4] independently defined an acid as a compound or ion with a tendency to lose a proton, and a base as a compound or ion with a tendency to gain a proton. This can be expressed by the general equilibrium shown below

$$A \rightleftharpoons B + H^+$$

Acid Base + Proton

On losing a proton the acid A becomes a base B. The base will then tend to regain the proton and revert to the acid A. The acid and base arising from this equilibrium are commonly referred to as a conjugate acid - base pair.

The Lowry - Brönsted definition allows for three different types of acid, molecular, cationic and anionic. Molecular acids are those such as hydrochloric and sulphuric which lose protons to give the chloride and hydrogen sulphate ions as conjugate bases. Cationic acids like the hydroxonium and ammonium ions lose protons to give water and ammonia as conjugate bases. Anionic acids are anions such as hydrogen sulphate which lose a proton to form their conjugate base.

The definition also allows for two different types of base. Molecular bases such as ammonia and ethylamine, which combine with protons to give the corresponding cations, and anion bases such as the hydroxide and acetate ions, which combine with protons to give uncharged molecules.

Although this definition applies to a wide range of systems it suffers from two major faults. The acid must contain hydrogen and nothing is specified about the atomic structure of the base.

1.1.2 THE SOLVENT SYSTEM DEFINITION

The solvent system definition was developed from the

fundamental ideas of E.C. Franklin by chemists exploring the chemistry of a number of non aqueous systems[5].

Within this classification an acid is defined as any substance that yields, either by direct dissociation or by interaction with the solvent, the cation characteristic of that solvent. A base is defined as any substance that yields either by direct dissociation or by interaction with the solvent, the anion characteristic of the solvent. Both donor and acceptor acids and bases can be defined. A donor acid is a substance that can split off solvent cations or unite with solvent molecules to form cations. An acceptor acid is a substance that can combine with solvent anions. Similarly for bases, a donor base is a substance that can split off solvent anions or unite with solvent molecules to form anions, and an acceptor base is a substance that can combine with solvent cations.

The solvent system definition is unsatisfactory because acid base phenomena are not restricted to self ionising solvents.

The Arrhenius, Lowry, Brönsted and solvent system definitions of acids and bases all have their faults and are restricted in their application. A much more wide ranging definition was first proposed by G.N. Lewis in 1923[6] and further emphasised in 1938[7].

1.1.3 THE LEWIS ACID-BASE DEFINITION

Lewis defined a basic substance as one "which has a lone pair of electrons which may be used to complete the stable group of another atom," and an acidic substance as one "which can employ a lone pair from another molecule in completing the stable group of its own atoms." He also proposed that one of the main operational criteria of an acid be that a stronger acid be able to displace a weaker acid from its acid base complexes.

The fundamental acid base reaction is the forward step of equilibrium 1.

$$\underset{\text{Acid}}{A} + \underset{\text{Base}}{B} \rightleftharpoons \underset{\text{Adduct}}{A:B} \qquad 1$$

Equilibria 2 - 4 show the related heterolytic processes which follow from the fundamental relationship.

$$A^1 + A^2 : B \rightleftharpoons A^2 + A^1 : B \qquad 2$$

$$B^1: + A : B^2 \rightleftharpoons B^2: + A : B^1 \qquad 3$$

$$A^1: B^1 + A^2: B^2 \leftrightharpoons A^1B^2 + A^2B^1 \qquad 4$$

The Lewis definition covers the previously discussed definitions due to Lowry and Brönsted and the solvent system definitions. For example equilibrium 5 shows a typical Brönsted-Lowry acid-base equilibrium. This is equivalent to equilibrium 3 with the proton in 5 representing the Lewis acid in 3.

$$B^1 + B^2 : H^+ \leftrightharpoons B^1 : H^+ + B^2 \qquad 5$$

Similarly for the solvent systems approach.

Equilibrium 6 shows the reaction occurring in liquid ammonia between the solvent systems acid NH_4Cl and the solvent systems base $NaNH_2$.

$$NH_4^+ + Cl^- + Na^+ + NH_2^- \rightleftharpoons 2NH_3 + Na^+ + Cl^- \qquad 6$$

This equilibrium can be rewritten as shown in 7.

$$\underset{\text{Adduct}}{NH_4^+} + \underset{\text{Base}}{NH_2^-} \rightleftharpoons \underset{\text{Adduct}}{NH_3} + \underset{\text{Base}}{NH_3} \qquad 7$$

The Lewis definitions are widely applicable. Unfortunately they suffer from the absence of a uniform scale of acid or base strengths. Instead these are made variable by dependence upon the reaction or method used for their evaluation hence the evolution of the hard/soft acid/base formalism of R.G. Pearson.[8]

Lewis proposed that a strong acid should be able to displace a weaker acid from its acid base complexes. Accordingly the study of a large number of displacement reactions of the type shown in equation 1.1 should allow an ordering of the strengths of acids in a given series towards a particular base.

$$A^1 + B : A \longrightarrow B : A^1 + A \qquad \text{equation 1.1}$$

A more quantitive measure may be obtained by measuring the enthalpy change accompanying the following reaction for a series of acids and a reference base.

$$A + B \rightarrow A : B$$

Based on Hess's Law and the assumption that the displacement that occurs has a negative ΔH, the order of acidity toward the reference base may be taken as the order of exothermicity of the reaction. In practice this type of reaction has been studied most frequently in solution, occasionally with formation of an insoluble product or reactant or both. Indirectly related properties such as solubilities or sublimation temperatures have also been used as criteria for acidity orders. In these cases differences in solvation energies of products and reactants, or lattice energy effects, or both, may obscure acidity differences. A further complication occurs in the assumption that the order of the acid strength is independent of the reference base. Within recent years it has been shown that the order of acid strengths is indeed affected by the reference base chosen.[9, 10]

Fluoride ion affinities are most commonly used when comparing the acidities of inorganic fluorides. There have been several investigations of the relative additives of inorganic fluorides based on fluoride ion affinities. The results of these studies in which a wide variety of approaches and fluoride ion donors have been used are summarised in table 1.1.

TABLE 1.1 LEWIS ACIDITY ORDERS

ORDER	FLUORIDE DONOR	REFERENCE	METHOD
$BF_3 > TaF_5 > NbF_5 > TiF_4 > PF_5 > SbF_3 > WF_6 > SiF_4 \sim CrF_3$	HF + xylene	11	Solvent extraction of $ArH^+ MF^-_{n+1}$
$AsF_5 \sim BF_3 > PF_5 \sim WF_6 > NbF_5 \sim TaF_5 > SiF_4 \sim SbF_3 \sim CrF_3$	MF and/or HF	12	Solubility of MF or Lewis acid
$SbF_5 > AsF_5 > BF_3 > PF_5$	$CF_3{-}SF_3$	13	Decomposition pressure
$AsF_5 > PF_5 > BF_3$	MF^-_{x+1} in CH_2Cl_2	14	Displacement reaction
$SbF_5 > AsF_5 > PF_5 \sim BF_3$	HF	15	Cryoscopy conductivity
$AsF_3 > BF_3 > SiF_4 > AsF_5 > PF_5 > PF_3$	SF^-_6	16	Rate of F^- Transfer
$AsF_5 > BCl_3 > PF_5 > BF_3 > SiF_4 > AsF_3 \sim HCl > SO_2 > SF^{\cdot}_5 \sim SF_4$		17	Ion cyclotron resonance studies

The orders obtained are similar although there are occasional positional changes between studies emphasising the dependance of the order on the fluoride ion donor and reaction method used.

The most recent order of acidities is based on an ion cyclotron resonance study[17] of gas phase ion affinities. The gas phase ion affinity is defined as the negative enthalpy change for the reaction.

$$A(g) + X^-(g) \rightarrow AX^-(g)$$

All comparisons of Lewis acidity discussed in this work are based on this scale as it is independant of external factors.

Although ion cyclotron resonance studies give an acidity scale which is independant of extraneous factors, the reliability of individual measurements such as F^- ion affinities will depend on the reliability of ancillary data used in the appropriate enthalpy cycle. An example of this is the disagreement over the fluoride ion affinity of boron trifluoride. Altshuller[18] published a value of -296 KJ mol^{-1} which was accepted by several authors[17, 19] as the basis for other fluoride ion affinities and electron affinities. Sharpe[20] proposed a value of -380 KJ mol^{-1} based on the data of Bills and Cotton.[21] Although this value is in agreement with other fluoride ion affinities and electron affinities it was only confirmed in 1983 by Bartlett and coworkers[22] who calculated a value of

-384 ± 25 KJ mol^{-1}. It is therefore most important to check the validity of all data used in these calculations very carefully.

Although the original Lewis definitions were based on homogeneous systems they can be applied to heterogeneous gas-solid reactions if the acid-base definitions are restated as follows.

A Lewis acid site on a solid surface is a site which has an unoccupied orbital with a high affinity for an electron pair, so that a major decrease in energy is obtained when such a site shares an electron pair donated by an adsorbed base molecule. Lewis base sites on the surface are those which have electron pairs available at a high energy level and a major decrease in energy is obtained if they share this electron pair with an adsorbed electron pair acceptor.

It would seem therefore that the Lewis acid base definitions are the most suitable for describing heterogeneous gas solid reactions, and that ion cyclotron resonance studies give the most reliable measure of Lewis acidity so long as the reliance of the absolute values of fluoride affinities on the accuracy of the data used to calculate them is noted.

The chemistry of the fluorides studied is briefly discussed in section 1.2 to 1.4. As CsF and SF_4 were involved more often than any of the other fluorides, a more detailed review of their properties is presented.

1.2 CHEMISTRY OF THE LEWIS ACIDS

The reactions of the Lewis acids AsF_5, BF_3, and F_2CO with CsF have been studied. In addition to these systems the reactions of AlF_3, NbF_5, CsF and βUF_5 with SF_4 which can behave as both a Lewis acid and a Lewis base have also been studied.

AsF_5 , BF_3, CO_2 and F_2CO are all gases at room temperature their Lewis acid strengths increase in the order:

$$CO_2 < F_2CO < BF_3 < AsF_5$$

AsF_5 and BF_3 are both strong Lewis acids and react readily with fluorides ion donors to form adducts containing the AsF_6^- and BF_4^- anions respectively. [23, 24]

The AsF_6^- anion is octahedral as shown in figure 1.1[25] BF_4^- is slightly distorted from tetrahedral symmetry. Figure 1.2 shows the atomic arrangement in $(SF_3)^+ (BF_4)^-$ [26]

Carbonyl fluoride is a weak Lewis acid which is used in organic synthesis to fluorinate unsaturated compounds. Its reaction with

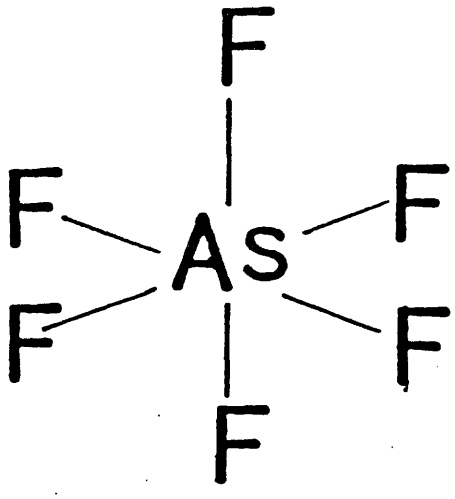

Figure 1·1 The structure of AsF_6^-

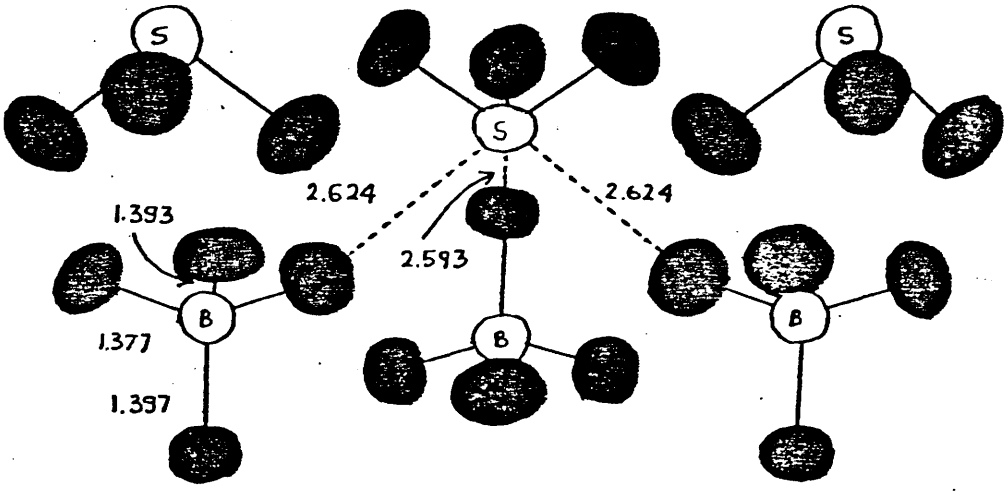

Figure 1·2 The structure of $BF_4^-SF_3^+$

CsF has been widely studied and it has been shown that if the reaction is carried out in the presence of acetonitrile $Cs^+ OCF_3^-$ is formed.[27] No reaction has been reported in the absence of acetonitrile.

Spectroscopic studies of the OCF_3^- anion have indicated that it has C_{3v} symmetry.[28] Examination of the band positions indicates that the C-O bond is intermediate between a single and a double bond, thus suggesting that resonance species are involved. This is supported by the x-ray single crystal diffraction analysis of $TAS^+ CF_3O^-$ (figure 1.3)[29] which shows that the C-F bonds of the CF_3O^- anion are exceptionally long and the C-O bond short compared with the corresponding gas-phase experimental values for CF_3OR. The C-O bond length approaches that for the C=O bond in $CF_2=O$.

The presence of resonance structures is also indicated by the results of Mulliken population analysis which show that each F in the CF_3O^- carries an additional charge. Figure 1.4 shows the four hyperconjugative resonance structures which are proposed to contribute to the bonding in CF_3O^-.

The reaction between caesium fluoride and CO_2 is more complex and the published results have aroused a great deal of controversy.

In 1971 Martineau and Milne[30] reported the preparation of $Cs_2CO_2F_2$ from the reaction of CO_2 with CsF in acetonitrile.

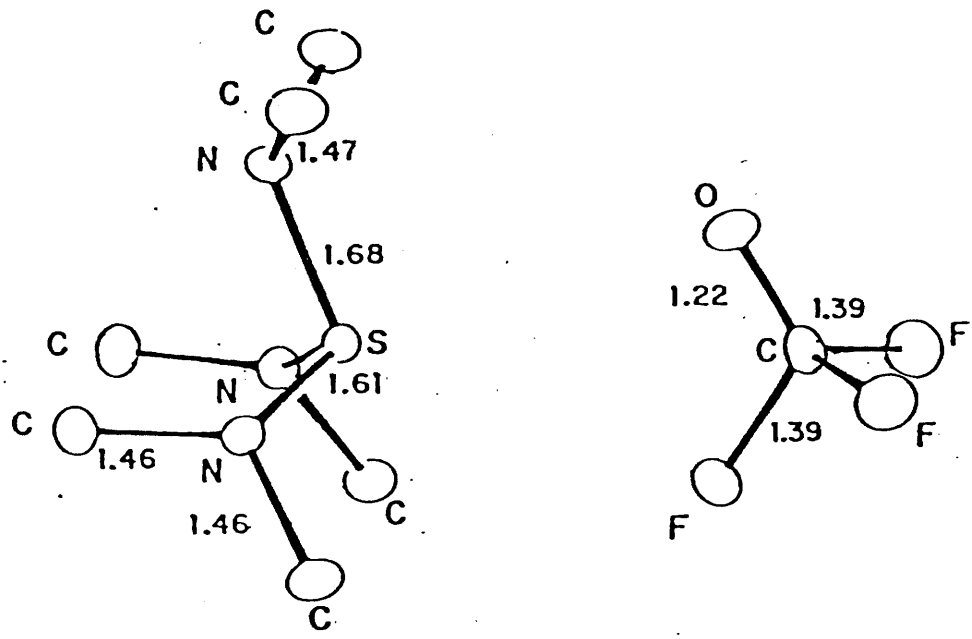

Figure 1·3 The structure of $TAS^{+}CF_3O^{-}$

TAS = tris(dimethylamino) sulfonium

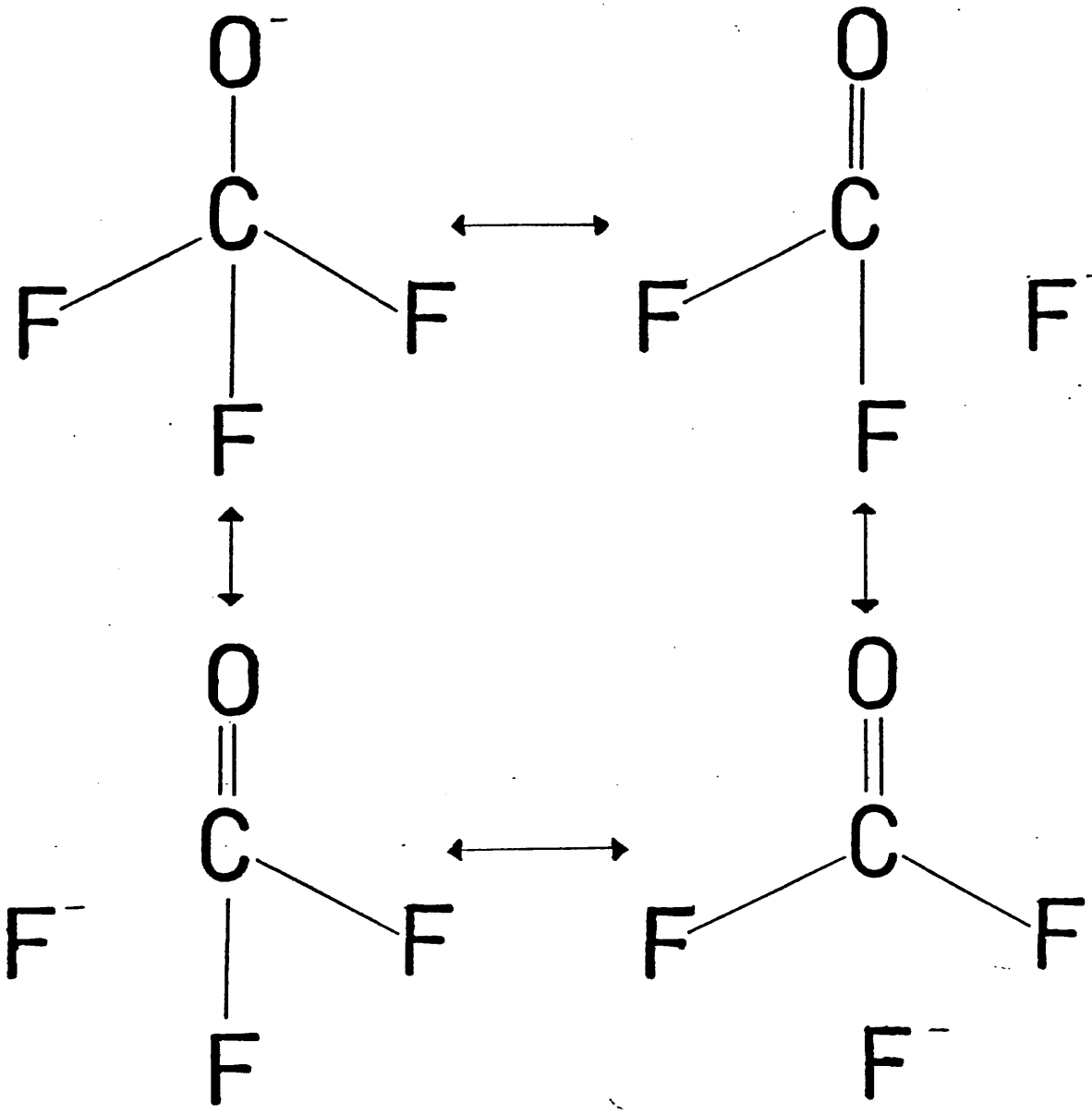

Figure 1·4 CF_3O^- Resonance structures

the product being characterised spectroscopically and on the basis of Cs and F analyses.

Subsequent attempts to reproduce these results have not been successful. In 1979 Lawlor and Passmore[31] suggested that rather than observing the $CO_2F_2^{2-}$ anion, Martineau and Milne were in fact observing hydrolysis products caused by the presence of water in their acetonitrile.

Further doubt was cast on the validity of Martineau and Milne's results by David and Ault[32] in 1985. They carried out a matrix isolation study of the $CO_2F_2^{2-}$ anion and their infra-red data did not agree with that of Martineau and Milne. David and Ault explained this disagreement by suggesting like Lawlor and Passmore in 1979 that Martineau and Milne had obtained infra red spectra of a hydrolysis product rather than of $Cs_2CO_2F_2$.

Both aluminium trifluoride and niobium pentafluoride are white crystalline solids. The AlF_3 unit cell has a distorted hexagonal close packed structure with each aluminium surrounded by three fluorine atoms at a distance of 1.70A^{o} and three at 1.89A^{o}. NbF_5 adopts the molybdenum pentafluoride structure. This consists of tetrameric units containing four metal atoms with four coplanar bridging fluorine atoms as shown in figure 1.5[34] AlF_3 is involatile at room temperature whereas NbF_5 is slightly volatile and is readily hydrolised by moist air. NbF_5 forms a number of fluorine bridged complexes with Lewis bases such as SeF_4[23] hence radiotracer studies of NbF_5 with gaseous

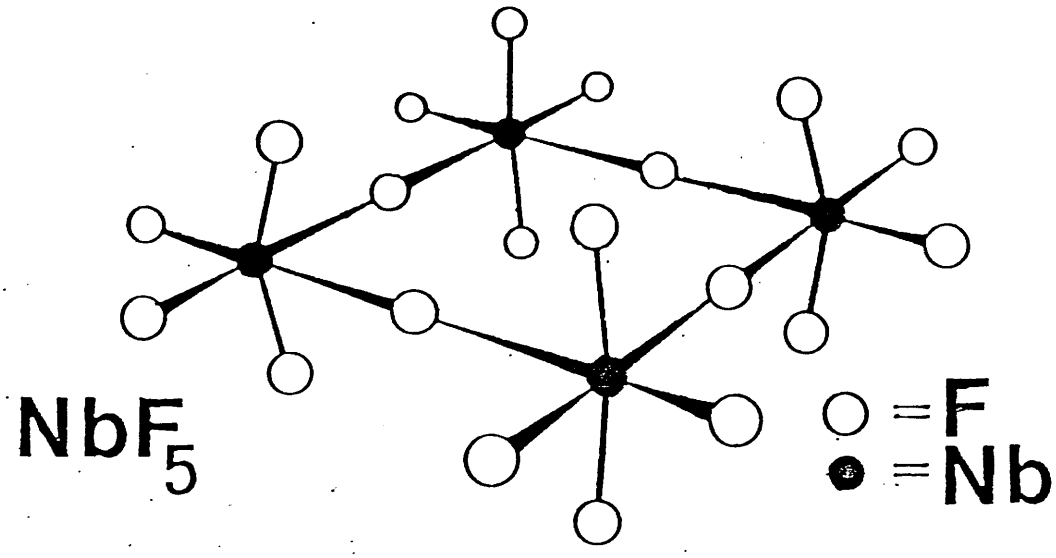

Figure 1·5 The structure of NbF_5

Lewis bases should provide information on the formation of these fluorine bridged species.

Like caesium fluoride, aluminium trifluoride is a widely used catalyst in organic chemistry[35] so its use in this work allows comparison of the reactions of both a solid Lewis acid, that is AlF_3 and a solid Lewis base that is CsF with SF_4.

1.3 STRUCTURE AND CHEMISTRY OF SULPHUR TETRAFLUORIDE

SF_4 is a colourless gas at room temperature. Its structure is that of a distorted trigonal bipyramid in which two fluorine atoms and the unshared electron pair are in the equatorial positions and the other two fluorines are in the axial positions. (figure 1.6)[36,37]

SF_4 reacts with a wide range of Lewis acids as shown below to form adducts containing the SF_3^+ cation.

$$SF_4 + MF_n \rightarrow SF_3^+ MF_{n+1}^-$$

MF = BF_3, PF_5, AsF_5, SbF_5, HF, IrF_5, AsF_3

The SF_3^+ cation exhibits C_{3v} symmetry as shown in figure 1.7. Figures 1.2 and 1.8 show the crystal structures of the adducts $SF_3^+ BF_4^-$ [26] and $(SF_3^+)_2 GeF_6^{2-}$. [22]

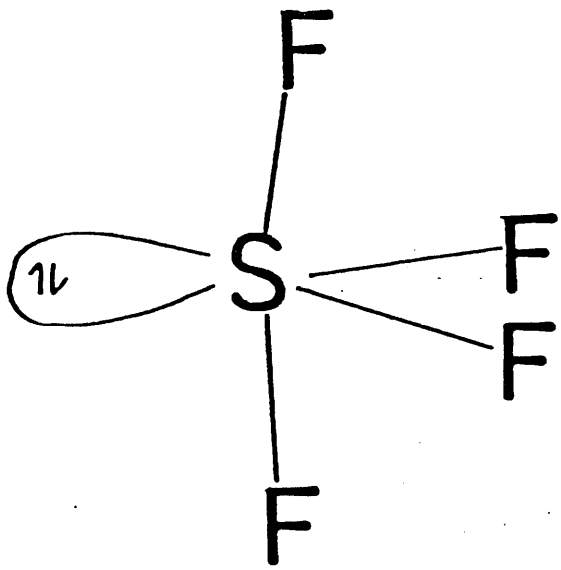

Figure 1·6 The structure of SF_4

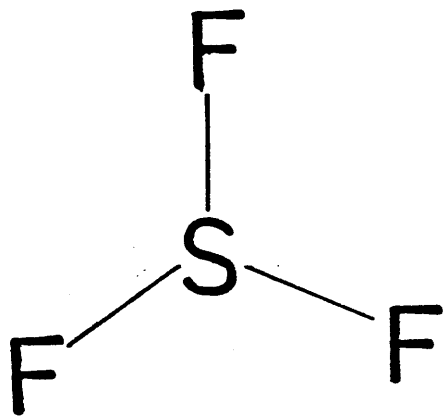

Figure 1·7 The structure of SF_3^+

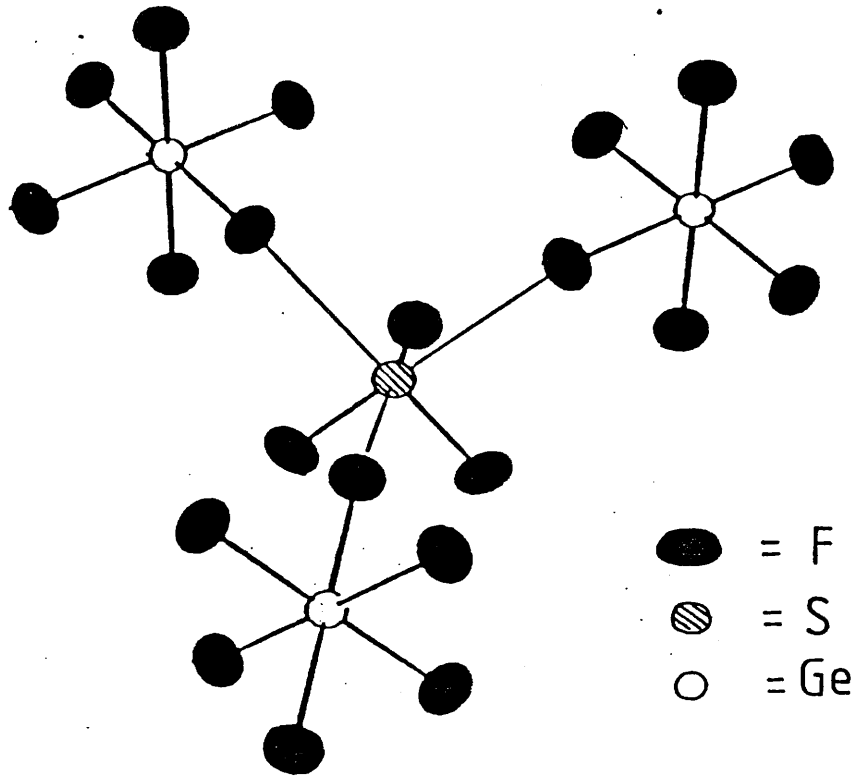

Figure 1·8 The structure of $(SF_3^+)_2GeF_6^{2-}$

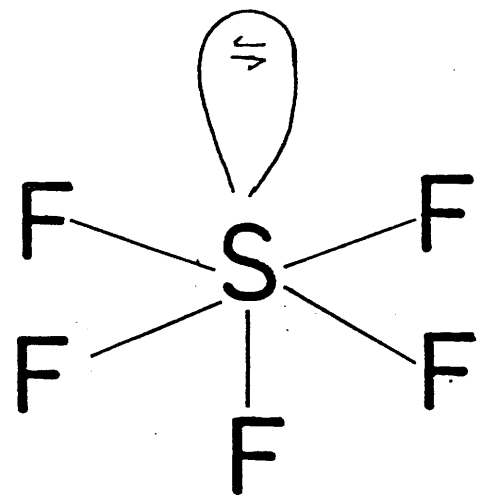

Figure 1·9 The structure of SF_5^-

Sulphur tetrafluoride also reacts with CsF [38] or Me_4NF [39] to form adducts containing the SF_5^- anion. The structure of the anion has been characterised spectroscopically as being square pyramidal (C_{4v}).[40] (Figure 1.9)

In addition to the Lewis acid base type reactions previously described, SF_4 is also widely used in organic reactions as a fluorinating agent most commonly for fluorination of a carbonyl group as indicated in the following examples: [41]

1. 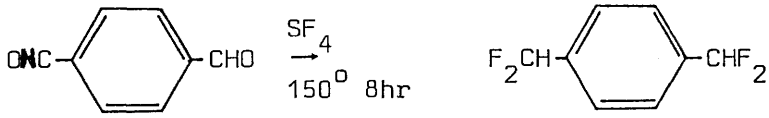

2. $CH_3(CH_2)_n CHO \xrightarrow[50\text{-}60^o,\ 8hr]{SF_4} CH_3(CH_2)_n CHF_2$

3. $R CO_2H + SF_4 \rightarrow RCOF + HF + SOF_2$

4. $R COF + SF_4 \xrightarrow{HF} RCF_3 + SOF_2$

Fluorination by SF_4 is not restricted to carbonyl oxygen. Oxygen doubly bonded to arsenic, iodine or phosphorus is similarly replaced by two fluorine atoms. SF_4 is also very useful for replacing the hydroxyl groups of primary, secondary and tertiary alcohols, carboxylic acids and sulphonic acids with a fluorine atom.

SF_4 can also be used to introduce fluorine into organic compounds by replacement of chlorine, bromine or iodine atoms

by fluorine, although relatively high temperatures are required. For example metathesis of carbon tetrachloride with sulphur tetrafluoride requires a temperature of 225-235°.

$$CCl_4 \xrightarrow[225\text{-}235^{o}]{SF_4} CCl_3F + CCl_2F_2 + CClF_3$$

The previous examples show that SF_4 can undergo a wide range of chemical reactions, and exhibit both Lewis acid and Lewis base behaviour. This, together with the availability of ^{18}F and ^{35}S radiotracers makes SF_4 a very useful substance for the study of Lewis acid-base reactions.

1.4 CAESIUM FLUORIDE AS A CATALYST AND A BASE

Alkali metal fluorides have been widely used as catalysts in a whole range of synthetic reactions. They are fairly strong bases and have a number of advantages over other bases. Reactions conducted in the presence of alkali metal fluorides give high yields, proceed selectively and without formation of any by-products. Reactions involving conventional bases such as hydroxides or alkali metal carbonates usually result in the formation of unwanted by products. The ability of a metal fluoride to act as a catalyst depends on the nucleophilic properties of F^- so it is vitally important that the CsF is dry because of the strength of the hydrogen bonds formed by the fluoride ion.

Studies carried out with various alkali metal fluorides have shown caesium fluoride to be the most active. The overall

order of activity generally found in synthetic and catalytic work is: [42]

$$CsF > RbF > KF \gg NaF > LiF$$

Illustrative examples of the use of alkali metal fluorides in synthetic reactions are given below.

1.4.1 Elimination of hydrogen halides

The basic properties of alkali metal fluorides were first observed in dehydrohalogenation reactions. In the reaction of 3 - chloropropanoic acid with potassium fluoride, the formation of acrylic acid was observed. [43]

$$Cl - CH_2 - CH_2 - COOH \xrightarrow[68\%]{KF} H_2C = CH - COOH$$

In the presence of alkali metal fluorides fluoro-amino groups are converted to fluoroimino and nitrile groups.

$$F_2N - CH_2 - \underset{\diagdown}{\overset{F}{}}CH - NF_2 \xrightarrow{CsF} N \equiv C - CF = NF \qquad 44$$

Reaction of haloorganic compounds with alcohols or phenols in the presence of metal fluorides leads to the formation of ethers.

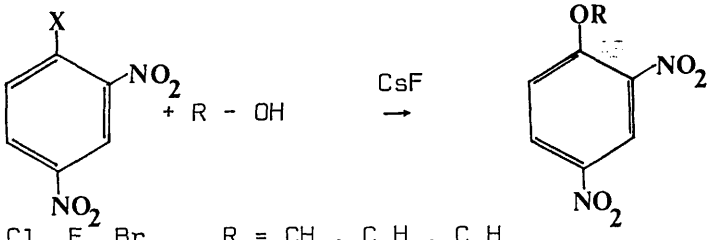

45

x = Cl, F, Br, R = CH_3, C_2H_5, C_6H_5

1.4.2 MICHAEL REACTIONS

The nucleophilic addition of an enolate or analogous anion to the carbon-carbon double bond of an unsaturated ketone, aldehyde, nitrile or carboxylic acid derivative is a process known as the Michael reaction. The use of alkali metal fluorides in these reactions instead of the traditionally used amines, alkoxides, ammonium salts of organic acids, or alkali hydroxides makes it possible to carry out the reactions under milder conditions and increases the yields of reaction products.[46]

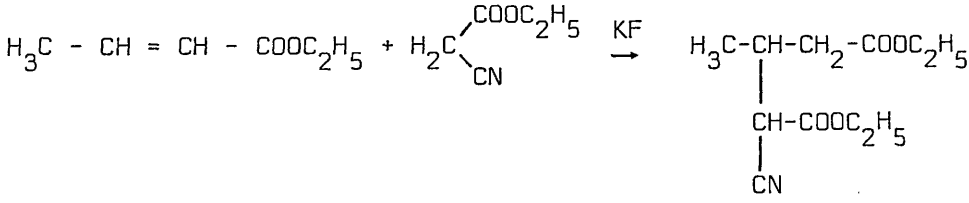

1.4.3 KNOEVENAGEL REACTIONS

The condensation of an active methylene compound and an aldehyde or ketone with elimination of water from the intermediate aldol product is known as the Knoevenagel reaction.[46]

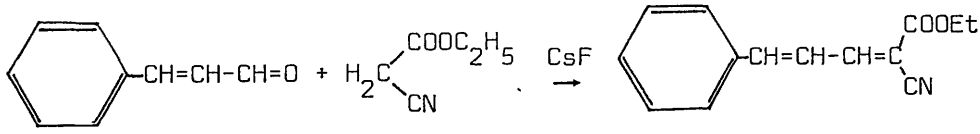

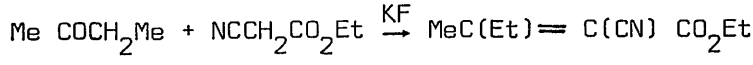

1.4.4 DECARBOXYLATION

The use of alkali metal fluorides as decarboxylating agents was first discovered in 1948 by Nesmeyanov and coworkers[43] when they isolated chloroform when attempting to obtain trifluoroacetic acid from trichloroacetic acid in the presence of potassium fluoride.

$$Cl_3C - COOH \xrightarrow[70\text{-}100\%]{KF} Cl_3CH$$

This reaction proved to be applicable to a wide range of acids. Heating of dicarboxylic acids with potassium fluoride results in partial decarboxylation which leads to cyclic ketones.[48]

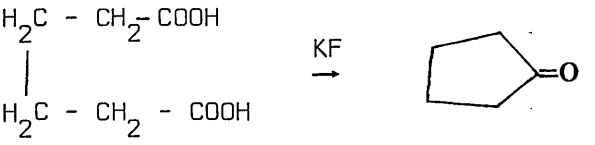

1.4.5 REACTIONS OF FLUORINE CONTAINING COMPOUNDS

When heated with caesium fluoride in the presence of a solvent, F-buta-1,3-diene is transformed to F-but-2-yne.[49]

$$F_2C = CF - CF = CF_2 \xrightarrow{CsF} F_3C - C\equiv C - CF_3$$

In the presence of caesium or potassium fluoride,

F-methylenecyclopentane is almost quantitatively isomerised to give F-1 methylcyclopentene.

50

Alkali metal fluorides also catalyse a number of processes which lead to fluorine containing long chain polymers.

$$n\ F_2C = CF_2 \xrightarrow{CsF} C_8F_{18} + C_{10}F_{21} + C_{12}F_{24} \qquad 51$$

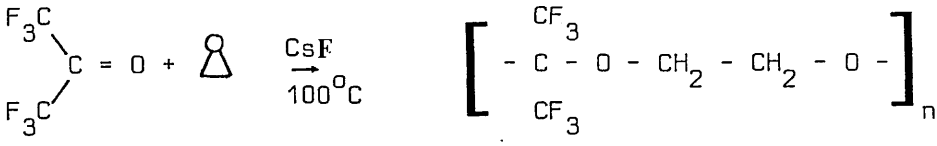

mol mass = 118000

1.4.6 REACTIONS OF CARBONYL CONTAINING COMPOUNDS

CF_3OCl, C_2F_5OCl and other similar compounds can be prepared at low temperature by caesium fluoride catalysed addition of chlorine monofluoride to the appropriate carbonyl compound. [53]

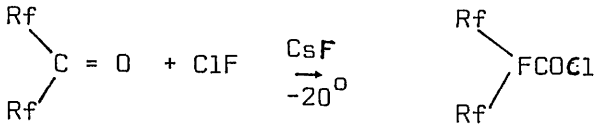

similarly

Carbon dioxide and carbonyl fluoride both react with fluorine in the presence of caesium fluoride.

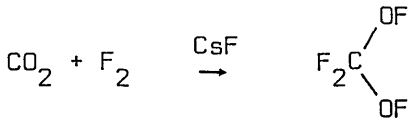

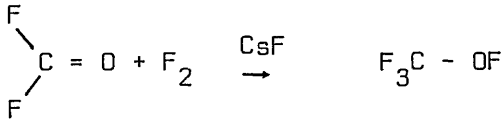

1.4.7 THE CHLOROFLUORINATION OF SF_4

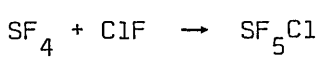

When no caesium fluoride is present a temperature of 350°C is required.[56] In the presence of caesium fluoride this reaction occurs readily at room temperature.[57]

1.5 DISCUSSION OF GENERALLY ACCEPTED MECHANISMS

Ionic fluorides with their variable basicity and relatively low nucleophilicity towards carbon have proved to be versatile proton abstractors in a variety of base assisted reactions where the strength of the base required has varied from weak to very strong and the role of the base has been catalytic and non catalytic. The fluoride ion method is particularly well suited to reactions such as Michael additions, alkylations, esterifications, eliminations and Knoevenagel condensations. These reactions are thought to occur via strong H bonding of the electron donating fluoride ion to the acceptor molecule with resulting enhancement of the nucleophilicity of the acceptor molecule. The role of the metal fluoride in reactions such as the chlorofluorination of sulphur tetrafluoride and halogen addition reactions is not as clearly understood. Mechanisms proposed for these reactions have usually involved intermediates related to complex fluoroanions, but in many cases the validity of this approach has been questioned.

In 1973 Kennedy and Cady studied the reaction of carbonyl fluoride with fluorine in the presence of various fluorides as catalysts.[58] In the presence of CsF, RbF or KF the reaction proceeds as shown below at - 78°C

$$CF_2O + F_2 \longrightarrow CF_3OF$$

The mode of action of the CsF is proposed to be:

$$CF_2O + CsF \rightarrow Cs^+ CF_3O^- \quad \text{followed by}$$
$$CsCF_3O + F_2 \rightarrow CsF + CF_3OF$$

Doubts about this mechanism were first expressed by Lustig and coworkers in 1967.[55] Their explanation stated "It is probable that the metal fluoride either reacts directly with or polarizes the carbon-oxygen double bond to such an extent that a polar intermediate is formed, which is the active species in the fluorination." One reason for their caution is that some compounds which are catalytically fluorinated do not appear to involve extensive combination with the metal fluoride. For example the uptake of CO_2 by CsF is very small, but CO_2 reacts with fluorine in the presence of CsF to give $CF_2(OF)_2$. Kennedy and Cady have shown that the reaction of COF_2 with fluorine is also catalized by CsF, HF, $KAgF_4$ and CsCl. With these salts the CF_3O^- anion could not be formed as an intermediate. This would suggest that Lustig and coworkers vague proposal of a 'polar intermediate' may in fact be closer to the true mechanism than that involving formation of the trifluormethoxide anion.

A similar difference of opinion occurred over the mechanism for the chlorofluorination of sulphur tetrafluoride. This reaction occurs readily at room temperature in the presence of caesium fluoride. The generally accepted mechanism for

this reaction involves reaction between $Cs^+ SF_5^-$ and gaseous chlorine monofluoride.

$$SF_4\ (g) + CsF\ (s) \rightleftharpoons Cs^+ SF_5^-\ (s)$$

$$Cs^+ SF_5^-\ (s) + ClF\ (g) \longrightarrow SF_5Cl\ (g) + CsF\ (s)$$

This mechanism was shown to be incorrect by Kolta and coworkers in 1982.[59] As a result of radiotracer studies involving (^{36}Cl) chlorine monofluoride and (^{35}S) sulphur tetrafluoride, they proposed that the mechanism could best be described by the following five equilibrium reactions.

$$SF_4\ (g) + CsF\ (s) \leftrightharpoons CsF\ SF_4\ (ads)$$

$$CsF\ SF_4\ (ads) \leftrightharpoons Cs^+ SF_5^-\ (s)$$

$$ClF\ (g) + CsF\ (s) \rightleftharpoons CsF\ ClF\ (ads)$$

$$CsF\ ClF\ (ads) \rightleftharpoons Cs^+ ClF_2^-\ (s)$$

$$CsF\ ClF\ (ads) + CsF\ SF_4\ (ads) \rightleftharpoons SF_5Cl\ (g) + 2CsF\ (s)$$

with CsF ClF (ads) and CsF SF_4 (ads) as the active species rather than Cs SF_5 (s) and ClF (g).

These results, together with those of Kennedy and Cady show that the mechanisms of reactions catalysed by ionic fluorides are not as straightforward as was first thought. They cannot simply be assumed to occur via formation of a fluoroanion.

This work was carried out in an attempt to identify the species present on the surface of a solid fluoride during reaction with a gaseous fluoride. The species were identified by using radiotracers and by infra-red spectroscopy. Comparison of the results obtained with those in the literature indicated that there are many similarities between the species involved in a reaction on the surface of the solid and the species involved in reaction within the bulk of the solid.

ooOoo

CHAPTER TWO

CHAPTER 2 EXPERIMENTAL

2.1 EQUIPMENT

Most of the reactants used in this work are either air or moisture sensitive. In order to ensure anhydrous and oxygen free conditions, all experimental work was performed in vacuo (10^{-4} Torr) or in an inert atmosphere box ($H_2O < 10ppm$).

2.1.1 THE VACUUM SYSTEM

Several different vacuum lines were used during the course of this work. The basic system consisted of a Pyrex glass vacuum line which was pumped by means of a mercury diffusion pump, together with an oil sealed rotary pump. The pumps were protected from any volatile material in the line by waste traps which were cooled in liquid nitrogen.

The main components of the vacuum line were a manometer or pressure gauge (Heise) to measure the pressure of gas or vapour contained in the line, a vacustat which was used to measure the efficiency of the pumping system and a main manifold. The type of main manifold fitted depended on the operation being carried out. The simplest manifold consisted of outlets to which reaction vessels were attached by

means of cone and socket joints which were sealed with Kel-F grease. Other manifolds had reaction vessels and secondary manifolds connected directly to them. Reactions were carried out either in glass reaction vessels fitted with polytetrafluoroethylene (Rotaflo) stopcocks or in Monel metal pressure vessels (Hoke) fitted with Monel valves (Whitey). To ensure that as much as possible of the moisture adsorbed on the surface of the glass was removed, the glass vessels and line were flamed out with a gas/oxygen flame while the line was being pumped.

2.1.2 GAS UPTAKE APPARATUS

In order to follow manometrically the uptake of gas by a solid the apparatus shown in figure 2.1 was used. This consisted of a constant volume manometer, a small volume manifold, a bulb B to increase the volume of the manifold if necessary and a socket fitted with a Rotaflo stopcock onto which the sample bulb was attached. The volume of the system was accurately calibrated before use. Pressure changes were measured using a cathetometer.

The constant volume manometer is shown in more detail in figure 2.2. The mercury level was manipulated by applying air or vacuum to the reservoir by means of the two way stopcocks so that the mercury in the right hand limb was always brought to a reference mark before a measurement was taken.

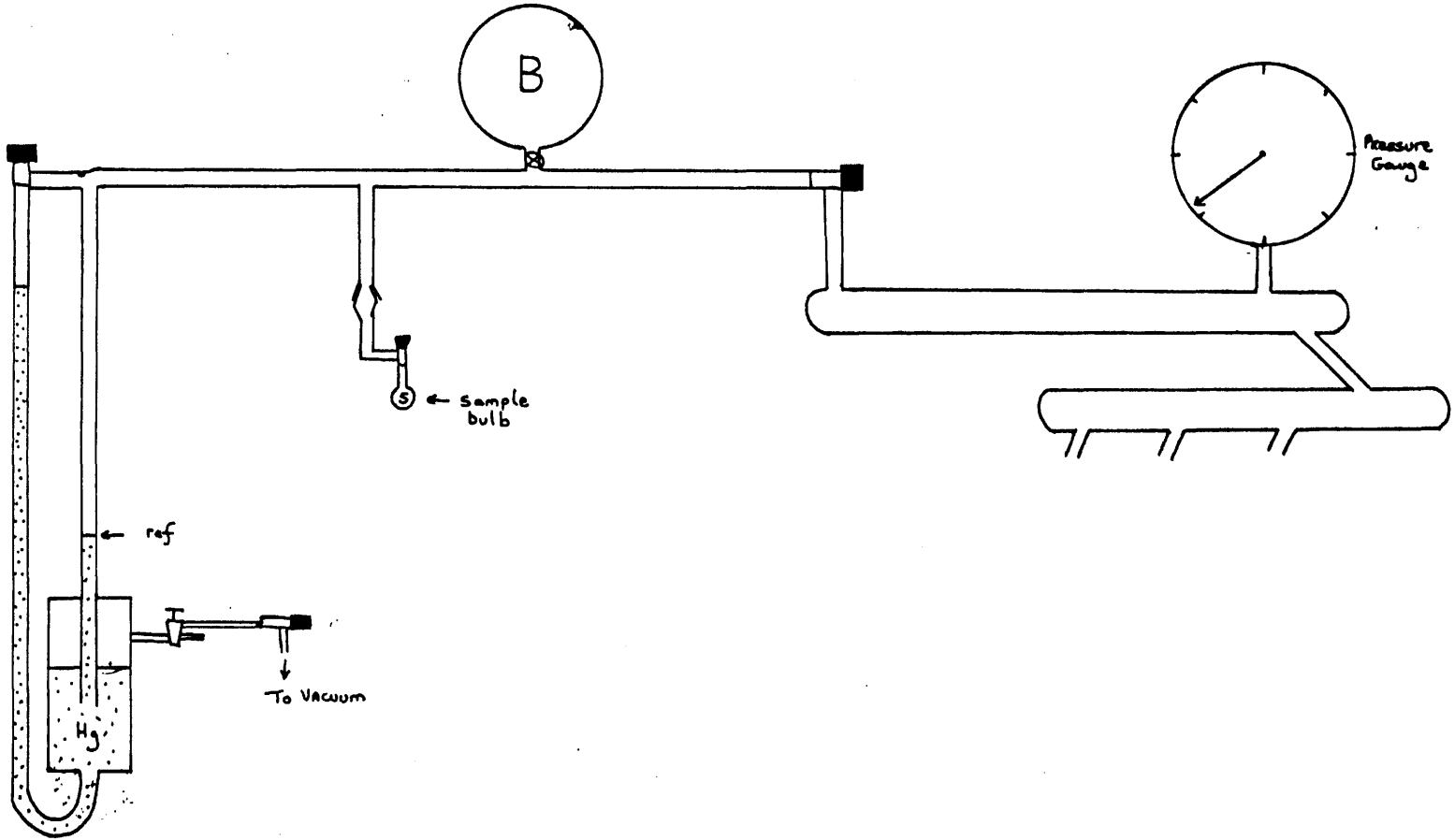

Figure 2·1 Constant volume apparatus

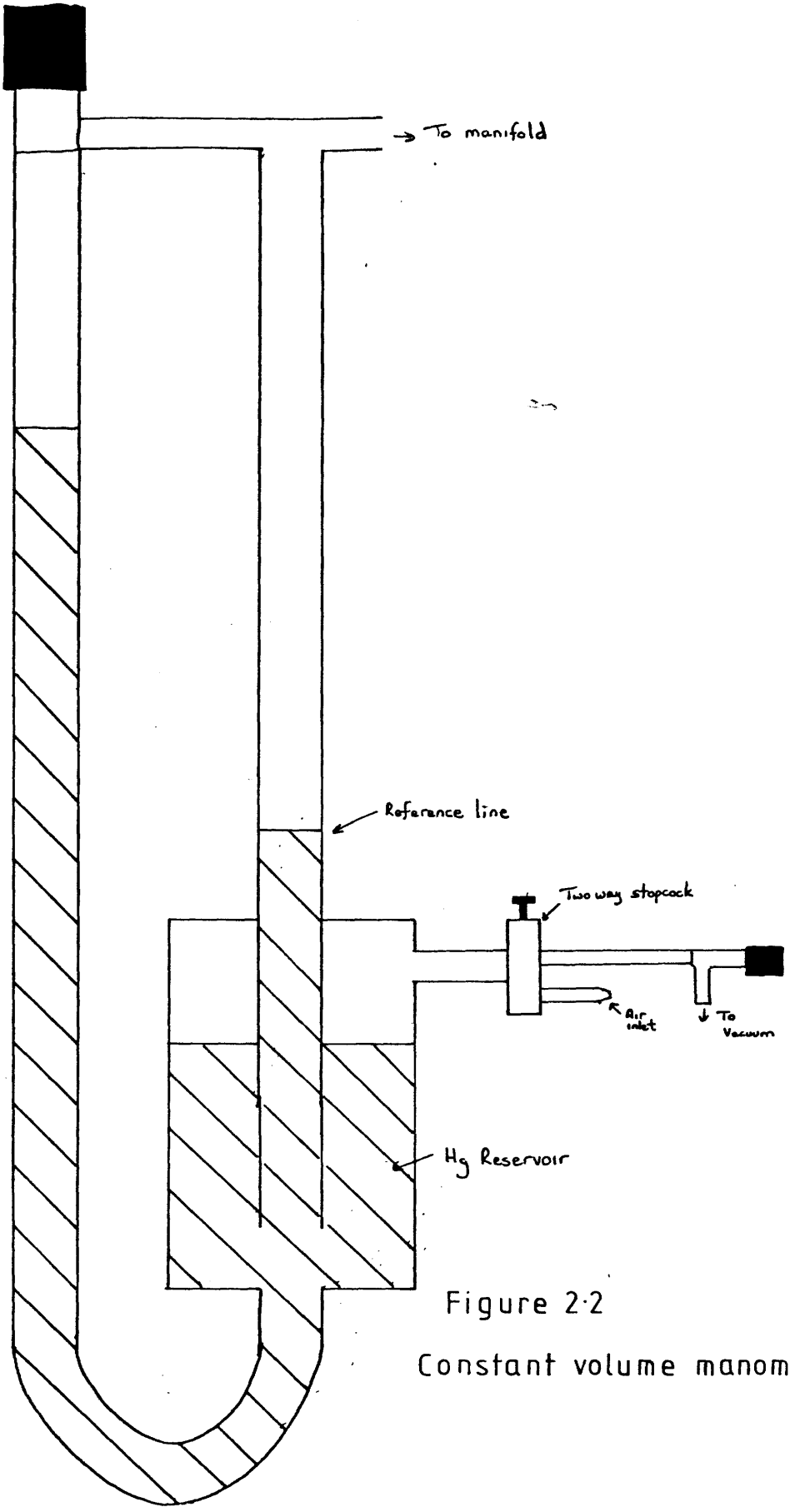

Figure 2·2

Constant volume manometer

2.1.3 THE INERT ATMOSPHERE BOX

An argon atmosphere Lintott box ($H_2O < 10ppm$) was used when handling and storing all samples. Vessels were evacuated and in the case of glass vessels flamed out before being transferred to the box. The box contained a balance which allowed samples to be weighed in this dry atmosphere.

2.1.4 INFRA-RED SPECTROSCOPY

The IR work was performed on a Perkin Elmer 580 or 983 spectometer. The spectra were obtained as Nujol and Fluorube mulls, between AgCl plates or in a gas IR cell equipped with AgCl windows. All mulls were prepared in the inert atmosphere box due to their sensitivity to moisture and air.

2.2 PREPARATION AND PURIFICATION OF REAGENTS

2.2.1 PURIFICATION OF ACETONITRILE

HPLC or spectroscopic grade MeCN was refluxed over anhydrous $AlCl_3$ for one hour before being distilled into a flask containing $KMnO_4$ and Li_2CO_3 over which it was refluxed for 0.25 hours. The MeCN was distilled into another flask containing $KHSO_4$ over

which it was refluxed for one hour before being transferred to a flask containing CaH_2 and again refluxed for 1 hour. It was then distilled into another flask containing P_2O_5 and distilled for half an hour before being finally refluxed over a fresh sample of P_2O_5 for a further half hour. The MeCN was then transferred, without exposure, to atmospheric moisture, to vessels containing previously activated 3A molecular sieves. It was degassed in vacuo, allowed to stand at room temperature for 24 hours, then vacuum distilled onto fresh 3A sieves before being used.

2.2.2 PURIFICATION OF DI-ETHYL ETHER

Analar Et_2O was purified by adding small pieces of freshly cut sodium until no further reaction was observed. The Et_2O was then degassed in vacuo and allowed to stand over activated 3A molecular sieves for 24 hours. Before use the Et_2O was vacuum distilled onto fresh 3A molecular sieves.

2.2.3 PURIFICATION OF PYRIDINE

Analar pyridine was purified by degassing in vacuo then drying over activated 3A molecular sieves.

2.2.4 PURIFICATION OF AsF_5 AND BF_3

Arsenic pentafluoride (Ozark-Mahoning) and boron trifluoride (Matheson Inc) were purified by trap to trap distillation over NaF at - 80°C and stored over NaF at - 196°C. NaF removes any HF which may be present.

2.2.5 PURIFICATION OF CO_2

Carbon dioxide was obtained in the form of dry ice (Distillers Co.) In this form it contains a high proportion of water. The water was removed by first crushing the solid CO_2 followed by three trap to trap distillations over fresh P_2O_5 at - 80°C. The CO_2 was then transferred into a large volume bulb containing P_2O_5 and left at room temperature for twelve hours before use.

2.2.6 PREPARATION AND PURIFICATION OF F_2CO

Carbonyl fluoride was prepared by the reaction of carbonyl chloride with sodium fluoride in acetonitrile.

In a typical preparation carbonyl chloride (3.0g, 30.4 m mol) was condensed onto sodium fluoride (16g 360 m mol) in acetonitrile (30 ml) and the reaction

mixture kept at 20°C for 36 hours in a stainless steel pressure vessel (300 ml). Fractionation of the volatile components gave carbonyl fluoride (1.9g 28.8m mol).

The carbonyl fluoride was purified by trap to trap distillation at - 80°C and stored in a stainless steel pressure vessel until required to prevent reaction with glass to form silicon tetrafluoride.

2.2.7 PURIFICATION OF IF_5

Iodine pentafluoride was purified by trap to trap distillation over NaF followed by shaking at room temperature with Hg metal. The IF_5 was stored over a fresh sample of Hg at room temperature until required for use.

2.2.8 PREPARATION OF Li BF_4

Lithium tetrafluorobate was prepared by the reaction of boron trifluoride with lithium fluoride (B.D.H.) in acetonitrile.

Boron trifluoride (5.71g 84m mol) was condensed onto lithium fluoride (2g 76.9m mol) in acetonitrile

(10 ml) and the reaction mixture was shaken at room temperature for 72 hours. Removal of the solvent and volatile material gave $LiBF_4$ (6.96g 7.4 mmol).

2.2.9 PURIFICATION OF $(NbF_5)_4$

Niobium pentafluoride (Fluorochem Ltd) was purified by sublimation using the apparatus shown in figure 2.3. The crude niobium pentafluoride was placed in flask A and heated using an oil bath to 70°C. Pure NbF_5 was trapped in the U tube by cooling it to - 196°C in liquid nitrogen. When the sublimation process was complete the U tube was sealed off at points C1 and C2 and transferred to an inert atmosphere box where it was stored until required.

2.2.10 PREPARATION AND PURIFICATION OF FNO

Nitrosyl fluoride was prepared by the reaction of nitrogen dioxide (Matheson Inc) with caesium fluoride (BDH).

Nitrogen dioxide (4 m mol) was condensed onto caesium fluoride (10g 66m mol) and the vessel allowed to reach room temperature. After four days 3.6m mol of nitrosyl fluoride were produced.

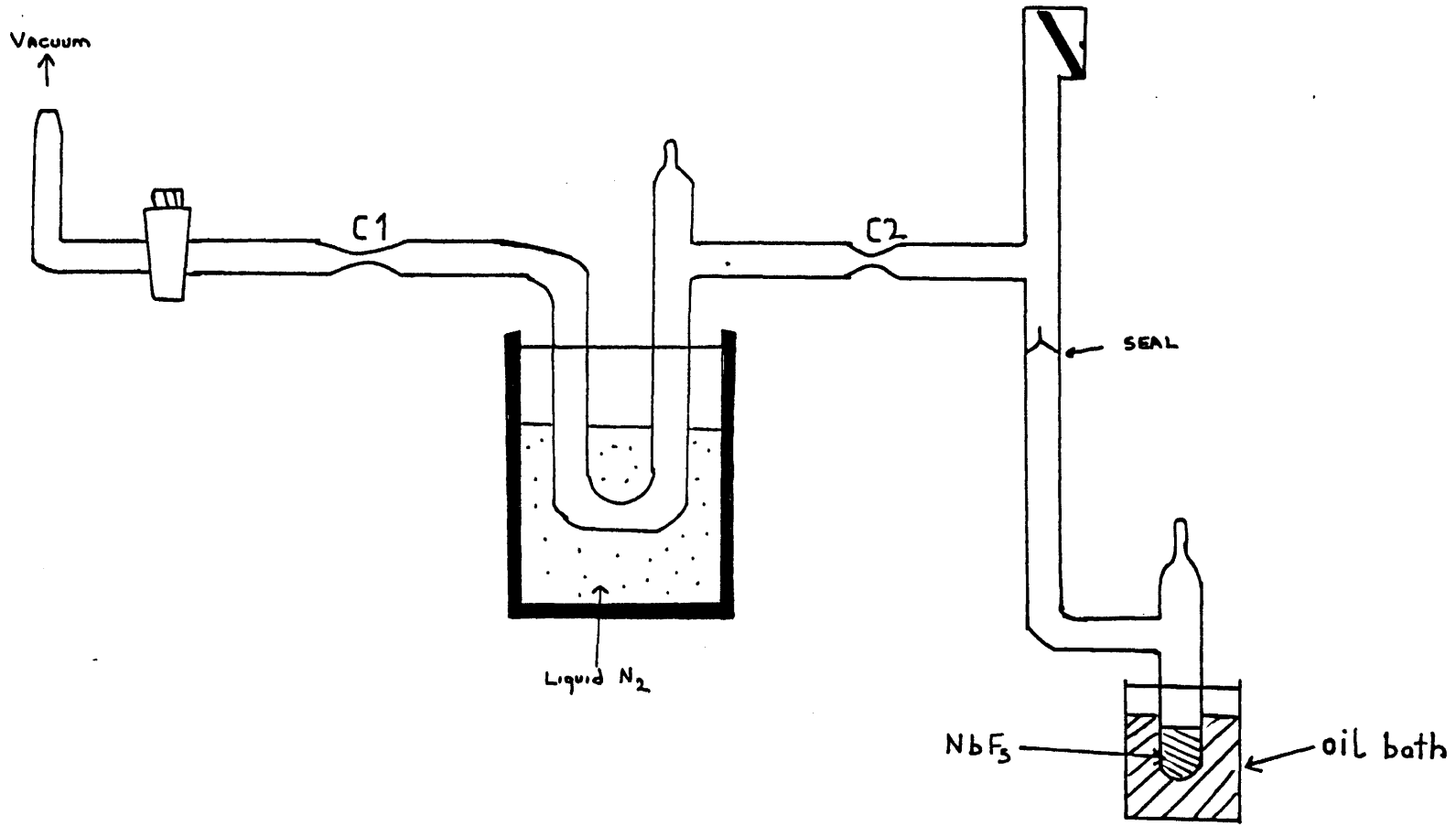

Figure 2·3 NbF_5 sublimation apparatus

The rate of reaction could be increased in two ways. If the vessel containing the nitrogen dioxide and caesium fluoride was heated to 120°C the reaction was complete within three hours. If the caesium fluoride was pretreated with hexafluoroacetone (see chapt. 3) the reaction was complete within ten minutes.

2.2.11 PREPARATION AND PURIFICATION OF SF_4 [63]

Sulphur tetrafluoride was prepared by fluorination of elemental sulphur by iodine pentafluoride.

Purified iodine pentafluoride (45m mol) was condensed into a stainless steel pressure vessel containing elemental sulphur (7m mol). The vessel was then heated at 373K for 5 hours followed by 473K for 48 hours. After reaction the volatile material was removed at 195K and condensed into a similar vessel over NaF.

The SF_4 was purified by reation with BF_3 at 195K forming the adduct $SF_3^+ \ BF_4^-$ [26] Unreacted material was removed by pumping at this temperature, and the adduct decomposed by adding the calculated quantity of dry diethyl ether at 195K.[24] The infra-red spectrum of the product showed no sign of any impurities.

2.2.12 PREPARATION OF β-UF_5 [64]

β-uranium pentafluoride was prepared by the reaction of purified uranium hexafluoride on iodine in iodine pentafluoride according to equation 2.1.

$$10\ UF_6 + I_2 \rightarrow 10UF_5 + 2IF_5 \qquad \text{Equation 2.1}$$

In a typical preparation I_2 (0.36m mol) and UF_6 (6m mol) in IF_5 (20m mol) were shaken at room temperature for 1 hour. Removal of the colourless volatile material gave uranium pentafluoride (0.35m mol).

Aluminium trifluoride (Ozark Mahoning 99.5%) was used as received. Caesium fluoride (BDH Optran grade) was used as received or treated with hexafluoroacetone as described in chapter 3.

2.3 RADIOCHEMICAL TECHNIQUES

Radiotracer methods are widely used for monitoring exchange reactions and for studying surface catalysed processes. Their main advantage is their sensitivity in detecting small numbers of atoms or molecules when these are radioactive.

Before 1934 only the heavy elements with naturally occurring radioactive isotopes could be used to follow the movement of atoms or molecules during reactions. Artificial radioactivity

was discovered by Curie and Joliot early in 1934.[65] They discovered that aluminium foil which had been bombarded with α particles gave off radiation after the bombardment had ceased (equation 2.2). Following this discovery many more radioisotopes were produced by other groups of workers using similar bombardment techniques.

$$^{27}_{13}Al + ^{4}_{2}He \rightarrow ^{30}_{15}P + ^{1}_{0}n \qquad \text{equation 2.2}$$

Because of the low neutron fluxes available at this time, only short-lived radioisotopes of low specific activity could normally be produced. Since 1945, the successful operation of nuclear reactors and the development of particle accelerators have made available high particle fluxes. Consequently radioisotopes, both short and long-lived, of nearly all the elements have become available. This has removed most of the restrictions on the systems which could be examined and exchange reactions have provided much information on a wide variety of topics, for example molecular structure, bond types and reaction kinetics.[66, 67]

2.3.1 EXCHANGE REACTIONS

An exchange reaction occurs when atoms of a given element interchange between two or more forms of this element. Exchange reactions can be observed by labelling one of the elements with a radioisotope and following the position of the isotope. The general equation for an isotopic exchange reaction

may be written:

$$AX + BX^* \rightleftharpoons AX^* + BX$$

Where * designates the distinguishable (radioactive or stable) isotope. The rate of disappearance of the isotopic species from an initially unlabelled reactant is described by a first order rate law regardless of the number of atomic species which participate, since there can be no change in the concentration of the reactants.[68] It is possible therefore to carry out quantitative investigations of exchange reactions. Results can be expressed in terms of the fraction of activity exchanged (f) where (f) is defined by equation 2.3.[69,70]

$$f = \frac{\text{fraction of activity in the initially unlabelled compound}}{\text{fraction of fluorine (mg-atom) in the initially unlabelled compound}}$$

equation 2.3

f is determined experimentally using either equation 2.4 or 2.5

$$f = \frac{A_1}{A_1+A_2}\left(\frac{xm_1}{xm_1+ym_2}\right)^{-1}$$

equation 2.4

$$f = (A_o-A_2)\,\frac{(xm_1 + ym_2)}{A_o x m_1}$$

equation 2.5

where A_1 and A_2 counts s^{-1} are the count rates, corrected for decay, after exchange between m_1 and m_2 m mol of reactants (1 being inactive initially) containing respectively x and y F atoms. A_o counts s^{-1} is the corrected count rate of reactant 2 before exchange.

Equations 2.4 and 2.5 should in theory give the same answer providing that the radiochemical balance is $>95\%$ that is $A_o = A_1 + A_2$. In practice this is not always the case since there are three possible situations which can arise.

1. Fluorine exchange with no retention of the gas by the solid. In this case either equation may by used and the value of f obtained indicates the degree to which exchange has occurred. f = 0 corresponds to no exchange and f = 1 corresponds to complete exchange, that is a random distribution of activity. This situation was observed in the reactions of $SF_3{}^{18}F$ with AlF_3 and $(NbF_5)_4$ reported in chapter 5 of this work.

2. Retention of the gas by the solid with no fluorine exchange. In this case equation 2.4 would give a value of $f > 1$ and equation 2.5 would give a value of f = 0. Therefore as soon as uptake of gas occurs equation 2.4 becomes invalid and equation 2.5 must be used. This situation was

observed in the reactions of $AsF_4{}^{18}F$, $BF_2{}^{18}F$ and $SF_3{}^{18}F$ with CsF reported in chapter 4 of this work.

3. Fluorine exchange and retention of gas by the solid. In this case equation 2.4 will give a value of $f > 1$. Since equation 2.5 depends on the specific count rate of the gas before and after reaction, a true measure of the fraction exchanged will be obtained if this equation is used. This situation was observed in the reaction of ^{18}F FCO with CsF reported in chapter 4 and also in the reactions of AsF_5, BF_3 and SF_4 with $Cs^{18}F$ at high temperature reported in chapter 2.

Equation 2.5 will give a true measure of the fraction exchanged whereas equation 2.4 will only give a true result if there is no uptake of gas. If an f value of >1 is obtained when using equation 2.4 this suggests that uptake of gas has occurred and equation 2.5 must be used if an accurate f value is required.

2.3.2 CHOICE OF ISOTOPE

In general the choice of isotope is determined by three factors. These are:

a) The availability of the isotope

b) The length of its half life

c) The ease of detection

The three radioisotopes used in this work are ^{14}C, ^{18}F and ^{35}S, the longest lived radioactive isotopes of each element. All three are readily detected. ^{14}C and ^{35}S are β^- emitters detectable using Geiger Müller counters with βmax 0.155 MeV and 0.167Me V respectively, both also have long half lives (^{14}C $t_{\frac{1}{2}}$ = 5730y, ^{35}S $t_{\frac{1}{2}}$ = 87.4d).

^{18}F is a γ emitter (γ max=0.51 MeV) and is detectable using a scintillation counter. Although ^{18}F is the longest lived radioactive isotope of fluorine, its half life is only 109.72$^{+}_{-}$ 0.06min[71] This introduces experimental problems that must be overcome. Due to the short half life no more than one working day is available for each experiment since after six half lives only 1-2% of the starting activity is left. All synthesis and purification must therefore be carried out as quickly as possible.

Figure 2.4 shows the kinetic relationship between incorporation and decay of fluorine - 18. The formation of the ^{18}F labelled compound during the chemical reaction competes with the radioactive decay of ^{18}F. Reaction times longer than t limit lead to less net activity in the product.

Figure 2·4

Kinetic relationship between incorporation and decay of ^{18}F

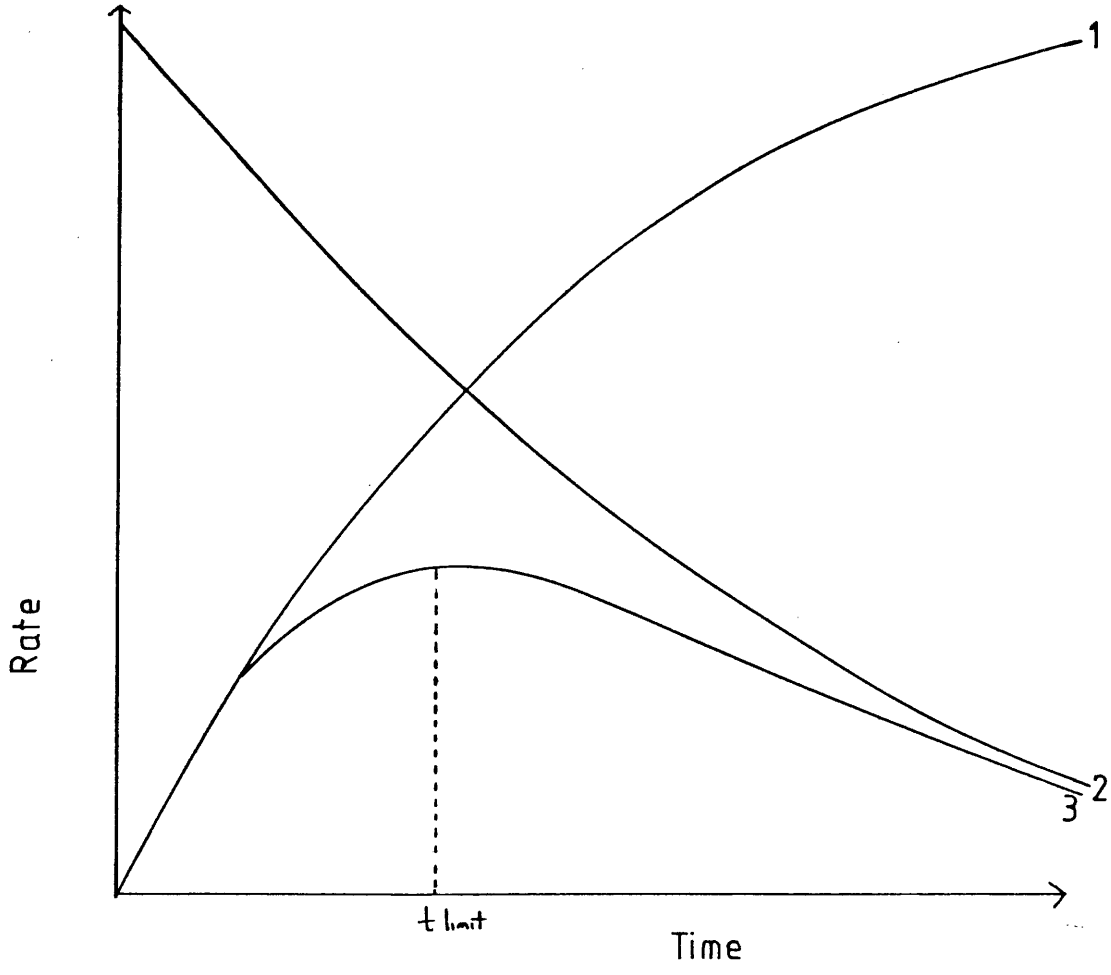

1 = Product formation

2 = Decay curve of ^{18}F

3 = Incorporation of ^{18}F in the labelled product

When using radiotracers to study a particular system it is better if two different isotopes are used, since comparable results obtained from two different sets of tracer experiments are more conclusive than a single set of data obtained for one radioisotope.

The use of two different isotopes to study the same system helps in characterising the species involved and also in distinguishing the reaction processes which are occurring. For example, by using both ^{18}F and ^{35}S labelled SF_4 and ^{18}F and ^{14}C labelled COF_2, it is possible to determine whether growth of activity in the solid is due to fluorine exchange or uptake of the gas by the solid.

Fluorine -18 is an energetic γ emitter which gives information about the overall bulk reaction as all activity present in the sample can be detected. Sulphur -35 and carbon -14 are both weak β^- emitters. Due to absorption of the radioactivity by the solid only activity originating from the surface of the solid can be detected in systems involving these isotopes. Comparison of ^{18}F results with those from ^{35}S or ^{14}C labelled samples allows the surface and bulk species to be differentiated.

In this work the results of reactions involving BF_3 and AsF_5 are based only on ^{18}F radiotracer work and those of CO_2 on ^{14}C work only as no other suitable isotopes were available.

COUNTING OF ^{14}C AND ^{35}S SAMPLES

2.4.1 GEIGER MÜLLER (G.M.) COUNTERS

Carbon-14 and sulphur-35 both decay by beta (β^-) emission A β^- particle is an electron which is ejected from the nucleus. Emission of a beta particle leaves the mass number of the isotope unchanged since the number of nucleons present is unaltered, but the atomic number is increased by one.

Samples labelled with ^{14}C and ^{35}S were counted using a Geiger Müller tube. A Geiger Müller tube consists of an earthed cylindrical case filled with a gas, usually argon, together with a low concentration of an organic substance often alcohol or methane. A positively charged electrode is suspended along the centre of the tube. Radiation enters the tube through a thin mica window and interacts with the gas to produce an electrical pulse. The electrical pulses are recorded by a electronic scaler which produces an output which is proportional to the strength of the initial ionising radiation.

2.4.2 PLATEAU CURVE

In a GM counter no counts are recorded until the applied potential is large enough to attract the free electrons to the anode. When this point known

as the Geiger threshhold is reached (Vt) the count rate begins to rise rapidly until a plateau is reached where the count rate increases only very slowly with voltage. (figure 2.5).

The plateau is never flat due to the generation inside the counter of spurious discharges caused by secondary electron emission. This occurs when the positive ions produced in the initial ionisation reach the cathode and cause secondary electron emission from the surface. This secondary electron emission is usually supressed by the addition of an organic quench gas such as CH_4. As the potential increases the quench gas cannot cope with the large number of spurious discharges and the count rate begins to rise rapidly until the counter begins to discharge.

Plateau regions were determined regularly for every Geiger Müller tube used by sweeping through the voltage region whilst monitoring the count obtained from a caesium-137 source. Figure 2.5 shows a typical plateau curve obtained. The working voltage was set in the middle of the plateau region.

Figure 2·5 G.M. Tube plateau curve

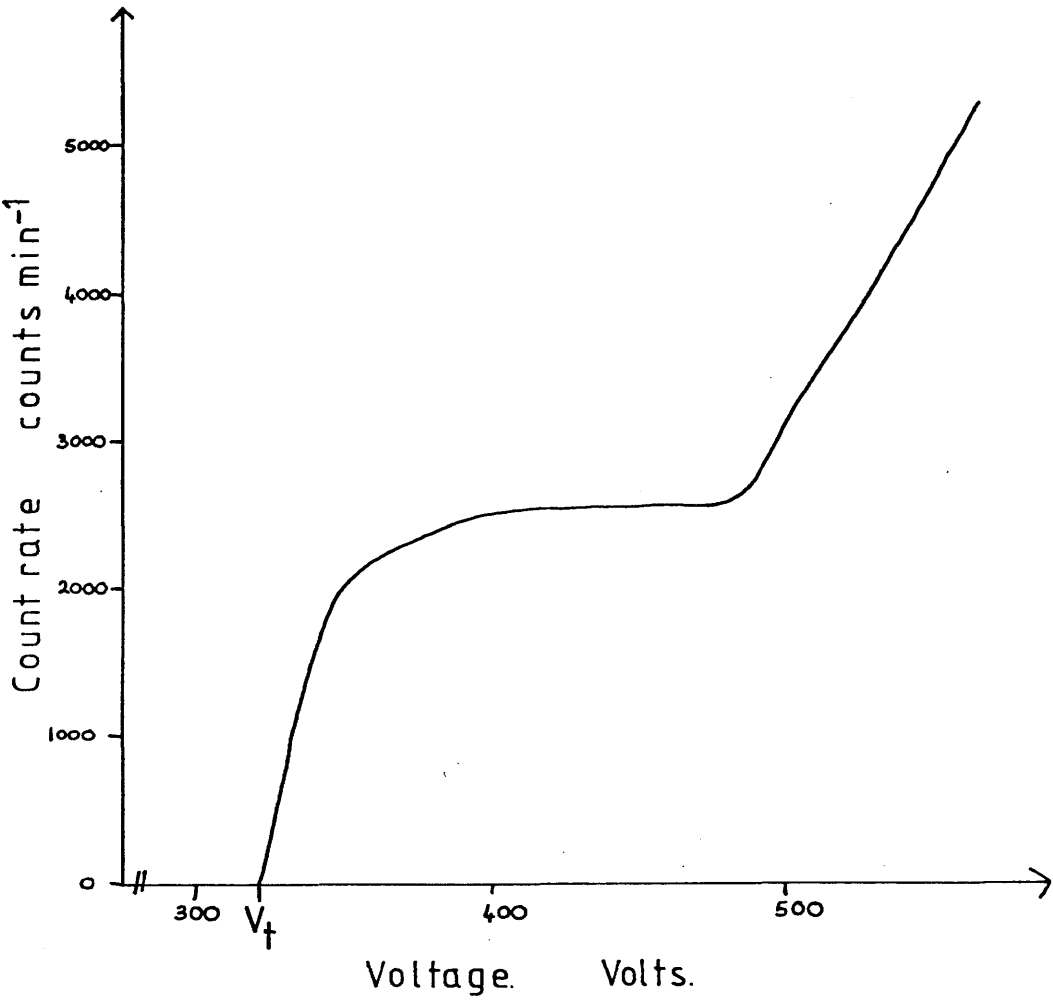

2.4.3 DEAD TIME

Immediately after the collection of electrons in a GM discharge a sheath of positive ions surrounds the central wire. These positive ions reduce the voltage gradient below the value necessary for ion multiplication, and the counter cannot record another event until the positive ions reach the cathode. As a result each pulse from the GM tube is followed by a period during which no particles can be detected. This insensitive period is known as the dead time of the counter, as in accurate counting experiments a correction is necessary for counts lost in such periods especially if the counting rate is high.

The true count rate (Nt) is related to the observed count rate No by the relation:

$$Nt = \frac{No}{(1 - No\tau)} \qquad \text{equation 2.6}$$

where τ is the dead time.

2.4.4 DETERMINATION OF DEAD TIME

The dead times of the GM tubes used were determined by counting samples of $Cs^{18}F$ over periods of three half lives.

The decay of a radioisotope is described by equation 2.7

$$At = A_o e^{-\lambda t} \qquad \text{Equation 2.7}$$

where λ = decay constant

At = Activity of sample at time t

A_o = Activity of sample at time t = o

hence a plot of log At versus time should be a straight line with gradient $-\lambda$ and intercept $\log_e A_o$. When a plot of $\log_e$ (At) versus time was drawn a linear relationship was obtained for $t > 200$ min. At times $t < 200$ min a curve was obtained because at these times the count rate was high enough for the dead time to have a considerable effect.

The linear portion of the plot was extrapolated to time t = 0 using the known half life of ^{18}F fluorine (109.72 $\pm$ 0.06 minutes). This line gave Nt the true count rate which is related to No the observed count rate No by the relation:

$$Nt = \frac{No}{(1 - No\tau)} \qquad \text{Equation 2.6}$$

where τ is the dead time.

This calculation was performed using the first twenty points on the graph and the mean of these

Figure 2·6
Log count rate of $Cs^{18}F$ vs time

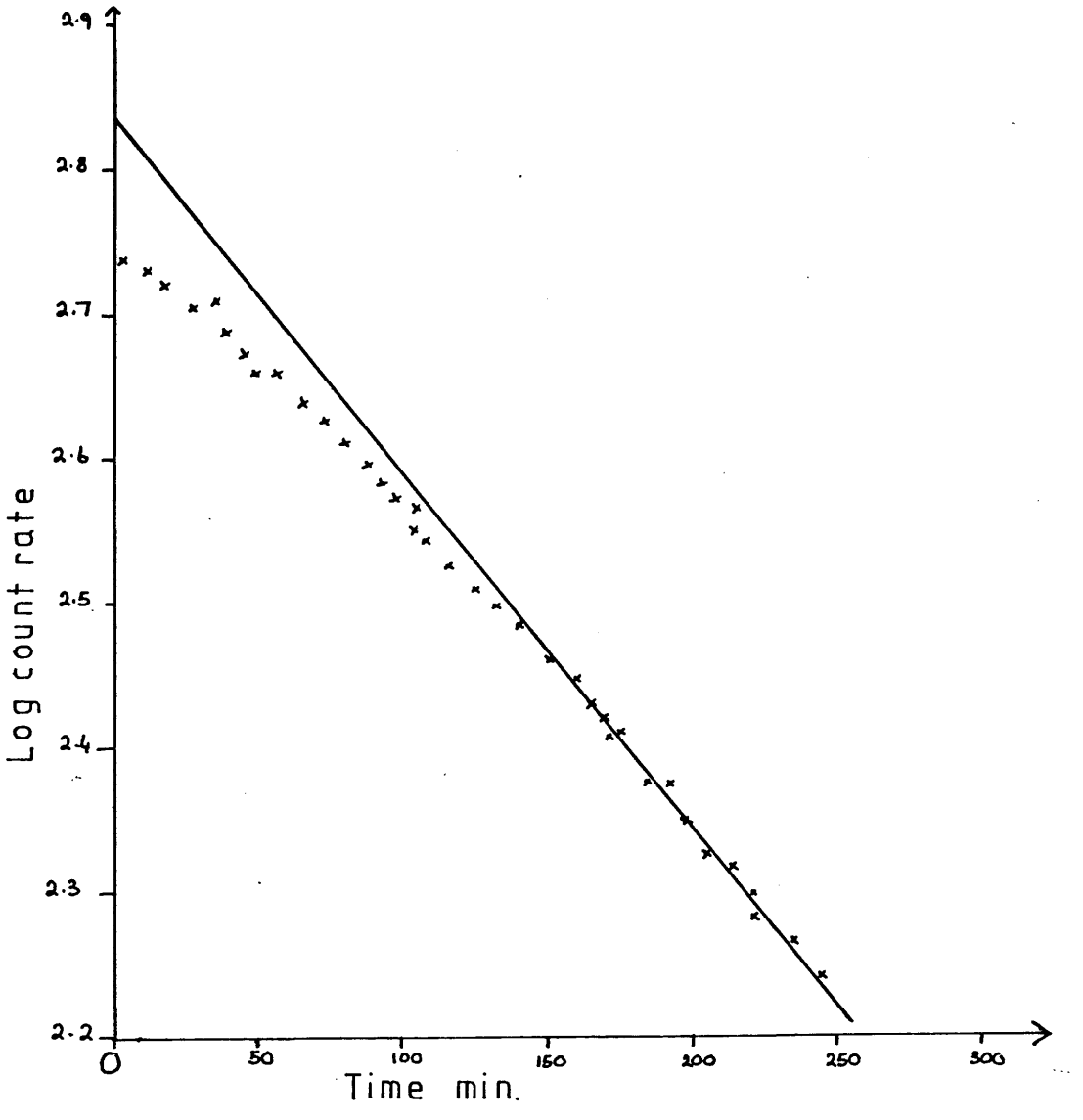

results was taken to be the dead time of the GM tube. Figure 2.6 shows both the experimentally observed line and the calculated true line.

2.5 COUNTING OF ^{18}F-FLUORINE SAMPLES

2.5.1 SCINTILLATION COUNTERS

^{18}F fluorine decays by positron emission (β^+). A positron is a positively charged electron which is ejected from the nucleus following the transformation within the nucleus of a proton into a neutron. As is the case with β^- emission, emission of a positron leaves the mass number of the isotope unchanged but in positron emission the atomic number decreases by one.

The emitted positrons interact with surrounding atoms in a manner very similar to that of an ordinary electron. When the positron has lost virtually all its initial kinetic energy, it combines with a negative electron and annihilation of both particles occurs. Annihilation of the positrons emitted by fluorine-18 results in the emission of γ radiation (γ max 0.51MeV) γ rays are high energy electromagnetic waves.

The γ rays produced in the annihilation process are counted using a Tl/NaI scintillation counter. (Ekco electronics instruments). The scintillation counter

basically consists of a large NaI crystal, a photomultiplier and an amplifier.

When ionising radiation passes through the NaI light is emitted in a short pulse. The size of the pulse is proportional to the energy given up by the radiation to the scintillator. The light from the scintillator liberates electrons at the photocathode of the photomultiplier, the number being proportional to the energy, electrons are accelerated by a dc voltage to the first electrode where each electron liberates another four or so. This is repeated down the tube so that in a 10 stage tube there is a gain of 4^{10}. The resulting pulse is then fed to an amplifier and then to a scaler where it is recorded.

To achieve maximum pulse height, the scintillator crystal is surrounded by a reflector, and the space between the crystal and the photomultiplier filled with paraffin oil or silicone oil of high viscosity to improve the light transmission.

Before use the scaler and scintillation counter were calibrated using a standard caesium-137 γ - source and then with a sodium-22 source which emits γ-rays of the same energy as those emitted by ^{18}F (0.51MeV).

In each case a γ-ray spectrum was obtained by monitoring the counts from the source while varying

Figure 2·7 γ-ray spectrum of ^{22}Na

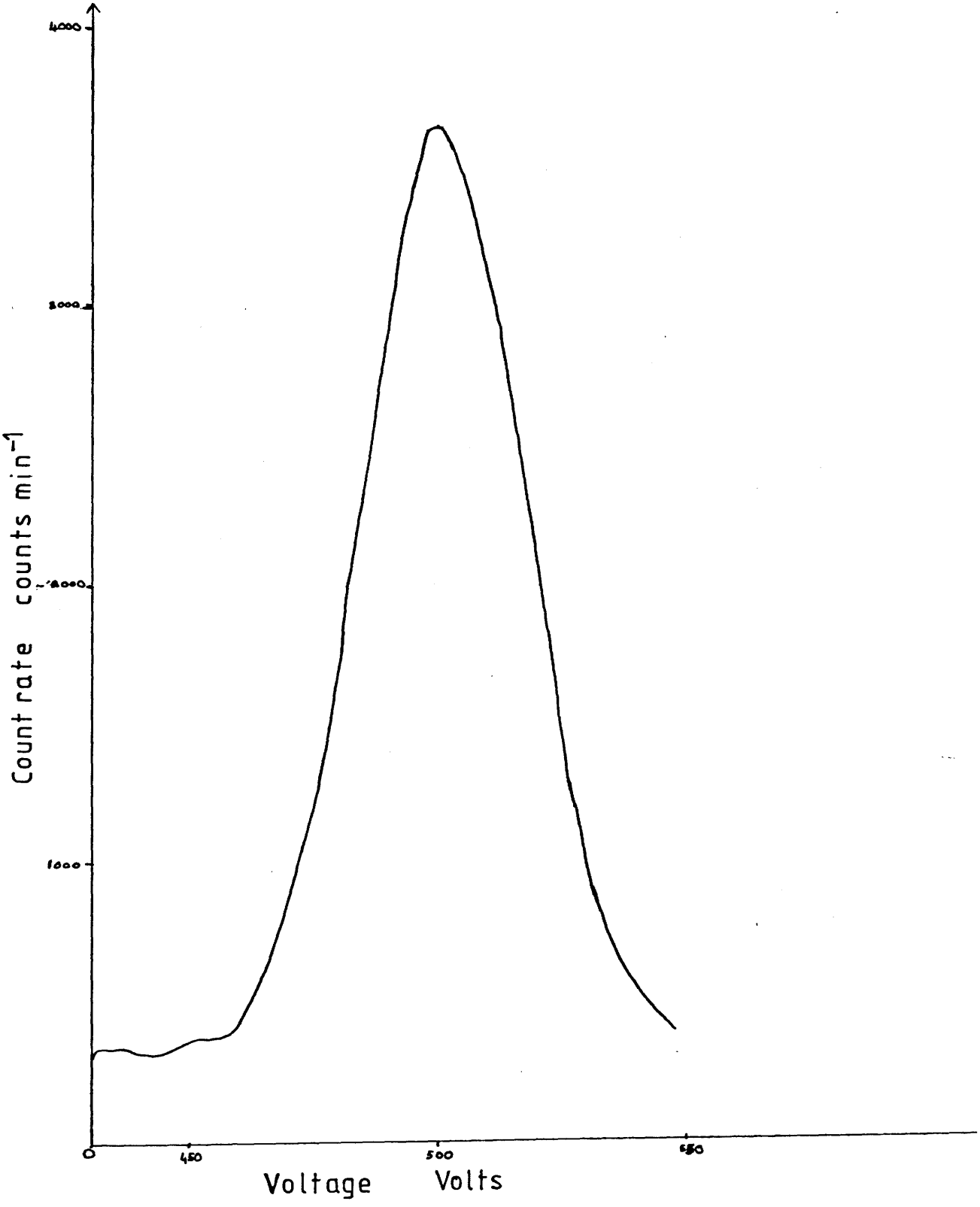

the applied voltage. The γ-ray spectrum obtained for the sodium-22 source is shown in figure 2.7. During experiments the scaler was set to count at the position of the γ-peak $\pm$5%.

2.5.2 DECAY CORRECTION

The disintegration of the nuclei of a radioactive material follows an exponential law

$$Nt = N_o e^{-\lambda t} \qquad \text{equation 2.8}$$

when No = Number of unstable atoms at time t = 0

Nt = Number of unstable atoms at time t

λ = decay constant

The rate of decay is indicated by the half life of the isotope

$$T_{\frac{1}{2}} = \frac{0.693}{\lambda} \qquad \text{equation 2.9}$$

Since the half life of fluorine-18 is (109.72$\pm$0.06 minutes) the rate of decay is such that significant decay occurs within the time taken to carry out one experiment. This means that all experimental data obtained must be corrected for decay before being analysed. All results were corrected to the time of the last measurement taken using equation 2.8. All calculations were carried out by microcomputer.

Listings and explanations of all computer programmes are given in the appendix.

2.6 BACKGROUND

The count recorded in any radiochemical analysis includes a contribution from sources other than the sample. Background activity can be traced to the existence of minute quantities of radon isotopes in the atmosphere, to the materials used in construction of the laboratory, to cosmic radiation, and to the release of radioactive materials into the earth's atmosphere. In order to obtain a true count it is necessary to correct the total count for background.

$$C_t = C_o - C_b \qquad \text{Equation 2.10}$$

where C_t = true count

C_o = observed count

C_b = background count

The level of background radiation can be reduced by shielding the counting equipment. The scintillation counter used for counting ^{18}F samples is encased in lead for this reason. The ^{14}C and ^{35}S samples were counted in a glass reaction vessel which could not be shielded and consequently a higher background count was obtained in these experiments.

2.7 STATISTICAL ERRORS

The decay of a radioisotope is a completely random process and is therefore subject to fluctuation due to the statistical nature of the process. This means that if a source of constant activity is measured in such a way as to exclude all other errors in measurement, the number of disintegrations observed in successive periods of fixed duration will not be constant. The probability W(m) of obtaining just m disintegrations in time t from N_o original radioactive atoms is given by the binomial expression:

$$Wm = \frac{N_o!}{(N_o-m)!m!} \; p^m \, (1 - p)^{N_o-m} \qquad \text{equation 2.11}$$

where p is the probability of a disintegration occurring within the time of observation. From this expression it can be shown[73] that the expected standard deviation for radioactive disintegration σ is given by:

$$\sigma = \sqrt{me^{-\lambda t}} \qquad \text{equation 2.12}$$

In practice the observation time t is short compared to the half life so λt is small. When this is so:

$$\sigma = \sqrt{m} \qquad \text{equation 2.13}$$

where m is the number of counts obtained. In this work all errors quoted on radiochemical measurements are the combination

of the uncertainty in the physical measurements such as weight of sample and pressure of gas, and the uncertainty in the count obtained.

2.8 ^{14}C AND ^{35}S COUNTING APPARATUS

Reactions involving carbon-14 or sulphur-35 labelled species were monitored using the apparatus shown in figure 2.8. This consisted of two intercalibrated GM tubes contained in a calibrated evacuable glass vessel which allowed the surface radioactivity to be determined directly.[74] In order to ensure an identical counting geometry for each GM tube care was taken to keep both tubes at the same height. A solid sample could be placed directly beneath either of the GM tubes by means of a movable glass sample boat. In order to test that only the GM tube with an active solid beneath it registered counts from the solid, the counts from both GM tubes were monitored with a 137-caesium source placed directly below one of the tubes. (Table 2.1).

The tube with the 137-caesium source under it gave a large count whereas the other tube gave only a background count.

GM tube counting characteristics vary slightly from tube to tube so the two contained in the counting vessel were intercalibrated before use by recording the counts obtained from different pressures of radioactive gas . A set of results obtained using $^{35}SF_4$ is illustrated in table 2.2.

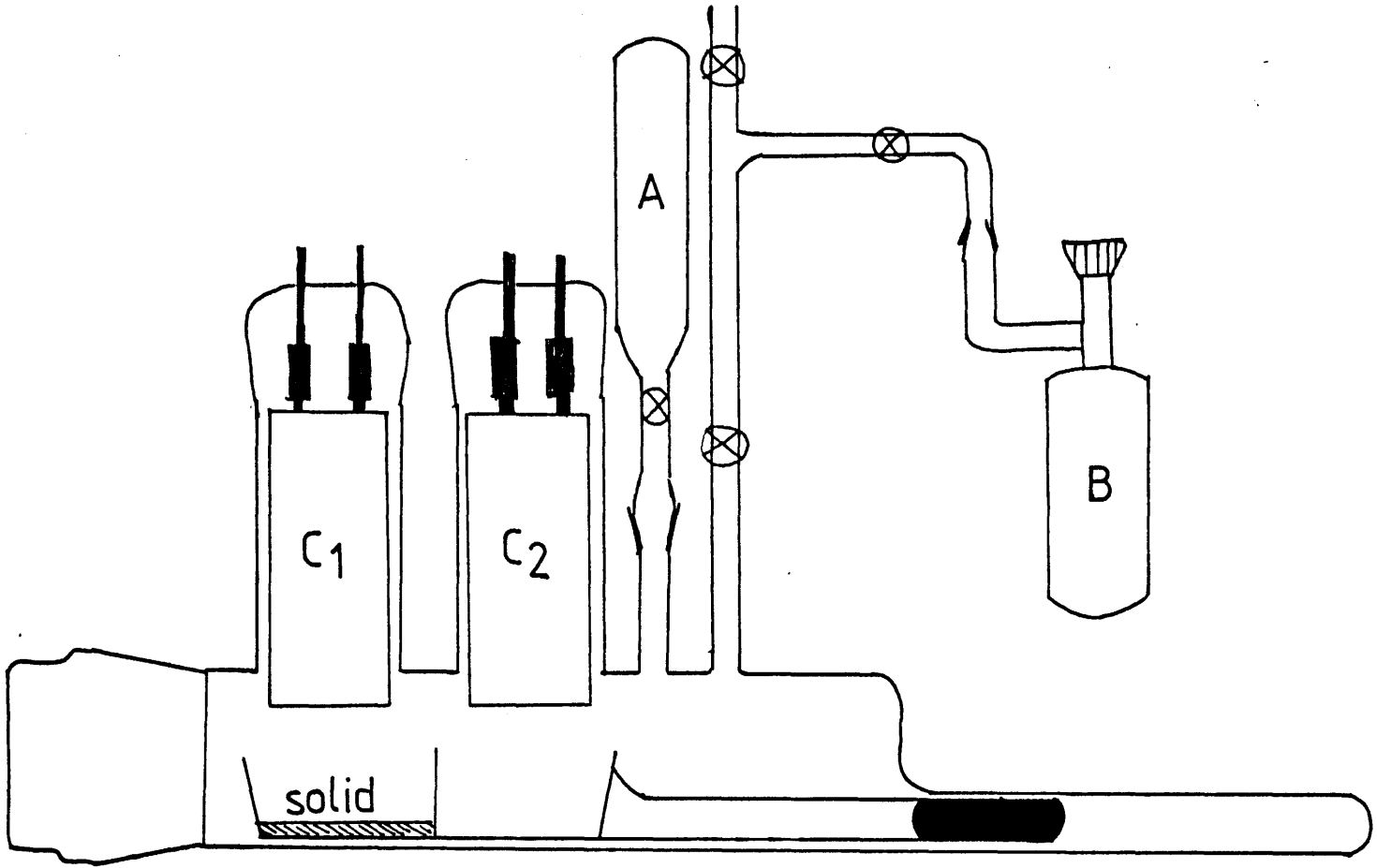

Figure 2·8 ^{35}S and ^{14}C counting apparatus

TABLE 2.1 OBSERVED COUNT RATES

POSITION OF ^{137}Cs	TUBE 1 COUNTS s^{-1}	TUBE 2 COUNTS s^{-1}
BACKGROUND	0.57	0.61
^{137}Cs under 1	85.23	0.65
^{137}Cs under 1	82.19	0.59
^{137}Cs under 1	83.36	0.62
^{137}Cs under 2	0.57	90.15
^{137}Cs under 2	0.59	89.79
^{137}Cs under 2	0.56	91.87

TABLE 2.2 $^{35}SF_4$ PRESSURE vs COUNT RATE

PRESSURE Torr	COUNT RATE TUBE 1 COUNTS SEC^{-1}	COUNT RATE TUBE 2 COUNTS SEC^{-1}
10 ± 1	59.56 ± 0.77	59.63 ± 0.77
19 ± 1	108.13 ± 1.04	109.76 ± 1.05
27 ± 1	154.35 ± 1.24	158.52 ± 1.26
54 ± 1	272.05 ± 1.65	276.03 ± 1.66
79 ± 1	418.51 ± 2.05	425.16 ± 2.06
116 ± 1	607.75 ± 2.47	616.57 ± 2.48
150 ± 1	784.29 ± 2.80	796.76 ± 2.82
210 ± 1	1090.81 ± 3.30	1105.46 ± 3.32
302 ± 1	1574.48 ± 3.97	1593.51 ± 3.99

A plot of pressure versus counts gives a straight line which passes through the origin as shown in figure 2.9.

The correlation factor for the two tubes was obtained by plotting the counts obtained from tube 1 against those obtained from tube 2. A straight line with gradient equal to the correlation factor was obtained (figure 2.10) typically 1.1 - 1.2.

Several different pairs of GM tubes were used in the course of this work. For each new pair, new plateau regions and correlation factor were determined.

Radiotracer experiments were carried out by first removing flask A from the counting vessel and loading it with an accurately weighed amount of the required solid in an inert atmosphere box. The flask was attached to the vacuum line and evacuated before being re-attached to the counting vessel which was then pumped for 30 minutes. After 30 minutes a measured pressure of radioactive gas was admitted to the counting cell and two 100 second counts taken. The average value of the counts obtained was taken as the activity of the gas before reaction. The radioactive gas was then removed from the counting vessel by condensing into Flask B. The flask containing the solid was then opened and the solid allowed to fall into the movable sample boat, which was then placed directly under one of the GM tubes. The GM tube which had the solid beneath it gave a count due to both the solid and the gas, whilst the other tube gave a count

Figure 2·9

$^{35}SF_4$ Count rate vs pressure

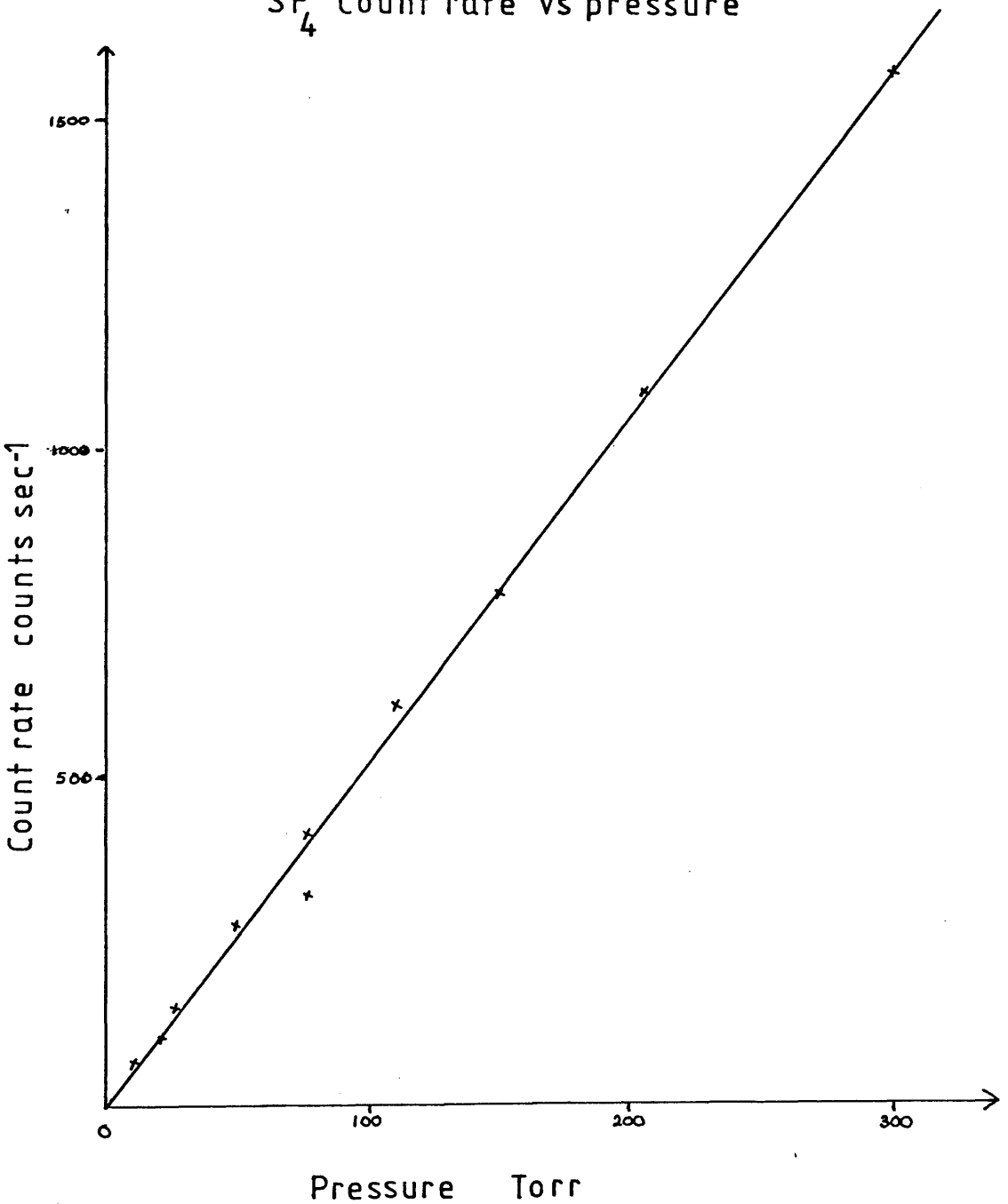

Figure 2·10
Count rate of G.M. tube1 vs count rate of G.M. tube 2

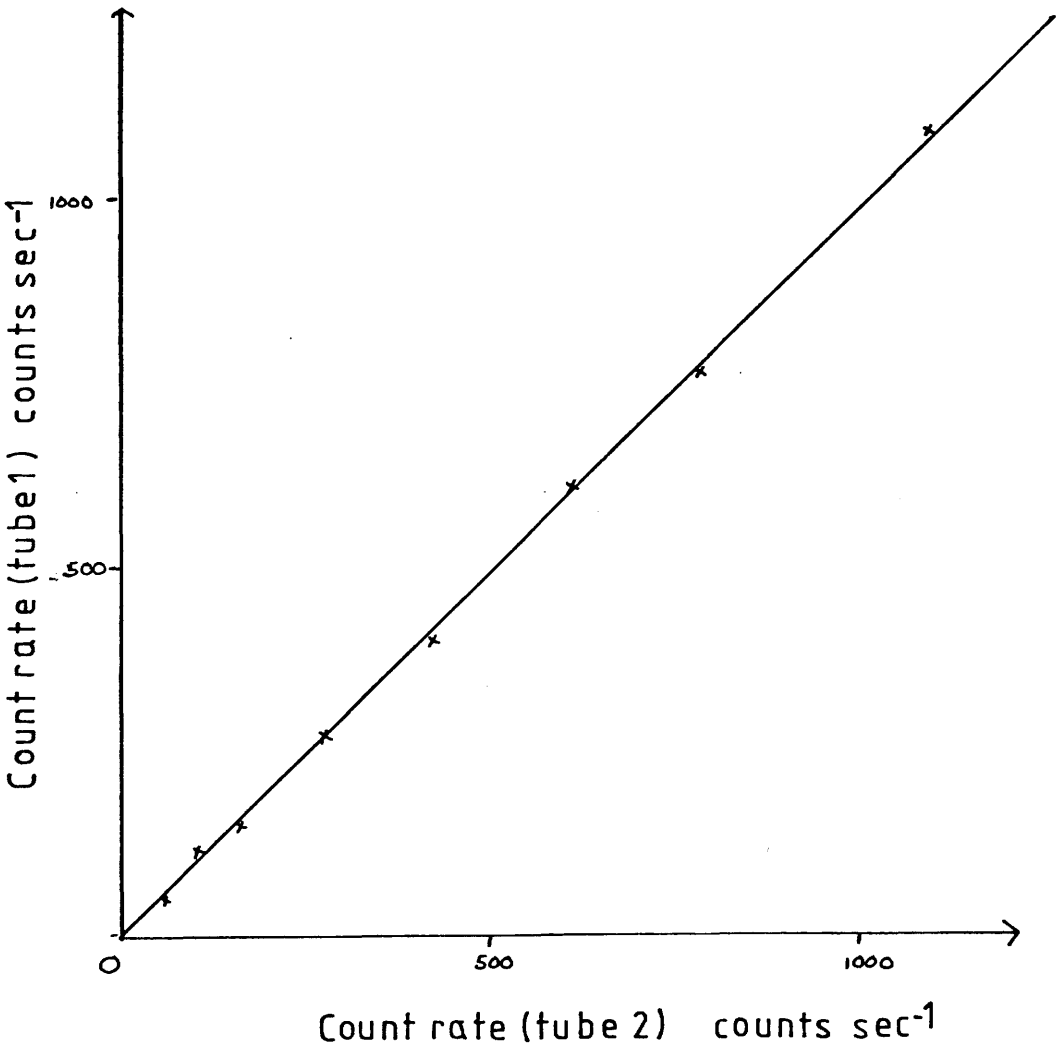

due only to the gas. The reaction was followed by monitoring the counts from both tubes over a period of time. The difference in counts between the two GM tubes gave a measure of the activity present on the surface of the solid and the overall drop in gas phase counts gave a measure of the total uptake of gas by the bulk of the solid.

2.9 FLUORINE-18 COUNTING APPARATUS

Reactions involving fluorine-18 labelled species were monitored using the counting vessels shown in figure 2.11. Type 1 was used to count standard samples of gas and type 2 was used to follow the reaction between fluorine-18 labelled gas and a non active solid.

A weighed amount of the required solid was placed in one limb of the twin limbed flask in an inert atmosphere box. The flask was then transferred to the vacuum line and evacuated for 30 minutes. A measured pressure of ^{18}F labelled gas was then admitted to the flask and the reaction followed by counting each limb alternately over a period of time. The limb containing the solid gave counts due to gas and solid, whilst the other limb gave counts due to gas alone. The difference between the two being a measure of the activity present in the solid. After reaction the radioactive gas was transferred from the twin limbed flask into a pre-weighed flask of type 1 and its specific count rate calculated. The specific count rate of the gas after reaction was then compared to the

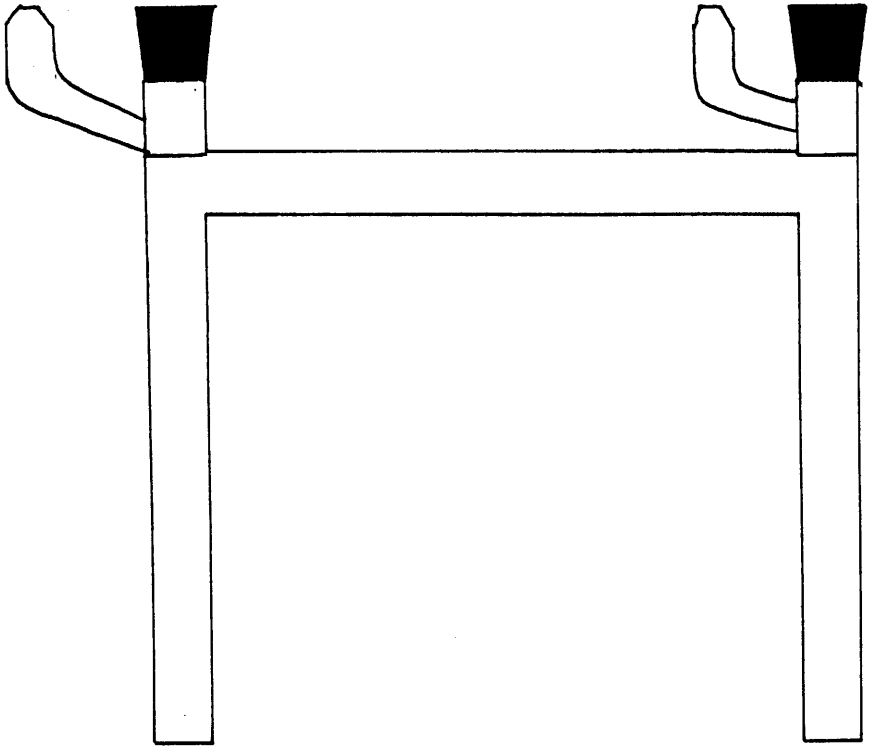

2

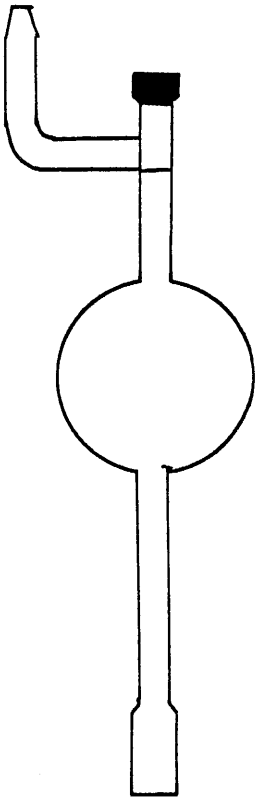

1

Figure 2·11 ^{18}F counting vessels

specific count rate of a sample of the gas taken before reaction to determine whether the activity in the solid was due to ^{18}F exchange between the solid and the gas or to uptake of the gas by the solid.

Fluorine-18 labelled samples were counted using a well type scintillation counter. A well counter is less efficient at counting materials in the gas phase than those in either solid or liquid phases since only the material which is actually in the well of the counter is counted. In order to overcome this problem $BF_2{}^{18}F$ and $AsF_4{}^{18}F$ were counted as their adducts[75,76] with MeCN. SF_4 was counted as its adduct with pyridine[77] and $COF^{18}F$ was counted as a solid at - 196°C by freezing in liquid nitrogen.

To test the validity of this method of counting, counting flasks were filled with varying amounts of labelled gas and the adducts formed. The samples were counted, a linear relationship between the amount of gas in the flask and count rate was obtained in each case. Figure 2.12 shows a plot of count rate vs amount of $BF_2{}^{18}F$.

2.10 PREPARATION OF RADIOCHEMICALLY LABELLED SPECIES

2.10.1 PREPARATION OF $Cs^{18}F$

Fluorine-18 was prepared in the Scottish Universities Research Reactor, East Kilbride using the irradiation

Figure 2·12

Count rate vs amount of $BF_2^{18}F.Et_2O$

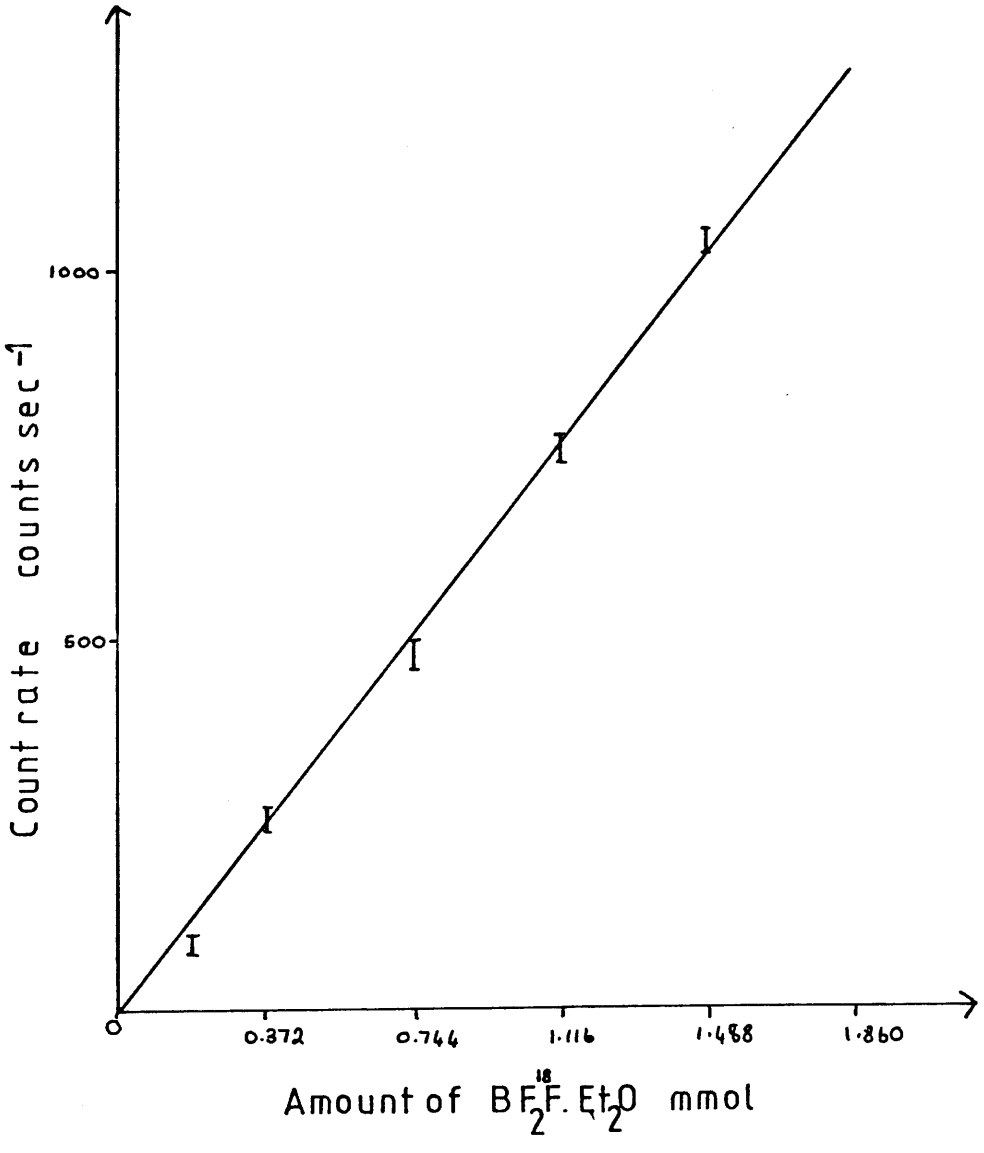

scheme $^{6}Li\ (n,\alpha)t : {}^{16}O\ (t, n)^{18}F$.[78] This scheme requires ^{6}Li and ^{16}O to be intimately mixed. To achieve this Li_2CO_3 (BDH Analar) is used as the target material.

Li_2CO_3 (2g) was irradiated with a neutron flux of 3×10^{12} n $cm^{-2}s^{-1}$ for 30 minutes. The $Li^{18}F$ produced in the irradiation was converted to $H^{18}F$ by reaction with 50% H_2SO_4. The $H^{18}F$ was distilled into a solution of CsOH at $0^{o}C$. The solution was then neutralised by addition of HF and evaporated to dryness on a hotplate to give $Cs^{18}F$ as a finely divided white powder. Before being used to label gaseous fluorides the $Cs^{18}F$ was further dried by heating at $120^{o}C$ under vacuum for 30 minutes. Irradiation of 2g of lithium carbonate gave rise to a yield of ^{18}F of between 40 μCi and 65 μ Ci.

2.10.2 PREPARATION OF $B^{18}FF_2$ $AsF_4{}^{18}F$ $COF^{18}F$ AND $SF_3{}^{18}F$

^{18}F labelled boron trifluoride, arsenic pentafluoride and carbonyl fluoride were prepared by high temperature exchange with $Cs^{18}F$ in a Monel metal pressure vessel. Previous work has shown that $Cs^{18}F$ undergoes high temperature fluorine exchange more readily than any other Group 1 fluoride.[70,79]

^{18}F labelled sulphur tetrafluoride prepared by this method has a specific count rate which is too low,

so labelled SF_4 was prepared by first labelling BF_3 then forming its adduct with SF_4[26] and allowing the adduct to exchange at room temperature for twenty minutes before decomposing with measured amounts of dry diethyl ether.

Various reaction conditions were used in order to determine those which gave the greatest incorporation of ^{18}F. The results of these experiments for each type of gas labelled are listed in tables 2.3 - 2.6

From the results listed in table 2.3 it can be seen that increasing the temperature of reaction and pressure of gas increase the incorporation of ^{18}F in BF_3. Table 2.4 lists the results of a series of experiments in which the $Cs^{18}F$ was activated before use by reaction with hexafluoroacetone for 30 min then heating under vacuum at $120^{o}C$ for 30 min . These results show that pretreatment with hexafluoroacetone has a much greater effect on the amount of ^{18}F incorporated than increasing pressure or temperature. This is due to an increase in the surface area of the caesium fluoride caused by reaction with hexafluoroacetone (see chapt 3) and hence a greater solid surface available for reaction with the BF_3.

Since pretreatment of the $Cs^{18}F$ with hexafluoroacetone had such a marked effect on the incorporation of ^{18}F

TABLE 2.3

BF_3 LABELLING

EFFECT OF TEMPERATURE AND PRESSURE ON ^{18}F INCORPORATION

Pressure of BF_3 Torr	Temp ^oC	Exchange Time min	Activity of $Cs^{18}F$	Counts in 100 sec Gas Phase m mol^{-1}
510	85	60	30 μ Ci	648
510	85	60	25 μ Ci	616
510	100	60	30 μ Ci	912
510	100	60	25 μ Ci	750
760	125	60	30 μ Ci	1028
760	125	60	30 μ Ci	1358

TABLE 2.4

BF_3 LABELLING

EFFECT OF PRESSURE ON ^{18}F INCORPORATION AFTER TREATMENT OF $Cs^{18}F$ with $(CF_3)_2CO$

Pressure of BF_3 Torr	Temp ^oC	Exchange Time min	Activity of $Cs^{18}F$	Counts in 100 sec Gas Phase m mol^{-1}
760	125	60	45 μ Ci	2467
760	125	60	35 μ Ci	1906
1010	125	60	45 μ Ci	3586
1010	125	60	55 μ Ci	6690
1010	125	60	55 μ Ci	5915
1010	125	60	55 μ Ci	6203

in BF_3 the $Cs^{18}F$ was treated in this way before determining optimum conditions for the labelling of AsF_5 and F_2CO. The results of these experiments are listed in tables 2.5 and 2.6. These results also show a dependence on temperature and pressure. Table 2.7 lists the optimum conditions for labelling each type of gas.

During the exchange reaction between $Cs^{18}F$ and BF_3 approximately 6m mol of BF_3 were retained by the $Cs^{18}F$ (6m mol). Infra red examination of the solid after reaction shows bands which can be assigned to BF_4.

This, together with the fact that increasing temperature and pressure increase incorporation of ^{18}F, indicates that the exchange reaction occurs in two distinct stages. The first stage is adsorption of BF_3 and reaction to form BF_4^- and then exchange between BF_4^- and BF_3.

In the experiment involving AsF_5 and F_2CO uptake of gas was observed although to a lesser extent than that observed for BF_3. Infra red examination of the CsF after reaction indicated the presence of AsF_6^- and COF_3^- suggesting that ^{18}F exchange occurs in the same way as in the CsF BF_3 system.

TABLE 2.5

AsF_5 LABELLING

EFFECT OF TEMPERATURE AND PRESSURE ON ^{18}F INCORPORATION

Pressure of AsF_5 Torr	Temp ^oC	Exchange Time min	$(CF_3)_sCO$ Pretreat	Activity of $Cs^{18}F$	Counts in 100 sec Gas Phase
760	85	60	N	45 μ Ci	1356 m mol^{-1}
1010	125	60	N	35 μ Ci	1780
1010	125	60	Y	45 μ Ci	3471
1010	100	60	Y	40 μ Ci	3159

TABLE 2.6

F_2CO LABELLING

EFFECT OF TEMPERATURE AND PRESSURE ON ^{18}F INCORPORATION

Pressure of F_2CO Torr	Temp ^oC	Exchange Time min	$(CF_3)_2CO$ Treatment	Activity of $Cs^{18}F$	Counts in 100 sec Gas Phase
760	100	60	N	65 μ Ci	5876 m mol^{-1}
1010	100	60	N	60 μ Ci	6499
1010	100	60	Y	65 μ Ci	11898

TABLE 2.7

OPTIMUM LABELLING CONDITIONS

Gas Type	Pressure Torr	Temp ^oC	Exchange Time	$(CF_3)_2CO$ Treatment
AsF_5	1010	125	60 min	Y
BF_3	1010	100	60 min	Y
F_2CO	1010	100	60 min	Y

2.10.3 PREPARATION OF ^{18}FNO

Several methods were tried in an attempt to produce nitrosyl fluoride of high enough specific count rate to be useful for exchange reactions.

The first method tried was that of Ratcliffe and Shreeve.[62] NO_2 (2m mol) was condensed onto the $Cs^{18}F$ in a stainless steel pressure vessel at -196°C and the vessel left at room temperature for 1 hour. Due to the short half life of ^{18}F (110 minutes) this was the maximum time that could be allowed for reaction. Under these conditions very little ^{18}FNO was produced.

In an effort to improve on this the caesium fluoride was pretreated with hexafluoroacetone before use by condensing into the vessel $(CF_3)_2CO$ (10m mol). The vessel was left at room temperature for 30 min and then heated at 120°C for 30 min.

When this pretreated $Cs^{18}F$ was treated with NO_2 the result was as in the previous attempt, a negligable yield of $NO^{18}F$.

In a second paper Ratcliffe and Shreeve[62b] state that reaction between CsF and NO_2 is complete in 15 minutes if the reaction is carried out at 300°C.

A third preparation was attempted in which the $Cs^{18}F$ was first pretreated with hexafluoroacetone and the reaction with NO_2 carried out at 250°C (the limit of the available heating coil). The amount of ^{18}F NO produced in this reaction was too small to be of any use.

The main factor affecting the yield appears to be the small amount of $Cs^{18}F$ produced by the reactor as the reaction of CsF with NOF requires CsF to be in excess. In view of this it was decided to add to the $Cs^{18}F$ produced by the reactor 10g (65.8m mol) of hexafluoroacetone activiated caesium fluoride, as activated caesium fluoride is known to react instantaneously with NO_2 and the addition of 10g of CsF would give the required excess.

This preparation resulted in a reasonable yield of $NO^{18}F$ (2m mol) but with a very low specific count rate (3.5 count s^{-1}) which was too low to be of use in radiotracer experiments.

Attempts to label NOF by high temperature exchange with $Cs^{18}F$ were also unsuccessful resulting in $NO^{18}F$ of too low specific count rate to be of any use. As a result no further work with nitrosyl fluoride was carried out.

2.10.4 PREPARATION AND PURIFICATION OF $^{35}SF_4$ [63]

^{35}S labelled sulphur tetrafluoride was prepared from elemental sulphur and iodine pentafluoride according to equation 2.14

$$5S + 4IF_5 \rightarrow 5SF_4 + 2I_2 \qquad \text{equation 2.14}$$

Rhombic (^{35}S) - sulphur (1 m Ci, specific activity 30 m Ci mg - atom^{-1}, The Radiochemical Centre, Amersham) was dissolved in dry CS_2 and diluted by addition to a Monel metal pressure vessel containing inactive sulphur (7.0m mol) also dissolved in CS_2. The CS_2 was removed under vacuum and purified iodine pentafluoride (44.8m mol) added by vacuum distillation. The vessel was heated at 100^{o}C for 12 hours followed by 200^{o}C for 48 hours. After reaction the volatile material was removed at -80^{o}C and condensed into another monel vessel containing predried sodium fluoride.

The $^{35}SF_4$ was purified by reaction with BF_3 at -80^{o}C to form $^{35}SF_3^+$ BF_4^{-}[26]. Unreacted material was removed by pumping at this temperature. The adduct was decomposed by adding a calculated amount of dried diethyl ether at -80^{o}C[24]. The infra red spectrum of the $^{35}SF_4$ (table 2.8) contained no bands attributable to SF_6, SOF_2 or SiF_4.

TABLE 2.8

INFRA RED SPECTRUM OF $^{35}SF_4$ (cm^{-1})

This work	Literature SF_4[80]	SF_6	SOF_2	SiF_4[81]
			1308	
				1010
		939		
887 s	892 $\nu_1 A_1$			
860 s	867 $\nu_6 B_1$			
			801	
730 vs	730 $\nu_8 B_2$		721	
		614		
550 w	558 $\nu_2 A_1$			
530 w	532 $\nu_7 B_1$		526	
	475 $\nu_3 A_1$			
			393	390
	353 $\nu_9 B_2$			
			326	
	226 $\nu_4 A_1$			

The $^{35}SF_4$ was diluted with inactive SF_4 (1:2 ratio) to give a working specific count rate of 258 $\pm$ 3 count s^{-1} m mol^{-1}. The ^{35}S count rate was determined using the counting vessel described in section 2.8 (figures 2.8). A linear count rate vs pressure relationship was obtained and is shown in figure 2.9.

2.10.5 PREPARATION AND PURIFICATION OF $F_2{}^{14}CO$

^{14}C labelled carbonyl fluoride was prepared from carbonyl chloride and sodium fluoride.

^{14}C - carbonyl chloride (1m Ci, The Radiochemical Centre, Amersham) was supplied as a solution in toluene contained in a glass vial. The glass vial and a Monel metal pressure vessel were cooled to -78^{o}C in solid CO_2. When cold the glass vial was cut open and the contents quickly transferred into the cooled metal vessel. The vial was rinsed with a small amount of toluene ($<$10 ml) and the washings added to the metal vessel. The vessel was then degassed and the $Cl_2{}^{14}CO$ transferred to a second metal vessel at -80^{o}C by vacuum distillation. Inactive Cl_2CO (80m mol) was then added to dilute the radioactive sample.

$Cl_2{}^{14}CO$ (30m mol) and Cl_2CO (45 m mol) were condensed into a pressure vessel containing NaF (41g, 900m mol) and 40 ml of acetonitrile. The vessel was then left at room temperature with occasional shaking for 36 hours.

$F_2{}^{14}CO$ was removed at -80^oC and purified by trap to trap distillation. The $F_2{}^{14}CO$ had a specific count rate of 135 ± 2 count s^{-1} m mol^{-1}. A linear count rate vs pressure relationship was obtained and is shown in figure 2.13.

2.10.6 PURIFICATION OF $^{14}CO_2$

$^{14}CO_2$ (2m mol, 1m Ci) which had been prepared by the addition of acid to $Ba^{14}CO_3$ was dried by three trap to trap distillations over fresh P_2O_5 at -80^oC. It was then diluted with non radioactive CO_2 to give a specific activity of 2150 ± 5 counts s^{-1} m mol^{-1} before being transferred to a large volume storage bulb containing fresh P_2O_5 and left at room temperature for twelve hours before use. A linear count rate vs pressure relationship was obtained and is shown in figure 2.14.

ooOoo

Figure 2·13

Count rate of $F_2^{11}CO$ vs pressure

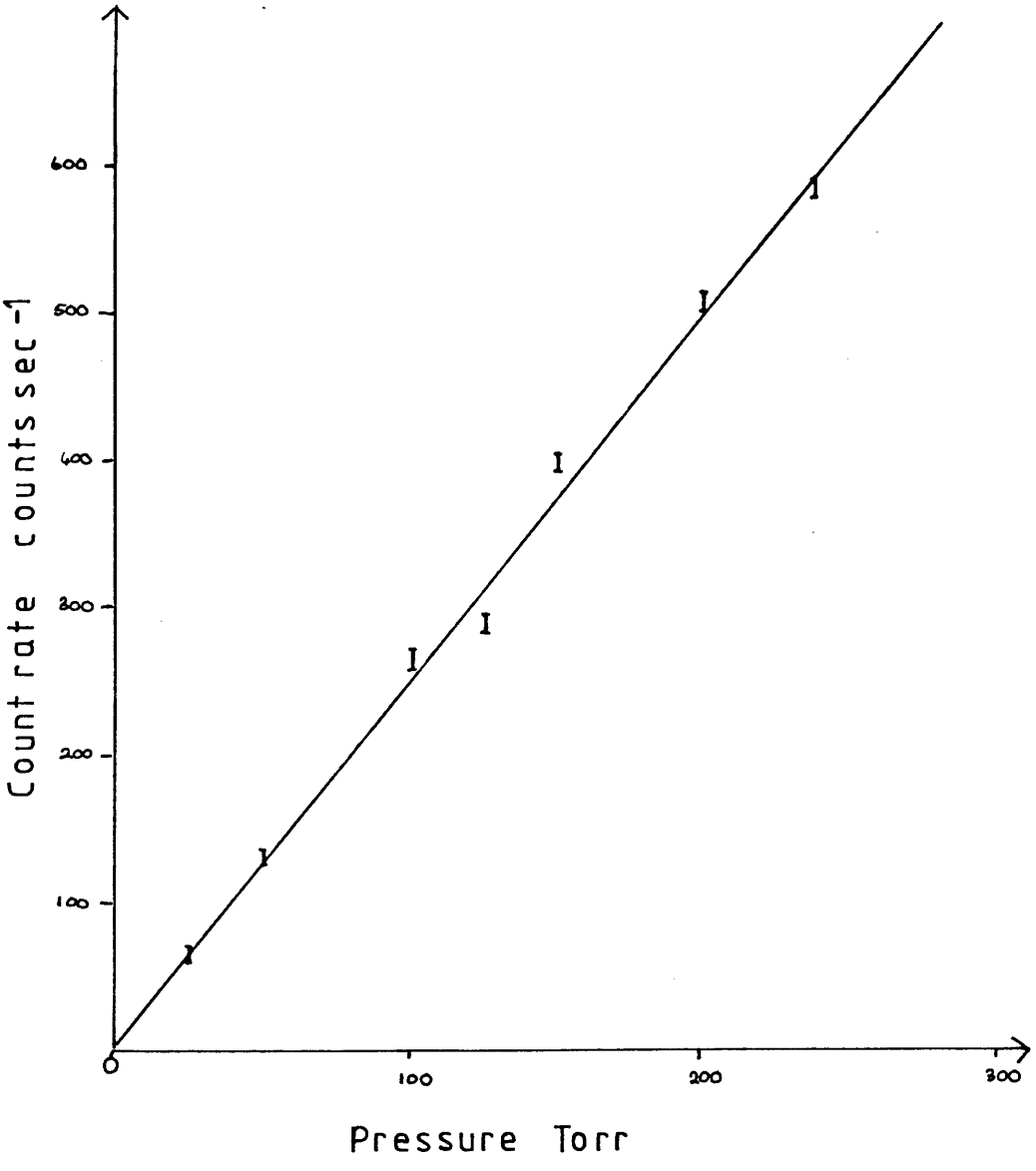

Figure 2·14

Count rate of $^{14}CO_2$ vs pressure

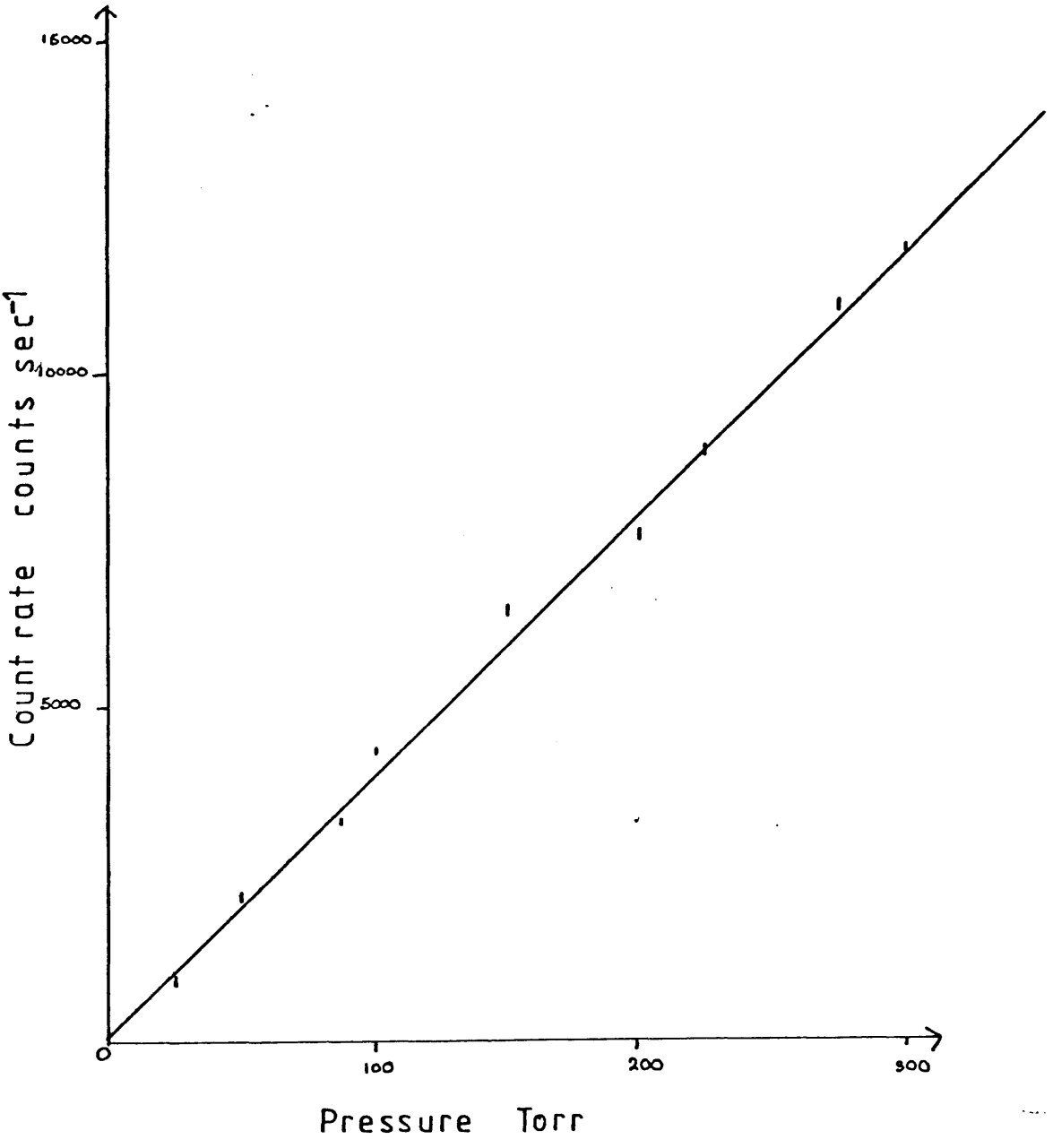

CHAPTER THREE

CHAPTER 3

ACTIVATION OF CAESIUM FLUORIDE

INTRODUCTION

When caesium fluoride is used as a catalyst it is usually pretreated in some way. Methods of pretreatment range from simply heating and grinding in an inert atmosphere to formation and subsequent thermal decomposition of a chemical adduct.[55,57,82]

The caesium fluoride used in this work was pretreated by reaction with $(CF_3)_2CO$ in MeCN to form $Cs^+ OCF(CF_3)_2^-$, and then decomposed by heating under vacuum to leave activated CsF. This activation process is known to increase the surface area[83] and also to enhance the reactivity[57] of the caesium fluoride. The effect of treating the caesium fluoride with F_2CO in MeCN was also studied and the results compared with those of $(CF_3)_2CO$ activated CsF.

Before carrying out any radiotracer experiments with activated CsF the increase in surface area was determined using the ^{85}Kr B.E.T. method[83]. Surface areas are normally measured by determining the amount of gas adsorbed at a given temperature as a function of pressure. When the surface area to be measured is small, that is below $5m^2 g^{-1}$, the change in pressure cannot be measured accurately by conventional techniques. For these small areas krypton-85 is used as the adsorbate and the small changes in pressure can be

accurately determined. This is done by calibrating the pressure against the count rate of the krypton in counts sec^{-1}.

3.1 EXPERIMENTAL

3.1.1 ACTIVATION OF CsF BY TREATMENT WITH $(CF_3)_2CO$

Activated caesium fluoride was prepared according to the reaction scheme shown below using a variation of the method described by Redwood and Willis.[84]

$$CsF(s) + (CF_3)_2CO(g) \rightleftharpoons Cs^+(solv) + (CF_3)_2FCO^-(solv)$$

$$CsF(s) + (CF_3)_2CO(g) \xleftarrow{\Delta} Cs^+ OCF(CF_3)_2^- (s)$$

Caesium fluoride (4g, 26m mol, BDH Optran grade) was ground in an inert atmosphere box and placed in a stainless steel pressure vessel (Hoke Inc.) together with four stainless steel ball bearings. The vessel was sealed and evacuated and hexafluoroacetone (30m mol), together with acetonitrile (5ml) added by vacuum distillation. The vessel was allowed to warm to room temperature and shaken for twelve hours. After twelve hours the acetonitrile and unreacted hexafluoroacetone were removed by vacuum distillation. The infra red spectrum of the product at this stage consisted of ten bands (Table 3.1). The results of a C and F analysis show that the product is $Cs\ OCF(CF_3)_2$.

TABLE 3.1

Infra red spectrum of Cs $OCF(CF_3)_2$ (cm^{-1})

1450	m	ν CO
1350	w	ν CF
1250	s	ν CF
1210	s	ν CF
1150	s	ν CF
1100	s	ν CF
960	s	ν CC
780	w	υ CF
730	w	δ CF
630	w	δ CF

TABLE 3.2

Infra red spectrum of $(CF_3)_2$ CO (cm^{-1}) [85]

1805	m	ν CO	A1
1340	sh	ν CF	B1
1265	w	ν CF	B1
1250	s	ν CF	A1
970	s	ν CC	B1
780	w	υ CC	A1
720	sh	δ CF	B1
640	w	δ CF	A1

$CsOCF(CF_3)_2$ requires C 11.32%, F 41.82%

Found C 11.24%, F 41.54%

The vessel was heated under vacuum at 125°C for sixteen hours to decompose the adduct formed. After heating the CsF was transferred to an inert atmosphere box where it was ground in an agate mortar and pestle, and stored in a sealed glass vessel until required for use. After activation the caesium fluoride is an off white colour and resembles talc in appearance.

3.1.2 PREPARATION OF $Cs\ OCF_3$

Caesium fluoride (2g, 13m mol) was ground in an inert atmosphere box and placed in a stainless steel pressure vessel equipped with a valve. Carbonyl fluoride (15 m mol) and acetonitrile (5ml) were added by vacuum distillation. The vessel was allowed to warm to room temperature and shaken for twelve hours. After twelve hours the acetonitrile and unreacted carbonyl fluoride were removed by vacuum distillation. The vessel was then transferred to an inert atmosphere box where the $Cs\ OCF_3$ (13 m mol) produced was stored in a sealed glass vessel until required for use.

TABLE 3.3

Infra red spectrum (cm^{-1}) of solid Cs OCF_3 Nujol Mull

Present work	Literature[28]	Assignment
2000 bw		$\nu_3 + \nu_1$ HF_2^- [86]
1825 w		$\nu_2 + \nu_1$ HF_2^-
1560 vs br	1560 vs br	ν_1 A_1 CO str
1455 s		ν_3 CO_3^{2-} [87]
1230 s		ν_2 HF_2^-
960 b vs	960 vs br	ν_4 E CF_3 asym str
805 s	813 s	ν_2 A_1 CF_3 sym str
595 m	595 mw	ν_3 A_1 sym CF_3 def
570 ms	574 ms	ν_5 E OCF def
420 w	423 w	ν_6 asym CF_3

The infra red spectrum of the trifluoromethoxide consisted of ten bands (table 3.3).

3.1.3 DECOMPOSITION OF $Cs\ OCF_3$

$Cs\ OCF_3$ (1g, 4.6m mol) was placed in a stainless steel pressure vessel equipped with a valve and heated under vacuum at $120^{o}C$ for three hours. The vessel was allowed to cool and transferred to an inert atmosphere box. Infra red examination of the product showed that the trifluoromethoxide anion was no longer present.

3.1.4 SURFACE AREA DETERMINATION

Surface areas were determined by the B.E.T. method using the radio-isotope ^{85}Kr as adsorbate. The apparatus was a modified version of that described by Aylmore and Jepson [88] and consisted of a calibrated system connected to a standard vacuum line system. The calibrated section, constructed from Pyrex glass consisted of two sets of bulbs each with a mercury reservoir, a ^{85}Kr storage bulb (B), a thin walled counting vessel (C) and the adsorbent sample bulb (S). This system is shown in figure 3.1.

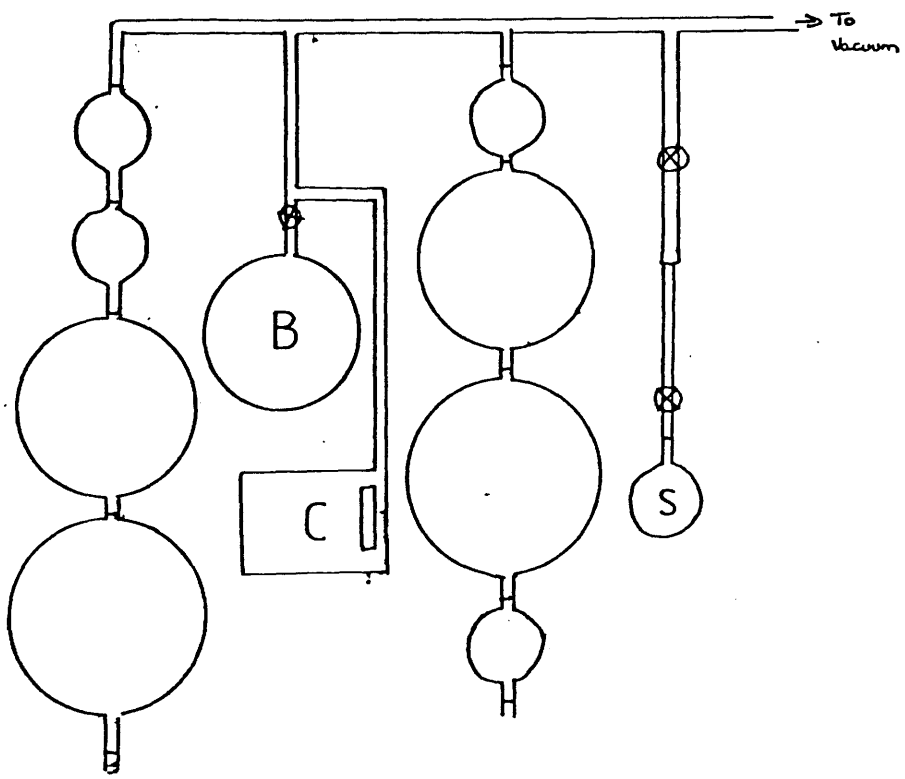

Figure 3·1 B.E.T. Apparatus

The calibrated section was also connected to reservoirs containing ^{85}Kr ($t_{\frac{1}{2}}$ = 10.6y, β max = 0.67 MeV Radiochemical Centre Amersham) and inactive Kr (BOC Ltd) and to a trap containing charcoal activated at 578 K in vacuo which was used to prepare diluted ^{85}Kr of a suitable working activity.

A calibration curve of ^{85}Kr count rate versus pressure was determined (Figure 3.2). Pressures were measured using a Pirani gauge and ^{85}Kr activities determined using a Geiger-Müller counter (Mullard 2P 1481) externally mounted immediately below the counting vessel C. The counting vessel was surrounded by lead to cut down the effect of background radiation. Twenty minutes were required for equilibrium to be attained after each pressure change. The count rates were reproducible, the time of counting being adjusted to give a total count of $\geqslant 10^4$, to minimise counting errors.

The sample bulb(S) was loaded with an accurately weighed sample (0.2 - 0.5g, 1.3 - 3.3m mol) of caesium fluoride in an inert atmosphere box, and degassed overnight. ^{85}Kr was admitted to the manifold and by filling the bulbs with mercury the volume of the system was changed thus altering the pressure, P. For every surface area determination a graph of volume versus temperature/pressure was drawn. This

Figure 3·2

Count rate of ^{85}Kr vs pressure

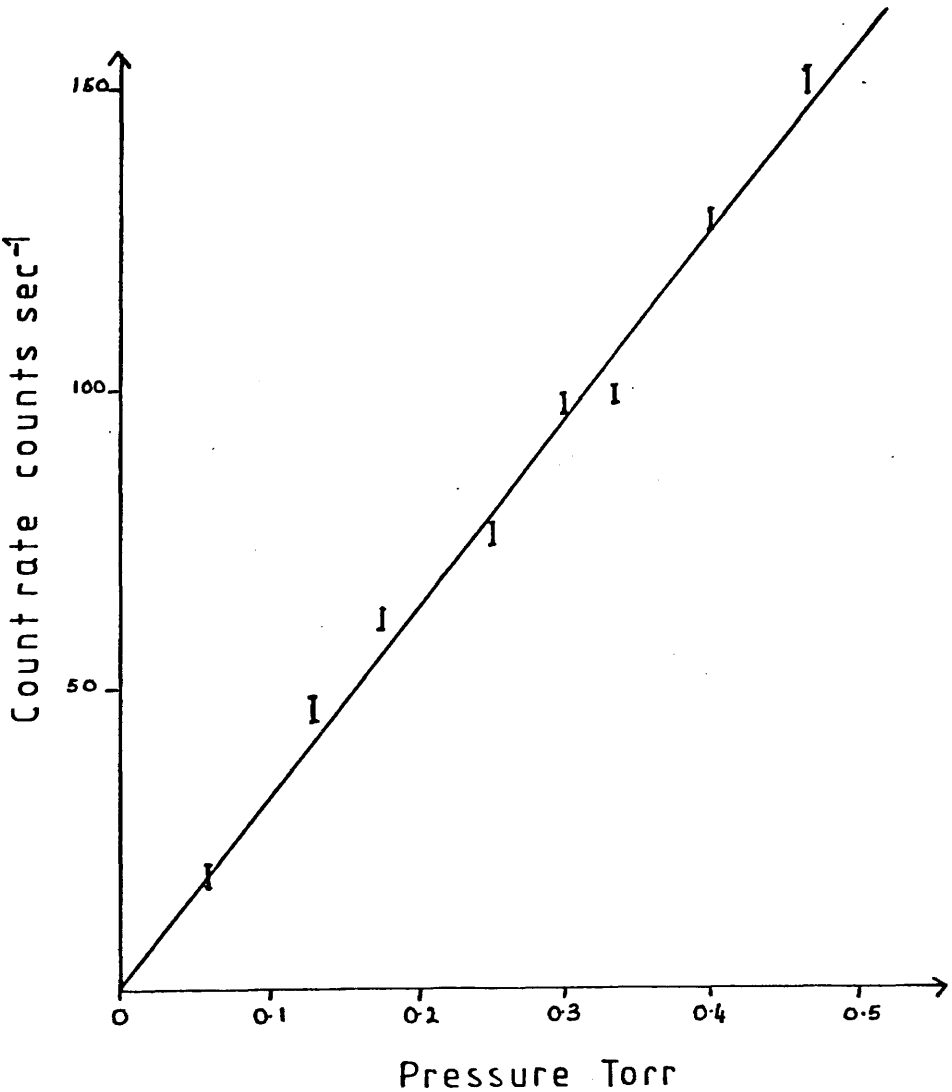

gave a straight line which intercepted the y axis at a volume equal to the dead space of the apparatus. The sample bulb was then cooled to 77K in liquid nitrogen. A correction was made to take account of the effective volume of the apparatus when part of the system was cooled to 77K. The corrected volume versus temperature/pressure plot should be a line parallel to the room temperature line with an intercept equal to the dead space plus the temperature corrected volume. This was verified experimentally by carrying out an experiment with no CsF in the sample bulb.

With the bulb held at 77K a second volume versus temperature/pressure relationship was obtained. This was a straight line with the same intercept as the temperature corrected line but with a different gradient. The amount of ^{85}Kr adsorbed was calculated by taking the difference in volume, ΔV, between these two lines. The number of Kr molecules adsorbed (n) is given by equation 3.1.

$$n = \frac{P\Delta V}{T} \quad \frac{N}{R} \quad \frac{1}{760} \times 10^{3} \qquad \text{Equation 3.1}$$

Where P = Pressure (Torr)

ΔV = Change in volume (ml)

N = Avagadro number (6.022×10^{23})

T = Temperature at which the adsorption isotherm is determined, that is 77K

R = Gas constant (0.082 l at mol^{-1} K^{-1})

The B.E.T. equation (equation 3.2) states that

$$\frac{P}{n(Ro-P)} = \frac{1}{NmC} + \frac{C-1}{NmC}\frac{P}{Po} \qquad \text{Equation 3.2}$$

where n = amount adsorbed at pressure P

P^o = saturated vapour pressure of the gas at the adsorption temperature

C = constant for any particular gas/solid system

Nm = quantity of gas required to form a monolayer

Therefore a graph of $\frac{P}{n(Po-P)}$ versus P/Po gives a straight line with gradient $\frac{C-1}{NmC}$ and intercept $\frac{1}{NmC}$.

Thus the surface area was calculated from equation 3.3.

$$\text{The surface area} = \frac{19.5 \times 10^{-20}}{\text{wt of sample}} \; m^2 \; g^{-1} \qquad \text{Equation 3.3}$$

where 19.5×10^{-20} m^2 is the molecular area of Kr.

A typical calculation is shown in table 3.4 and in figures 3.3 and 3.4.

From figure 3.3

$$\text{Gradient} = 0.7389 \times 10^{-18}$$

$$\frac{C-1}{NmC} = 0.7389 \times 10^{-18}$$

TABLE 3.4

SURFACE AREA DETERMINATION OF ACTIVATED CsF

Volume ml	Counts sec^{-1}	Temp ^oC	Pressure Torr	$T/P \times 10^{-3}$ $^oC\ Torr^{-1}$	
183.37	47.06	20.1	0.131	0.153	Room Temp.
120.30	61.72	20.7	0.177	0.117	
60.73	86.87	20.7	0.256	0.081	
31.20	111.55	21.1	0.333	0.063	
0.00	153.30	21.0	0.463	0.045	
Volume ml	Counts sec^{-1}	Temp ^oC	Pressure Torr	$T/P \times 10^{-3}$ $^oC\ Torr^{-1}$	
183.37	37.15	21.4	0.100	0.214	Liquid N_2
120.30	45.32	21.6	0.126	0.171	Temp.
60.73	60.48	21.7	0.173	0.125	
31.20	71.97	22.2	0.209	0.106	
0.00	89.77	22.0	0.265	0.083	

ΔV ml	$\cap \times 10^{-18}$	p^o-p Torr	$\cap(p^o-p) \times 10^{18}$	$\frac{P}{\cap(p^o-p)\times 10^{18}}$	$\frac{P}{Po}$
62	0.773	2.390	1.847	0.054	0.040
53	0.833	2.364	1.969	0.064	0.051
43	0.927	2.317	2.148	0.080	0.069
39	1.016	2.881	2.317	0.090	0.084
34	1.123	2.225	2.499	0.106	0.106

Figure 3·3

Volume vs ($T/P \times 10^{-3}$)

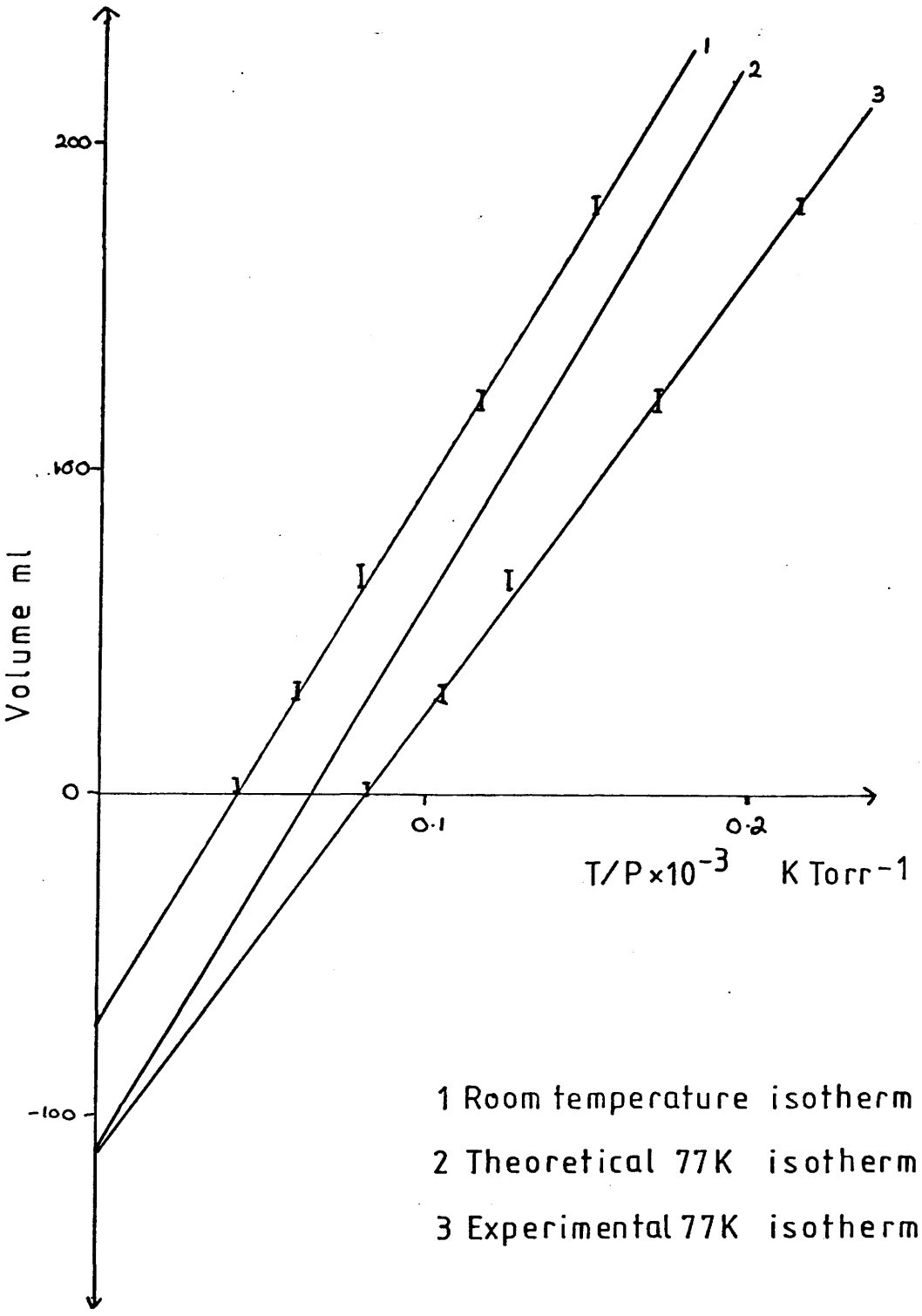

1 Room temperature isotherm

2 Theoretical 77K isotherm

3 Experimental 77K isotherm

Figure 3·4

$P/x(P^{\circ}-P)$ vs P/P°

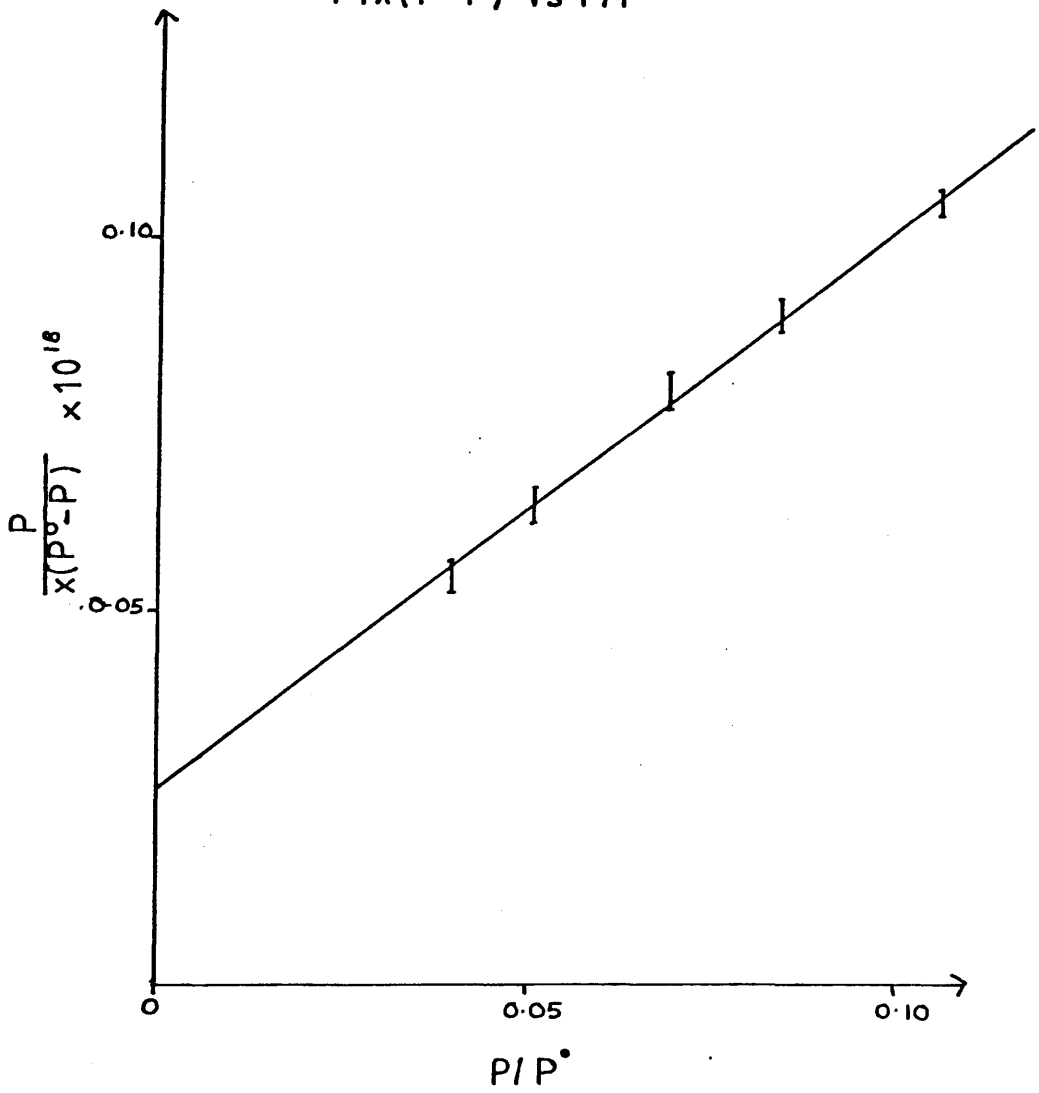

$$\text{Intercept} = 0.0262 \times 10^{-18}$$

$$\frac{1}{NmC} = 0.0262 \times 10^{-18}$$

$$Nm = 1 \Big/ \frac{C-1}{NmC} + \frac{1}{NmC}$$

$$Nm = 1.307 \times 10^{18}$$

$$\text{The surface area} = \frac{Nm \times \text{molecular area of Kr}}{\text{sample weight}}$$

$$= \frac{1.307 \times 10^{18} \times 19.5 \times 10^{-20}}{0.0908}$$

$$= 2.808 \quad m^2 g^{-1}$$

3.2 RESULTS

3.2.1 THE $(CF_3)_2CO$ ACTIVATION PROCESS

The infra red spectrum of $Cs(OCF(CF_3)_2)$ consists of ten bands (Table 3.1). The band at 1450 cm^{-1} is assigned to the CO stretching mode by analogy with the frequencies in the ions CO_3^{2-} (1410 - 1450 cm^{-1}), $HCOO^-$ and CH_3COO^- (near 1570 cm^{-1}) and CF_3COO^- (1700 cm^{-1})[84]. Comparison of this frequency with the CO stretching frequency in $(CF_3)_2CO$ (table 3.2) shows a shift of approximately four hundred wave numbers, consistent with a change from a CO double bond to a CO single bond. This suggests that the

reaction of hexafluoroacetone with caesium fluoride results in the formation of an ionic product, not just a simple adduct.

The infra red spectrum of the heptafluoroisopropoxide after heating under vacuum at 125^{o}C for 16 hours shows the same ten bands as those listed in table 3.1, indicating that complete decomposition does not occur as was previously thought.[84] In an effort to quantify the amount of the anion remaining, fluorine and carbon analyses were carried out on a sample of the heptafluoroisopropoxide after heating. The results of these analyses are given below:

$Cs(OCF\ (CF_3)_2)$ requires C 11.32%, F 41.82%

Found after heating C 0.29%, F 12.44%

Mole ratio of carbon : fluorine before heating = 1:2.33

Mole ratio of carbon : fluorine after heating = 1:27

The results of the analyses after heating correspond to a solid comprising approximately 99.5% CsF and 0.5% $Cs(OCF\ (CF_3)_2)$. Thus all references in this work to activated caesium fluoride actually refer to a solid of this composition.

3.2.2 PREPARATION AND DECOMPOSITION OF $CsOCF_3$

The preparation of caesium trifluormethoxide by reaction of carbonyl fluoride with caesium fluoride in acetonitrile was first reported in 1965 by M E Redwood and C J Willis.[27] The $CsOCF_3$ formed was reported to be crystalline and stable with respect to decomposition at room temperature. Its rate of decomposition at 80^oC was reported to be very slow with less than 10% decomposition after 80 minutes. It has since been discovered that Cs OCF_3 can be completely decomposed by heating under vacuum at 120^oC for three hours.[89] The caesium fluoride which remained after reaction was similar in appearance to that obtained after treatment with hexafluoroacetone and had a similar B.E.T. surface area.

When $Cs(OCF(CF_3)_2)$ is decomposed a small amount of the heptafluoroisopropoxide anion is retained. There is no evidence for the retention of any of the trifluoromethoxide anion when Cs OCF_3 is decomposed. With this in mind a sample of caesium fluoride was pretreated by formation and subsequent decomposition of Cs OCF_3, and its reactions with ^{18}F labelled BF_3 were studied. The results obtained from these experiments were compared to those obtained from hexafluoroacetone pretreated caesium fluoride in an attempt to determine whether or not the small amount

of retained $^{-}OCF(CF_3)_2$ anion has any effect on the reactions (See Chapter 4 section 4.2.5).

The CF_3O^- anion has C_{3v} symmetry and has therefore six vibrational modes, 3 A_1 and 3E, all of which are infra red active. Assignment of all six modes has been accomplished by comparison with the vibrational spectrum of the isoelectronic ONF_3[28]. The infra red spectrum of the trifluoromethoxide prepared in section 3.1.2 contained ten brands. The IR spectrum of Cs OCF_3 prepared by Redwood and Willis[84] also showed more bands than expected for a simple CF_3O^- anion of C_{3v} symmetry. These extra bands are due to hydrolysis products, as Cs OCF_3 is readily hydrolysed to give HF, Cs HF_2 and H_2CO_3. The band at 1230 cm^{-1} corresponds to the ν_2 mode of HF_2^-. The bands at 1825 and 2000 cm^{-1} correspond to the combination modes $\nu_2 + \nu_1$ and $\nu_3 + \nu_1$ of HF_2^-[86]. The band at 1455 corresponds to the ν_3 mode of the CO_3^{2-} anion.[87]

After decomposition by heating under vacuum for 3 hours at 120°C the infra red spectrum contained no bands which could be assigned to the OCF_3^- anion.

3.2.3 SURFACE AREA DETERMINATION OF CAESIUM FLUORIDE

When a gas is allowed to come into contact with the surface of a solid, the gas may be adsorbed by the

surface depending upon the experimental conditions. This adsorption is either chemical or physical in nature depending on the type of bond formed between the gas molecules, the adsorbate, and the solid surface, the adsorbent. Chemical adsorption involves the formation of chemical bonds between the adsorbate and the adsorbent. In consequence chemical adsorption is limited to the formation of a monolayer at the surface, and is limited to certain solid/gas systems, for example, hydrogen and transition metals.[90] In contrast physical adsorption can, in principle occur between all gases and all solids provided the temperature is not considerably in excess of the boiling point of the adsorbate. Unlike chemical adsorption, in the physically adsorbed state, no chemical bonds are formed between the adsorbate and the adsorbent; forces similar to those responsible for the cohesive properties of liquids, for example van der Waals' forces are involved. Because of this, physical adsorption is not restricted to a monomolecular layer, multi layers may be built up on the surface.

The extent of coverage of the surface by the adsorbate is related to the pressure of the adsorbate gas. To determine the surface area of a sample it is necessary to determine when the adsorbed monolayer is complete.

The first important treatment of adsorption was developed by Langmuir.[91] In his model, the surface of the solid was regarded as an array of adsorption sites. A state of dynamic equilibrium was postulated in which the rate at which molecules arriving from the gas phase and condensing on to bare sites is equal to the rate at which molecules evaporate from occupied sites.

The rate at which the gaseous species is adsorbed is proportional to the number of molecules colliding with the solid surface, which in turn is proportional to the partial pressure p_a, at a fixed temperature. The adsorption rate must also be proportional to the number of empty sites, assuming that the surface is energetically uniform. If the fraction of the sites covered is θ, then R_a, the rate of adsorption per unit surface area may be written as:

$$R_a = K_a p_a (1 - \theta) \qquad \text{Equation 3.4}$$

where K_a is the rate constant for adsorption.
R_a the rate of desorption of the adsorbed species, is proportional to the amount of adsorbate on the surface.

Thus

$$R_d = K_d \theta \qquad \text{Equation 3.5}$$

where K_d is the rate constant for desorption.

At equilibrium, the rates of adsorption and desorption are equal and the extent of coverage at equilibrium, θe, may be obtained by equating Ra and Rd to give:

$$\theta e = Kp_a / (1 + Kp_a), \qquad \text{Equation 3.6}$$

$$\text{where } K = \frac{ka}{kd}$$

Equation 3.6 is known as the Langmuir adsorption isotherm. In deriving this equation Langmuir assumed that adsorption was restricted to a monolayer.

The major difficulty to be overcome with physical adsorption is that, because of the close similarity with the liquefaction of gases, adsorbed monolayers are not complete before further adsorbed layers begin to form on top of the first layer.

By introducing a number of simplifying assumptions Brunauer, Emmett and Teller[92] extended the Langmuir theory to cover multilayer physical adsorption. When extended to the second layer, the Langmuir mechanism requires that the rate of condensation of molecules from the gas phase onto molecules already adsorbed in the first layer, shall be equal to the rate of evaporation from the second layer, that is

$$a_2 p\, s_1 = b_2 s_2 e^{-E_2/RT} \qquad \text{Equation 3.7}$$

and for the ith layer

$$a_i p s_{i-1} = b_i s_i e^{-E_i/RT} \qquad \text{Equation 3.8}$$

where si is the surface area covered by i layers of adsorbed molecules.

p is the pressure

E_i is the heat of adsorption of the ith layer

a_i, b_i are constants

The total surface area of the solid is given by

$$A = \sum_{i=o}^{\infty} si \qquad \text{Equation 3.9}$$

and the total volume adsorbed is

$$v = vo \sum_{i=o}^{\infty} is_i \qquad \text{Equation 3.10}$$

where vo is the volume of gas adsorbed on one square centimetre of the adsorbent surface when it is covered with a complete unimolecular layer of adsorbed gas.

It follows that:

$$\frac{V}{Avo} = \frac{V}{Vm} = \frac{\sum_{i=o}^{\infty} is_i}{\sum_{i=o}^{\infty} si} \qquad \text{Equation 3.11}$$

where Vm is the volume of gas adsorbed when the entire adsorbent surface is covered with a complete unimolecular layer.

The summation indicated in equation 3.11 can be carried out by making the simplifying assumptions that the evaporation-condensation properties of the molecules in the second and higher adsorbed layers are the same as those of the liquid state. This allows s_1, s_2 .... s_i to be expressed in terms of s_o.

$$s_1 = Ys_o, \text{ where } Y = (a_1/b_1)pe^{E_i/RT} \qquad \text{Equation 3.12}$$

$$s_2 = Xs_1, \text{ where } X = p/(g)e^{E/RT} \qquad \text{Equation 3.13}$$

$$S_3 = XS_2 = X^2S_1$$

$$s_i = xs_i = x^{i-1}s_1 = yx^{i-1}so = cx^{i}so \qquad \text{Equation 3.14}$$

$$\text{where } c = \frac{y}{x} = \frac{a_1 g}{b_i} e^{E_1 - E_L/RT}$$

$$g = \frac{b_i}{a_i}$$

E_L = heat of liquefaction

Substituting into equation 3.11 gives:

$$\frac{v}{Vm} = \frac{cso \sum_{i=1}^{\infty} ix^i}{so\left(1 + c\sum_{i=1}^{\infty} x^i\right)} \qquad \text{Equation 3.15}$$

The summation represented in the denominator is the sum of an infinite geometric progression.

$$\sum_{i=1}^{\infty} x^i = \frac{x}{1-x} \qquad \text{Equation 3.16}$$

The summation in the denominator can be treated similarly:

$$\sum_{i=1}^{\infty} ix^i = X\frac{d}{dx}\sum_{i=1}^{\infty} x^i = \frac{x}{(1-x)^2} \qquad \text{Equation 3.17}$$

It follows therefore that:

$$\frac{V}{Vm} = \frac{cx}{(1-x)(1-x+cx)} \qquad \text{Equation 3.18}$$

At the saturation pressure of the gas, Po, an infinite number of layers can build up on the adsorbent. To make $v = \infty$, when $p = p_o$, x must be equal to unity. Thus from equation 3.13

$$(Po/g)e^{E_L/RT} = 1 \quad \text{and} \quad x = P/P_o$$

Substituting into equation 3.18 gives the isotherm equation 3.19

$$v = \frac{Vm\ cP}{(Po-P)\ (1 + (c-1)(P/Po))} \qquad \text{Equation 3.19}$$

Equation 3.19 is the form of the B.E.T. equation used throughout this work.

The surface areas of the caesium fluoride samples were determined using the radio-isotope ^{85}Kr as adsorbate. The advantage of using a radioactive gas is that small changes in pressure can be determined relatively rapidly and with a high precision.

Three different types of caesium fluoride were examined:

Type 1 CsF (B.D.H. Optran Grade) ground in an agate mortar and pestle in an inert atmosphere box

Type 2 CsF (B.D.H. Optran Grade) pretreated by reaction with $(CF_3)_2CO$ as described in section

Type 3 CsF (B.D.H. Optran Grade) pretreated by reaction with F_2CO as described in section

Five surface area determinations were carried out on both hexafluoroacetone activated CsF and non activated CsF. Typical surface areas obtained were 0.25 $m^2 g^{-1}$ for non activated CsF and 2.55 $m^2 g^{-1}$ for activated CsF.

In these calculations the major source of error is graphical. If the error on each separate graph is calculated and the errors combined using the standard method for combination of errors, the error on the surface area determination of activated CsF is $\pm$ 0.51 $m^2 g^{-1}$.

A more satisfactory method than this is to carry out a number of surface area determinations and obtain the error limits by statistical analysis, Table 3.5 lists the results of five determinations on activated

CsF. The mean value of these five results is 2.547. The standard deviation is 0.360. Hence by this method the surface area of activated CsF is $2.55 \pm 0.36\ m^2 g^{-1}$. The disadvantage of this type of error calculation is that with such a small number of data points it cannot be assumed that the true value of the surface area agrees exactly with the mean of the results obtained, since further determinations would result in a different mean value. It is better therefore to determine an interval within which it is highly probable that the true value lies. This interval is called the reliability interval and the probability selected is called the reliability coefficient. The reliability interval L is given by equation 3.20.

$$L_{1,2} = \bar{X} \pm Kn\ R \qquad \text{Equation 3.20}$$

where L_1 = the lower limit of the reliability interval

L_2 = the upper limit of the reliability interval

$\bar{X}$ = the mean value

Kn = the reliability coefficient[93]

R = the range of the results

For the given five results the reliability interval in which the true result lies with a probability of 95% is:

$$2.55 \pm (0.51 \times 0.91)$$

$$= 2.55 \pm 0.46$$

TABLE 3.5

SURFACE AREA OF HEXAFLUOROACETONE ACTIVATED CsF

Sample Number	Surface Area $m^2 g^{-1}$
1	2.076
2	2.355
3	2.807
4	2.986
5	2.511

TABLE 3.6

SURFACE AREA OF NON ACTIVATED CsF

Sample Number	Surface Area $m^2 g^{-1}$
1	0.310
2	0.249
3	0.272
4	0.224
5	0.192

Therefore it is 95% certain that the true value of the surface area of activated caesium fluoride lies in the range 3.01 - 2.09 m^2g^{-1}.

Table 3.6 lists the results of five surface area determinations on non activated caesium fluoride. By applying equation 3.20 to these results, the reliability interval in which the true result lies with a probability of 95% is 0.31 - 0.19m^2g^{-1}.

Table 3.7 shows the results of three surface area determinations on caesium fluoride activated by formation and decomposition of $CsOCF_3$. For these three results the reliability interval in which the true result lies with a probability of 95% is 2.27 - 1.77m^2g^{-1}. The results of the surface area determinations on the three different types of CsF are summarised in table 3.8.

In an effort to reduce the error on each individual determination, the calculations were done using a programme written for the BBC microcomputer which employs linear regression analysis to obtain the line of best fit for each set of data. (Programme 1 in appendix)

TABLE 3.7

SURFACE AREA OF CsF ACTIVATED BY REACTION WITH F_2CO

Sample Number	Surface Area $m^2 g^{-1}$
1	1.910
2	2.051
3	2.101

TABLE 3.8

SUMMARY OF SURFACE AREA RESULTS

Type of CsF	Surface Area $m^2 g^{-1}$
$(CF_3)_2CO$ activated CsF	3.01 - 2.09
F_2CO activated CsF	2.27 - 1.77
Non activated CsF	0.31 - 0.19

3.3 DISCUSSION

The surface areas of hexafluoroacetone activated caesium fluoride and non activated caesium fluoride have previously been determined by Kolta and coworkers[83] using the apparatus described in section 3.1.4. The results obtained were much lower than those obtained in the present work. The values quoted are $0.04 m^2 g^{-1}$ for non activated CsF and $0.41 m^2 g^{-1}$ for hexafluoroacetone activated CsF.

This difference occurs because Kolta and coworkers used the vapour pressure of solid krypton in their calculations (P^o = 0.62 Torr at 77K) but if the solid is taken as the reference state the adsorption isotherm shows an unusually sharp upturn at the high pressure end. The usual practice, following Beebe,[94] is therefore to take P^o as the saturation vapour pressure of the supercooled liquid. (P^o = 2.49 Torr at 77K). All B.E.T. surface area calculations in this work are based on the saturation vapour pressure of the supercooled liquid.

Pretreatment of caesium fluoride with hexafluoroacetone in acetonitrile produces marked changes in both the appearance of the CsF and in its physical properties. The pretreatment process results in a ten fold increase in surface area and produces an off white, finely divided solid which resembles talc.

The increase in surface area is too large to be due simply to a reduction in the CsF particle size. The two most likely explanations for this large increase in surface area are:

1. Disruption of the crystal structure by $(CF_3)_2CO$

2. Formation of a porous structure

CsF reacts with $(CF_3)_2CO$ to produce $Cs^+ (OCF(CF_3)_2)^-$ as an ionic solid. Infra red examination of this product confirms that there is no free $(CF_3)_2CO$ present, it is all converted to $OCF(CF_3)_2^-$. To accommodate the large heptafluoroisopropoxide anion, the crystal lattice must undergo some form of expansion. After $Cs(OCF(CF_3)_2)$ has been heated under vacuum, examination of the solid by infra red spectroscopy has shown that some $OCF(CF_3)_2^-$ is retained. Although the solid contains only 0.5% $CsOCF(CF_3)_2$ after heating this must prevent the CsF from returning to its original crystal structure, hence the surface area must increase.

When CsF reacts with F_2CO in acetonitrile $CsOCF_3$ is formed. When the trifluoromethoxide is heated under vacuum the solid is completely decomposed to leave only CsF. The surface area of this CsF is $1.91 m^2 g^{-1}$ compared to $2.55 m^2 g^{-1}$ for hexafluoroacetone activated CsF. This shows that the retained DCF $(CF_3)_2^-$ can only have a minor effect on the surface area of the CsF since treatment with F_2CO produces a similar effect with no trifluoromethoxide retained to affect the crystal structure.

Thermal decomposition reactions of the type shown below

Solid A → Solid B + gas

are known to produce porous solids. For example the production of lime by calcination of limestone[94] or chalk where the loss of a volatile component leads to the development of a pore system with its associated increased surface area. The decomposition of $CsOCF(CF_3)_2$ is a reaction of this type and it is therefore reasonable to assume that a porous solid is formed.

The pore systems of solids are of many different kinds. The individual pores may vary greatly both in size and in shape within a given solid, and between one solid and another. Pores are usually classified according to their average width as proposed by Dubinin.[95] This classification is summarised in table 3.9.

In a micropore the interaction energy of the solid with a gas molecule is significantly higher than in a wider pore, owing to the proximity of the walls and the overlap of their potential fields. The amount adsorbed at a given relative pressure is correspondingly enhanced. If micropores are present in a sample the specific surface area derived by the B.E.T. procedure will be erroneously high.[96]

This problem is encountered with hexafluoroacetone activated potassium fluoride. With activated KF it is impossible to obtain reproducible results from sample to sample.[97]

TABLE 3.9

CLASSIFICATION OF PORES ACCORDING TO THEIR WIDTH

Pore Type	Width
Micropores	Less than 20 A^{o}
Mesopores	Between 20 and 500 A^{o}
Macropores	Greater than 500 A^{o}

The average value obtained is much greater than that obtained for caesium fluoride, 21.08 - 9.31m^2g^{-1} compared to 3.01 - 2.09m^2g^{-1}.

In order to calculate the B.E.T. surface area it is necessary to plot three adsorption isotherms, one at room temperature, one at 77K and a theoretical 77K isotherm which should be parallel to the room temperature line and intercept the y axis at the volume equal to the dead space of the system when the sample bulb is immersed in liquid N_2. For normal B.E.T. behaviour the intercepts of the theoretical isotherm and that determined at 77K should be the same. The experimentally determined 77K isotherms of activated KF intercept the y axis at points much greater than the volume of the dead space of the system. This suggests that an initial uptake of gas has taken place at low relative pressure which is consistent with capillary condensation in a microporous solid. Hexafluoroacetone pretreatment of potassium fluoride must therefore produce a solid which is almost wholly microporous whereas the same treatment of caesium fluoride produces a solid composed of larger pores.

ooOoo

CHAPTER FOUR

CHAPTER 4

REACTIONS OF GASEOUS LEWIS ACID FLUORIDES WITH CAESIUM FLUORIDE

INTRODUCTION

In order to test the appropriateness of molecular analogies in describing the interactions of gaseous Lewis acids with a solid Lewis base, the reactions between caesium fluoride and AsF_5, BF_3, CO_2, F_2CO and SF_4 were studied. The reactions were studied at room temperature using ^{18}F labelled species, together with ^{14}C and ^{35}S labelled species where appropriate.

4.1 EXPERIMENTAL

^{18}F labelled species were prepared by high temperature exchange with reactor produced $Cs^{18}F$ as described in section 2.10.2. $^{14}CO_2$, $F_2{}^{14}CO$ and $^{35}SF_4$ were prepared as described in sections 2.10.6, 2.10.5, 2.10.4.

The reactions between the ^{18}F labelled gases and caesium fluoride were followed using the types of reaction vessel shown in figure 2.11.

One limb of the vessel was loaded with a weighed amount of CsF (usually 0.50g 3.3m mol) in an inert atmosphere box. The vessel was removed from the box, attached to the vacuum line and evacuated. Using the pressure gauge attached to the main manifold a measured pressure of the labelled gas

(usually 300 Torr, which is equivalent to 1.1m mol of gas in the reaction vessel) was admitted to the reaction vessel. The growth of activity in the solid was followed by counting each limb of the reaction vessel alternately and subtracting the counts obtained from the limb with no CsF from the counts obtained from the limb containing the CsF. Figure 4.1 shows a typical set of results for the reaction between $AsF_4{}^{18}F$ and CsF. Line 1 shows the count rate due to the solid + gas, Line 2 shows the count rate due to the gas and line 3 shows the count rate due to the solid alone. All experimental results were corrected for radioactive decay and background counts using a programme written for the Dragon microcomputer. (Programme number 2 in appendix).

Experiments involving $^{14}CO_2$, $F_2{}^{14}CO$ and $^{35}SF_4$ were carried out in the reaction vessel shown in figure 2.8. Weighed amounts of CsF (usually 0.50g 3.3m mol) were loaded into the sample tube A in an inert atmosphere box. The sample tube was then evacuated and connected to the counting vessel. The counting vessel was pumped out for ten minutes and then isolated from the pump. Bulb B containing a known amount of labelled gas was opened and the pressure allowed to equilibrate. Three counts were taken and the average of these taken as the count rate of the gas before reaction. The gas was recondensed into the storage bulb and the flask containing the CsF opened to allow the CsF to fall into one section of the movable glass boat. The section containing the CsF was placed directly below one of the GM tubes and the labelled gas re-admitted to the counting vessel. Counts were taken at five minute intervals.

Figure 4·1

Reaction of $AsF_4^{18}F$ with CsF.

Solid count rate vs time

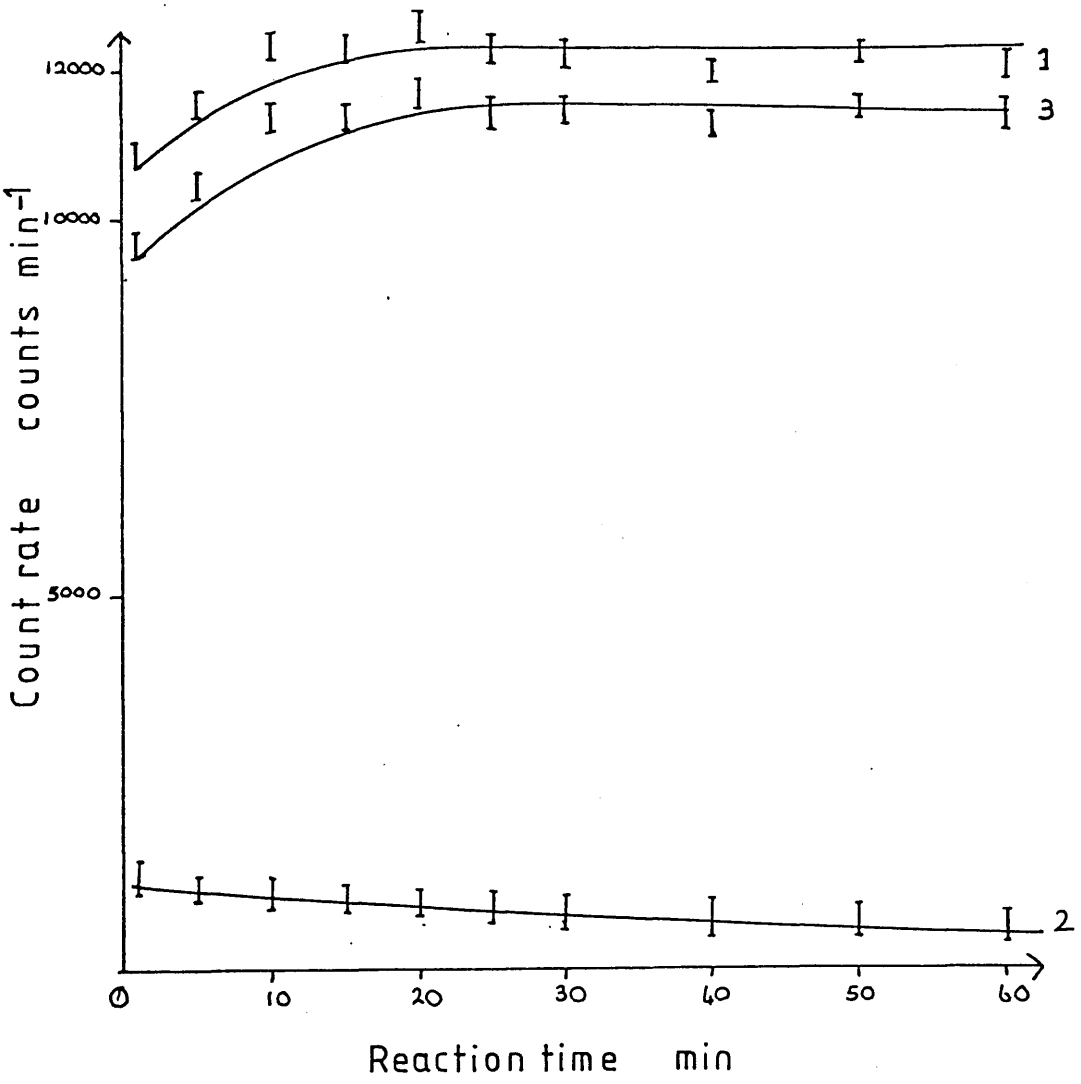

The count rates obtained were corrected for background, the dead time of the GM tubes and their intercalibration factor using a programme written for the BBC microcomputer (Programme number 6 in appendix).

Manometric measurements were carried out using the apparatus described in section 2.1.2. The sample bulb was loaded in an inert atmosphere box and evacuated for 15 minutes before admission of the gas. The gas was first admitted to the system with the sample bulb closed and a pressure measurement taken. The sample bulb was opened allowing the reaction to proceed. The amount of gas uptake was calculated from the total fall in gas pressure after applying a correction to take into account the volume change on opening the sample bulb.

4.2 RESULTS OF REACTION OF SF_4 WITH CsF

The reactions of both activated and non activated CsF with SF_4 have been investigated using both ^{18}F and ^{35}S labelled SF_4 and in the case of activated CsF by conventional manometric means.

The results of three experiments between $SF_3{}^{18}F$ and non activated CsF are summarised in table 4.1. Figure 4.2 shows a plot of solid count rate versus time for one of these experiments. This shows that the solid count rate rises rapidly and then begins to level off until an equilibrium level is reached after 35 minutes. Calculation of the

TABLE 4.1

REACTION OF $SF_3{}^{18}F$ WITH NON ACTIVATED CsF - SUMMARY OF RESULTS

Amount of CsF g m mol	Amount of $SF_3{}^{18}F$ Torr m mol	Specific Count Rate of $SF_3{}^{18}F$ Before Reaction counts min^{-1} m mol^{-1}	Specific Count Rate of $SF_3{}^{18}F$ After Reaction counts min^{-1} m mol^{-1}	Solid Count Rate After Reaction counts min^{-1}	Uptake m mol
0.50 ± 0.01 3.29 ± 0.06	300 ± 2 1.0 ± 65	4217 ± 65	4215 ± 65	181 ± 13	0.043 ± 0.003
"	"	3557 ± 60	3558 ± 60	142 ± 12	0.040 ± 0.0035
"	"	2516 ± 50	2509 ± 50	97 ± 10	0.0385 ± 0.004
"	"	2733 ± 52	2731 ± 52	127 ± 11	0.0465 ± 0.004

Figure 4·2

Reaction of $SF_3^{18}F$ with non-activated CsF

Solid countrate vs reaction time

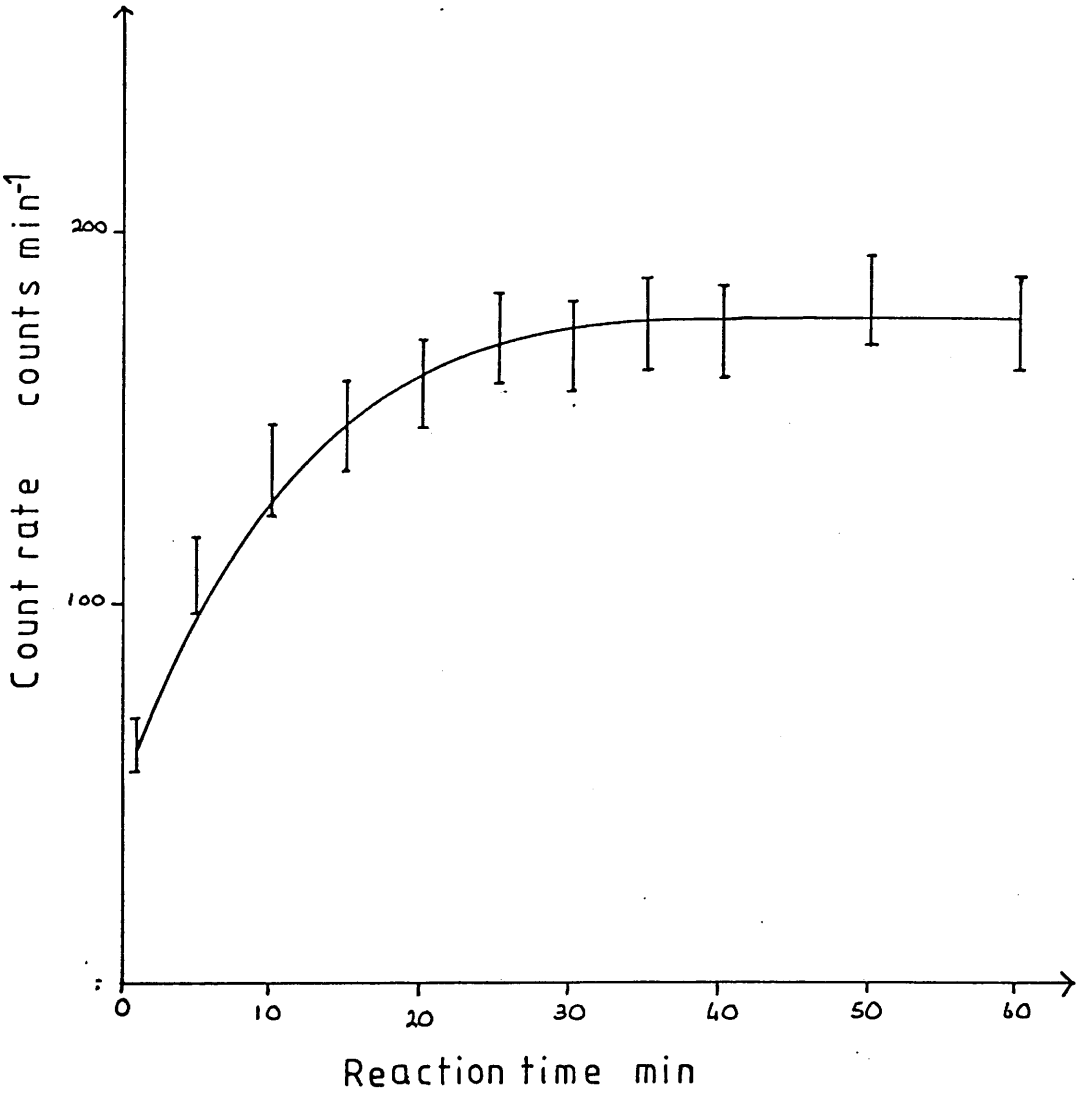

specific count rate before and after reaction shows that there is no change. This means that the activity in the solid is due to uptake of gas and not ^{18}F exchange. A sample of $SF_3{}^{18}F$ counted separately had a specific count rate of 4217 ± 65 counts min^{-1} m mol^{-1} so a solid count rate of 181 ± 13 counts min^{-1} is equivalent to an uptake of 0.043 m mol of $SF_3{}^{18}F$. The average uptake observed in the four experiments was 0.042 ± 0.004 m mol. The observed solid count rate in these experiments was very low. In order to ensure that a significant number of counts were recorded and to reduce the error on the count rate the counting period was extended to fifteen minutes. This procedure was used throughout this work whenever a low count rate was obtained.

Table 4.2 shows the infra red spectrum of the CsF after reaction, together with the infra red spectrum of $CsSF_5$ prepared by Christe and coworkers.[40] Comparison of the two sets of data shows that the reaction between $SF_3{}^{18}F$ and CsF has resulted in the formation of some $CsSF_5$.

In an attempt to distinguish between surface and bulk reactions an experiment was carried out using $^{35}SF_4$. The results from this reaction were inconclusive, with the surface count rate being barely detectable due to the low surface area of non activated CsF. For this reason the study of the reaction between $^{35}SF_4$ and non activated CsF was abandoned and all further experiments with $^{35}SF_4$ were carried out using activated CsF.

TABLE 4.2

INFRA RED SPECTRUM OF CsF AFTER REACTION WITH $SF_3{}^{18}F$

Activated CsF		Non Activated CsF	Literature $CsSF_5$[40]	Assignment
1250				CF str
1210				CF str
1150				CF str
1110				CF str
793	s	790	793s	A_1 ν_1
590	vsbr	590	590 vsbr	E ν_1
			520 wsh	A_1 ν_2
460	s	465	466 s	A_1 ν_3
			430 sh	E ν_8

The results of four reactions between $SF_3{}^{18}F$ and activated CsF are listed in table 4.3. Figure 4.3 shows a plot of solid count rate versus time for the first experiment. The solid count rate rises rapidly at first and then begins to level off until an equilibrium level of 1560 $\pm$ 40 counts min^{-1} is reached after 35 minutes. There is no change in the specific count rate of the gas so this solid count rate is due to gas uptake. A sample of $SF_3{}^{18}F$ counted separately had a specific count rate of 5270 $\pm$ 73 counts min^{-1} m mol^{-1} so the observed solid count rate is equivalent to an uptake of 0.296 $\pm$ 0.006 m mol. The average uptake observed in the four experiments is 0.296 $\pm$ 0.009 m mol. Infra red examination of the CsF after reaction showed bands due to SF_5^-. (Table 4.2)

The experiments listed in table 4.3 were all carried out using an initial pressure of 300 torr of $SF_3{}^{18}F$. The results of a further six experiments carried out using pressures of 50, 75, 100, 150, 200 and 250 Torr are listed in table 4.4.

These experiments show that uptake is independant of initial pressure over the range 100-300 Torr and corresponds to 0.09 $\pm$ 0.02 m mol (m mol CsF)$^{-1}$. In order to verify the results of the reactions involving varying pressures of $SF_3{}^{18}F$, a manometric study was carried out using the constant volume apparatus described in section 2.1.2. The results of this study shown in figure 4.4, confirm that the uptake of

TABLE 4.3

REACTION OF $SF_3{}^{18}F$ WITH ACTIVATED CsF - SUMMARY OF RESULTS

Amount of CsF g m mol	Amount of $SF_3{}^{18}F$ Torr m mol	Specific Count Rate of $SF_3{}^{18}F$ Before Reaction counts min^{-1} m mol^{-1}	Specific Count Rate of $SF_3{}^{18}F$ After Reaction counts min^{-1} m mol^{-1}	Solid Count Rate After Reaction counts min^{-1}	Uptake m mol
0.50 ± 0.01 3.29 ± 0.06	300 ± 2 1.0 ± 0.01	5270 ± 73	5270 ± 73	1560 ± 40	0.30 ± 0.006
"	"	4117 ± 64	4109 ± 64	1276 ± 36	0.31 ± 0.009
"	"	1967 ± 44	1961 ± 44	560 ± 24	0.285 ± 0.01
"	"	2516 ± 50	2514 ± 50	729 ± 27	0.29 ± 0.01

Figure 4·3

Reaction of $SF_3^{18}F$ with activated CsF

Solid count rate vs reaction time

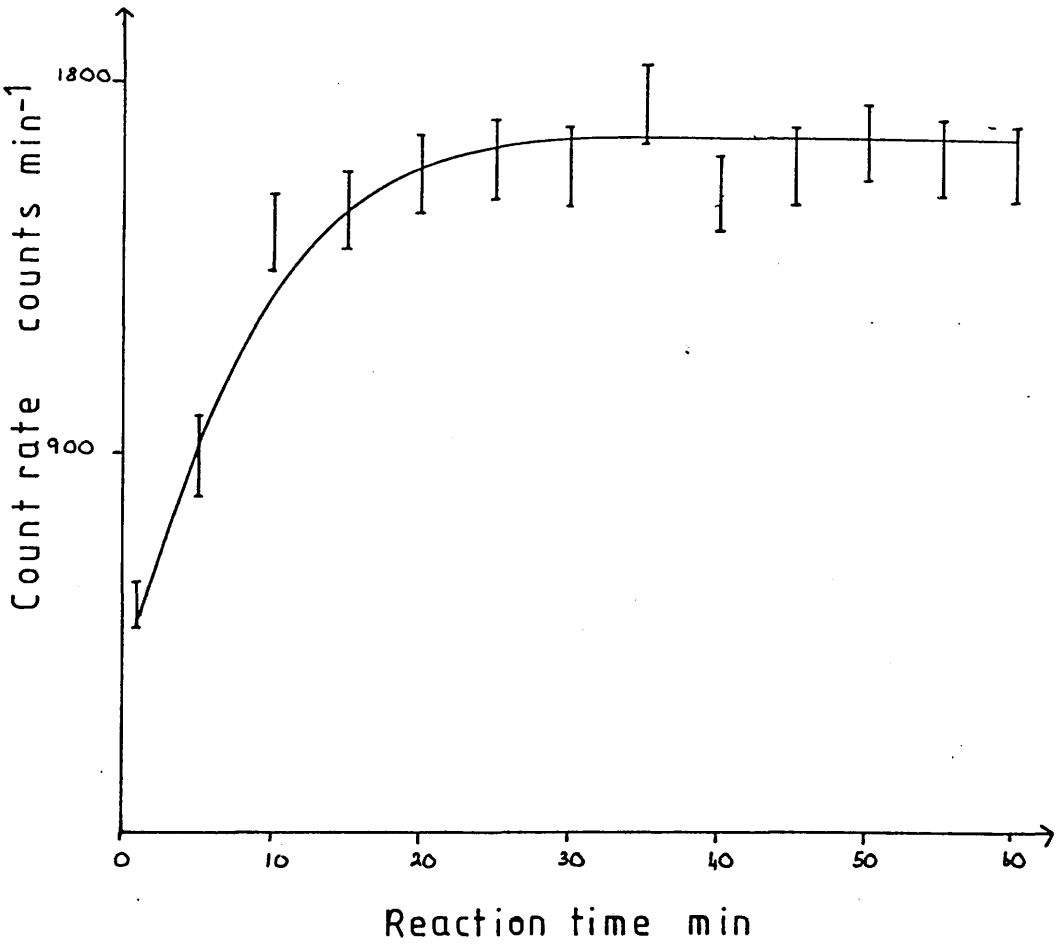

TABLE 4.4

VARIATION IN UPTAKE WITH INITIAL PRESSURE OF SF_4

RADIOCHEMICAL MEASUREMENTS

Pressure of SF_4 Torr	Uptake m mol (m mol CsF)$^{-1}$
50 $\pm$ 2	0.027 $\pm$ 0.003
75 $\pm$ 2	0.065 $\pm$ 0.005
100 $\pm$ 2	0.081 $\pm$ 0.006
150 $\pm$ 2	0.100 $\pm$ 0.007
200 $\pm$ 2	0.085 $\pm$ 0.007
250 $\pm$ 2	0.098 $\pm$ 0.007
300 $\pm$ 2	0.091 $\pm$ 0.007

Figure 4·4

Reaction of SF_4 with activated CsF

Amount adsorbed vs initial pressure

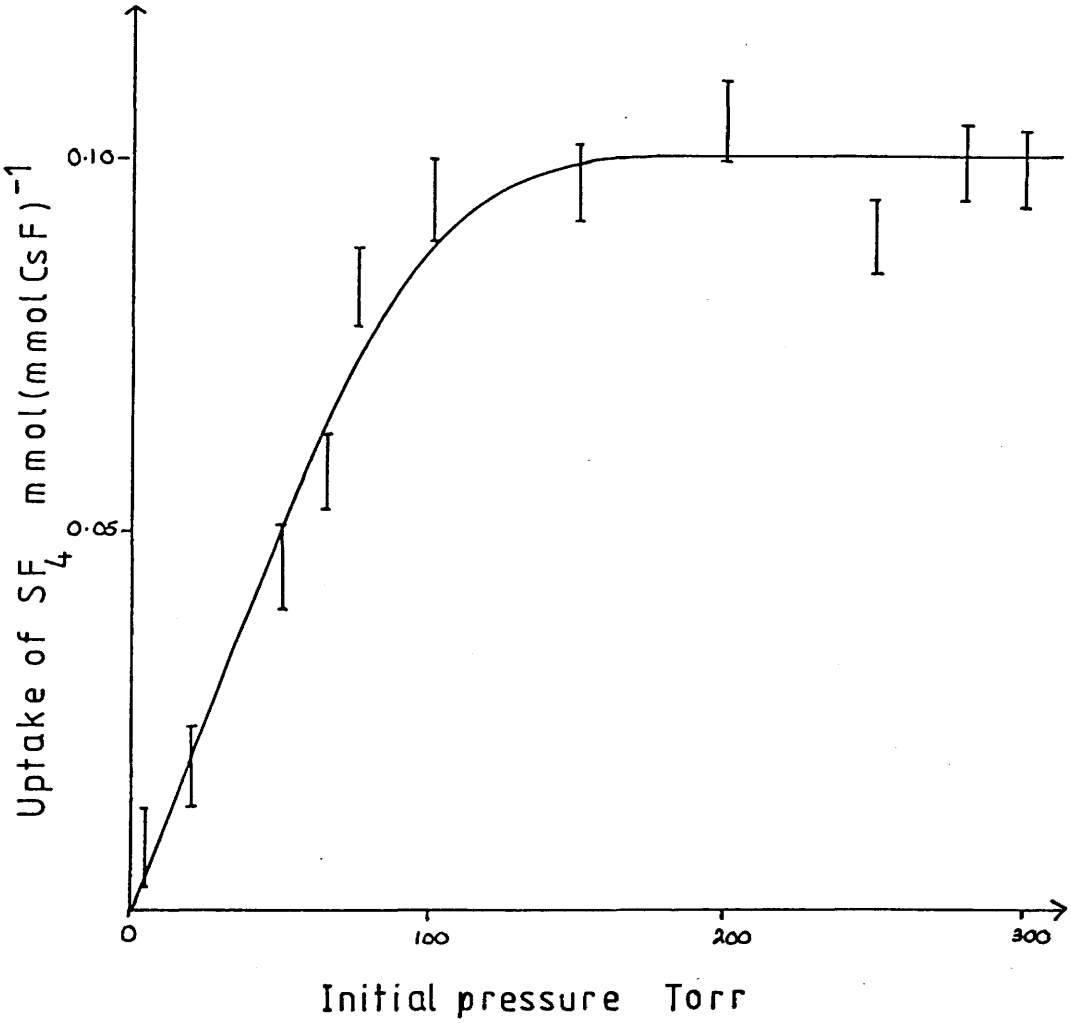

SF_4 by activated CsF is independent of initial pressure over the range 100-300 Torr. Infra red spectroscopic examination of the solid after reaction is consistent with the formation of $CsSF_5$. (Table 4.2)

The reaction between $^{35}SF_4$ and activated CsF was studied at 23 different pressures between 2 and 308 Torr. Figures 4.5, 4.6 and 4.7 are plots of solid count rate versus time at initial pressures of 52, 110 and 296 Torr. The solid count rate increases rapidly until an equilibrium level corresponding to a surface uptake of 0.010 m mol (m mol CsF)$^{-1}$ is reached after 10 minutes. A plot of the amount of $^{35}SF_4$ adsorbed on the surface of the CsF versus initial pressure (figure 4.8), shows that the amount of surface coverage is independant of the initial pressure at all pressures greater than 10 Torr. When the $^{35}SF_4$ is removed from the counting vessel 85% of the total surface counts are also removed. This means that the major surface species is weakly adsorbed with only 15% of the total surface count rate due to a permanently adsorbed species. Infra red examination of CsF after reaction with $SF_3{}^{18}F$ shows that some $CsSF_5$ is formed hence it is reasonable to assume that the permanently adsorbed surface species is the SF_5^- anion. If the permanently adsorbed species is assumed to be SF_5^-, the weakly adsorbed species is most likely to be adsorbed molecules of SF_4.

When $^{35}SF_4$ is readmitted to the counting vessel the observed solid count rate is 90% of the count rate observed during the

Figure 4·5

Reaction of $^{35}SF_4$ with activated CsF

Surface count rate vs reaction time

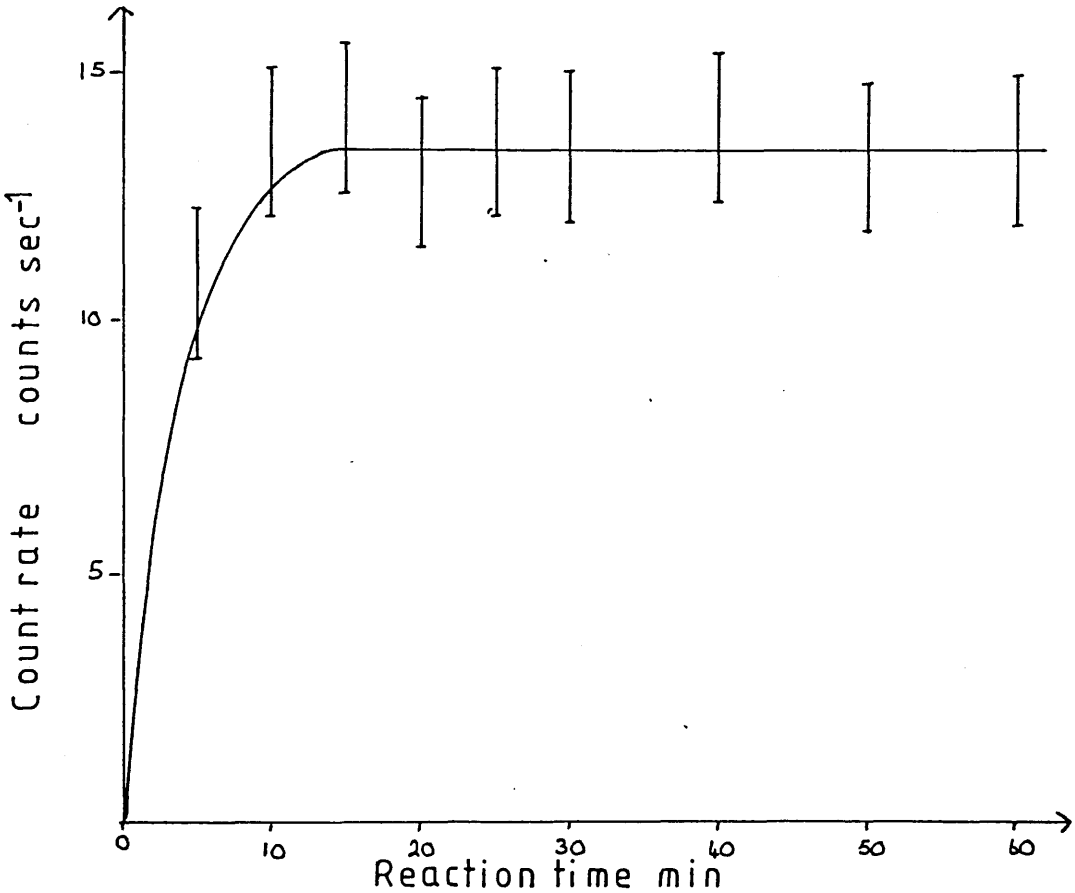

Initial pressure =52 Torr

Specific count rate of $^{35}SF_4$ =1450 counts sec^{-1} $mmol^{-1}$

Figure 4·6

Reaction of $^{35}SF_4$ with activated CsF

Surface count rate vs reaction time

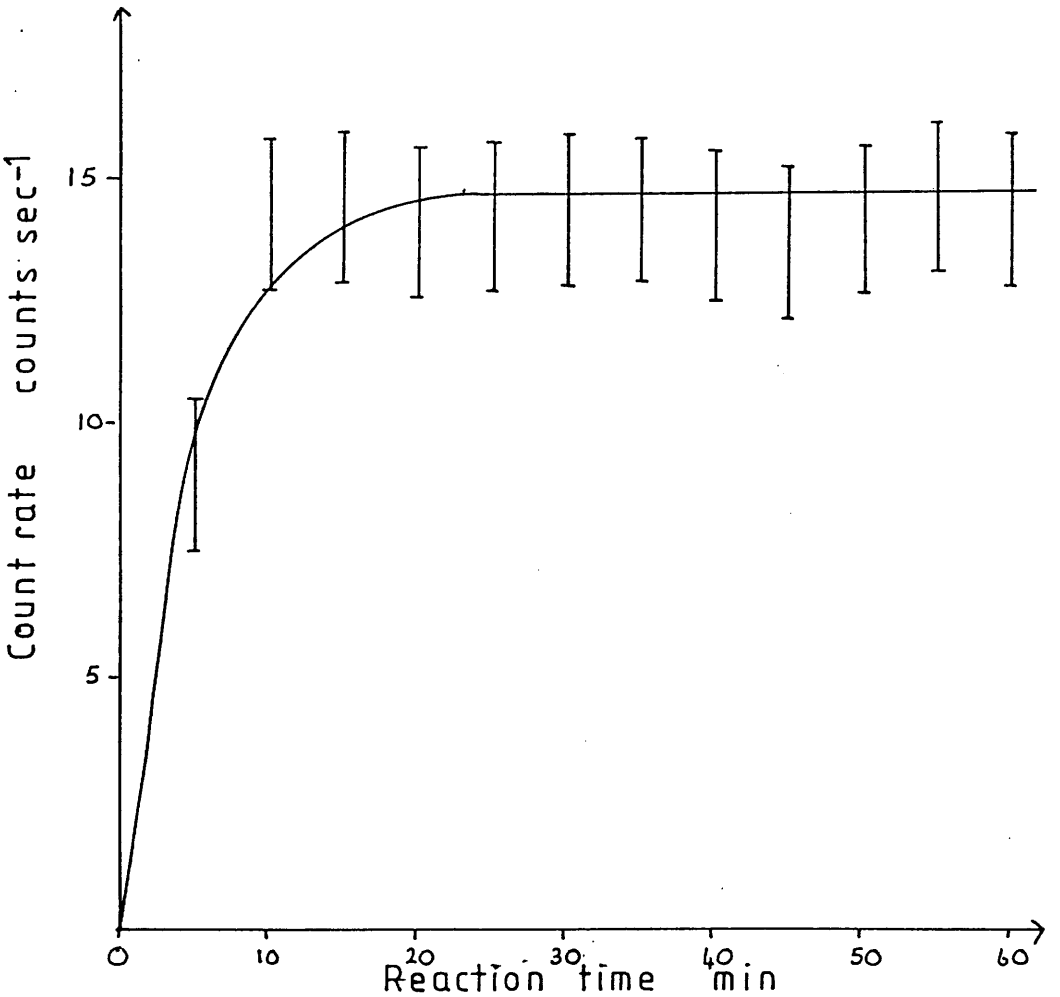

Initial pressure = 110 Torr

Specific count rate of $^{35}SF_4$ = 1450 counts sec^{-1} $m\,mol^{-1}$

Figure 4·7

Reaction of $^{35}SF_4$ with activated CsF

Surface count rate vs reaction time

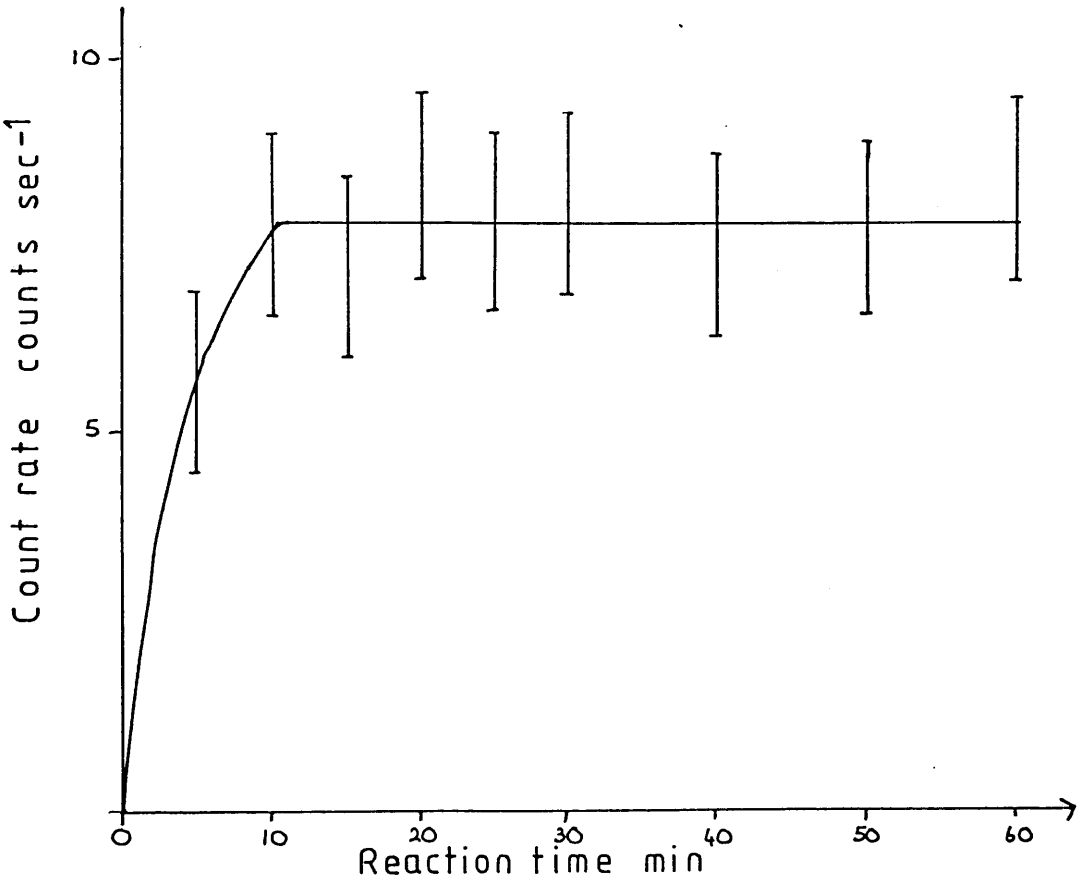

Initial pressure = 296 Torr

Specific count rate of $S^{35}F_4$ = 853 counts $sec^{-1} mmol^{-1}$

Figure 4·8 Reaction of $^{35}SF_4$ with activated CsF

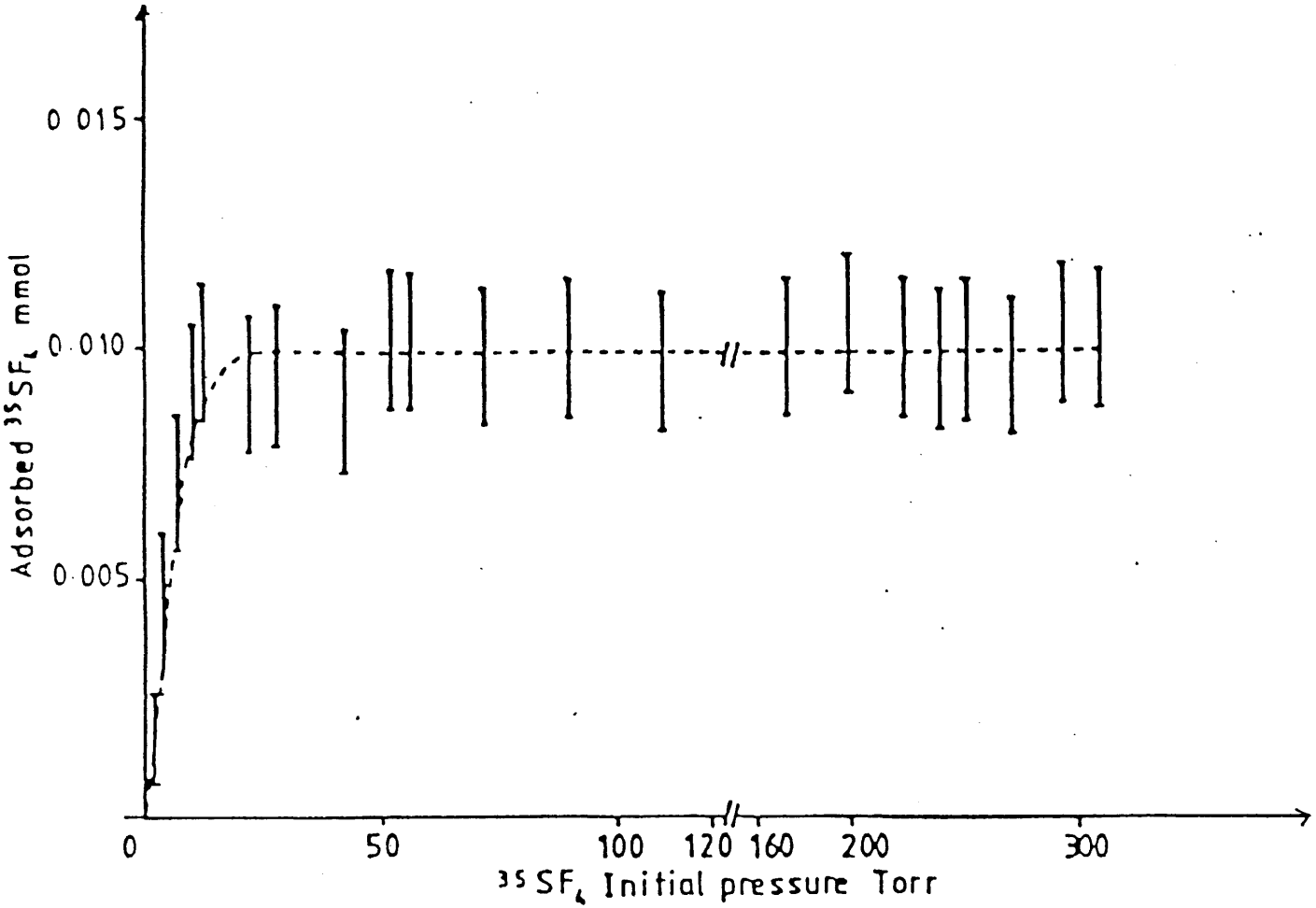

Amount of $^{35}SF_4$ adsorbed on surface of CsF vs initial pressure

first admission. The fall in gas phase counts is equivalent to 20% of the decrease observed during the first admission. After two further admissions of $^{35}SF_4$ no further fall in gas phase counts is observed. These results show that there is a slow build up of SF_5^- on the surface of the CsF and that diffusion of SF_4 into the bulk of the solid is very slow.

The overall uptake of $^{35}SF_4$, calculated from the fall in gas phase counts is 0.10 ± 0.02 m mol (m mol CsF)$^{-1}$ which is the same as that calculated from the experiments involving $SF_3{}^{18}F$. The results of the reactions between SF_4 and activated CsF are summarised in table 4.5.

4.3 DISCUSSION OF SF_4 RESULTS

SF_4 reacts readily at room temperature with both activated and non activated CsF to form $CsSF_5$. Complete reaction does not occur with the amounts reacting being 0.10 m mol (m mol CsF)$^{-1}$ for activated CsF and 0.013 m mol (m mol CsF)$^{-1}$ for non activated. The ratio of uptakes is 10:1, the same as the ratio of the surface areas.

No fluorine exchange is observed in either reaction.

Due to the low level of uptake by non activated CsF $^{35}SF_4$ did not provide any useful information. With activated CsF, studies using $^{35}SF_4$ showed that there are two distinct

TABLE 4.5

SF_4 + ACTIVATED CsF SUMMARY OF RESULTS

	Uptake m mol (m mol CsF)$^{-1}$
Overall uptake calculated from both ^{35}S and ^{18}F experiments	0.10 ± 0.02
Surface uptake	0.0030 ± 0.0005
Amount permanently retained on surface	0.00045 ± 0.0001

No fluorine exchange is observed at room temperature

species present on the surface of the solid one which is weakly adsorbed and one which is permanently adsorbed. The major surface species is weakly adsorbed SF_4 with only 15% of the total surface activity due to permanently adsorbed SF_4. Since infra red studies have shown that SF_5^- is the major bulk species the permanently adsorbed surface species is also assumed to be SF_5^-.

Since the specific count rate of the adsorbed $^{35}SF_4$ and the surface area of the CsF are known it is possible to estimate the number of F^- ions present in the sample, and to compare this with the number of $^{35}SF_4$ molecules adsorbed. This can be done as follows:

BET surface area of activated CsF = 3.011 - 2.09 $m^2 g^{-1}$

Weight of sample = 0.50g

Surface area of sample = 1.505 - 1.040 m^2

Length of unit cell edge = 6.008$\mathring{A}$

Area of one face of unit cell = 36.096$\mathring{A}^2$

Assuming a perfect surface composed of a regular geometric array of unit cell faces:

Number of unit cell faces required to cover surface = (2.88 - 4.17) x 10^{18}

Number of surface F^- ions per unit cell = 2

(Figure 4.9 shows the unit cell of CsF)

Number of surface F^- ions in sample = (5.77 - 8.34) x 10^{18}

Surface count rate corresponds to (5.99 $\pm$ 2.13) x 10^{18} molecules

Although there is good agreement between these two estimates, it does not rule out the possibilities that SF_4 is weakly

Figure 4·9 CsF unit cell

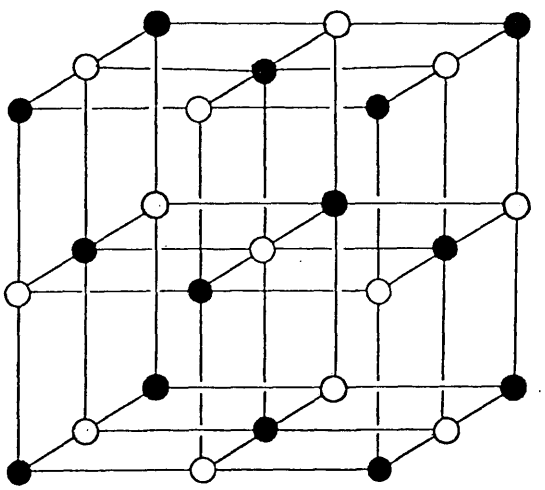

● = F^-

○ = Cs^+

Number of F^- ions per face is $(4 \times 1/4) + 1 = 2$

adsorbed at sites other than F^- or that multiple adsorption occurs since many assumptions have been made in arriving at these estimates. The main assumptions are:

1. The surface of the CsF has no defects and is composed of a regular array of unit cell faces.

2. The unit cell edge length of activated CsF is the same as that of non activated CsF.

3. All of the surface F^- ions in the sample are equally available.

This comparison also does not take into account the small amount of the heptafluoroisopropoxide anion retained by the CsF after activation. When these facts are taken into account the number of F^- ions calculated is probably an over estimate.

Figures 4.10, 4.11 and 4,12 show the species present on the surface of the CsF based on the assumption that adsorption takes place at F^- sites. The structure of the SF_5^- anion is shown in figure 4.10. SF_5^- is assumed to be the permanently adsorbed species. There are two possibilities for the weakly adsorbed species, both of which have similar structures to the SF_5^- anion. Figure 4.11 shows SF_4 adsorbed with the lone pair in an axial position and figure 4.12 shows the lone pair in an equatorial position. Since the structure of the SF_5^- anion has been characterised as

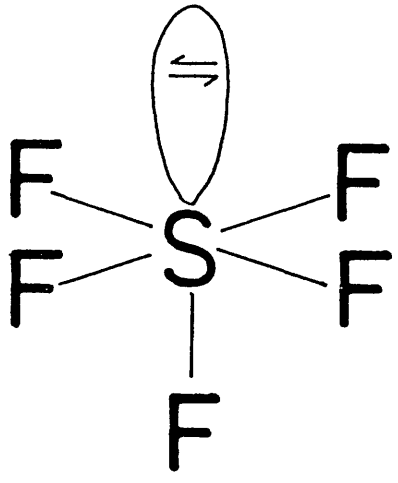

Figure 4·10 SF_5^-

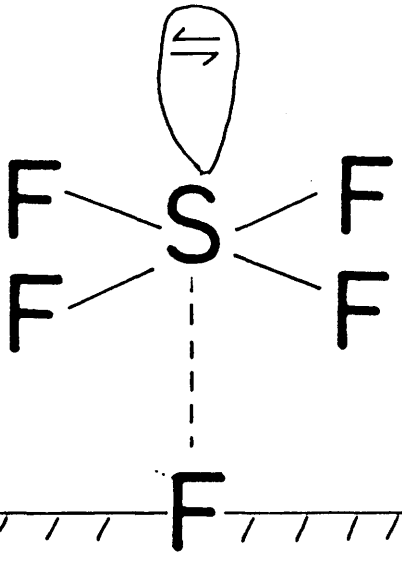

Figure 4·11 SF_4(ads)

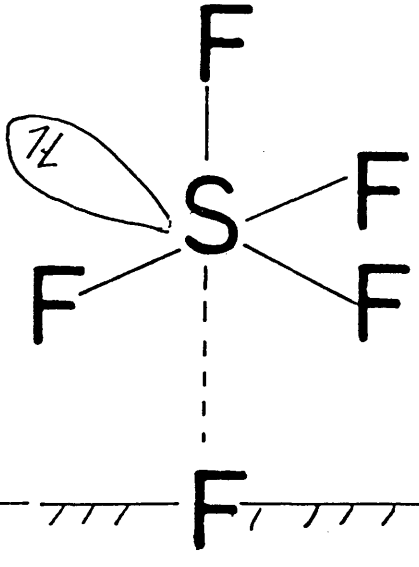

Figure 4·12 SF_4(ads)

being C_{4v}[40] as shown in figure 4.10 the weakly adsorbed species is most likely to have the structure shown in 4.11, with the lone pair in an axial position.

SF_5^- is the major bulk species and the minor surface species. The fact that no fluorine exchange is observed is due to the SF_5^- anion being co-ordinatively saturated. Since SF_5^- is only the minor surface species the absence of ^{18}F exchange also indicates that in the weakly adsorbed state, the S-F bonds of the adsorbed SF_4 retain their integrity. In other words at no time during the reaction do the four S-F bonds of the SF_4 become equivalent to the bond between the S and the F^- ion on the surface.

4.4 RESULTS OF REACTION OF F_2CO WITH ACTIVATED CsF

The reaction between F_2CO and activated CsF was studied using both ^{18}F and ^{14}C labelled F_2CO, which allowed differentiation between surface and bulk reactions, and by manometric methods. After each reaction the CsF was examined by infra red spectroscopy. Three experiments were carried out using $F^{18}FCO$; the results are listed in table 4.6 Figure 4.1.3 is a plot of solid activity versus time for experiment 1. This shows that there is a rapid initial increase in solid activity over the first 30 minutes of the reaction followed by a second period in which the growth of solid activity is much slower. The specific count rate of the $F^{18}FCO$ before reaction was 7139 ± 85 counts min^{-1} m mol^{-1} and the specific count rate of the $F^{18}FCO$ after reaction was 5842 $\pm$ counts min^{-1} m mol^{-1}

TABLE 4.6

REACTION OF $F^{18}FCO$ WITH ACTIVATED CsF - SUMMARY OF RESULTS

Amount of CsF g m mol	Amount of $F^{18}FCO$ Torr m mol	Specific Count Rate of $F^{18}FCO$ Before Reaction counts min^{-1} m mol^{-1}	Specific Count Rate of $F^{18}FCO$ After Reaction counts min^{-1} m mol^{-1}	Fraction Exchanged	Uptake m mol
0.50 ± 0.01 3.29 ± 0.06	300 ± 2 0.944 ± 0.01	7139 ± 85	5927 ± 76	0.344	0.194 ± 0.002
"	"	7139 ± 85	5919 ± 76	0.346	0.201 ± 0.002
"	"	5130 ± 71	4370 ± 66	0.300	0.198 ± 0.002

Average uptake = 0.198 m mol

Figure 4·13

Reaction of ^{18}FFCO with activated CsF

Solid count rate vs reaction time

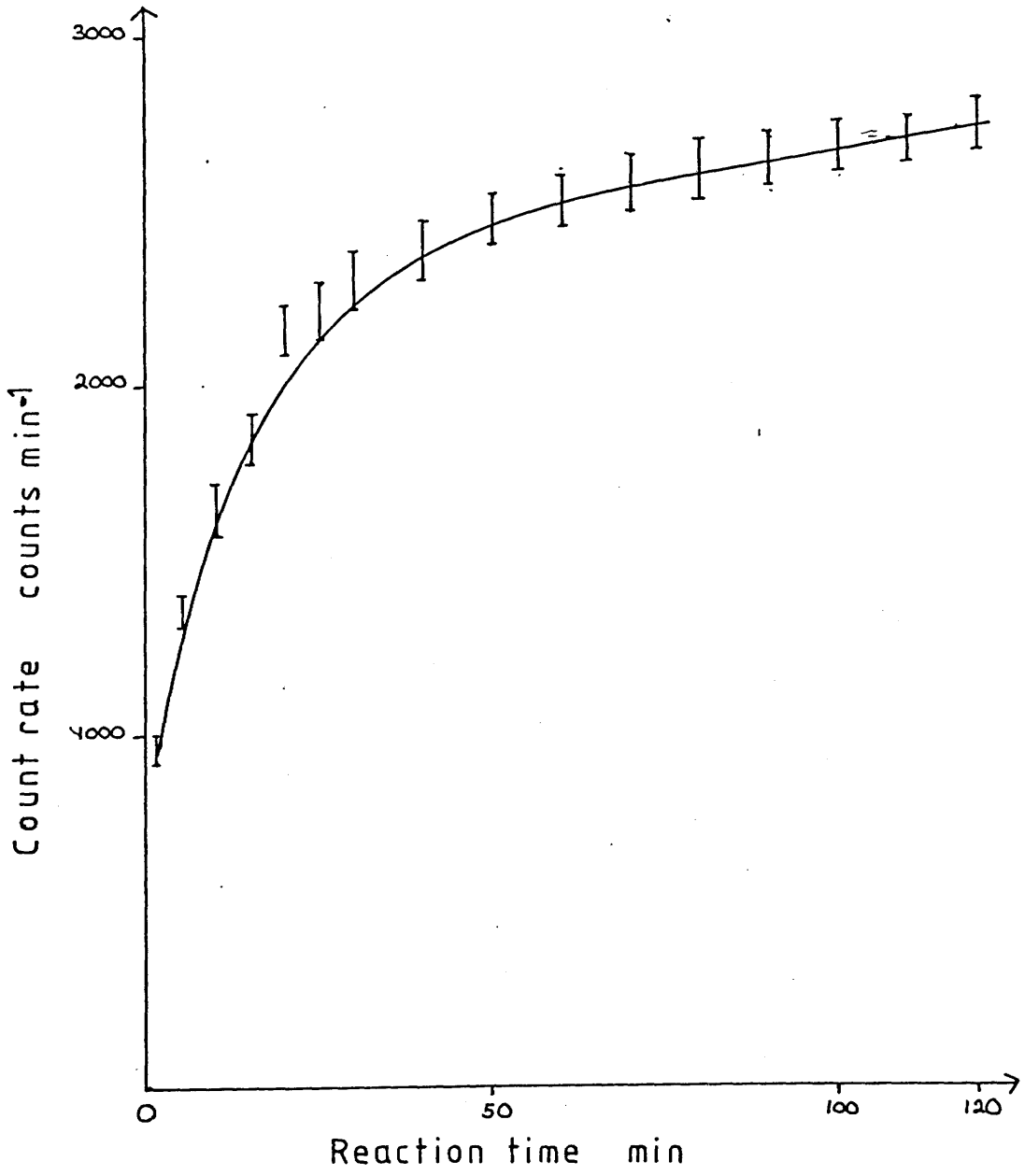

indicating that ^{18}F exchange had occurred. The amount of gas recovered after the reaction was less than the starting amount indicating that in addition to ^{18}F exchange uptake of gas had also occurred.

Using equation 2.5 the fraction of ^{18}F exchanged was calculated, and using this figure the count rate due to gas uptake was calculated by subtracting the count rate due to exchange from the count rate of the CsF after 2 hours. The calculation is now shown in detail for experiment 1 in table 4.6.

The fraction exchanged (f) is given by $f = \frac{(A_o - A_2)(n_1 m_1 + n_2 m_2)}{A_o n_1 m_1}$

where m (m mol) = quantitiy of a species with n exchangeable F atoms.

subscripts 1 and 2 refer to the initially inactive and active species respectively.

A = count rate (counts s^{-1}) after exchange

A_o = count rate of reactant 2 before exchange

Weight of CsF = 0.28g = 1.842 m mol

Pressure of F_2CO = 300 Torr = 0.944 m mol

Count rate of gas before reaction = 7139 counts min^{-1} $(m\ mol)^{-1}$

Count rate of gas after reaction = 5927 counts min^{-1} $(m\ mol)^{-1}$

$$f = \frac{(7139 - 5927)(1.842 + (2 \times 0.944))}{7139 \times 1.842}$$

$f = 0.344$

100% exchange would result from a statistical distribution of ^{18}F among all the fluorine atoms present.

Total number of fluorine atoms = 1.842 + 1.888

= 3.73 mg atoms

Specific count rate of gas = 7139 counts min (m mol)$^{-1}$

Amount of F_2CO = 0.944 m mol

Count rate of F_2CO = 6739 counts min^{-1}

For 100% exchange 3.73 ≡ 6739 counts min^{-1}

1.0 mg atom ≡ 1806 counts min^{-1}

CsF contains 1.842 mg atom F so for 100% exchange count rate of solid would be 1.842 x 1806 counts min^{-1}

= 3326 counts min^{-1}

Calculated level of exchange is 34.4%

so count rate of solid due to exchange is $\frac{34.4}{100}$ x 3326

= 1144 counts min^{-1}

The count rate of the solid after reaction is 2532 counts min^{-1}

So count rate due to uptake of gas is 2532 - 1144

= 1388 counts min^{-1}

The specific count rate of the F_2CO is 7139 $\pm$ 85 counts min^{-1} m mol^{-1} so a count rate of 1388 counts min^{-1} is equivalent to an uptake of 0.194 $\pm$ 0.002 m mol of $F^{18}FCO$.

In each case the infra red spectrum of the solid after reaction shows bands due to the F_3CO^- anion (Table 4.7)

The reaction between $F_2{}^{14}CO$ and activated CsF was studied at

TABLE 4.7

Infra red frequencies of $CsOCF_3$

This Work	Literature[28]	Assignment
1560	1560	$\nu_1 A_1$ CO str
955	960	ν_4 E CF_3 asym str
810	813	ν_2 A_1 CF_3 sym str
590	595	ν_3 A_1 sym CF_3 def
575	574	ν_5 E, OCF def
420	423	ν_6 E, asym CF_3

nine different pressures between 20 and 308 Torr. Surface count rates were measured directly and the overall drop in gas phase counts was used as a measure of the uptake of gas by the bulk solid. Each reaction was followed for 1 hour before removing the $F_2{}^{14}CO$ from the counting vessel to determine the count rate of the CsF surface in the absence of gas.

Plots of solid activity versus time at initial $F_2{}^{14}CO$ pressures of 20, 100 and 308 Torr are shown in figures 4.14, 4.15 and 4.16.

The surface reaction between $F_2{}^{14}CO$ and activated CsF is complete before the first count is taken and the surface count rate remains constant at 6.1 ± 1.6 counts sec^{-1} throughout the experiment. The $F_2{}^{14}CO$ used had a specific count rate of 1000 counts sec^{-1} m mol^{-1}, so a surface count rate of 6.1 ± 1.6 counts sec^{-1} is equivalent to a surface uptake of 0.0061 ± 0.0016 m mol of $F_2{}^{14}CO$. This surface count rate is independant of initial $F_2{}^{14}CO$ pressure as shown by figure 4.17.

When the $F_2{}^{14}CO$ is removed from the counting vessel the surface count rate drops to barely above background level indicating that 95% of the surface activity is dependant upon there being a pressure of $F_2{}^{14}CO$ in the counting vessel with only a very small amount of the F_2CO being permanently adsorbed. The uptake of gas by the bulk solid is also dependant on the initial pressure of F_2CO in the vessel. In order to check this pressure dependance a series of

Figure 4·14

Reaction of $F_2{}^{14}CO$ with activated CsF

Solid count rate vs reaction time

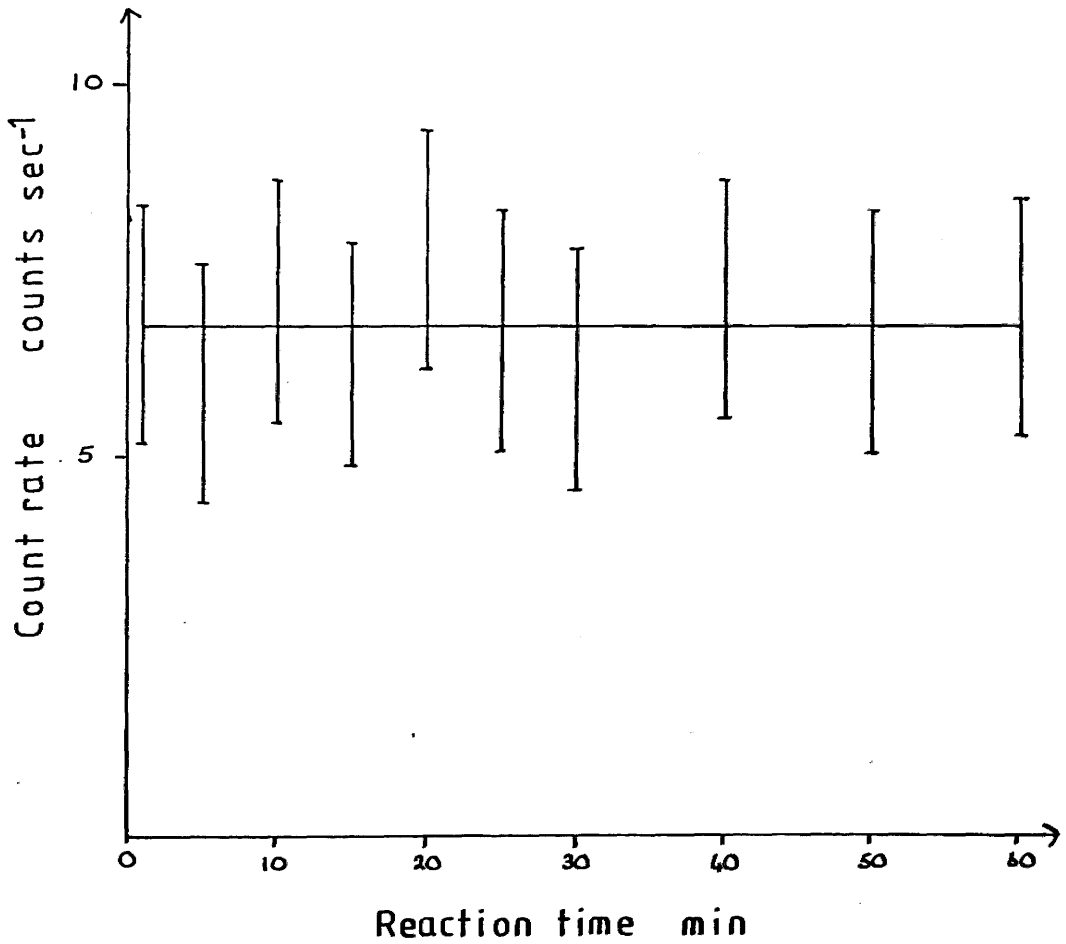

Initial pressure =20 Torr

Figure 4·15

Reaction of $F_2{}^{16}CO$ with activated CsF

Solid count rate vs reaction time

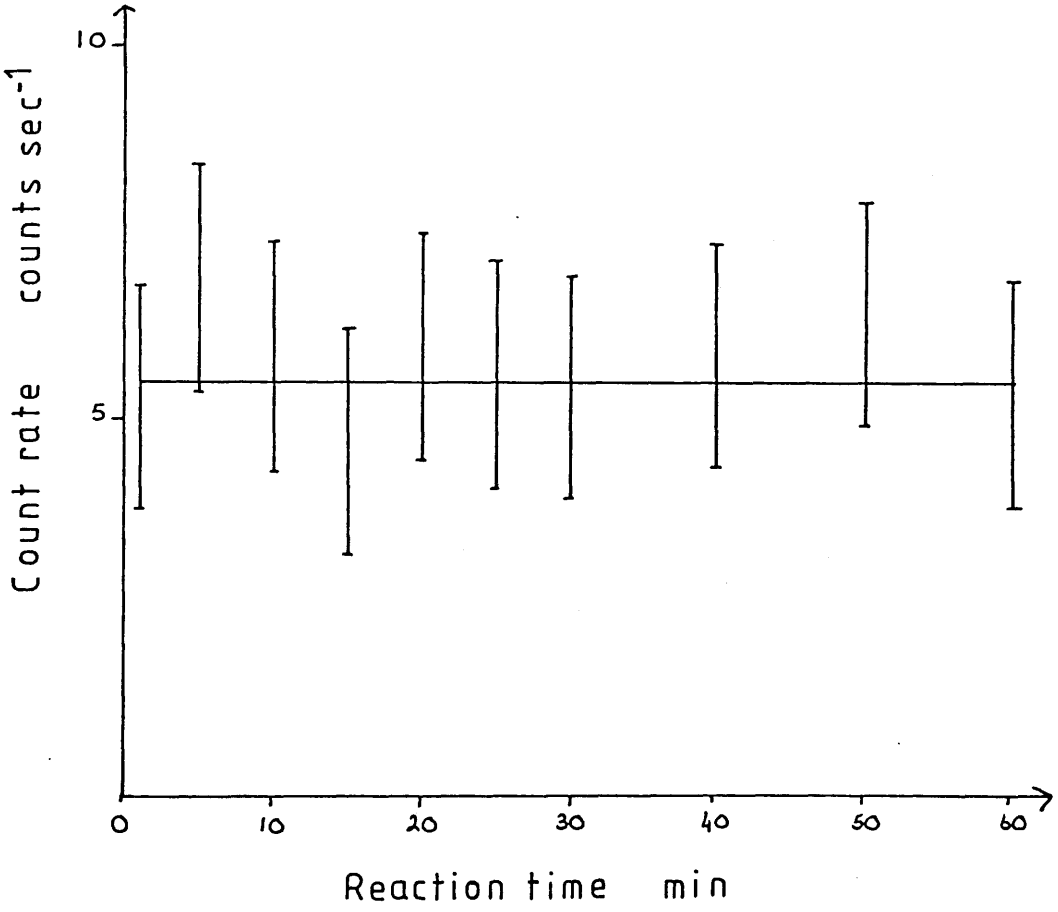

Initial pressure = 100 Torr

Figure 4·16

Reaction of $F_2{}^{14}CO$ with activated CsF

Solid count rate vs reaction time

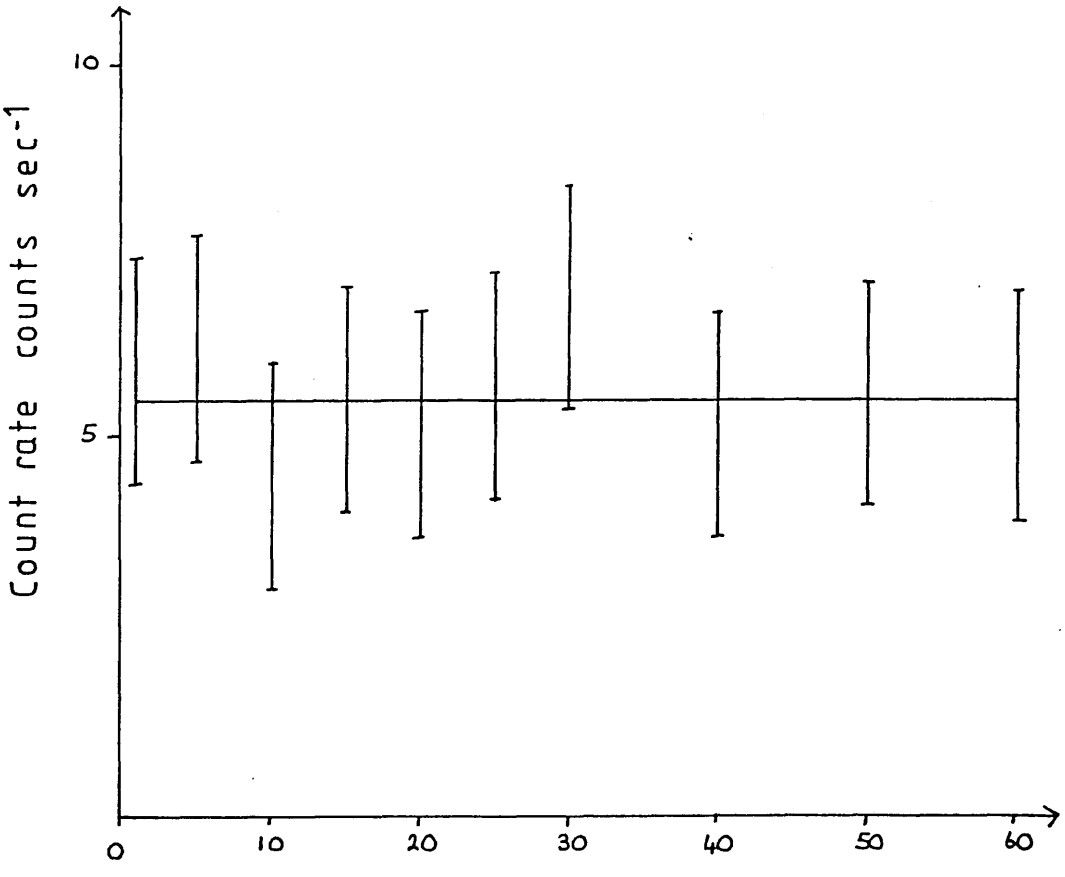

Initial pressure = 308 Torr

Figure 4·17

Reaction of $F_2{}^{14}CO$ with activated CsF

Solid count rate vs initial pressure

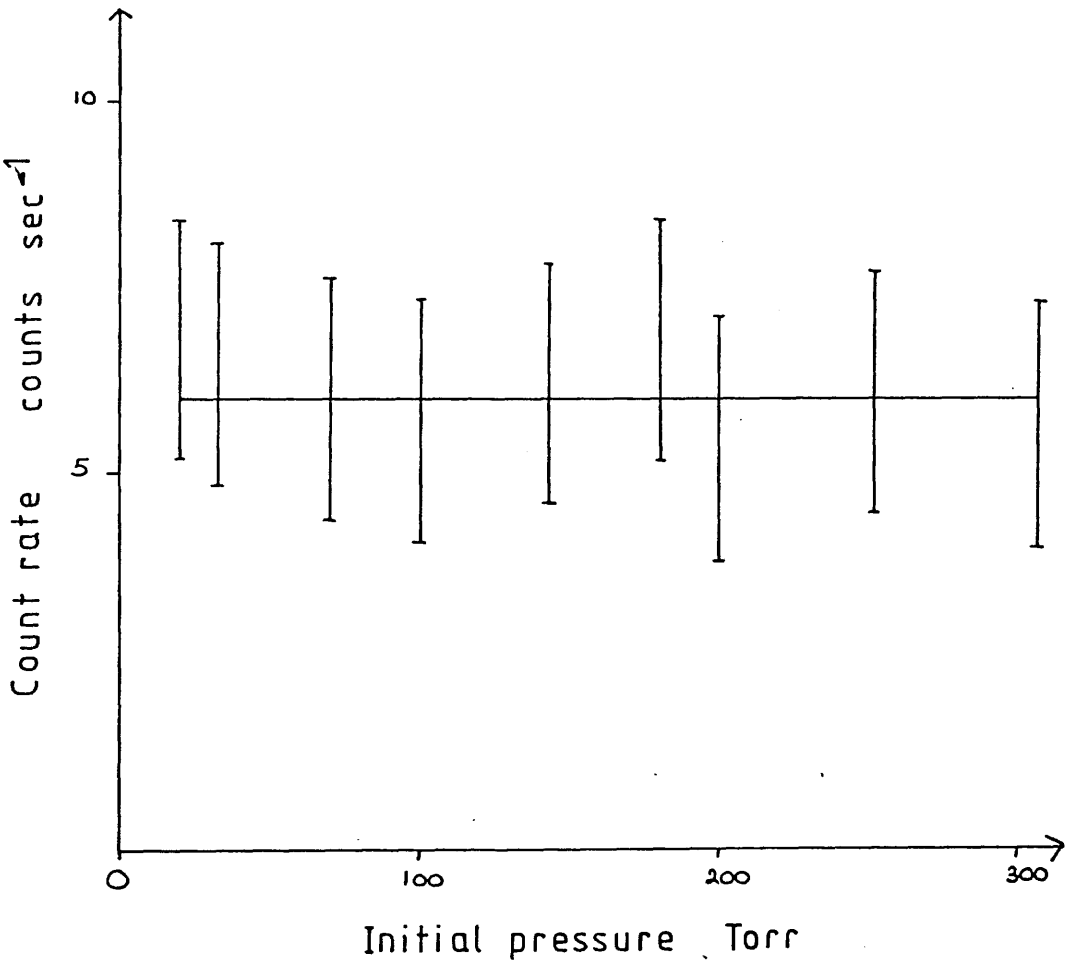

experiments was carried out using the constant volume manometer described in section 2.12. Measurements were carried out at 10 different pressures. The results are shown in figure 4.18, together with the uptakes calculated from the drop in overall gas phase counts in the $F_2{}^{14}CO$ experiments. The two sets of data show very good agreement thus indicating that the fall in gas phase counts gives a reliable measure of the uptake of gas by the solid. Figure 4.17 shows that the uptake of F_2CO by bulk CsF is totally dependant upon the initial pressure of F_2CO in the system. When the samples were re-weighed after the constant volume experiments the increase in weight in each case was less than half that required for the uptake of F_2CO indicated by the drop in pressure (Table 4.8). This shows that the removal of the F_2CO from the counting vessel must also remove more than half of the F_2CO adsorbed within the bulk of the solid. For example the drop in pressure at 300 Torr is equivalent to an uptake of 0.25 m mol of F_2CO per m mol of CsF whereas the increase in weight after reaction is equivalent to an uptake of 0.11 m mol of F_2CO per m mol CsF. Infra red examination of the CsF after reaction reveals the presence of the F_3CO^- anion as was the case in the reaction of $F^{18}FCO$ with CsF (Table 4.7).

4.5 DISCUSSION OF F_2CO RESULTS

The reaction between F_2CO and activated CsF is rapid at room temperature. More than one type of species is present

Figure 4·18

Reaction of F_2CO with activated CsF

Uptake of F_2CO vs initial pressure

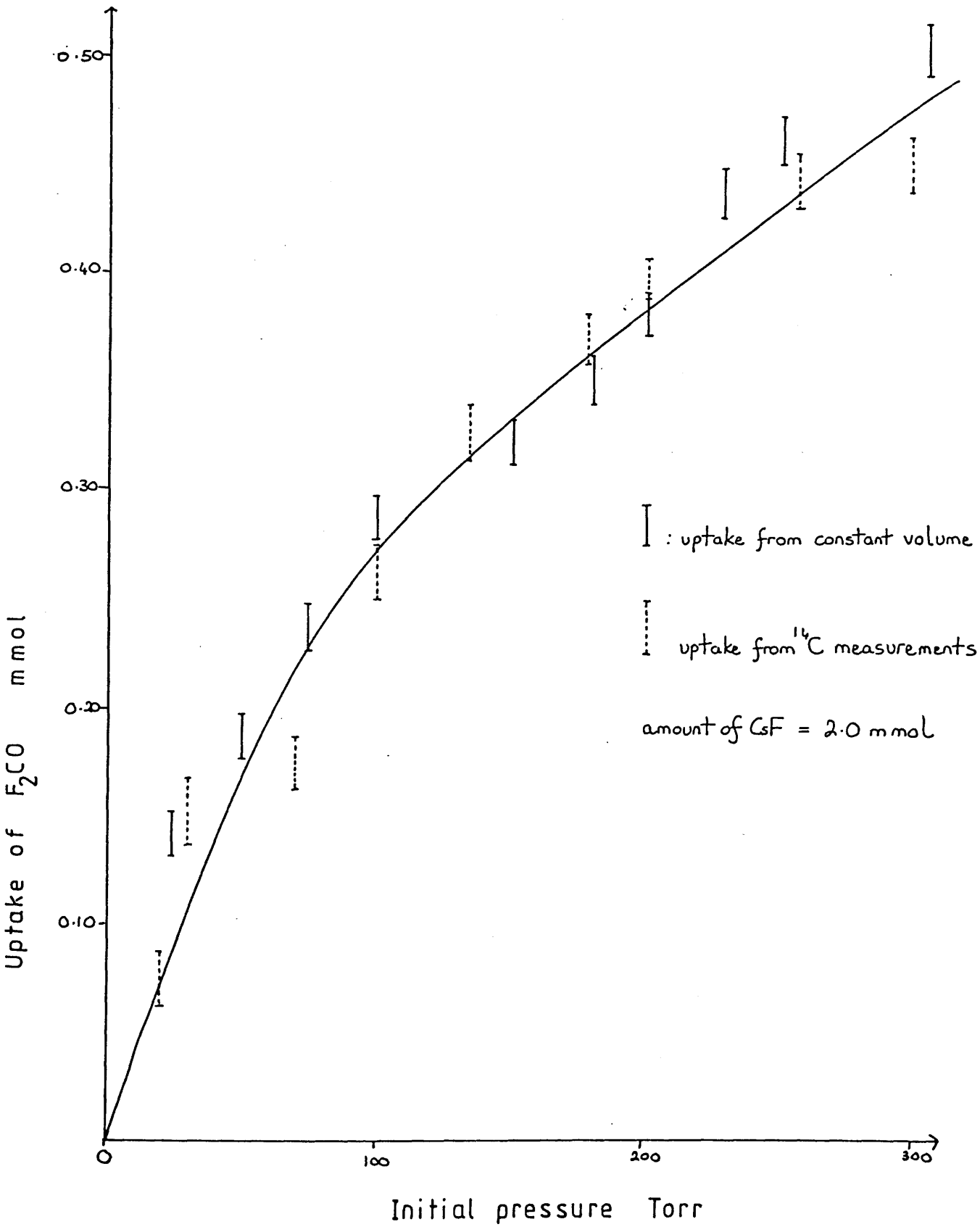

TABLE 4.8

UPTAKE OF F_2CO BY ACTIVATED CsF

Initial Pressure Torr	Uptake Calculated from Fall in Pressure m mol (m mol CsF)$^{-1}$	Uptake Calculated From increase in weight of CsF m mol (m mol CsF)$^{-1}$
24	0.0712 $\pm$ 0.01	0.0270 $\pm$ 0.005
50	0.106 $\pm$ 0.01	0.048 $\pm$ 0.005
74	0.119 $\pm$ 0.01	0.052 $\pm$ 0.005
100	0.142 $\pm$ 0.01	0.067 $\pm$ 0.005
150	0.161 $\pm$ 0.01	0.081 $\pm$ 0.005
180	0.175 $\pm$ 0.01	0.086 $\pm$ 0.005
200	0.191 $\pm$ 0.01	0.094 $\pm$ 0.094
228	0.220 $\pm$ 0.01	0.102 $\pm$ 0.005
250	0.232 $\pm$ 0.01	0.110 $\pm$ 0.005
304	0.253 $\pm$ 0.01	0.121 $\pm$ 0.005

on the surface of the solid and also within the bulk of the solid.

There are two surface species present one which is permanently adsorbed probably as F_3CO^- on the basis of the infra red results, and one which is weakly adsorbed and can be pumped away. These same two species appear to be present in the bulk of the solid as well as on the surface because on removing the F_2CO from the reaction vessel the amount of gas which is adsorbed by the CsF falls by more than 50%.

In the reaction between CsF and $F^{18}FCO$ both uptake of gas and fluorine exchange are observed. There are two possible explanations for this fluorine exchange. The first is that the weakly adsorbed species is adsorbed in such a way as to make the fluorine from CsF equivalent to the two from F_2CO and the second is equivalence between F_3CO^- and F_2CO (ads) is possible. It is probable that the weakly adsorbed F_2CO molecules are adsorbed in such a way as to allow all the fluorines to become equivalent. The evidence for this comes from a matrix isolation study by B.S. Ault[99] in which he reports the formation of an unusual complex from the reaction of formaldehyde with CsF in an argon matrix. This reaction did not give rise to the expected fluoride ion transfer and formation of the CH_2FO^- anion. No C-F stretching mode was observed and the C = O stretching mode was shifted by only 50-60 cm^{-1} compared with a shift of 400 cm^{-1} when F_3CO^- is formed from F_2CO. This suggests that the fluoride ion is interacting weakly with the carbon centre

of the CH_2O but not actually forming a bond.

A similar type of reaction may occur between the weakly adsorbed F_2CO and the CsF to give the species shown in figure 4.19.

Figure 4.19

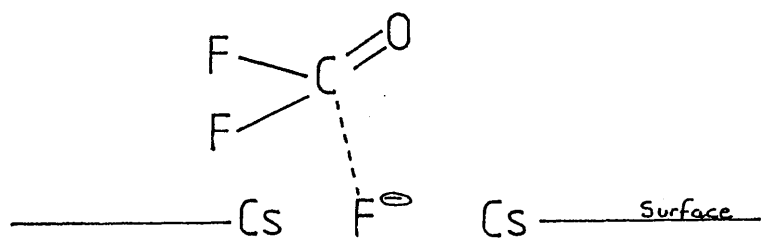

If this reaction occurs there may be a point at which all the fluorines become equivalent and exchange is possible.

The possibility of equivalence between F_3CO^- and F_2CO (ads) seems unlikely based on the findings of Redwood and Willis in 1965.[27] They reported that $CsOCF_3$ was stable with respect to decomposition at room temperature. The infra red and Raman study of the F_3CO^- ion by Christe and coworkers does however indicate that two or more resonance forms of the anion exist. This view is supported by a later matrix isolation study of $CsOCF_3$ by B.S. Ault.[100] In the infra red spectrum of $CsOCF_3$, there is a band at $960cm^{-1}$ which is assigned to the doubly degenerate CF_3 stretching mode. In the matrix isolation study the degeneracy of the band is lost and it appears as two separate bands at 919 cm^{-1} and 1039 cm^{-1}. The other band positions also show slight differences from their expected

values. The CF_3 frequencies have decreased by 350 cm^{-1} compared with CF_4. The CO stretch is at a lower frequency than expected for a double bond and higher than that of a single bond.

Further evidence for the existence of resonance structures is supplied by W B Farnham and coworkers[29] in their study of the crystal and molecular structure of $\left[\left((CH_3)_2N\right)_3S^+\right]\left[F_3CO^-\right]$. The X-ray single crystal diffraction analysis shows that the C-F bond lengths are exceptionally long (1.390 and 1.397 Å) and the C-O bond length is quite short (1.227Å) compared with the corresponding gas-phase experimental values for CF_3OR (R=F, CF_3). The C-O bond length is close to that for the C=O bond in $CF_2=O$. In addition the FCF bond angles are very small compared to those of CF_3OR.

Mulliken population analyses indicate that there is an additional charge of -0.2e on each F in CF_3O^-. This excess charge implies that each of the resonance structures b-d contribute approximately 20% to the bonding in CF_3O^- while (a) contributes 40%.

Figure 4.20

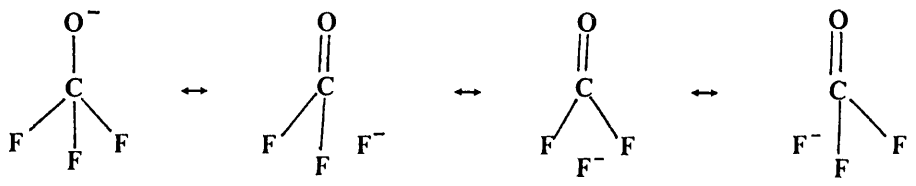

(a) (b) (c) (d)

The existence of these resonance forms provides a ready mechanism for the equivalence of F_3CO^- and F_2CO (ads) as the proposed weakly adsorbed species can be readily envisaged as a precursor to these resonance species as shown in figure 4.21.

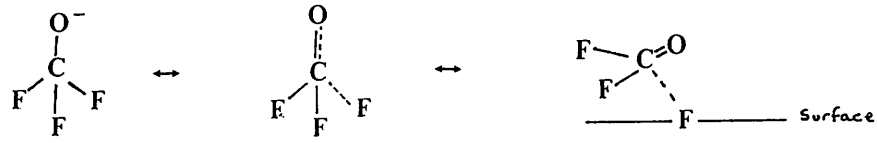

(a) (b) (c)

Therefore, based on the evidence presented the two possible explanations for fluorine exchange can be combined to provide an overall description of the ways fluorine exchange can occur.

In the weakly adsorbed state, the two fluorines from the F_2CO become equivalent to the fluorine from CsF. When this occurs the structure of the adsorbed species is similar to the structure of the F_3CO^- anion. This allows fluorine exchange to occur either between F_2CO (ads) and F^- or between F_3CO^- and F_2CO (ads).

4.6 RESULTS OF REACTION OF BF_3 WITH CsF

As there are no suitable radioisotopes of boron, the reaction between BF_3 and CsF was studied using ^{18}F

labelled BF_3 alone. The results obtained are comparable with those from a conventional manometric study of this system carried out at the same time.

Four experiments involving $BF_2{}^{18}F$ and non activated CsF were carried out. Their results are summarised in table 4.9. Figure 4.22 shows a plot of solid count rate versus time for experiment number 3. There is a rapid rise in solid count rate until an equilibrium level is reached after 30 minutes. There is no change in the specific count rate of the $BF_2{}^{18}F$ before and after reaction so the increase in the solid count rate is due to uptake of $BF_2{}^{18}F$ by the caesium fluoride. Since the specific count rate of the $BF_2{}^{18}F$ is known for each experiment, the observed solid count rates can be converted to amounts of $BF_2{}^{18}F$ adsorbed. The calculated amounts of adsorbed $BF_2{}^{18}F$ are shown in table 4.9. The average uptake observed is 0.088 ± 0.004 m mol.

Treatment of caesium fluoride with non radioactive BF_3 before reaction with $BF_2{}^{18}F$ prevents any uptake of the $BF_2{}^{18}F$. Table 4.10 shows the results of a reaction between $BF_2{}^{18}F$ and non activated CsF treated with BF_3. The observed counts are very low because they are gas phase counts and material in the gas phase cannot be efficiently counted in a well scintillation counter.

If the caesium fluoride is first treated with $BF_2{}^{18}F$ to produce a radioactive solid and then allowed to react

TABLE 4.9

REACTION OF $BF_2{}^{18}F$ WITH NON ACTIVATED CsF - SUMMARY OF RESULTS

Amount of CsF g m mol	Amount of $BF_2{}^{18}F$ Torr m mol	Specific Count Rate of $BF_2{}^{18}F$ Before Reaction counts min^{-1} m mol^{-1}	Specific Count Rate of $BF_2{}^{18}F$ After Reaction counts min^{-1} m mol^{-1}	Solid Count Rate After Reaction counts min^{-1}	Uptake m mol
0.50 ± 0.01 3.29 ± 0.06	300 ± 2 1.00 ± 0.01	14326 ± 120	14362 ± 120	1275 ± 36	0.089 ± 0.003
"	"	9513 ± 97	9511 ± 97	894 ± 30	0.094 ± 0.003
"	"	12118 ± 110	12115 ± 110	1030 ± 32	0.085 ± 0.003
"	"	5316 ± 73	5313 ± 73	457 ± 21	0.086 ± 0.004

Figure 4·22

Reaction of $BF_2^{18}F$ with non activated CsF

Solid counts vs reaction time

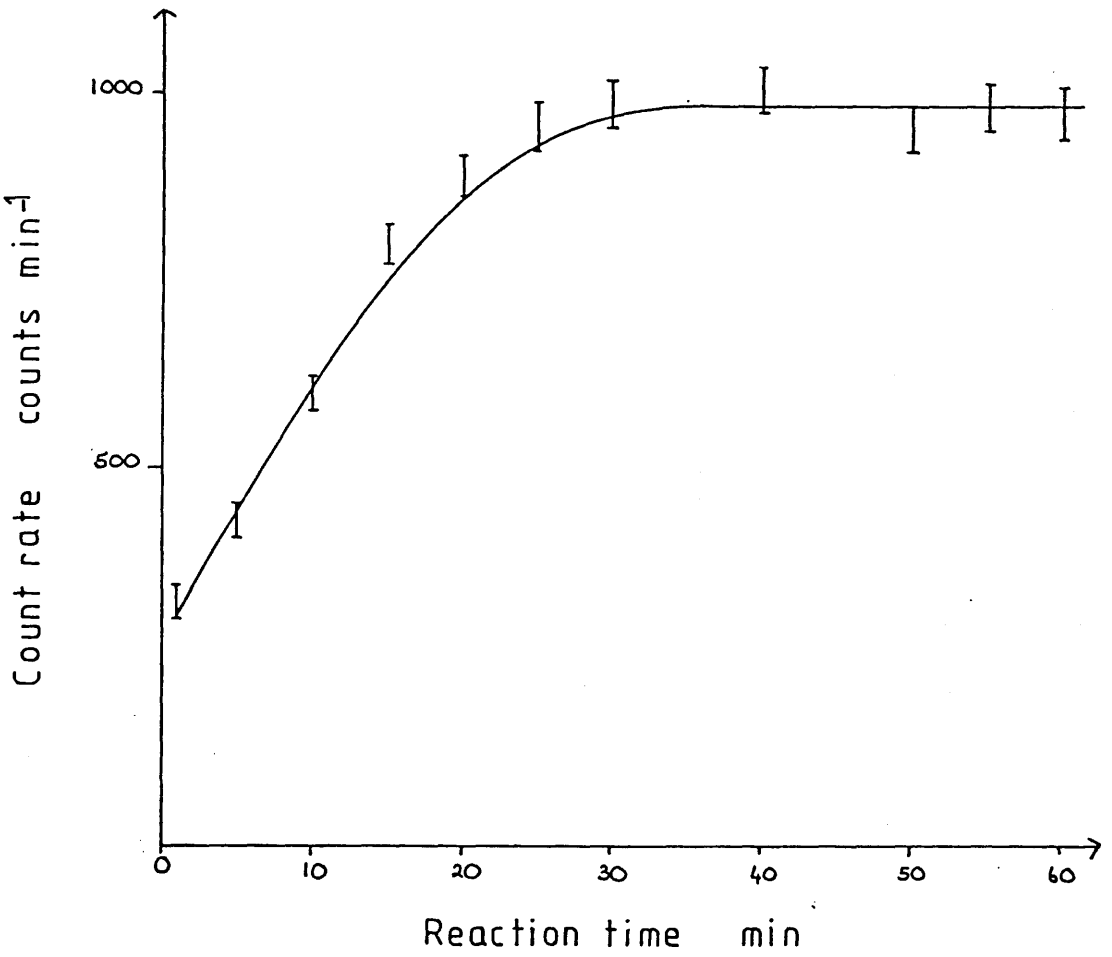

TABLE 4.10

RESULTS OF REACTION OF $BF_2{}^{18}F$ WITH NON ACTIVATED CsF TREATED WITH BF_3

Time min	Solid + Gas counts min^{-1}	Gas Counts counts min^{-1}	Solid Counts counts min^{-1}
2	439	422	17
9	454	433	21
17	446	448	-2
25	412	425	-13
32	436	416	20
38	435	436	-1
43	456	420	36
52	407	437	-30
58	434	454	-20
64	424	402	22
72	456	433	23

Count rate of solid after reaction = 28 counts min^{-1}

Specific count rate of $BF_2{}^{18}F$ before = 6870 counts min^{-1} m mol^{-1}

Specific Count rate of $BF_2{}^{18}F$ after = 6870 counts min^{-1} m mol^{-1}

with non radioactive BF_3 no ^{18}F exchange is observed. This also indicates that the adsorbed $BF_2{}^{18}F$ molecules do not exchange with the gas phase BF_3 molecules. The results of this experiment are listed in table 4.11.

The results of four reactions between $BF_2{}^{18}F$ and activated CsF are given in table 4.12. The results obtained are similar to those of the reaction between $BF_2{}^{18}F$ and non activated CsF, with a rapid increase in the solid count rate which reached an equilibrium level after 30 minutes as shown in figure 4.23. The only difference is that with non activated CsF, only a small proportion of the $BF_2{}^{18}F$ was taken up by the caesium fluoride whereas with activated caesium fluoride all of the gas present in the reaction flask is taken up by the solid.

In an effort to determine the total amount of BF_3 which would react with 0.50g of activated CsF two adsorption experiments were carried out using the constant volume apparatus described in section 2.1.2. 0.50g of activated CsF was loaded into a sample bulb and the line filled with BF_3 to a pressure of 300 Torr. The overall drop in pressure was measured after 45 minutes. After correction for the change in total volume on opening the sample bulb, the fall in BF_3 pressure was equivalent to uptakes of 3.21 $\pm$ 0.10 m mol and 3.15 $\pm$ 0.10 m mol of BF_3 by 3.28 $\pm$ 0.06 m mol and 3.16 $\pm$ 0.06 m mol of activated CsF respectively. These results show that activated CsF will react with BF_3 in a 1:1 mole ratio at room temperature.

TABLE 4.11

RESULTS OF REACTION OF BF_3 WITH NON ACTIVATED CsF TREATED WITH $BF_2{}^{18}F$

Time min	Solid Counts Counts min^{-1}	Gas Counts Counts min^{-1}
2	1584	4
7	1536	2
12	1597	5
17	1532	1
22	1527	0
27	1555	2
37	1598	4
45	1569	1
55	1581	1
65	1526	5
70	1544	7

Count rate of BF_3 after reaction = 34 counts min^{-1}

Specific count rate of $BF_2{}^{18}F$ before = 16781 counts min^{-1} m mol^{-1}

Specific count rate of $BF_2{}^{18}F$ after reaction = 16781 counts min^{-1} m mol^{-1}

TABLE 4.12

REACTION OF $BF_2{}^{18}F$ WITH ACTIVATED CsF, SUMMARY OF RESULTS

Amount of CsF g m mol	Amount of $BF_2{}^{18}F$ Torr m mol	Specific Count Rate of $BF_2{}^{18}F$ Before Reaction Counts min^{-1} m mol^{-1}	Count Rate of $BF_2{}^{18}F$ After Reaction Counts min^{-1}	Count Rate Of Solid After Reaction Counts min^{-1}	Uptake m mol
0.50 ± 0.01 3.29 ± 0.06	300 ± 2 1.0 ± 0.01	15003 ± 123	65 ± 8	14995 ± 120	1.00 ± 0.01
"	"	12118 ± 110	51 ± 7	12056 ± 110	1.00 ± 0.01
"	"	6870 ± 83	43 ± 7	6869 ± 83	1.00 ± 0.01
"	"	16781 ± 130	81 ± 9	16750 ± 130	1.00 ± 0.01

Figure 4·23

Reaction of $BF_2^{18}F$ with activated CsF

Solid count rate vs reaction time

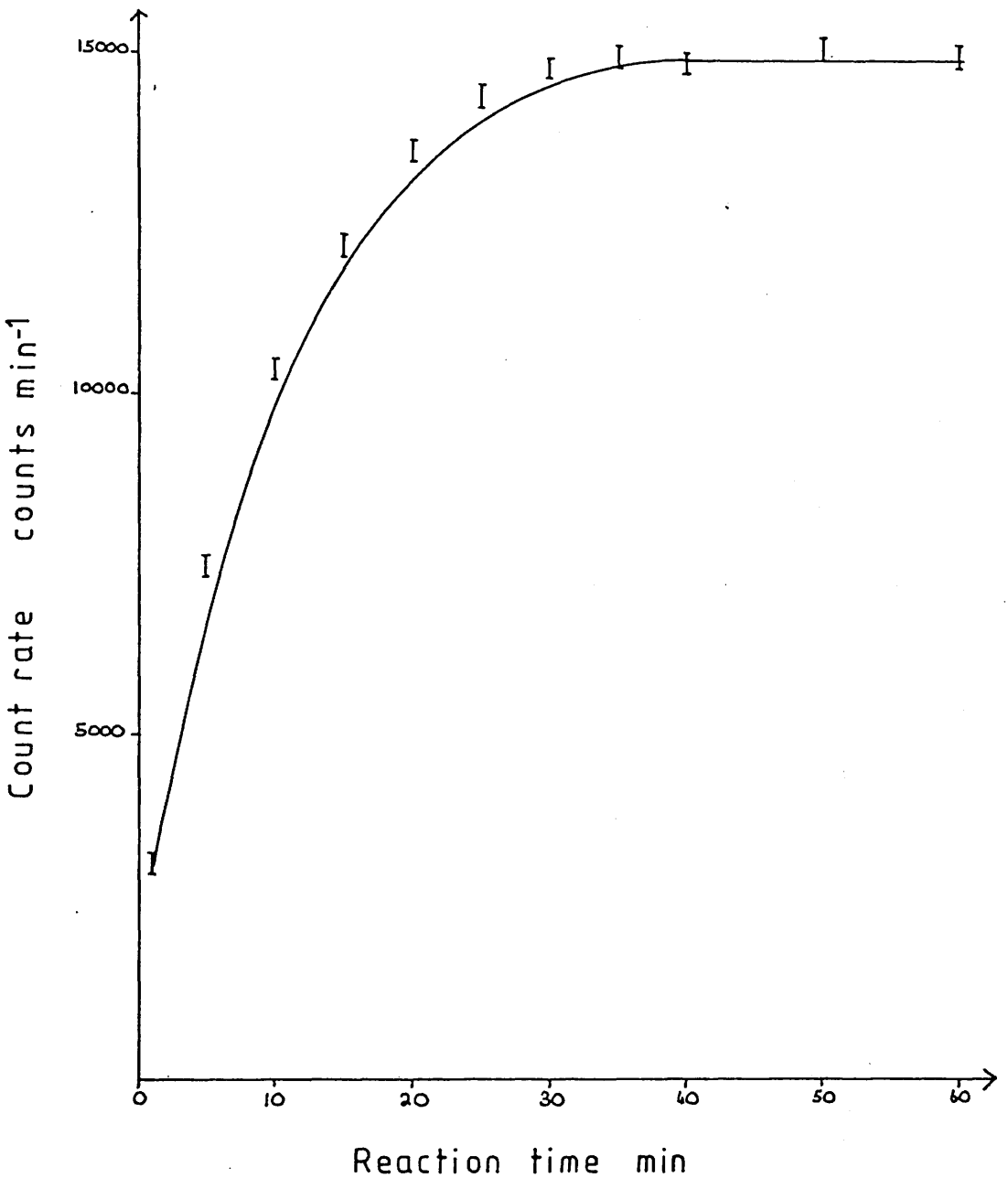

Table 4.13 shows the results of an experiment in which a sample of activated CsF was treated with non radio-active BF_3 before reaction with $BF_2{}^{18}F$. After one hour there is no detectable solid count rate.

Table 4.14 shows the results of an experiment in which the activated CsF was treated first with $BF_2{}^{18}F$ and then with non radioactive BF_3. In this case there is a barely detectable growth in the gas phase count rate. There is no detectable change in the specific count rate of the $BF_2{}^{18}F$ before and after reaction.

In this work the caesium fluoride was activated by treatment with hexafluoroacetone in acetonitrile and subsequent thermal decomposition of the adduct formed as described in chapter 3 section 3.1.1. Subsequent examination of this activated caesium fluoride revealed that 0.5% of the heptafluoroisopropoxide anion is retained after decomposition. In an effort to determine whether or not the retained anion plays any part in the reactions of activated caesium fluoride, two samples of caesium fluoride were activated by other means. The first sample was activated by heating under vacuum at 250^{o} for 8 hours followed by grinding in an agate mortar and pestle. The second sample was treated with F_2CO as described in chapter 3 sections 3.1.2 and 3.1.3.

TABLE 4.13

REACTION OF $BF_2{}^{18}F$ WITH ACTIVATED CsF TREATED WITH BF_3

Time min	Solid + Gas Counts Counts min^{-1}	Gas Counts Counts min^{-1}	Solid Counts counts min^{-1}
1	451	456	-5
5	447	441	6
10	463	455	8
15	431	437	-6
20	457	442	15
25	423	419	4
30	435	437	-2
40	419	407	12
50	472	480	-8
60	414	404	10

Count rate of solid after reaction = 43 counts min^{-1}

Specific count rate of $BF_2{}^{18}F$ before = 6638 $\pm$ 81 counts min^{-1} m mol^{-1}

Specific count rate of $BF_2{}^{18}F$ after reaction = 6632 $\pm$ 81 counts min^{-1} m mol^{-1}

TABLE 4.14

REACTION OF BF_3 WITH ACTIVATED CsF TREATED WITH $BF_2{}^{18}F$

Time min	Solid & Gas Counts Counts min^{-1}	Gas Counts Counts min^{-1}	Solid Counts Counts min^{-1}
1	21820	1	21819
6	21044	3	21041
12	21457	4	21453
18	21389	2	21387
24	21359	3	21356
34	21110	3	21107
43	21271	5	21266
49	21097	8	21091
57	21101	5	21096
63	20958	9	20949

Count rate of gas after reaction = 67 counts min^{-1}

Specific count rate of $BF_2{}^{18}F$ before = 6637 $\pm$ 81 counts min^{-1} m mol^{-1}

The results of the reaction of $BF_2{}^{18}F$ with CsF activated by heating are shown in figure 4.24. As with hexafluoroacetone activated CsF there is a rapid initial increase in solid count rate and an equilibrium level is reached after 30 minutes. Unlike the reaction of $BF_2{}^{18}F$ with hexafluoroacetone activated CsF all of the $BF_2{}^{18}F$ does not react with the CsF. The maximum uptake of BF_3, measured using the constant volume apparatus, corresponds to 0.33m mol of BF_3 to 1 m mol of CsF. With hexafluoroacetone activated CsF the maximum uptake is 1.1.

F_2CO activated CsF reacts with $BF_2{}^{18}F$ in a similar manner, to the thermally activated CsF as shown by figure 4.25. This shows a rapid initial increase in solid count rate which reaches an equilibrium value after 30 minutes. All of the $BF_2{}^{18}F$ in the reaction vessel is taken up by the CsF. Measurements carried out using the constant volume apparatus show that the maximum uptake of BF_3 corresponds to 0.95 m mol of BF_3 to 1 m mol of CsF.

In addition to the reactions already described the reaction between $BF_2{}^{18}F$ and $NF_4\ BF_4$ was studied. Figure 4.26 shows a plot of solid count rate versus time for this reaction. The solid count rate increases rapidly until an equilibrium value is reached after approximately 20 minutes. The specific count rate of the $BF_2{}^{18}F$ before reaction was 20095 ± 141 counts min^{-1} m mol^{-1} and after reaction it had dropped to 18702 ± 136 counts min^{-1} m mol^{-1}. This indicates

Figure 4·24

Reaction of $BF_2^{18}F$ with CsF activated by heating

Solid count rate vs reaction time

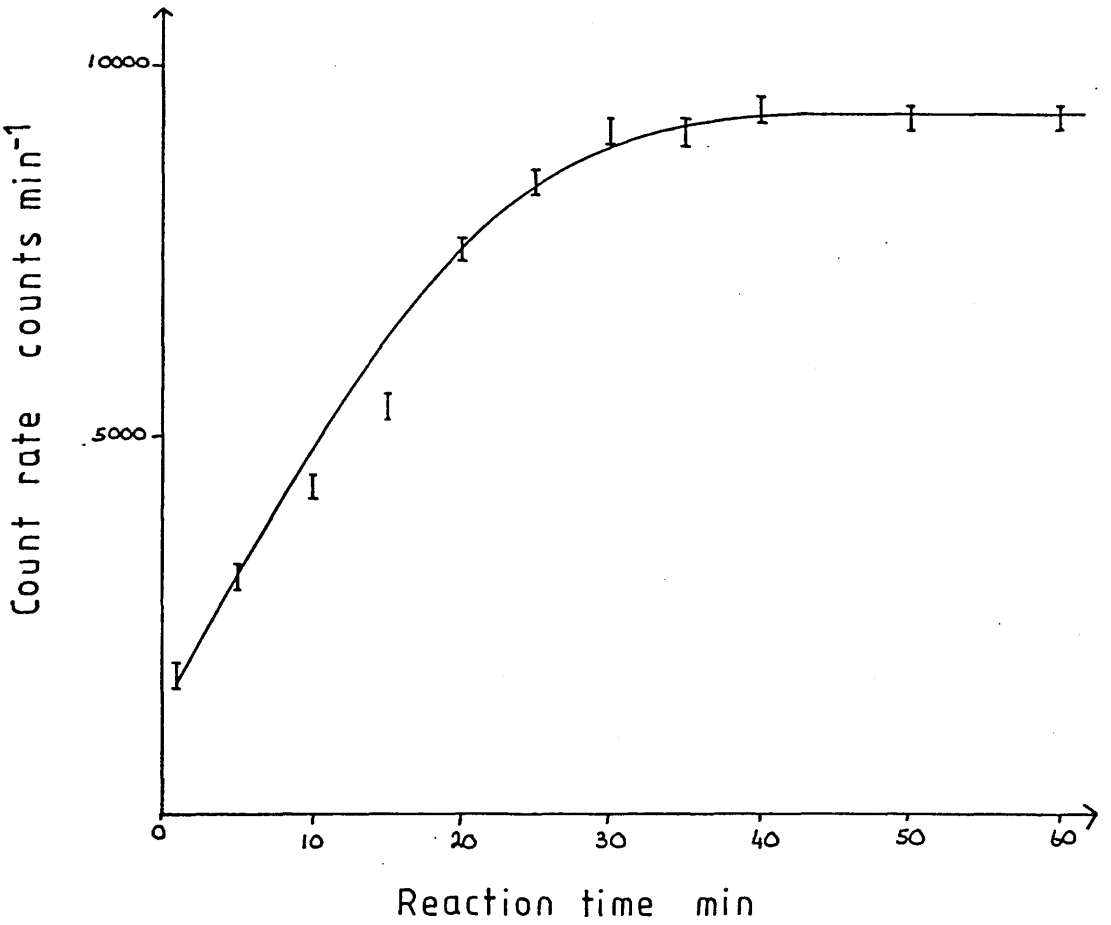

Figure 4·25

Reaction of $BF_2^{18}F$ with CsF activated by reaction with F_2CO.

Solid count rate vs reaction time

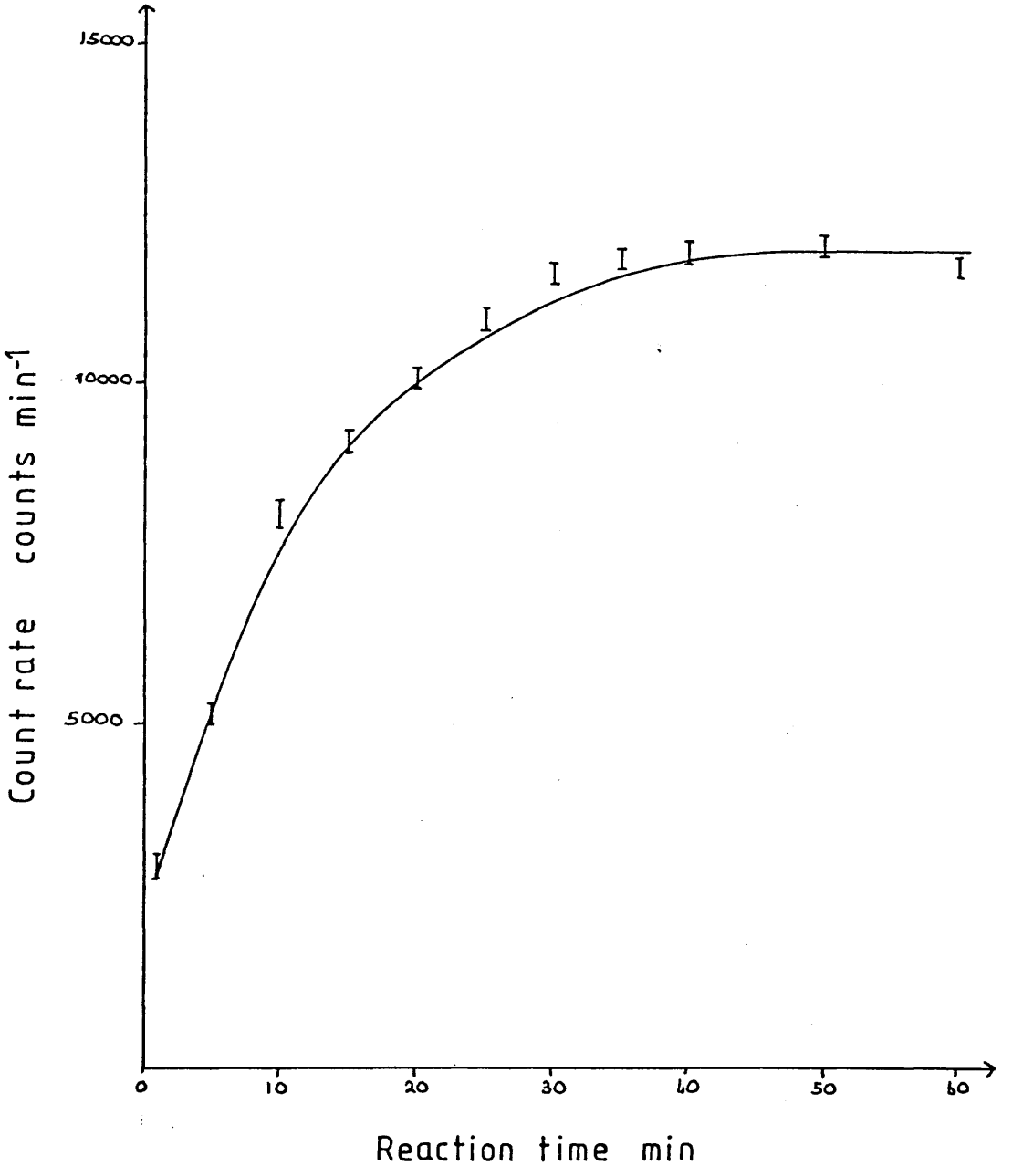

Figure 4·26

Reaction of $BF_2^{18}F$ with NF_4BF_4

Solid count rate vs reaction time

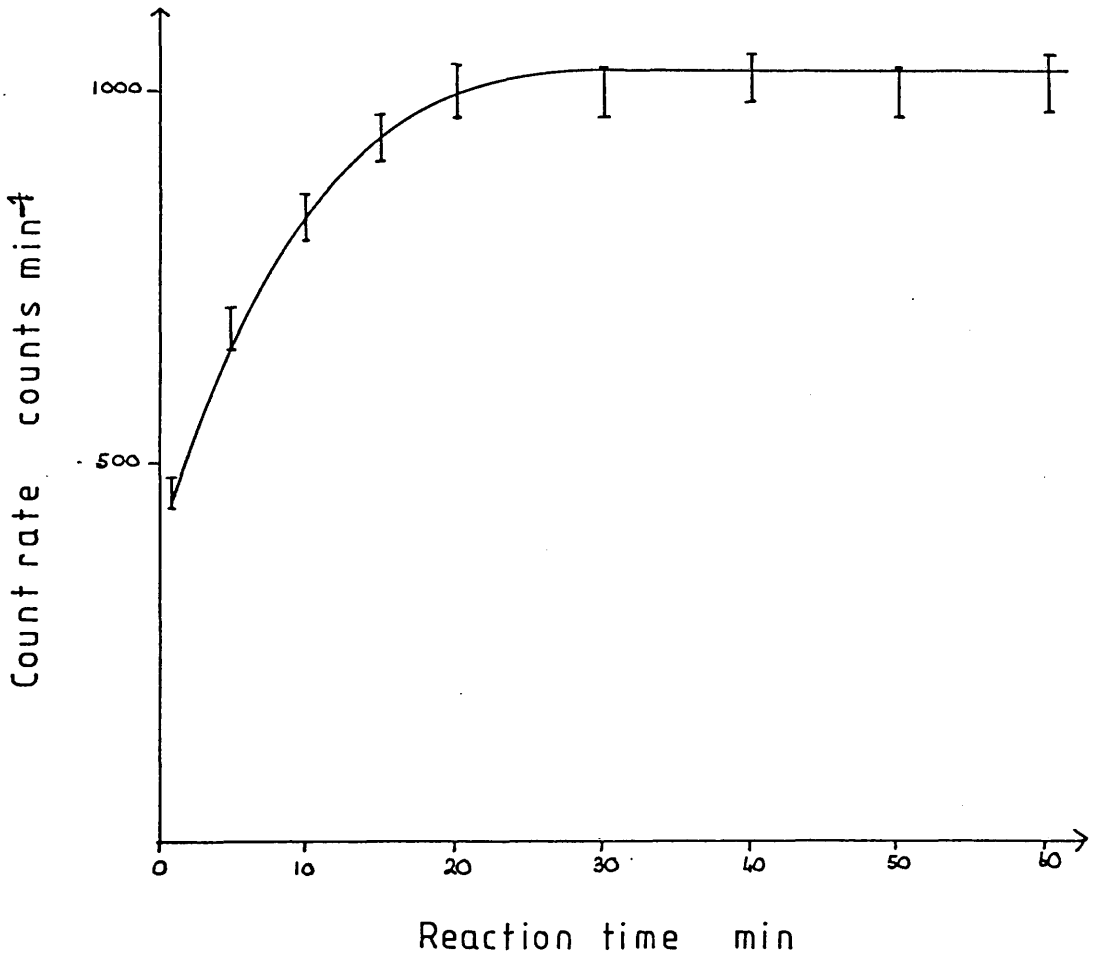

that the increase in solid activity is due to F exchange between BF_4^- and $BF_2{}^{18}F$. Using equation 2.4 and assuming that there is no exchange between $BF_2{}^{18}F$ and NF_4^+ [101] the fraction exchanged (f) is 0.087 $\pm$ 0.001. The fraction exchanged calculated from a second experiment is 0.080 $\pm$ 0.001.

The systems described so far have all been studied under heterogeneous conditions. Measureable ^{18}F exchange was observed between $BF_2{}^{18}F$ and NF_4BF_4. Fluorine exchange between BF_3 and BF_4^- has previously been observed under homogeneous conditions.[102] To show that the experimental techniques described in this work can be used to observe exchange under similar conditions the reactions between $BF_2{}^{18}F$ and Li BF_4 in MeCN and between $BF_2{}^{18}F$ and $CsBF_4$ in MeCN were studied.

The results are given in tables 4.15 and 4.16 and show that complete exchange is observed in the $BF_2{}^{18}F$/Li BF_4 system and 21% exchange is observed in the $BF_2{}^{18}F$/Cs BF_4 system.

4.7 DISCUSSION OF BF_3 RESULTS

Both activated and non activated CsF react readily with BF_3 at room temperature with uptake of gas always being observed. There are three possible species which could result from the uptake of gas - 1) Adsorbed BF_3 molecules, 2) the BF_4^- anion or 3) the $B_2F_7^-$ anion.

TABLE 4.15

REACTION OF $BF_2{}^{18}F$ WITH $Li\,BF_4$ IN MeCN

Count rate of $BF_2{}^{18}F$ before reaction	=	15966 counts min^{-1}
Amount of $BF_2{}^{18}F$	=	2.7 m mol
Reaction time	=	60 minutes
Count rate of $Li\,BF_4$ after reaction	=	9003 counts min^{-1}
Amount of $Li\,BF_4$	=	2.65 m mol
Count rate of $BF_2{}^{18}F$ after reaction	=	6856 counts min^{-1}
Fraction exchanged	=	1.02

TABLE 4.16

REACTION OF $BF_2{}^{18}F$ WITH $CsBF_4$ IN MeCN

Count rate of $BF_2{}^{18}F$ before reaction	=	17261 counts min^{-1}
Amount of $BF_2{}^{18}F$	=	2.0 m mol
Reaction time	=	60 minutes
Count rate of $Cs\,BF_4$ after reaction	=	2926 counts min^{-1}
Amount of $Cs\,BF_4$	=	1.95 m mol
Count rate of $BF_2{}^{18}F$ after reaction	=	14215 counts min^{-1}
Fraction exchanged	=	0.21

Many BF_4^- salts are known[103] and the tetrahedral structure of the anion has been well characterised spectroscopically[104,105] (Figure 4.27)

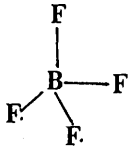

Figure 4.27

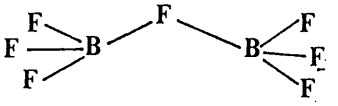

Figure 4.28

The $B_2F_7^-$ anion which has the structure shown in figure 4.28[106] exists at low temperatures in solution[106,107] and in the solid state with large cations[108] such as $(C_2H_5)_3NH^+$ but readily dissociates to give BF_3 and BF_4^-.

Infra red examination of both activated and non activated caesium fluoride after reaction with $BF_2{}^{18}F$ always produces a similar spectrum. Two weak bands are observed between 520 and 540 cm^{-1}, a medium band at 770 cm^{-1} and a strong band at 1060 cm^{-1}. With non activated CsF a weak broad band is observed in place of the two weak bands at 520 cm^{-1} and 540 cm^{-1} due to the small amount of BF_3 involved in the reaction. Table 4.17 lists the bands observed in the IR spectrum of CsF after reaction with BF_3 together with the literature values for BF_3[109], KBF_4[105] and $(Bu)_4NB_2F_7$[106]. Comparison of these data shows that the product of the reaction between CsF and BF_3 is $CsBF_4$ This is further supported by the results of the manometric studies previously described which show that BF_3 reacts

TABLE 4.17 INFRA RED SPECTRUM OF CsF AFTER REACTION WITH $BF_2{}^{18}F$

Solid after reaction	$BF_3{}^{109}$ cm^{-1}	$KBF_4{}^{105}$ cm^{-1}	$(Bu)_4NB_2F_7{}^{106}$ cm^{-1} (solution in CH_2Cl_2)
	1505 v3		
			1219
			1099
1070)		1078)	
)		)	
1060) vs br		1063) v3	1052
)		)	
1040)		1038)	
			1020
			833
768		773 ν_1	
	718 v2		
530		536)	
		) v4	
522		525)	
	482 v4		

with hexafluoroacetone activated CsF in a 1:1 mole ratio.

With non activated CsF there is a much smaller uptake of BF_3 with only 0.027 m mol of BF_3 reacting per m mol of CsF. The ratio of the amount of BF_3 reacting with non activated CsF to the amount reacting with activated CsF is approximately 1:40. The ratio of surface areas is 1:10. The large difference in uptakes is due to the amount of bulk reaction which occurs. In the reaction of activated caesium fluoride with $BF_2{}^{18}F$ the bulk reaction is complete and $CsBF_4$ is formed.

If non activated CsF is treated with BF_3 no further adsorption of gas can take place. This means that adsorption of BF_3 by non activated CsF is restricted to a limited number of specific sites, all of which are filled during the first reaction with BF_3.

The results of the reactions of BF_3 with CsF activated by treatment with F_2CO and with thermally activated CsF are similar to those of its reactions with hexafluoroacetone activated CsF.

Pre-treatment of CsF by repeated heating and grinding results in CsF with a surface area of $1.20 \pm 0.20\ m^2\ g^{-1}$. BF_3 reacts with this CsF giving a maximum uptake of 0.33m mol of BF_3 per m mol of CsF.

When CsF is activated by reaction with F_2CO it has a surface area of 2.27 - 1,77 $m^2\ g^{-1}$. BF_3 reacts with this CsF giving a maximum uptake of 0.95 m mol of BF_3 per m mol of CsF. When the differences in surface areas are taken into account the uptakes of gas by $(CF_3)_2CO$ activated CsF and F_2CO activated CsF are comparable. The uptake of gas by thermally activated CsF is much smaller suggesting that chemical pre-treatment of CsF does more than simply increase its surface area. The results obtained suggest that chemical pre-treatment produces a solid with a more open structure perhaps porous as proposed in chapter 3. The comparable results obtained from the two different types of chemically activated CsF show that the small amount of heptafluoroisopropoxide ion retained after activation by hexafluoroacetone does not play any part in the reactions of CsF activated in this way.

^{18}F exchange is observed in the homogeneous systems BF_3/ $LiBF_4$ in MeCN and $BF_3/CsBF_4$ in MeCN. Exchange is complete in the $BF_3/LiBF_4$ system but only 21% exchange is observed in the $BF_3/CsBF_4$ in MeCN which means that the $BF_3/CsBF_4$ system is not truely homogeneous.

When studying the heterogeneous systems, measurable ^{18}F exchange is only observed in the reaction of $BF_2\,^{18}F$ with $NF_4\ BF_4$. There is also a barely detectable increase in the gas phase count rate in the reaction of BF_3 with $CsBF_3\,^{18}F$ prepared from hexafluoroacetone activated CsF.

These results suggest that ^{18}F exchange between BF_3 and BF_4^- is very slow at room temperature, unless a solvent is present. The proposed mechanism for fluorine exchange in solution involves a slight initial dissociation of BF_4^- to give $BF_3 + F^-$ followed by the formation of a fluorine bridged $B_2F_7^-$ ion as shown below. [102]

$$\text{i} \quad BF_4^- \rightleftharpoons BF_3 + F^-$$

$$\text{ii} \quad BF_3 + BF_4^- \rightleftharpoons (F_3B\text{—}F\text{—}BF_3)^-$$

Complexation of BF_3 with the solvent is not directly involved in fluorine exchange.

The heterogeneous exchange reaction probably occurs via the same type of fluorine bridged intermediate. In view of this it is not surprising that fluorine exchange between $CsBF_4$ and BF_3 is not readily observed. The $B_2F_7^-$ ion has only been successfully isolated in the solid state with large cations. The salts formed readily dissociate to give BF_3 and BF_4^-. The critical factor in determining whether or not the $B_2F_7^-$ ion will be formed by reaction of BF_3 with the BF_4^- ion is proposed to be the distance between the tetrafluoroborate anion and the centre of positive charge in the cation. [108a] When bulky cations are present the distance between the charged centres is increased to such an extent that the interaction of the cation and the tetrafluoroborate anion becomes relatively weak. The co-ordinating power of the tetrafluoroborate anion toward a nucleophile thus approaches

its maximum potential value and it is able to co-ordinate with a free boron trifluoride molecule. Since $\left((CH_3)_4N^+\right)\left(BF_4^-\right)$ does not react with BF_3 [108a], $CsBF_4$ would not be expected to react to any great degree with BF_3 hence no ^{18}F exchange should be observed.

4.8 RESULTS OF REACTION OF AsF_5 WITH CsF

Due to the lack of a suitable As radioisotope only ^{18}F labelled AsF_5 was used to study the reaction of AsF_5 with CsF. The results of four reactions between $AsF_4{}^{18}F$ and non activated CsF are summarised in table 4.18. Figure 4.29 is a plot of solid count rate versus time for one of these experiments. This shows that there is a rapid rise in solid count rate until an equilibrium level is reached after 10 minutes. Comparison of the specific count rate of the $AsF_4{}^{18}F$ before and after reaction shows that within experimental error there is no change. This rules out ^{18}F exchange as the cause of the growth of the solid count rate. The increase in count rate must therefore be due to uptake of the gas by the solid. A sample of $AsF_4{}^{18}F$ counted separately had a specific count rate of 11398 ± 107 counts min^{-1} m mol^{-1} so the count rate of 5910 ± 77 counts min^{-1} in the CsF is equivalent to the uptake of 0.52 ± 0.007m mol of $AsF_4{}^{18}F$ in this experiment. The average uptake observed in the four experiments was 0.498 ± 0.015 m mol.

TABLE 4.18

REACTION OF $AsF_4{}^{18}F$ WITH NON ACTIVATED CsF - SUMMARY OF RESULTS

Amount of CsF g m mol	Amount of $AsF_4{}^{18}F$ Torr m mol	Specific Count Rate of $AsF_4{}^{18}F$ Before Reaction Counts min^{-1} m mol^{-1}	Specific Count Rate of $AsF_4{}^{18}F$ After Reaction Counts min^{-1} m mol^{-1}	Count Rate of solid Counts min^{-1}	Uptake m mol
0.50 ± 0.01 3.29 ± 0.06	300 ± 2 1.0 ± 0.01	11398 ± 107	11398 ± 107	5910 ± 77	0.520 ± 0.007
"	"	8932 ± 95	8930 ± 95	4377 ± 66	0.490 ± 0.007
"	"	10647 ± 103	10647 ± 103	5324 ± 73	0.500 ± 0.007
"	"	4236 ± 65	4235 ± 65	2033 ± 45	0.480 ± 0.010

Figure 4·29

Reaction of $AsF_4^{18}F$ with non activated CsF

Solid count rate vs reaction time

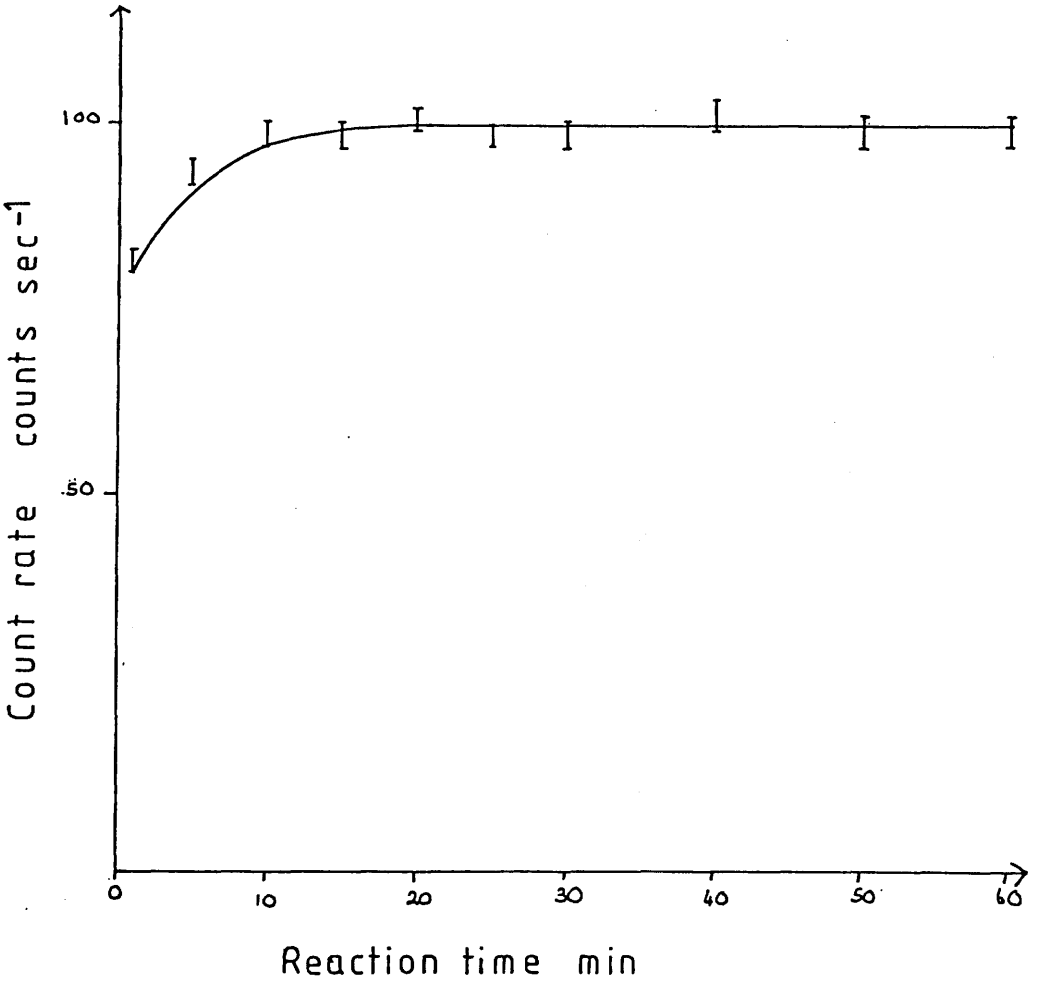

A sample of $AsF_4{}^{18}F$ was allowed to react with CsF to produce a radioactive solid. The labelled gas was removed and replaced by 300 Torr of non radioactive AsF_5. After one hour the gas phase count rate was barely above background level showing that the $AsF_4{}^{18}F$ adsorbed by the CsF does not exchange with the gas phase $AsF_4{}^{18}F$. The $AsF_4{}^{18}F$ on the surface of the CsF must therefore be permanently adsorbed.

The same result is obtained if CsF is first allowed to react with non radioactive AsF_5 and then with $AsF_4{}^{18}F$. Table 4.19 shows the results of one such reaction. The observed count rates are very low because they are gas phase count rates, and the well scintillation counter used cannot count materials in the gas phase very efficiently. The count rate of the CsF after reaction is barely above background level thus confirming there is no exchange at room temperature between adsorbed AsF_5 and AsF_5 in the gas phase.

A similar series of experiments was carried out with $AsF_4{}^{18}F$ and CsF activated by pretreatment with hexafluoroacetone. Table 4.20 shows the results of four reactions between $AsF_4{}^{18}F$ and activated CsF.

The results are similar to those obtained with non activated CsF. The solid count rate increases rapidly over the first ten minutes of the reaction before reaching its equilibrium level. This rapid increase is shown in figure 4.30. This increasing solid count rate must be due to uptake of gas

TABLE 4.19

RESULTS OF REACTION OF $AsF_4{}^{18}F$ WITH NON ACTIVATED CsF PRETREATED WITH AsF_5

Time (min)	Solid + Gas Counts min^{-1}	Gas Counts min^{-1}	Solid Counts min^{-1}
1	1089	1137	-48
6	1151	1171	-20
11	1118	1162	-44
16	1170	1149	+21
21	1164	1171	+7
26	1177	1150	+27
31	1159	1163	-4
35	1148	1140	+8
45	1176	1148	+28
55	1193	1182	+11

Count rate of solid after reaction = 134 counts min^{-1}

Average background count = 112 counts min^{-1}

Specific count rate of $AsF_4{}^{18}F$ = 10647 counts m mol^{-1} min^{-1}

TABLE 4.20

REACTION OF $AsF_4{}^{18}F$ WITH ACTIVATED CsF - SUMMARY OF RESULTS

Amount of CsF g m mol	Amount of $AsF_4{}^{18}F$ Torr m mol	Specific Count Rate of $AsF_4{}^{18}F$ Before Reaction Counts min^{-1} m mol^{-1}	Specific Count Rate of $AsF_4{}^{18}F$ After Reaction Counts min^{-1} m mol^{-1}	Count Rate of Solid After Reaction Counts min^{-1}	Uptake m mol
0.50 ± 0.01 3.29 ± 0.06	300 ± 2 1.0 ± 0.01	13567 ± 116	13567 ± 116	11538 ± 107	0.850 ± 0.007
"	"	7755 ± 88	7751 ± 88	6747 ± 82	0.870 ± 0.01
"	"	10647 ± 103	10647 ± 103	8837 ± 94	0.830 ± 0.009
"	"	4236 ± 65	4235 ± 65	3722 ± 61	0.880 ± 0.014

Figure 4·30

Reaction of $AsF_4^{18}F$ with activated CsF

Solid count rate vs reaction time

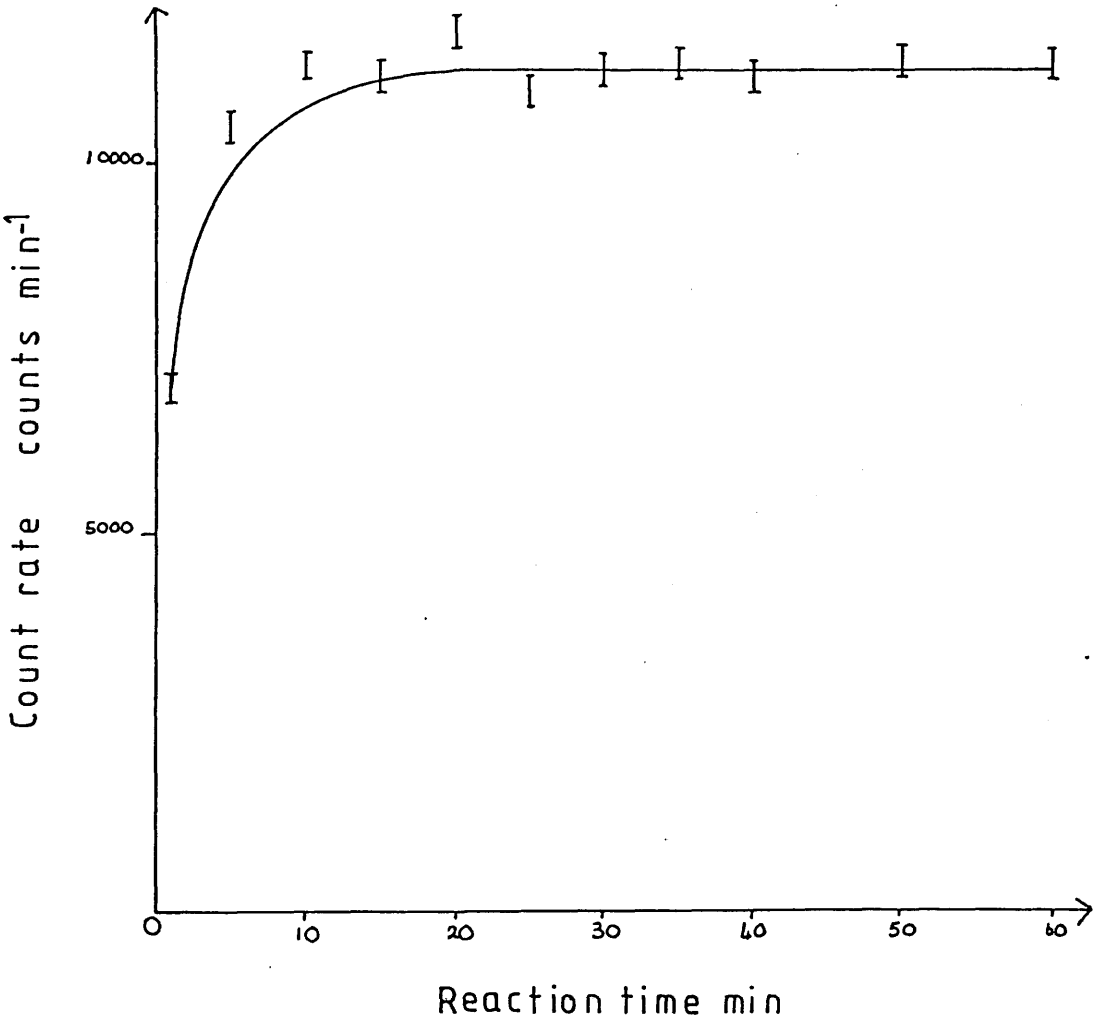

by the solid as there is no change in the specific count rate of the $AsF_4{}^{18}F$ before and after reaction. The $AsF_4{}^{18}F$ used in this experiment had a specific count rate of 13567 $\pm$ 116 counts min^{-1} m mol^{-1} so a solid count rate of 11538 $\pm$ 107 counts min^{-1} corresponds to an uptake of 0.850 $\pm$ 0.007 m mol of $AsF_4{}^{18}F$. The average uptake observed in the four experiments was 0.857 $\pm$ 0.020 m mol of $AsF_4{}^{18}F$.

Treatment of the activated CsF with AsF_5 prior to reaction with $AsF_4{}^{18}F$ has very little effect on the result obtained. There is still a rapid rise in solid count rate and the equilibrium level is reached after 10 minutes. The only difference observed is that the equilibrium count rate corresponds to an uptake of 0.777 $\pm$ 0.011 m mol of $AsF_4{}^{18}F$ compared to 0.857 $\pm$ 0.020 m mol for activated CsF which had not been pretreated with AsF_5. Figure 4.31 shows a plot of solid count rate versus time for this reaction.

During the reactions of $AsF_4{}^{18}F$ and activated CsF the reaction vessel became very hot and some sintering of the CsF was observed.

4.9 DISCUSSION OF AsF_5 RESULTS

The reaction of $AsF_4{}^{18}F$ with both activated and non activated CsF results in the uptake of gas with no ^{18}F exchange observed in either case. Similarly to the reaction of $BF_2{}^{18}F$ with CsF there are three different species which could be present on the

Figure 4·31

Reaction of $AsF_4^{19}F$ with activated CsF pretreated with AsF_5

Solid count rate vs reaction time

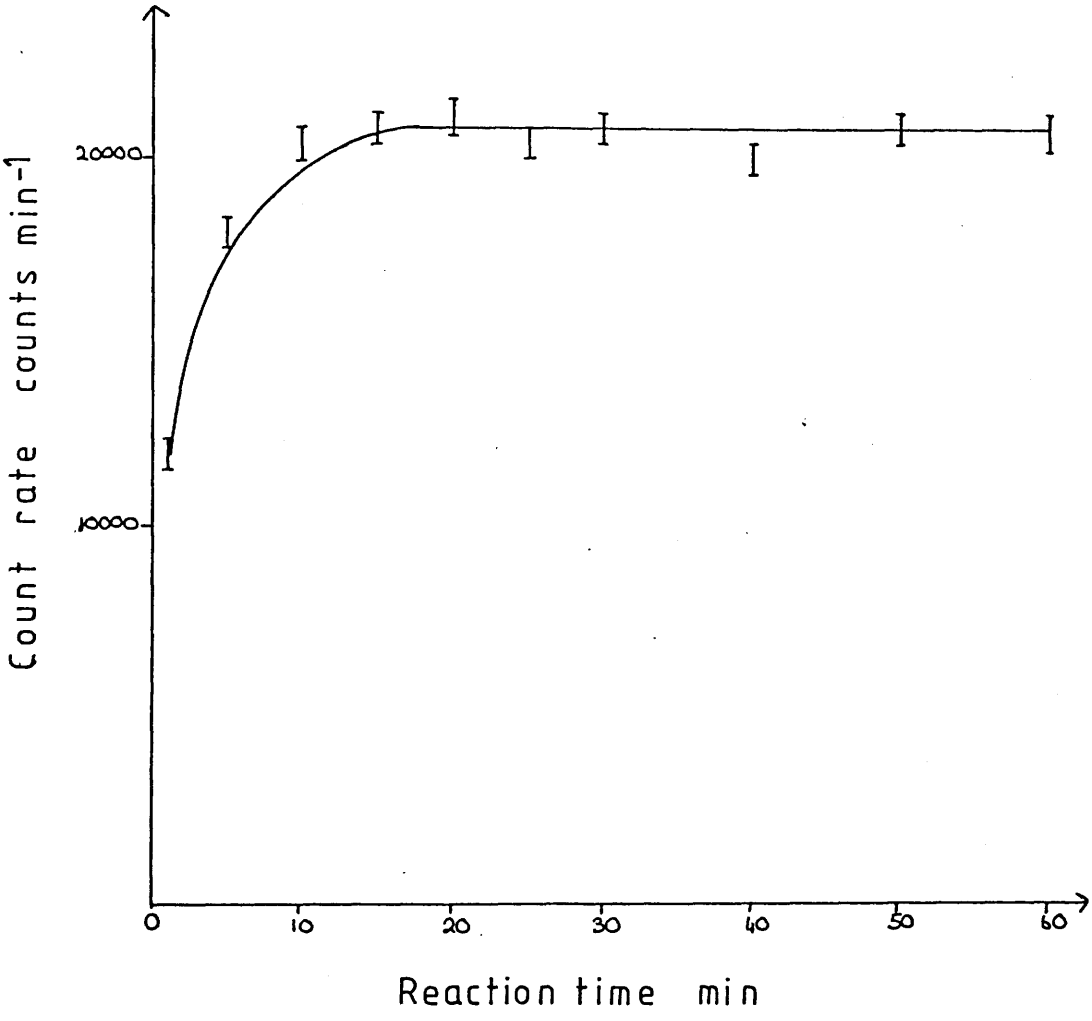

surface of the CsF, 1) an adsorbed molecule of AsF_5, 2) the AsF_6^- anion or 3) the $As_2F_{11}^-$ anion. The AsF_6^- anion has been well characterised spectroscopically[110] and many salts are known[111]. The $As_2F_{11}^-$ anion has been identified in solution[112] and isolated as the tetraethylammonium and tetrabutylammonium salts.[113] Both salts lose AsF_5 at temperatures above 0^oC. The release of AsF_5 is reversible and finely powdered solid Et_4NAsF_6 slowly absorbs gaseous AsF_5. No reaction has been observed between caesium hexafluoroarsenate and arsenic pentafluoride.[113] Figures 4.32 and 4.33 show the structures of the AsF_6^- and $As_2F_{11}^-$ anions.

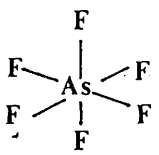

Figure 4.32

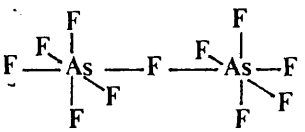

Figure 4.33

The infra red spectrum of the CsF after reaction with $AsF_4{}^{18}F$ is shown in table 4.21, together with the literature values for AsF_5 gas, $CsAsF_6$ and $Et_4NAs_2F_{11}$. Although the infra red spectrum of the CsF only shows one band it is reasonable to assume that $CsAsF_6$ has been formed. The band at 700 cm^{-1} is sharp and does not show any fine structure and there is no band in the 500 cm^{-1} region which rules out the possibility of the $As_2F_{11}^-$ anion. The absence of any other bands rules out the possibility of the surface species being adsorbed molecules of AsF_5.

TABLE 4.21

INFRA RED SPECTRUM OF CsF AFTER REACTION WITH $AsF_4{}^{18}F$

CsF	$CsAsF_6$ [110]	AsF_5 [114]	$Et_4NAs_2F_{11}$ [113]
		800 v_5E	
		785 v_3A_2	770-650 sbr
700 s v_3	699 s v_3F_{1u}		
			500 ms
	392 m v_4F_{1u}	400 v_4A_2	392 m
		366 v_6E	
		128 v_7E	

The ratio of the amount of $AsF_4{}^{18}F$ uptake by non activated CsF to the amount of uptake by activated CsF is 1:1.72. The ratio of surface areas is 1:10, so the uptake of $AsF_4{}^{18}F$ by activated CsF is much lower than expected. This is due to the high degree of sintering which occurs during the reaction which is highly exothermic. The sintering will reduce the available surface area and hence uptake of gas.

The uptake of $AsF_4{}^{18}F$ by non activated CsF can be prevented by treatment of the CsF with non radioactive AsF_5. This shows that adsorption of AsF_5 by CsF is limited to a set number of distinct sites which are quickly filled. Treating activated CsF in a similar way results in a slightly reduced uptake of $AsF_4{}^{18}F$. A possible explanation is that the heat given out during the reaction causes some of the large granules formed by sintering during the original reaction to break open and thus reveal a new surface for adsorption of gas.

4.10 RESULTS OF REACTION OF CO_2 WITH ACTIVATED CsF

The reaction of CO_2 with activated CsF was studied using ^{14}C labelled CO_2, by conventional manometric means, and by infra red spectroscopy.

The reaction between $^{14}CO_2$ and activated CsF was studied at nine different pressures between 25 and 300 Torr.

As ^{14}C is a soft β emitter only surface activities could be measured directly. A measure of the bulk reaction was obtained from the drop in gas phase counts within the closed reaction system. Each reaction was followed for 1 hour. After 1 hour the $^{14}CO_2$ was removed from the counting vessel and the activity on the solid in the absence of gas was measured. Figures 4.34, 4.35 and 4.36 are plots of solid activity versus time at initial $^{14}CO_2$ pressures of 25, 150 and 300 Torr. These figures show that the reaction between $^{14}CO_2$ and CsF is complete within the period before the first count is taken. The surface count rate is independent of initial pressure as shown in figure 4.37. At all $^{14}CO_2$ pressures studied a constant surface count rate of 50.12 ± 5.2 was obtained. The $^{14}CO_2$ used had a specific count rate of 3325 ± 15 counts s^{-1} m mol^{-1} so this surface count rate is equivalent to an uptake of 0.015 m mol of $^{14}CO_2$. When the $^{14}CO_2$ is removed from the counting vessel the surface count rate drops sharply to 8.58 ± 2.2 counts s^{-1}.

There seems to be no correlation between solid count rate retained after removal of the $^{14}CO_2$ and initial pressure of $^{14}CO_2$. This is illustrated by figure 4.38 which is a plot of solid count rate in the absence of gas versus initial $^{14}CO_2$ pressure.

Although the amount of CO_2 adsorbed on the surface of the CsF is independant of initial pressure, the total uptake of $^{14}CO_2$ calculated from the fall in gas phase counts is

Figure 4·34

Reaction of $^{14}CO_2$ with activated CsF

Solid count rate vs reaction time

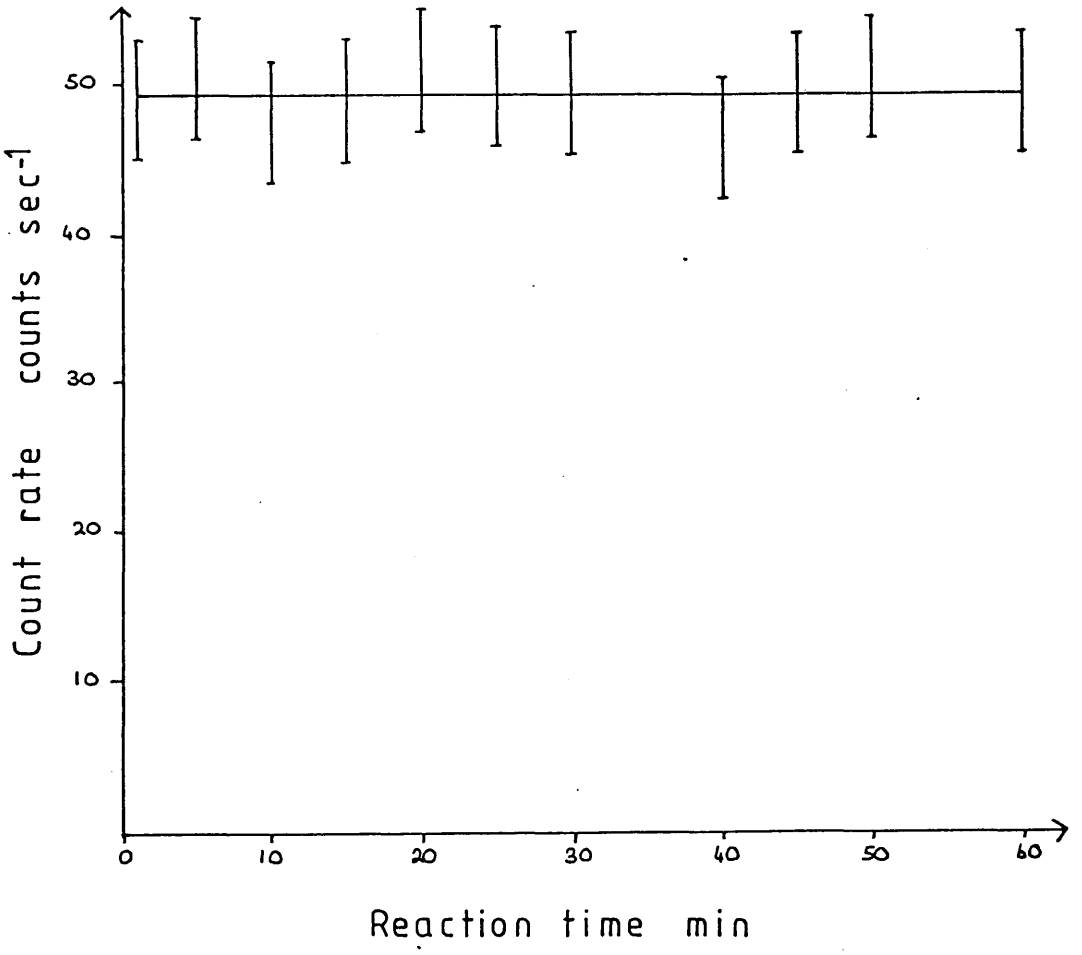

Initial pressure of $^{14}CO_2$ = 5 Torr

Figure 4·35

Reaction of $^{14}CO_2$ with activated CsF

Solid count rate vs reaction time

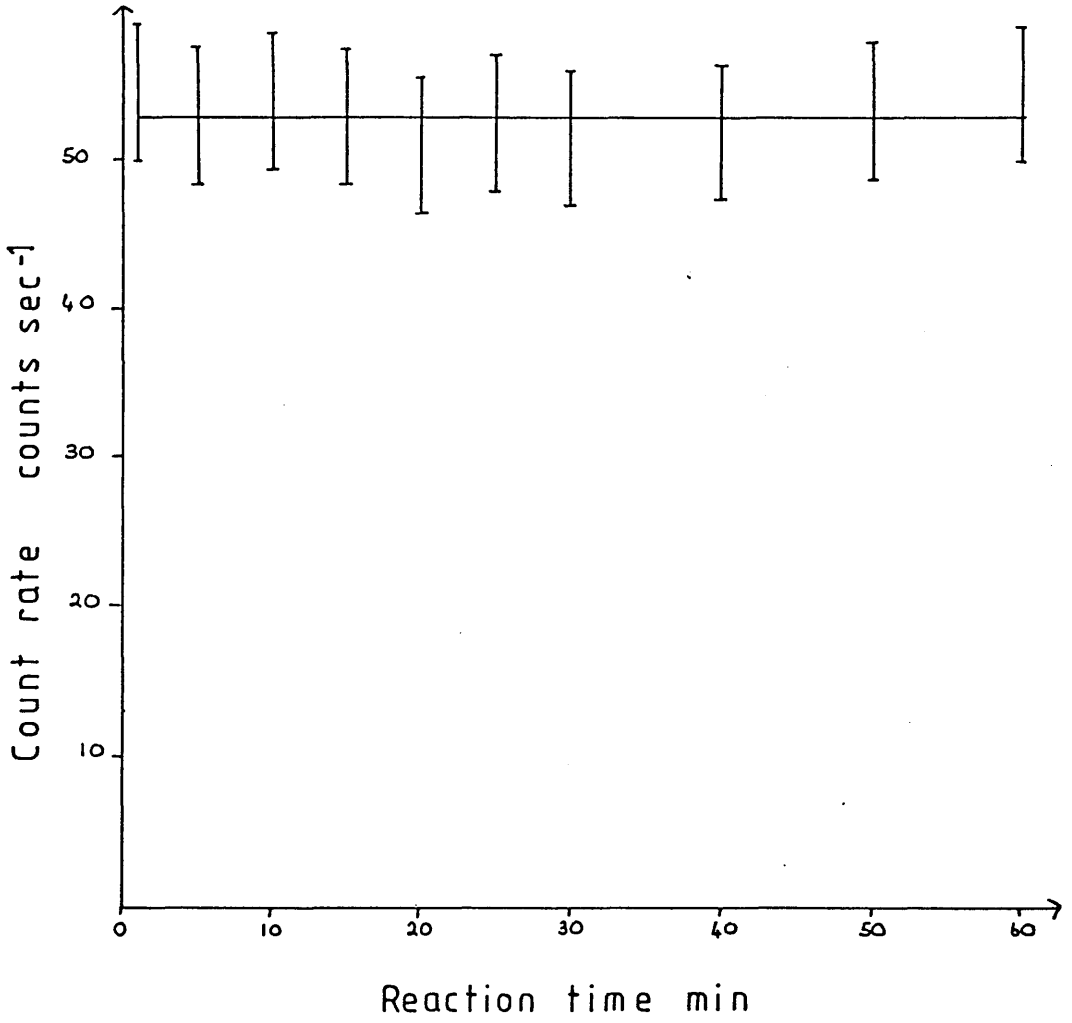

Initial pressure =150 Torr

Figure 4·36

Reaction of $^{14}CO_2$ with activated CsF

Solid count rate vs reaction time

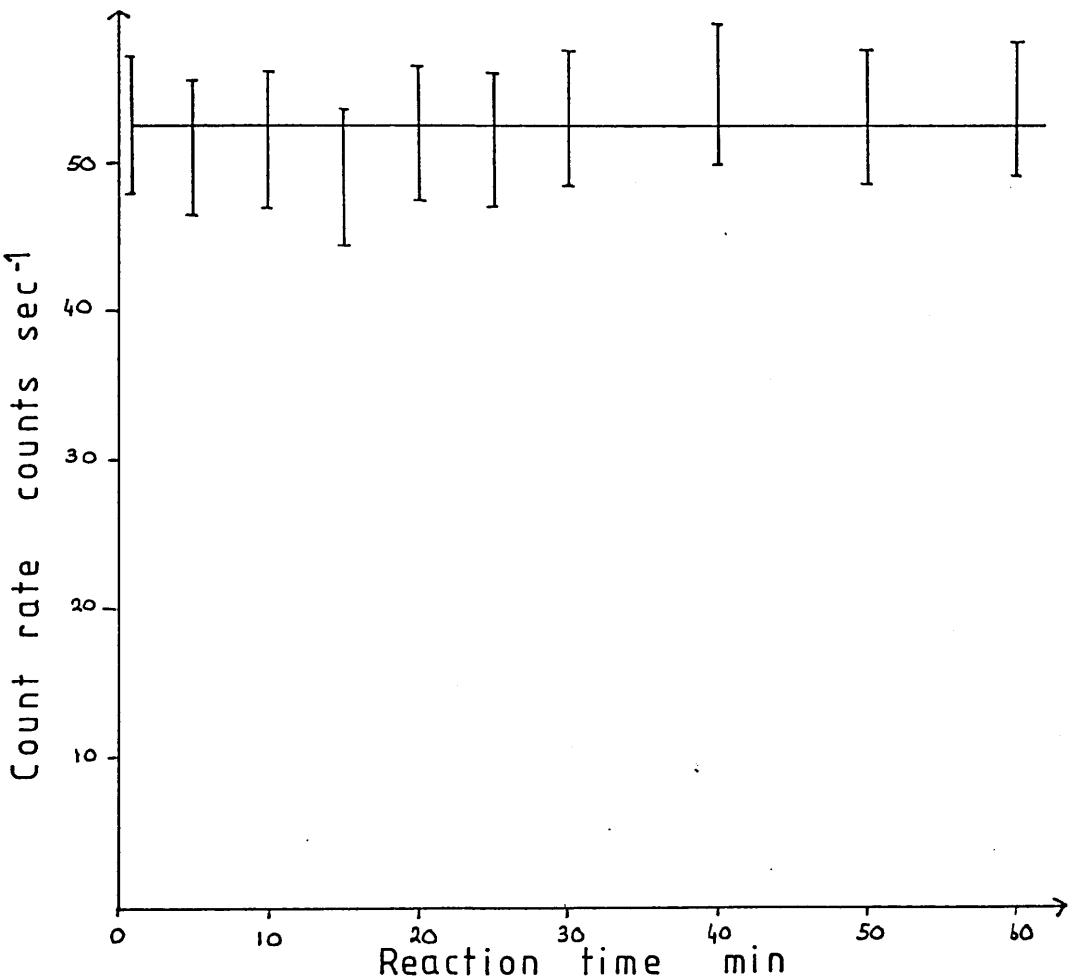

Initial pressure = 300 Torr

Figure 4·37

Reaction of $^{14}CO_2$ with activated CsF

Solid count rate vs initial pressure

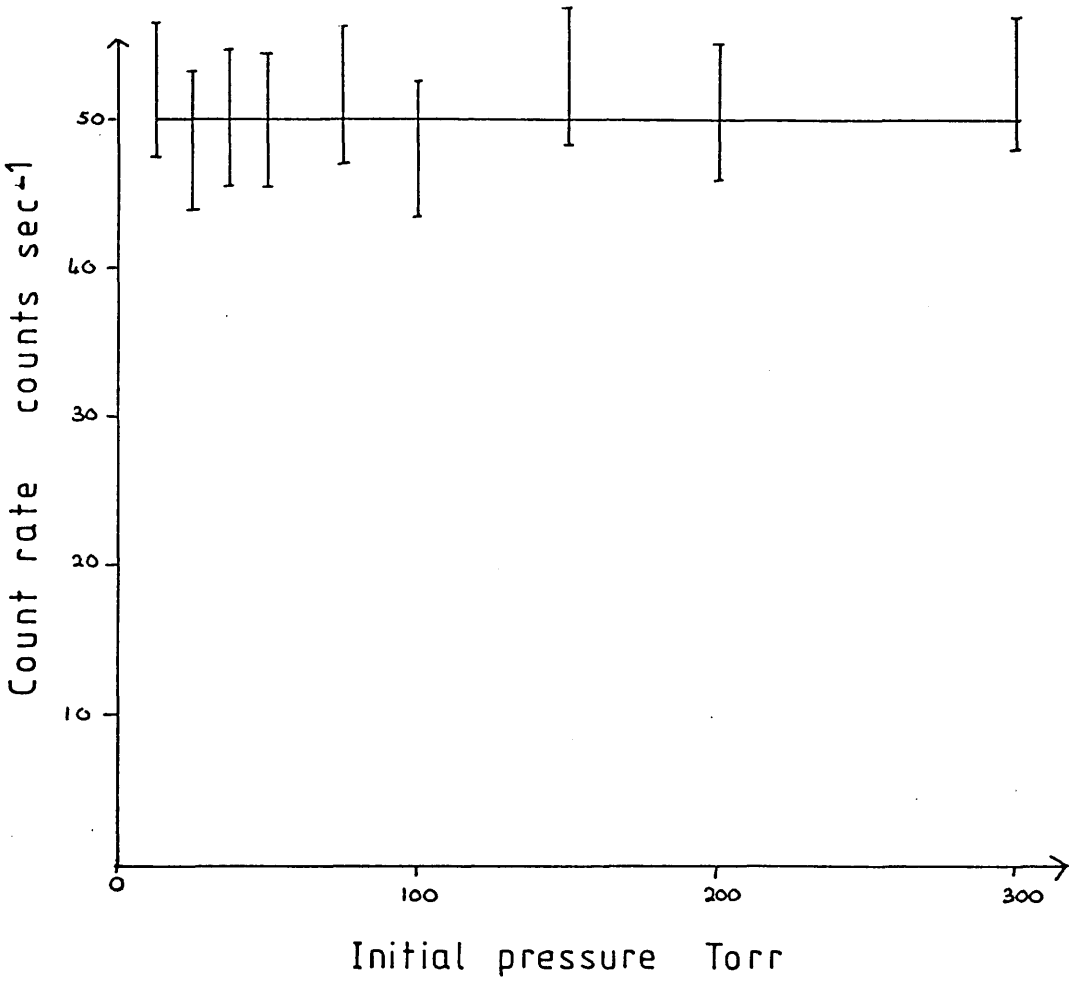

Figure 4·38

Reaction of $^{14}CO_2$ with activated CsF

Retained solid counts vs initial pressure

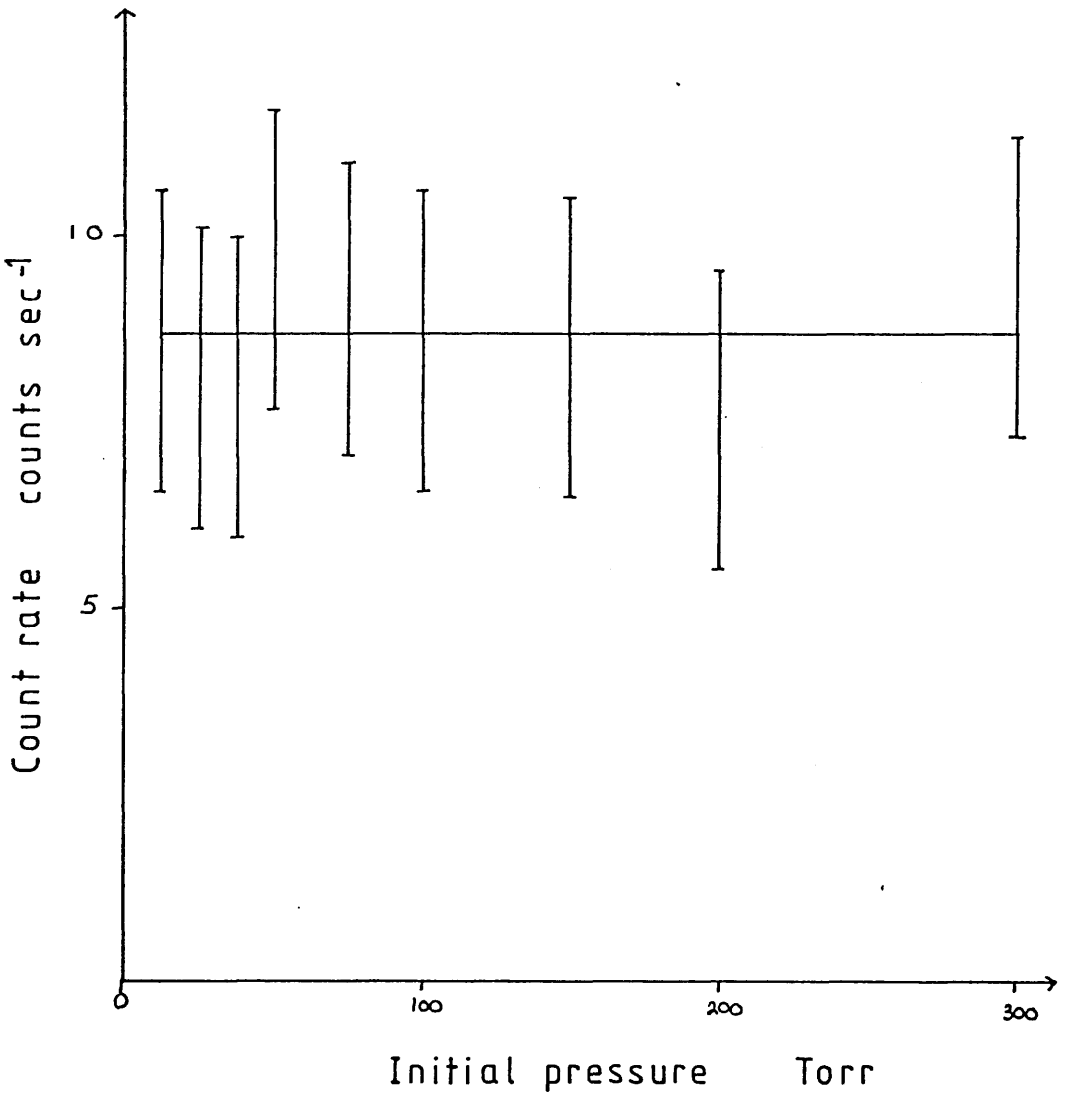

dependant on initial pressure. In the range of pressures studied the maximum uptake of 0.108 m mol of CO_2 occurred at 300 Torr the highest pressure studied. Figure 4.39 is a plot of total uptake of CO_2 versus initial CO_2 pressure. The results are summarised in table 4.22.

The experiments carried out with $^{14}CO_2$ indicated that the bulk uptake of CO_2 by activated CsF is pressure dependant. With this in mind the manometric studies were carried out using an initial pressure of 300 Torr, the maximum possible in this system.

Two experiments were carried out using 0.50g of activated CsF. Reductions in CO_2 pressure of 10.91 Torr and 12.12 Torr were observed. As the volume of the system is 156.689 cm^3 these pressure drops are equivalent to gas uptakes of 0.099 $\pm$ 0.020 and 0.110 $\pm$ 0.020 m mol. Infra red examination of the solid after reaction did not reveal any bands in addition to those due to activated CsF. In view of this it was decided to carry out the experiment in the presence of MeCN in an attempt to reproduce the results of Martineau and Milne.[30]

A reaction vessel containing activated CsF (3.0 m mol), CO_2 (10.0 m mol) and MeCN (10 ml) together with six ball bearings was shaken for 12 hours before removal of the solvent. The white product obtained was ground in an agate mortar and pestle and its infra red spectrum recorded as a Nujol mull

Figure 4·39

Reaction of $^{14}CO_2$ with activated CsF

Bulk uptake of CO_2 vs initial pressure

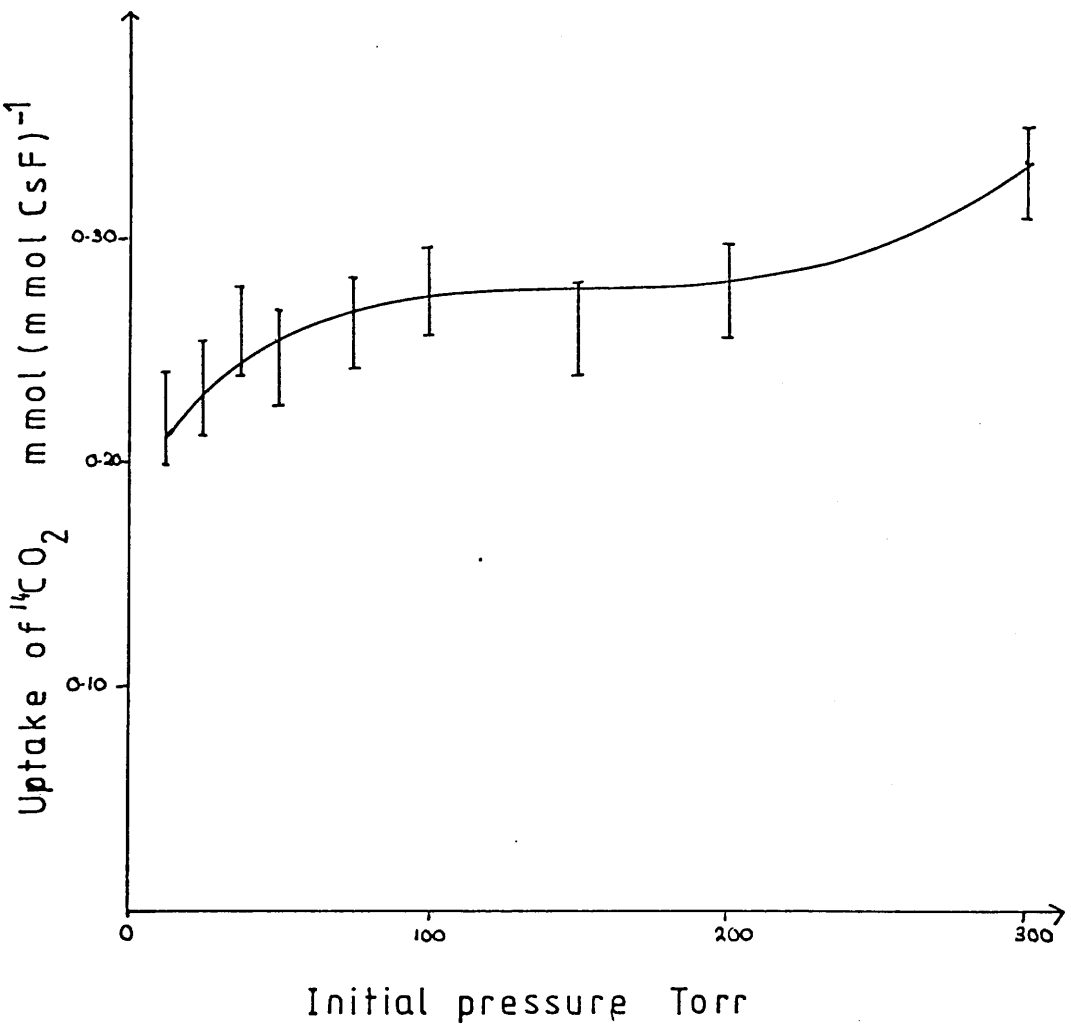

TABLE 4.22

SUMMARY OF RESULTS OF $^{14}CO_2$ + CsF REACTIONS	
	m mol (m mol CsF)$^{-1}$
Total uptake of CO_2	0.033
Surface uptake of CO_2	0.0045
Amount retained by CsF	0.00078

Figure 4·40

Reaction of CO_2 with activated CsF in MeCN

Infrared spectrum of reaction product

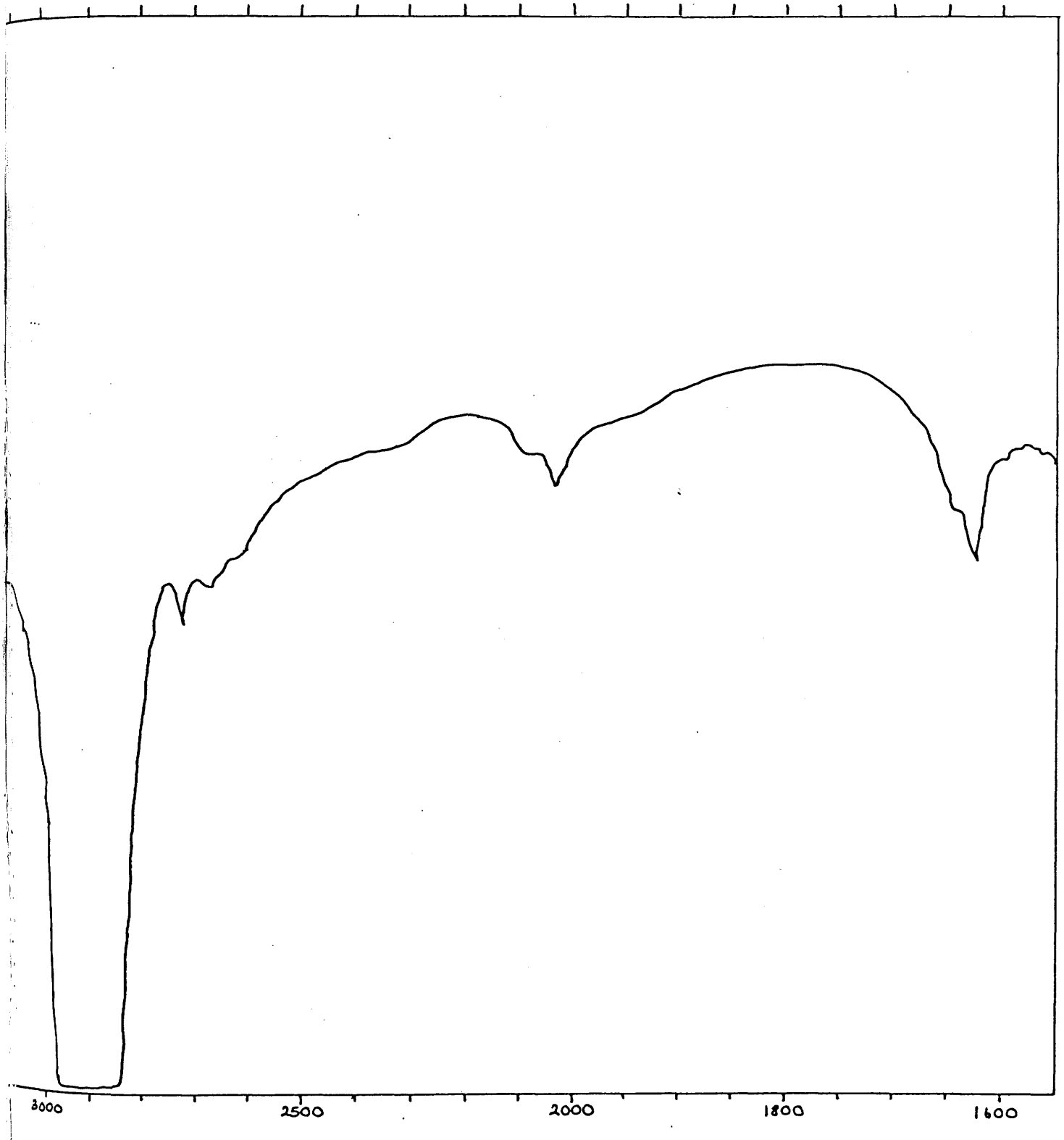

Figure 4·40 continued

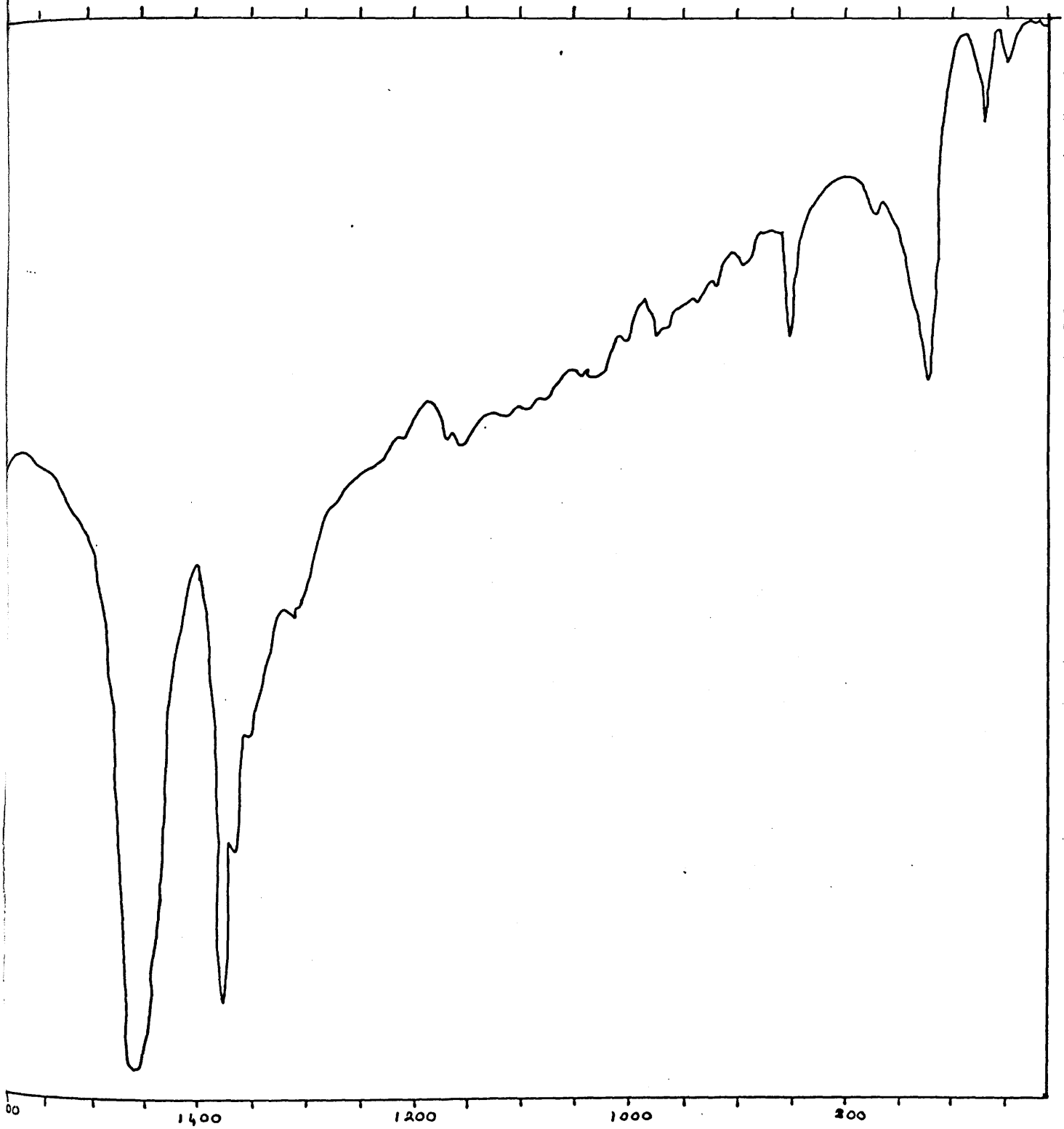

between AgCl plates (Figure 4.40). The details of the infra red spectrum obtained are listed in table 4.23, together with the infra red spectrum of the product obtained by Martineau and Milne in 1971.[30]

4.11 DISCUSSION OF CO_2 RESULTS

Since Martineau and Milne's claim to have prepared $Cs_2CO_2F_2$, there have been several unsuccessful attempts to reproduce their results. In 1979 Lawlor and Passmore[31] reported no reaction between CsF and CO_2 at pressures up to 110 atm. They also reported that CO_2 would not react with Et_4NF unless water was present. On the basis of these results they proposed that Martineau and Milne had obtained the infra red spectrum of a hydrolysis product rather than of the reported $Cs_2CO_2F_2$. Further evidence for this view was provided by S J David [32] and B S Ault [115] who reported matrix isolation studies of the $CO_2F_2^{2-}$ and CO_2F^- anions. None of the infra red bands observed in these studies correspond to any of those observed by Martineau and Milne (Table 4.24). In view of this David and Ault also suggested that Martineau and Milne had obtained the infra red spectrum of a hydrolysis product.

The infra red spectrum of the solid prepared in this work contains all the bands observed by Martineau and Milne, together with several other bands (Table 4.23). Comparison of this spectrum with those of CO_3^{2-}, HCO_3^- and HF_2^-, the

TABLE 4.23

REACTION OF CsF AND CO_2 IN MeCN

INFRA RED SPECTRUM OF REACTION PRODUCT

This work (cm^{-1})		Literature[30] Cs CO_2F_2		
2720	w			
2020	w			
1640	m			
1625	m			
1365	s			
1350	s			
1310	m			
1150	m			
1010	w	CO and CF stretching vibrations	1008	wsh
980	m		985	m
850	s		850	s
670	s			
650	w	deformations	680	s
			656	wsh

TABLE 4.24

COMPARISON OF INFRA RED SPECTRA (cm^{-1})

Ault[115] CO_2F^-	Ault[32] and David $CO_2F_2^{2-}$	Martineau and Milne[30] $CO_2F_2^{2-}$
1749 ν_4, B_2 C-O str	1382 C-O str	
1316 ν_2, A_1 C-O str		1008)
		985) CO AND CF
	930 C-F str	) stretches
883 ν_1, A_1 C-F str		)
		850)
	700 C-F dif	C-F
		680) deformations
		656)
	612 C-F def	

likely hydrolysis products, shows that $Cs_2CO_2F_2$ has definitely not been formed, as all of the observed bands can be assigned to one of three hydrolysis products (Table 4.25).

Although Martineau and Milne claim that the characteristic bands for CO_3^{2-} and HCO_3^- do not appear in their spectrum, the five bands observed could quite reasonably be assigned to these ions as shown in table 4.25.

TABLE 4.25

INFRA RED SPECTRUM OF REACTION PRODUCT

COMPARISON WITH SPECTRA OF HYDROLYSIS PRODUCTS (cm^{-1})

THIS WORK	$NaHF_2$ [86]	Cs_2CO_3 [116]	$KHCO_3$ [117]
2720	2755 $\nu_3 + 2\nu_1$		
2020	2100 $\nu_3 + \nu_1$		
1640			1648) ν_2
1625			1628) C-O str
		1461 ν_3, B_2	
1365			1368 ν_3
1310		1319 ν_3, A_1	C-O str
1150 vCF			
1010		1018 ν_1, A_1	
980			975 ν_5
850		870 ν_2, B_1	C-(OH) str
670		685 ν_4, A_1	
650			656 ν_9
			H Torsion

In addition to their infra red evidence. Martineau and Milne supported their claim with caesium and fluorine analyses and by comparison of the x-ray powder photograph of their product with that of Cs_2BeF_4. However, these results are not conclusive since Cs_2CO_3 would also give a similar x-ray powder pattern to Cs_2BeF_4 and a mix of Cs_2CO_3 and HF would give similar analytical results to $Cs_2CO_2F_2$ as shown below:

$Cs_2CO_2F_2$ requires	Cs 76.42%	F 10.92%
Cs_2CO_3 2HF requires	Cs 72.67%	F 10.38%

The results obtained in this work therefore show that Martineau and Milne did not prepare $Cs_2CO_2F_2$. They reported the infra red spectrum of a hydrolysis product rather than $Cs_2CO_2F_2$.

In addition to the results previously discussed Martineau and Milne also reported that dry CsF shows no tendency to adsorb carbon dioxide. The results of studies using $^{14}CO_2$ and constant volume manometer measurements show this observation to be false. Caesium fluoride will adsorb CO_2 at room temperature if the caesium fluoride is activated by treatment with hexafluoroacetone before use. The amounts involved are very small, 0.033m mol of CO_2 adsorbed per m mol of CsF, determined from both $^{14}CO_2$ and manometric measurements. The amount of CO_2 involved in the reaction is too small to be detected by infra red spectroscopy and can only be detected by

very accurate manometric work or by radiotracer techniques. This may explain why Martineau and Milne did not observe any uptake of CO_2 at room temperature. They also do not give any indication of how the CsF was treated before reaction. The fact that there have been several unsuccessful attempts to reproduce Martineau and Milne's work suggests that the method of CsF pretreatment is critical. None of the other attempts have used hexafluoroacetone pretreatment with heating being the most common treatment. In this work the use of hexafluoroacetone treated CsF resulted in the reproduction of Martineau and Milnes results at the first attempt.

The use of $^{14}CO_2$ allows bulk and surface reactions to be differentiated. The results obtained show that surface adsorption accounts for only a small proportion of the total gas uptake. The amount of surface adsorption is independant of initial pressure over the range of pressures studied but the adsorption is not permanent. If the $^{14}CO_2$ is removed from the counting vessel 83% of the surface activity is also removed. This suggests that there are two distinct adsorbed species present on the surface of the CsF, one which is weakly adsorbed and can be removed by pumping and one which is permanently adsorbed. The permanently adsorbed species is most likely to be CO_2F^- rather than $CO_2F_2^{2-}$

since David and Ault have shown that the $CO_2F_2^{2-}$ anion has limited stability even at low temperatures.[32] If CO_2F^- is assumed to be the permanently adsorbed species, the weakly adsorbed species is most likely to be a weakly adsorbed molecule of CO_2.

4.12 COMPARISON OF RESULTS

Both activated and non activated CsF react readily at room temperature with the Lewis acids studied. Experiments using two different isotopes have shown that the reaction occurs both in the bulk of the solid and on its surface. Two distinct species, one permanently adsorbed and one weakly adsorbed, have been identified on the surface of the CsF during reactions with CO_2, F_2CO and SF_4. Surface species could not be identified in the reactions of AsF_5 and BF_3 with CsF due to the lack of suitable radioisotopes.

In the reactions involving AsF_5, BF_3 and SF_4, uptake of gas occurs but there is no measurable ^{18}F exchange. ^{18}F exchange between BF_3 and $CsBF_4$ is observed in the presence of a solvent.

^{18}F exchange between $SF_3{}^{18}F$ and caesium fluoride at 150°C and 50°C was reported by Fraser and coworkers in 1972[70]

who quoted fractions exchanged of 0.2 at 150°C and 0.018 at 50°C. In this study there is no mention of any of the $SF_3{}^{18}F$ being retained by the CsF.

A later study of this system by the same workers published in 1978[118] reported f values of > 1 if the CsF was reground between each cycle of the pretreatment process. In this study it was suggested that a small quantitiy of SF_4 may be retained on the CsF surface. This together with the results reported in this thesis cast doubt upon the original results of Fraser and coworkers.

No ^{18}F exchange was observed between $Cs^{18}F$ and SF_4 at 50°C (section 2.10.2). Studies using $^{35}SF_4$ and infra red spectroscopy show that SF_4 is permanently adsorbed by the CsF. This means that the fraction exchanged of 0.018 at 50°C quoted by Fraser and coworkers[70] is wrong. The activity observed in the CsF must have been due to uptake of $SF_3{}^{18}F$ and not ^{18}F exchange. The value quoted for 150°C is also an over estimate as again no allowance has been made for uptake of gas.

Studies carried out using $^{35}SF_4$ show that there are two distinct species present on the surface of the CsF during the reaction. A permanently adsorbed species which is presumed to be SF_5^- and the major surface species which is weakly adsorbed SF_4. This confirms the findings of Kolta and coworkers in 1982[59] who proposed a weakly

adsorbed state of SF_4 as the active species in the CsF catalysed chlorofluorination of SF_4.

In the reaction of ^{18}F FCO with activated CsF both ^{18}F exchange and uptake of gas are observed. This reaction was studied by Fraser and coworkers in 1973[79]. ^{18}F exchange was observed at 15°C, 50°C and 150°C but as in the case of $SF_3{}^{18}F$ and CsF no allowance was made for the uptake of F_2CO by CsF. The fraction exchanged at 15°C (0.013) is much lower than that observed in this work (section 4.4). This difference is due to the different techniques used to activate the CsF before use. Fraser and coworkers activated their CsF by three cycles of pumping and heating in vacus at 150°C for 3 hours. The work reported in this thesis used CsF activated by treatment with $(CF_3)_2CO$ as described in chapter 3.

In all cases except with CO_2 the bulk reaction results in the formation of the anion of the Lewis acid. The reaction of BF_3 with activated CsF results in complete conversion of the CsF to $CsBF_4$. AsF_5 reacts with activated CsF to produce 30% $CsAsF_6$. The results of work involving repeated addition of AsF_5 to the same sample of CsF suggest that complete conversion to $CsAsF_6$ is possible if the solid is ground between each addition of gas.

The results reported in this chapter suggest that hexafluoroacetone activated CsF would be a useful

synthetic reagent. $CsAsF_6$, $CsBF_4$, $CsOCF_3$ and $CsSF_5$ are all formed at room temperature. $CsBF_4$ and $CsAsF_6$ are normally prepared by dissolving CsF or $CsHF_2$ in aqueous HF and passing AsF_5 or BF_3 through the solution until no further precipitate is formed. The preparation of $CsOCF_3$ from non activated CsF requires a solvent such as MeCN and the preparation of $CsSF_5$ normally requires a high temperature. The use of activated caesium fluoride would mean that these salts could be prepared at room temperature directly from a gas/solid reaction without the need for any solvents.

In the reaction of CO_2 with activated CsF the amount of gas adsorbed during the reaction is too small to be detected by infra red spectroscopy unless the reaction is carried out in the presence of a solvent. If the reaction is carried out in MeCN the infra red spectrum of the product indicates various hydrolysis products rather than the expected $CsCOF_2$ or $Cs_2CO_2F_2$.

All of the reactions studied are independent of initial gas pressure except those of CO_2 and F_2CO with activated CsF. The reaction of CO_2 with activated CsF shows a slight dependance on initial gas pressure whereas the uptake of gas in the reaction of F_2CO with CsF is directly related to the initial gas pressure. In the reaction of F_2CO with CsF there is more than one type of adsorbed species present in both the bulk of the solid and on its surface.

In all the systems studied surface coverage is independant of initial pressure at all pressures greater than 20 Torr and the amount adsorbed on the surface is the same, within experimental error, in each case. The number of molecules of gas adsorbed on the surface is of the same order of magnitude as the estimated number of surface F^- ions. This suggests that adsorption occurs at F^- sites. However, due to the many assumptions which have to be made in estimating the number of surface F^- ions, the possibility of adsorption at other sites or of multilayer adsorption cannot be ruled out.

Figure 4.41 shows a plot of uptake of gas versus time for the reaction of each of the Lewis acids studied with non activated caesium fluoride. Figure 4.42 shows a similar plot for the reactions with activated caesium fluoride. The amount of uptake of gas by non activated CsF is related to the Lewis acidity of the gas, that is the stronger the Lewis acid, the greater the uptake. The fluoride ion affinities of the various acids used are listed in table 4.26.

The order of uptake of gas by activated CsF is not so easily explained. Although AsF_5 is a stronger Lewis acid than BF_3, it reacts to a lesser extent. This may be due to the sintering which occurs during the reaction but it could also be due to the porosity of the activated CsF.

Figure 4·41

Uptake of Lewis acids by non activated CsF

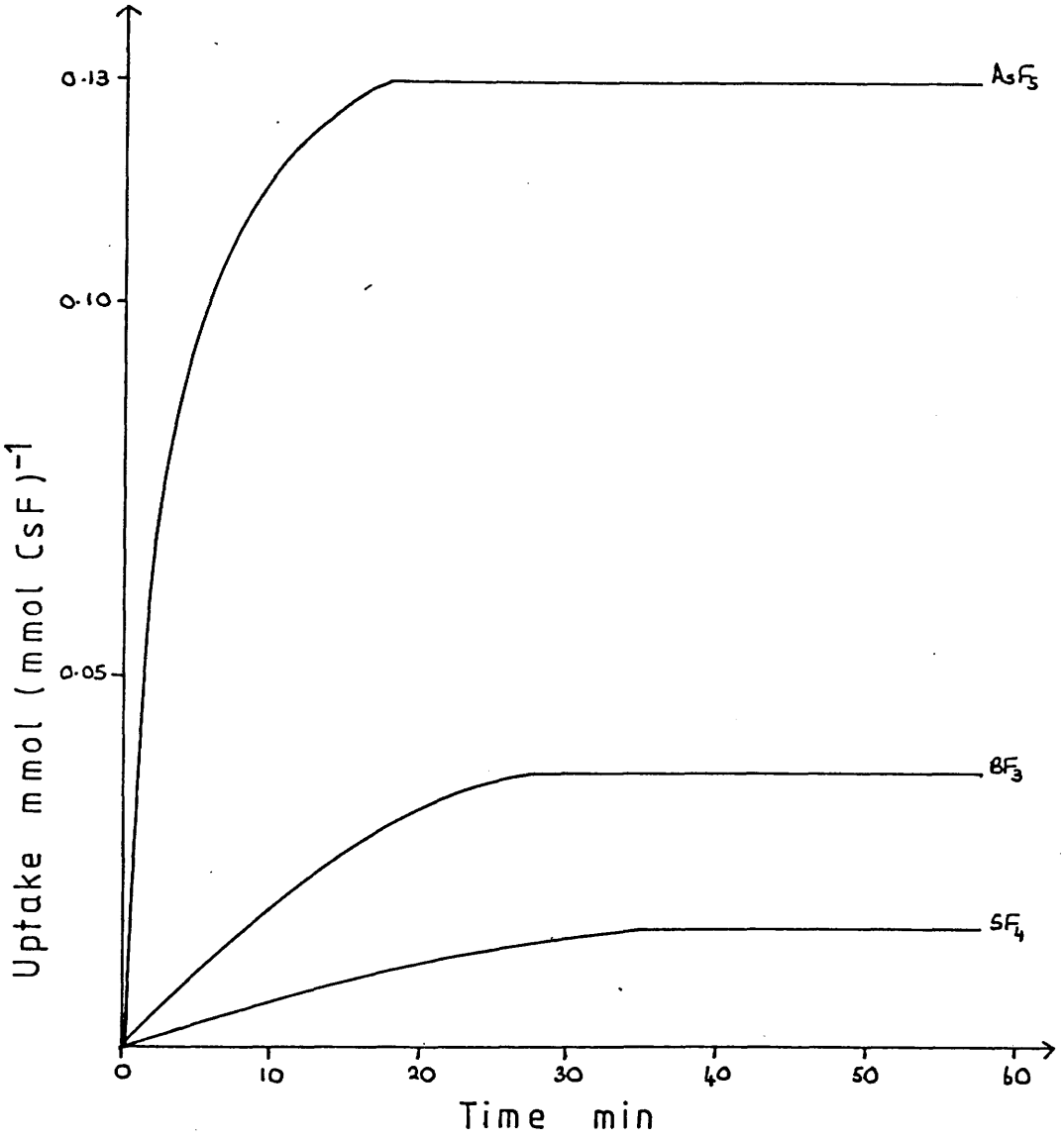

Figure· 4·42

Uptake of Lewis acids by activated CsF

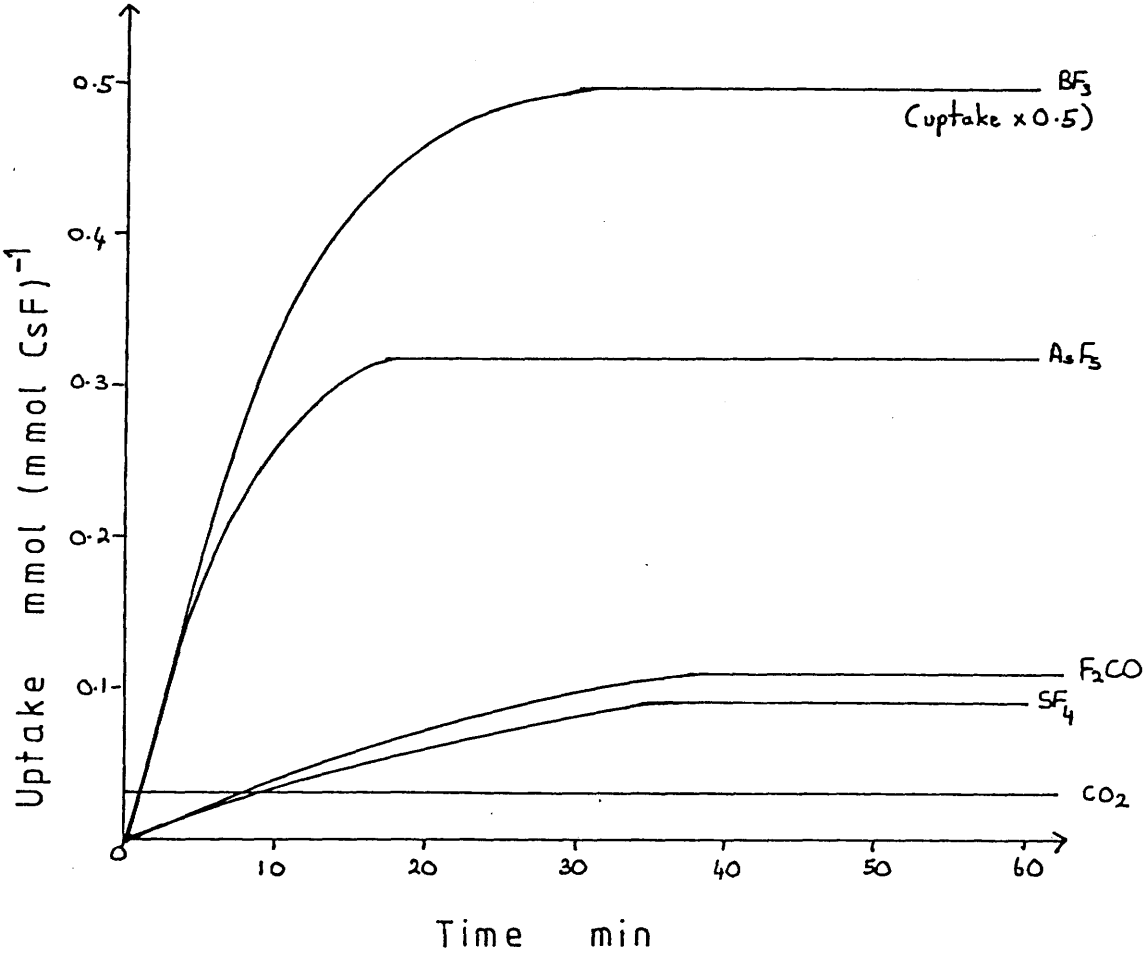

TABLE 4.26 LIST OF FLUORIDE ION AFFINITIES

ACID	kJ mol^{-1}	Ref
AsF_5	-464 ± 17	22
BF_3	-385 ± 25	22
CO_2	-138 ± 12	119
F_2CO	-146 ± 12	119
SF_4	~ 192	17

In chapter 3 it was suggested that pretreatment of CsF with hexafluoroacetone produced a porous solid. The rate of reaction of a gas with a porous solid is given by equation 4.1.[120]

$$r = \frac{kv}{\rho} \; Cg \; \eta \; W \qquad \text{equation 4.1}$$

where kv = reaction rate constant per unit volume of solid, sec^{-1}

Cg = gas phase concentration of adsorbent g-,mol cm^{-3}

η = effectiveness factor

ρ = particle density, gcm^{-3}

W = weight of sample, g

The effectiveness factor η represents the degree to which reaction occurs within the internal structure of a porous solid. A value of $\eta = 1$ indicates that the reaction occurs equally throughout the internal pore structure. Values of $\eta \ll 1$ indicate that the reaction occurs on the outside surface of individual particles, with the internal structure playing no part in the reaction due to strong pore diffusion resistances.

The effectiveness factor decreases with increasing particle size, increasing temperature or reaction rate, decreasing pore size and degree of product formation within the pore structure.

When the effectiveness factor is unity the reaction rate

and total adsorption capacity will be dictated by the chemical reactivity of the reactants. As the effectiveness factor decreases, chemical reactivity becomes less important, and other variables such as particle size, pore size and reactant structure become important. Therefore when comparing the results of a range of gases such as those discussed in this chapter, it is necessary to compare both effectiveness factors and reactivity.

No attempt was made to measure particle size or pore volume in this work. But since all the samples of activated CsF were treated in the same way and have B.E.T. surface areas within the range 2.08-3.01 m^2g^{-1} it is reasonable to assume that there were no major differences in particle size or pore volume between samples.

The pore volume of a porous solid is usually measured by mercury porosimetry which involves forcing mercury into the pores under very high pressure. This method cannot be readily applied to hygroscopic solids and it is debatable whether or not the volume of mercury forced into the solid gives a true measure of the pore volume available for adsorption of gas.

Assuming no major differences in particle size or pore volume between samples, the effectiveness factor of each gas will depend on its shape. The Lewis acids used are

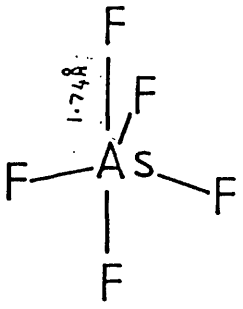

Figure 4·43

The structure of AsF_5 [121]

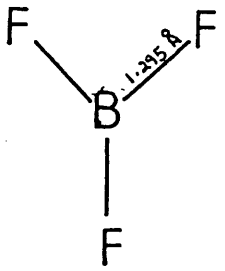

Figure 4·44

The structure of BF_3 [122]

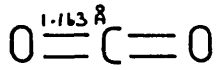

Figure 4·45

The structure of CO_2 [123]

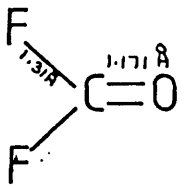

Figure 4·46

The structure of F_2CO [124]

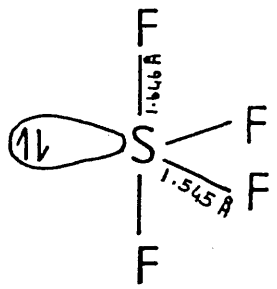

Figure 4·47

The structure of SF_4 [37]

drawn schematically in figures 4.43 to 4.47. Figure 4.43 shows that AsF_5 has a bulky trigonal bipyramid structure which will only fit into large pores. So despite the fact that it is the strongest Lewis acid, complete reaction with CsF would not be expected on the first admission of gas to the sample as AsF_5 will have a low effectiveness factor. BF_3 on the other hand is a planar molecule which will fit into a wider range of pores and so it will have a high effectiveness factor. The high effectiveness factor together with the strong Lewis acidity of BF_3 should result in complete reaction, as is observed experimentally. F_2CO will have a high effectiveness factor but due to its weak Lewis acidity uptake will be low. Similarly for SF_4 which is also a weak Lewis acid and which will have a lower effectiveness factor than F_2CO.

From figure 4.45, CO_2 would be expected to have an effectiveness value very close to unity. The low level of uptake in this case is due to the fact that CO_2 is a very weak Lewis acid.

The order of gas uptake can therefore be rationalised if both Lewis acidity and molecular shape are taken into account, thus supporting the view proposed in chapter 3 that activation of CsF by $(CF_3)_2CO$ produces a porous solid.

ooOoo

CHAPTER FIVE

CHAPTER 5

REACTIONS OF THE SOLID LEWIS ACIDS AlF_3 AND NbF_5 WITH SF_4

INTRODUCTION

Chapter 4 dealt with the reactions of gaseous Lewis acids with a solid Lewis base. In this chapter the reactions of the solid Lewis acids AlF_3 and NbF_5 with the Lewis base SF_4 are discussed. The reactions were studied at room temperature using both ^{18}F and ^{35}S labelled SF_4 which allowed bulk and surface reactions to be differentiated. The reaction of AlF_3 with SF_4 was also studied by conventional manometric methods.

5.1 EXPERIMENTAL

$SF_3{}^{18}F$ and $^{35}SF_4$ were prepared as described in chapter 2 sections 2.10.2 and 2.10.4. The reactions were followed using the techniques and apparatus outlined in chapter 4 section 4.1 and described in detail in chapter 2.

5.2 RESULTS OF REACTION OF SF_4 WITH AlF_3

The results of two reactions between $SF_3{}^{18}F$ and AlF_3 are summarised in table 5.1. Figure 5.1 shows a plot of surface count rate versus time for experiment 1 in table 5.1. There is a rapid initial rise in the solid count rate until an equilibrium level is reached after 25 minutes.

TABLE 5.1

REACTION OF $SF_3{}^{18}F$ WITH AlF_3 - SUMMARY OF RESULTS

Amount of AlF_3	Amount of $SF_3{}^{18}F$	Specific Count Rate of $SF_3{}^{18}F$ Before Reaction	Specific Count Rate of $SF_3{}^{18}F$ After Reaction	FRACTION EXCHANGED	
				Equation 2.4	Equation 2.5
0.50g 5.95 m mol	300 Torr 1.0 m mol	12326 ± 111 counts min^{-1} $m\ mol^{-1}$	9274 ± 96 counts min^{-1} $m\ mol^{-1}$	0.30	0.30
0.50g 5.95 m mol	300 Torr 1.0 m mol	5627 ± 75 counts min^{-1} $m\ mol^{-1}$	4160 ± 64 counts min^{-1} $m\ mol^{-1}$	0.31	0.31

Figure 5·1

Reaction of $SF_3^{18}F$ with AlF_3

Solid count rate vs reaction time

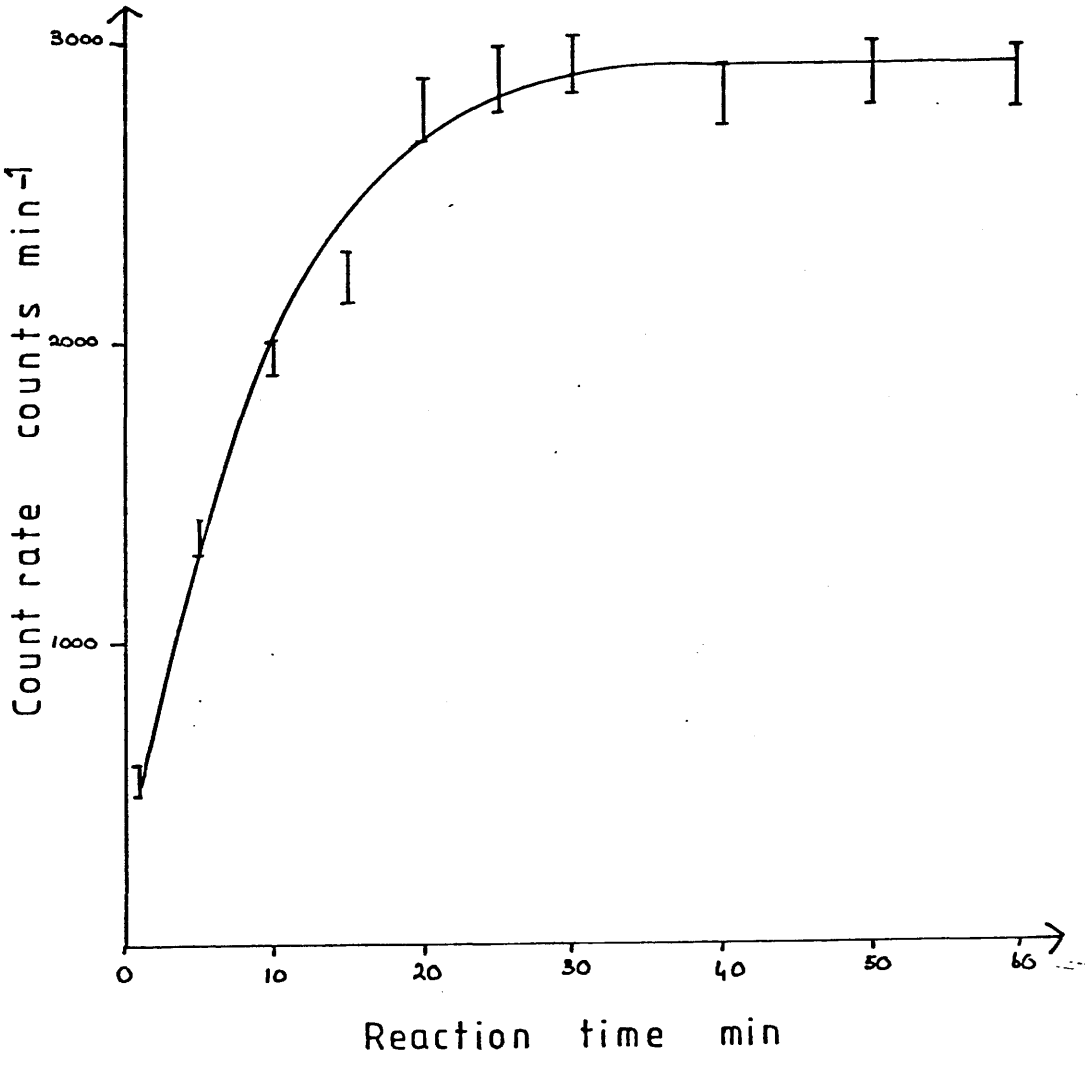

The specific count rate of the $SF_3{}^{18}F$ before reaction was 12326 $\pm$ 111 counts min^{-1} m mol^{-1}; after reaction it had fallen to 9274 $\pm$ 96 counts min^{-1} m mol^{-1} indicating that ^{18}F exchange had taken place. The fraction exchanged calculated using equation 2.4 is 0.30. Using equation 2.5 the fraction exchanged is also 0.30. The fact that identical values are obtained using these two different equations means that there is no uptake of gas with the increase in solid count rate due to ^{18}F exchange alone. This is confirmed by the infra red spectrum of the AlF_3 after reaction which showed no sign of either SF_3^+ or AlF_4^- ions. The fraction exchanged in experiment two was 0.31.

The reaction between $^{35}SF_4$ and AlF_3 was studied at 16 different pressures between 14 and 300 Torr. Each reaction was monitored for 1 hour before removal of the $^{35}SF_4$.

Figures 5.2, 5.3 and 5.4 are plots of solid count rate versus time at initial $^{35}SF_4$ pressures of 24, 150 and 300 Torr. These show that the reaction is complete within the five minutes before the first count is taken. The level of surface count rate is dependant on the initial pressure of $^{35}SF_4$ as shown by figure 5.5. The maximum count rate corresponds to a surface uptake of 0.22 $\pm$ 0.02 m mol of $^{35}SF_4$ from an initial pressure of 300 Torr.

For each pressure of $^{35}SF_4$ studied the drop in overall gas phase counts was equal to the growth in solid counts.

Figure 5·2

Reaction of $^{35}SF_4$ with AlF_3

Solid count rate vs reaction time

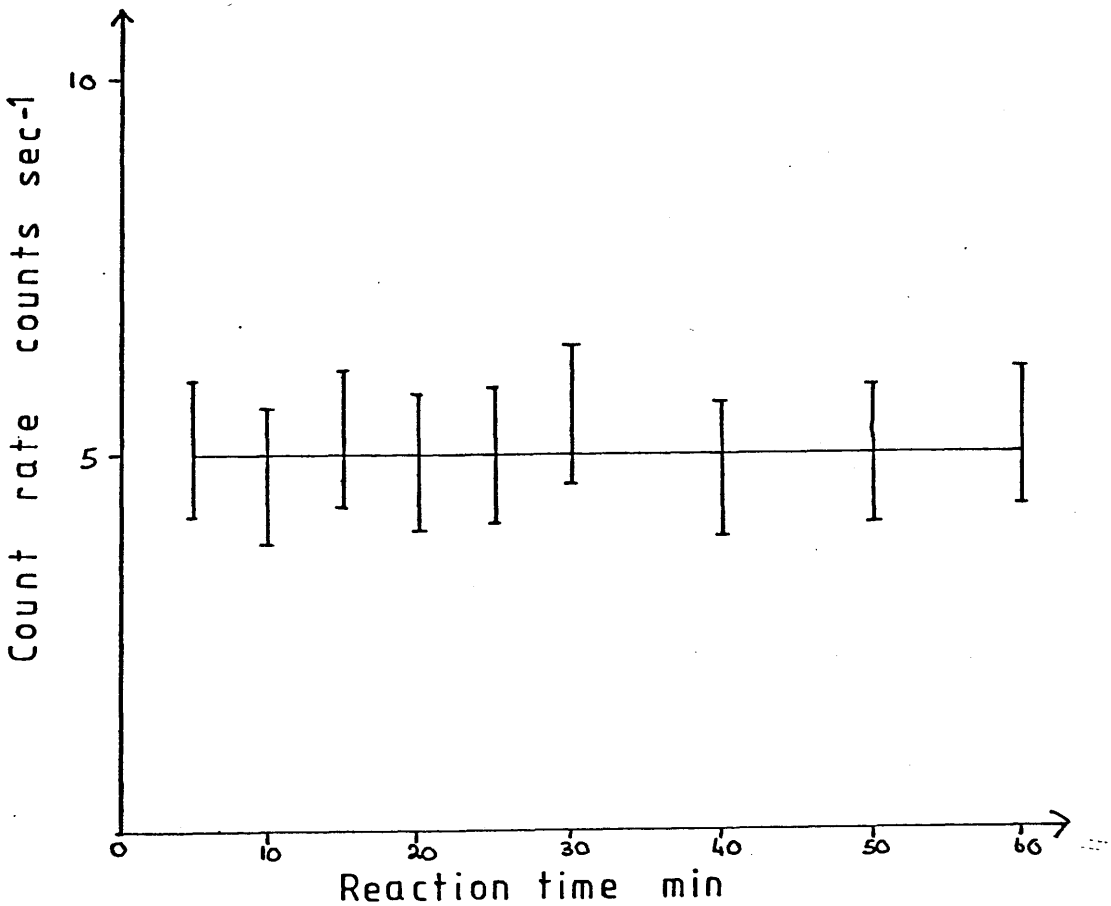

Initial pressure =24 Torr

Figure 5·3

Reaction of $^{35}SF_4$ with AlF_3

Solid count rate vs reaction time

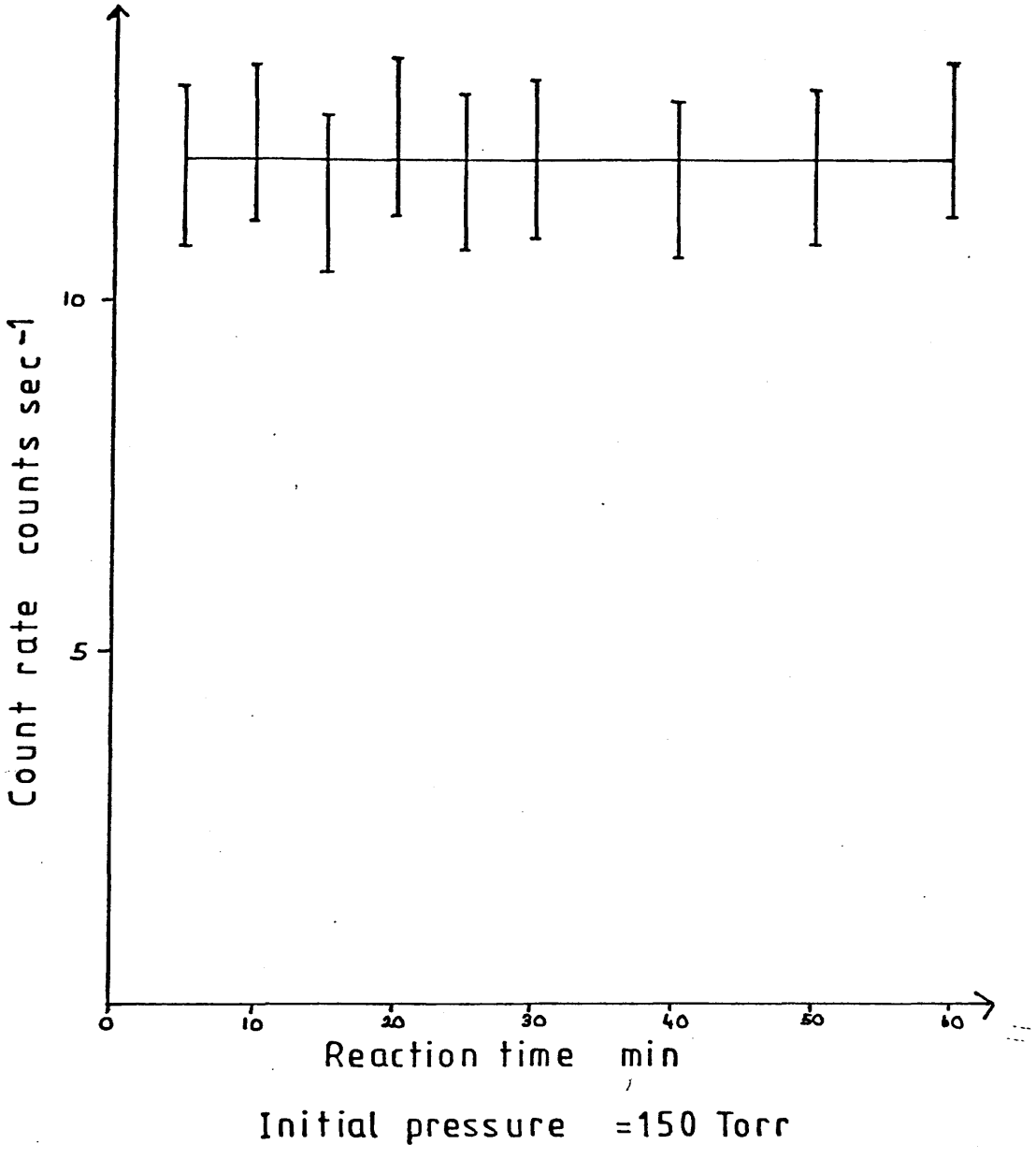

Initial pressure =150 Torr

Figure 5·4

Reaction of $^{35}SF_4$ with AlF_3

Solid count rate vs reaction time

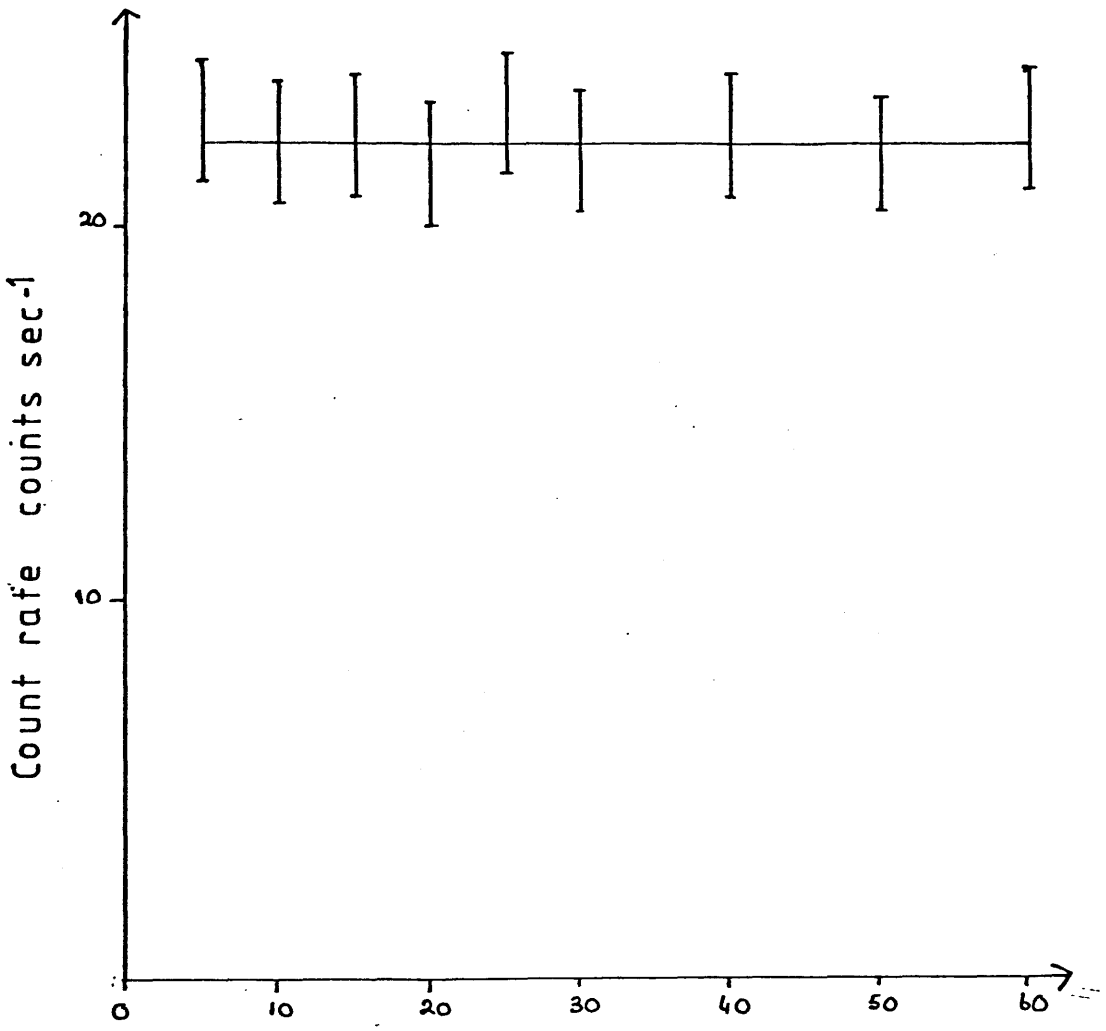

Initial pressure = 300 Torr

Figure 5·5

Reaction of $^{35}SF_4$ with AlF_3

Solid count rate vs initial pressure

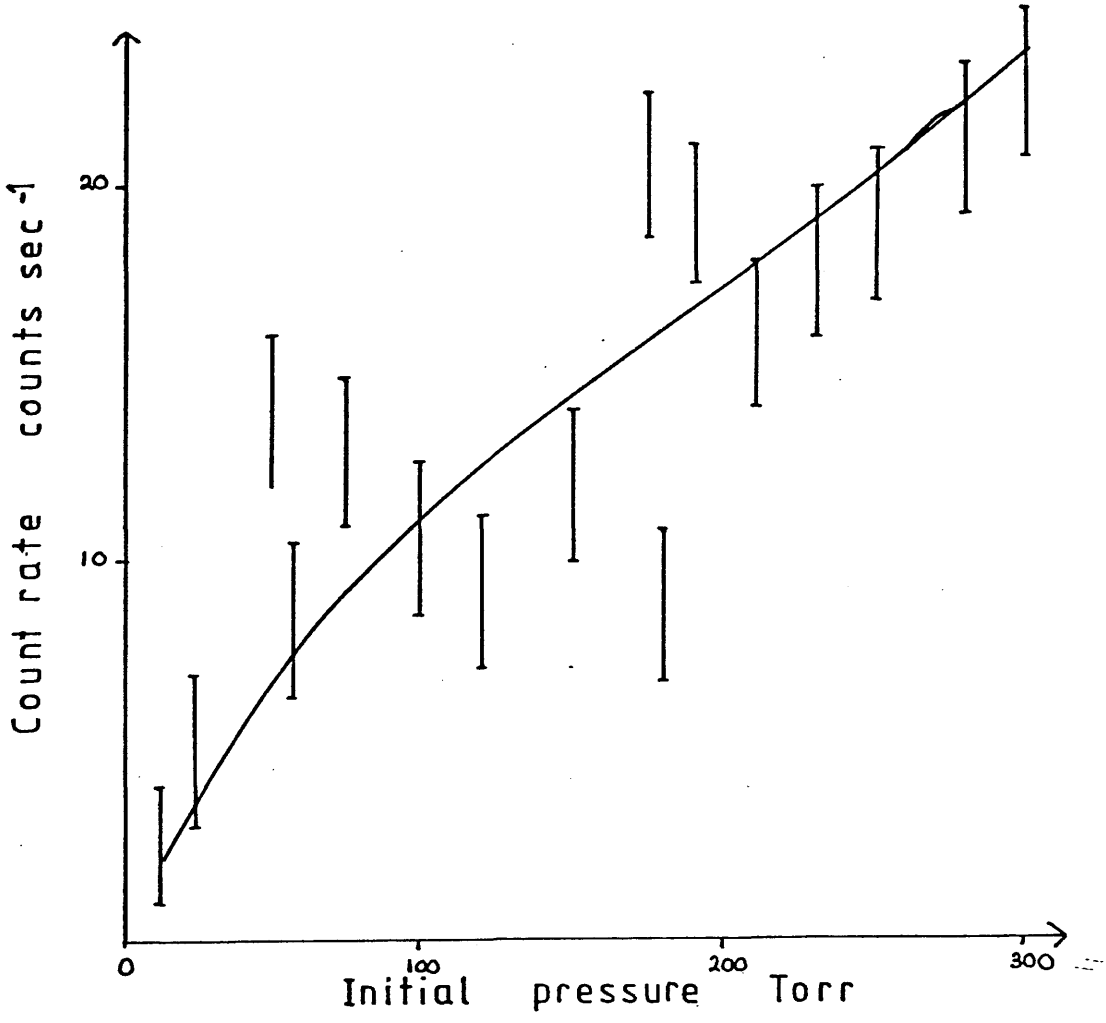

Figure 5·6

Reaction of SF_4 with AlF_3

Uptake of SF_4 vs initial pressure

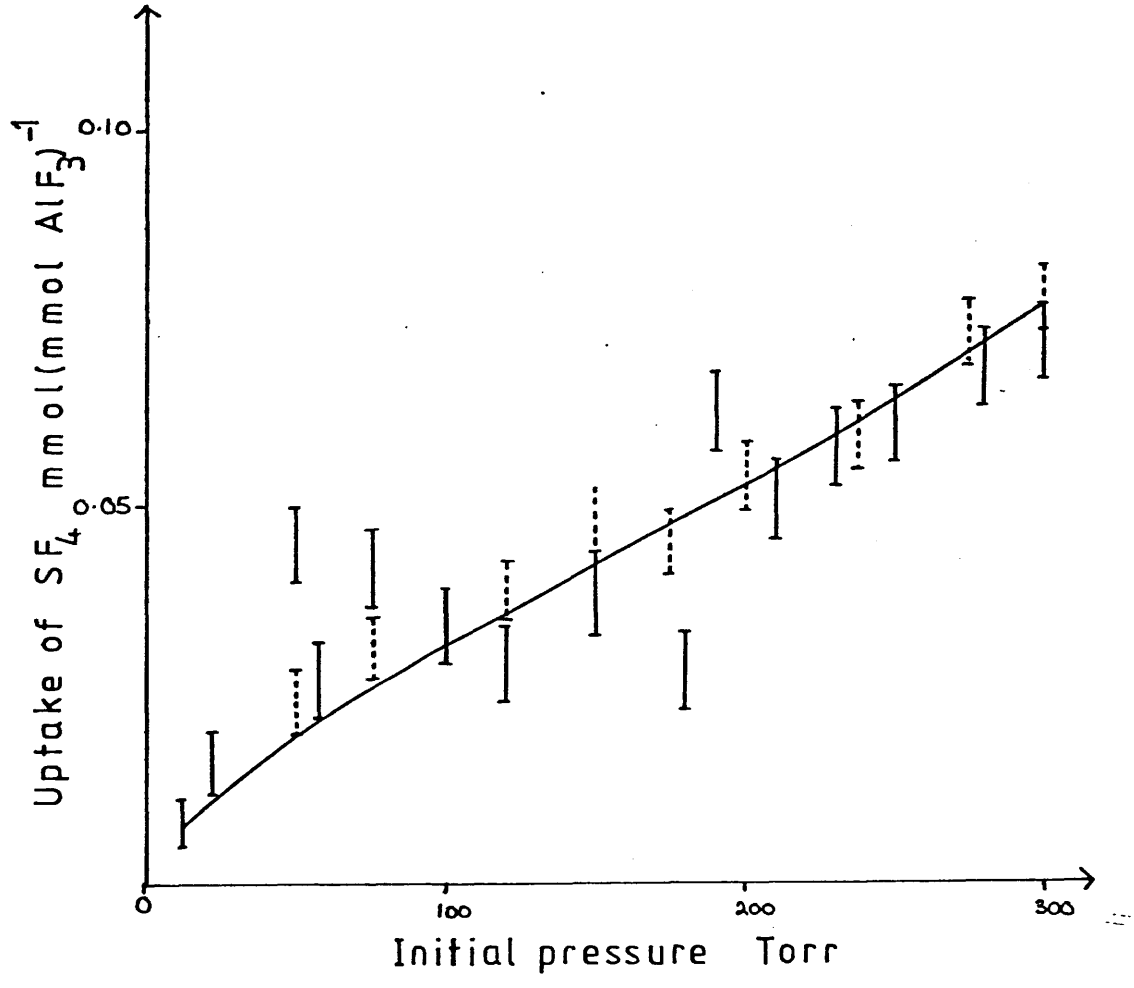

This shows that the reaction between $^{35}SF_4$ and AlF_3 is limited to surface adsorption with no bulk adsorption occurring in contrast to the reaction between $^{35}SF_4$ and activated CsF where both surface adsorption and bulk adsorption are observed.

When the $^{35}SF_4$ is removed from the counting vessel all of the surface adsorbed $^{35}SF_4$ is removed with the solid count rate falling to background level. If $^{35}SF_4$ is readmitted to the counting vessel the surface count rate returns to its original level. Removal of the gas again results in the complete removal of the surface activity with no indication of the formation of any permanently adsorbed species similar to those observed in the reaction between $^{35}SF_4$ and activated CsF.

The uptake of SF_4 by AlF_3 was studied at nine different pressures between 50 and 300 Torr using the constant volume manometer system described in chapter 2 section 2.12. The results are shown in figure 5.6 together with the uptakes calculated from the fall in the gas count rate in the $^{35}SF_4$ experiments. The two sets of data show very good agreement and confirm that the reaction between AlF_3 and SF_4 is dependant upon the initial pressure of gas and that the reaction is limited to the surface of the AlF_3 since the uptake of gas is equal to the measured surface uptake.

Figure 5·6

Reaction of SF_4 with AlF_3

Uptake of SF_4 vs initial pressure

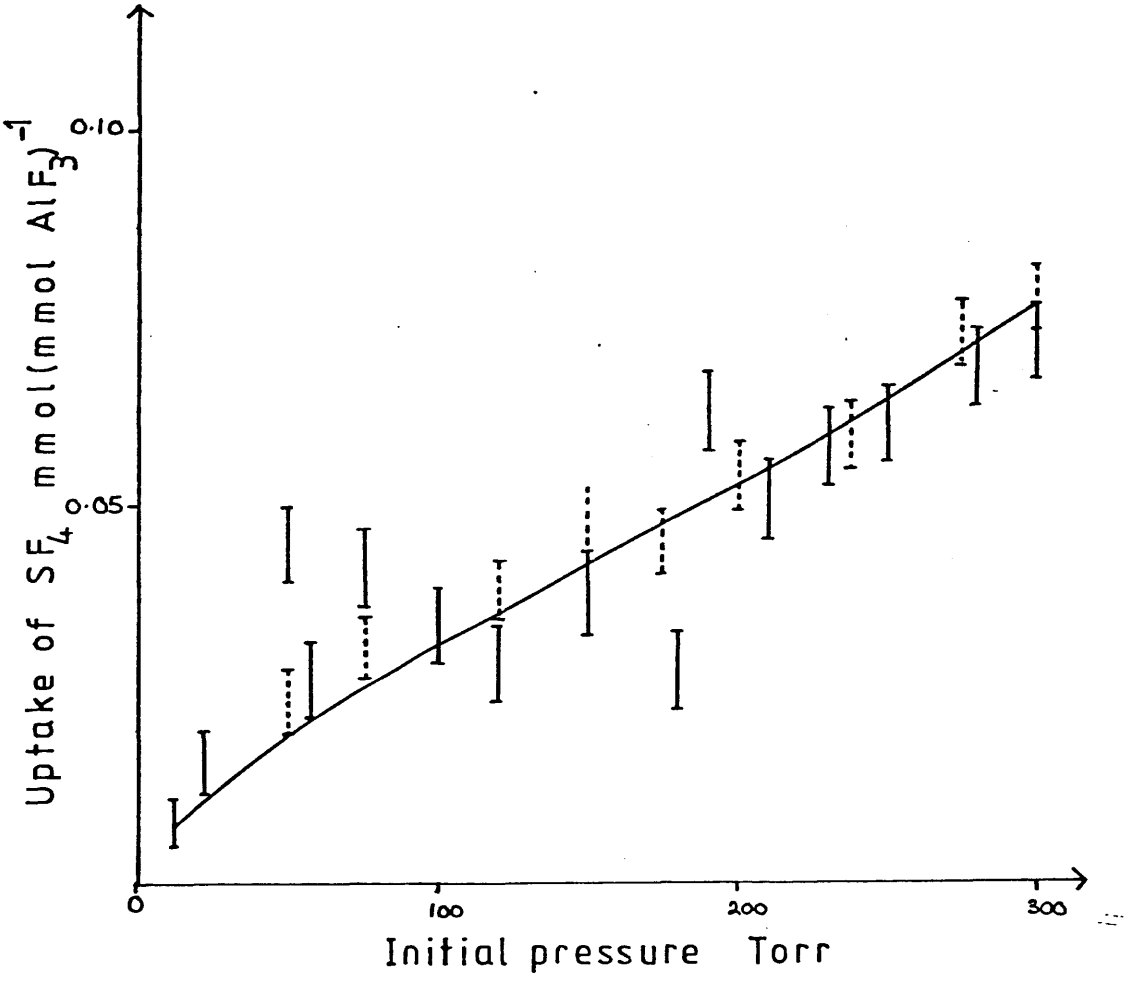

The surface area of AlF_3 was determined by the B.E.T. method using N_2 as adsorbate. A value of 22.3 $\pm$ 2.6 m^2 g^{-1} was obtained.

5.3 RESULTS OF REACTION OF SF_4 WITH NbF_5

Two experiments involving $SF_3{}^{18}F$ and NbF_5 were carried out. The results are summarised in table 5.2. The count rate of the solid rises rapidly until an equilibrium level is reached after 50 minutes, as shown by figure 5.7. Comparison of the $SF_3{}^{18}F$ specific count rate before and after reaction shows that the increase in solid count rate is due to ^{18}F exchange. The specific count rate of the $SF_3{}^{18}F$ before reaction was 15768 $\pm$ 125 counts min^{-1} m mol^{-1}. The specific count rate of the $SF_3{}^{18}F$ after reaction was 2762 $\pm$ 53 counts min^{-1} m mol^{-1}. Using equations 2.4 and 2.5 the fractions exchanged are 1.065 and 1.061 respectively. Those calculated for experiment 2 are 1.00 and 0.99. Since both equations give the same value, no uptake of gas has occurred, the increase in solid count rate is due to ^{18}F exchange. The infra red spectrum of the NbF_5 after reaction showed only bands due to NbF_5 (Table 5.3).

The reaction between $^{35}SF_4$ and NbF_5 was studied at 10 different pressures between 25 and 300 Torr. Each reaction was followed for 90 minutes before removal of the $^{35}SF_4$.

TABLE 5.2

REACTION OF $SF_3{}^{18}F$ WITH NbF_5 - SUMMARY OF RESULTS

Amount of NbF_5	Amount of $SF_3{}^{18}F$	Specific Count Rate of $SF_3{}^{18}F$ Before Reaction	Specific Count Rate of $SF_3{}^{18}F$ After Reaction	Fraction Exchanged
0.50 g 2.66 m mol	300 Torr 1.0 m mol	15768 ± 125 Counts min^{-1} m mol^{-1}	2762 ± 53 Counts min^{-1} m mol^{-1}	1.06
0.51 g 2.71 m mol	300 Torr 1.0 m mol	9765 ± 99 Counts min^{-1} m mol^{-1}	2239 ± 47 Counts min^{-1} m mol^{-1}	0.99

Figure 5·7

Reaction of $SF_3^{18}F$ with NbF_5

Solid count rate vs reaction time

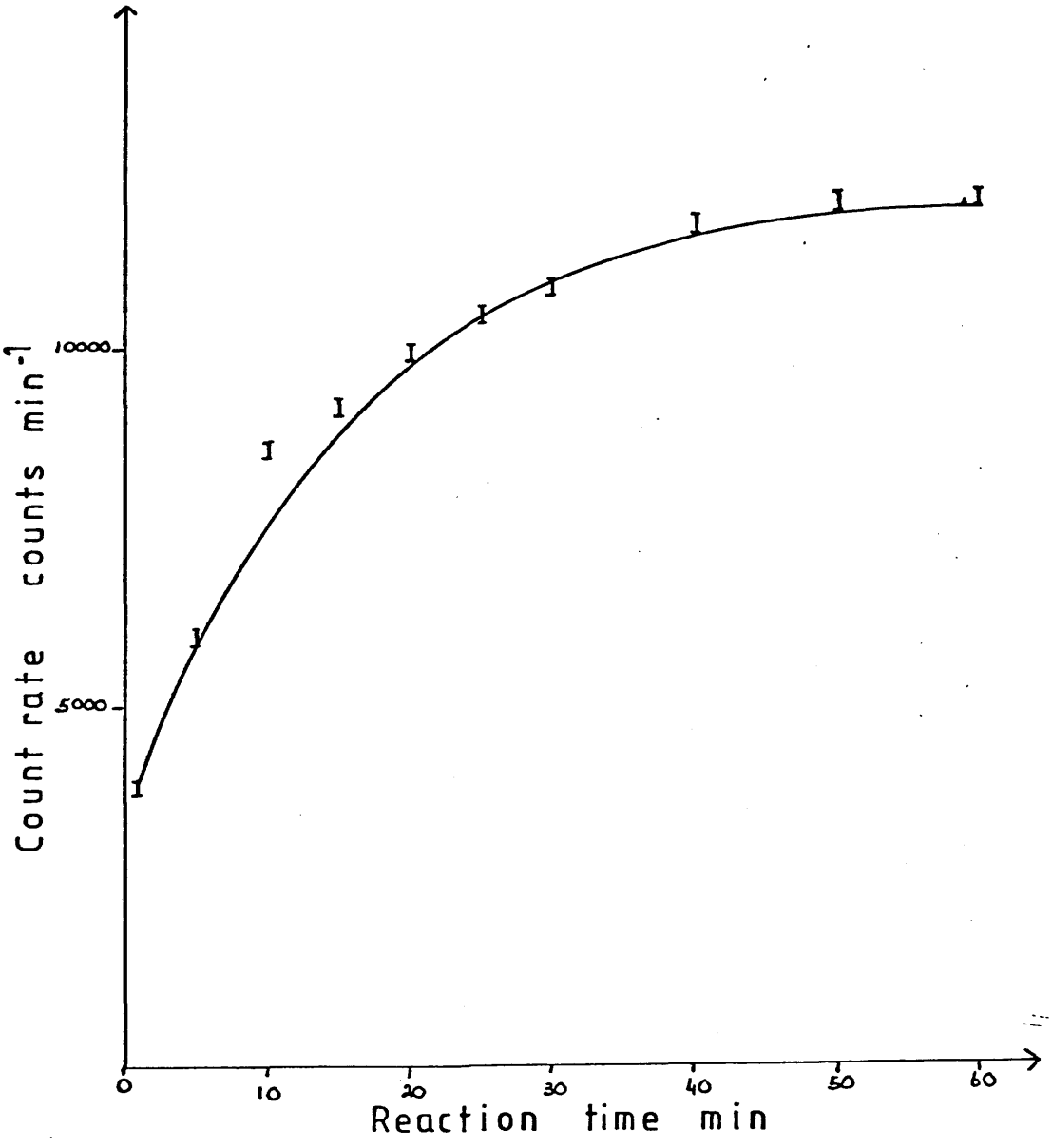

TABLE 5.3

INFRA RED SPECTRUM OF SOLID NbF_5 AFTER REACTION WITH $SF_3{}^{18}F$

THIS WORK	LITERATURE NbF_5	
	125	126
742 s	734 vs	746 s
720 vs		721 vs
700 s		700 vs
	688 s	692 sh
670 s		672 s
660 m	661 m	660 s
	514 ms	
490 sb	479 w	498 sb
	378 vs	

Figures 5.8, 5.9 and 5.10 are plots of solid count rate versus reaction time at initial pressures of 25, 125 and 305 Torr.

In each case there is a rise in solid count rate over the first 20 minutes followed by a decrease over the next 50 minutes. At low initial pressures of $^{35}SF_4$ the maximum surface count rate is very small. This surface count rate increases with initial $^{35}SF_4$ pressure until a constant level of 80-90 counts sec^{-1} is attained at all pressure greater than 100 Torr. The solid count rates after 70 minutes are also equal at pressures greater than 100 Torr. During the reaction the glass vessel becomes coated with an off white solid.

When the $^{35}SF_4$ is removed from the counting vessel the solid counts fall to background level indicating that all of the $^{35}SF_4$ has been removed from the surface.

If the same pressure of $^{35}SF_4$ is readmitted to the counting vessel the surface count rate follows the same pattern as that previously described. The count rate rises for the first 20 minutes and then falls over the next 50 minutes.

On removal of the gas there is a very small surface count remaining. This surface count rate is only detectable by counting for periods of 10,000 seconds or more.

Figure 5·8

Reaction of $^{35}SF_4$ with NbF_5

Solid count rate vs reaction time

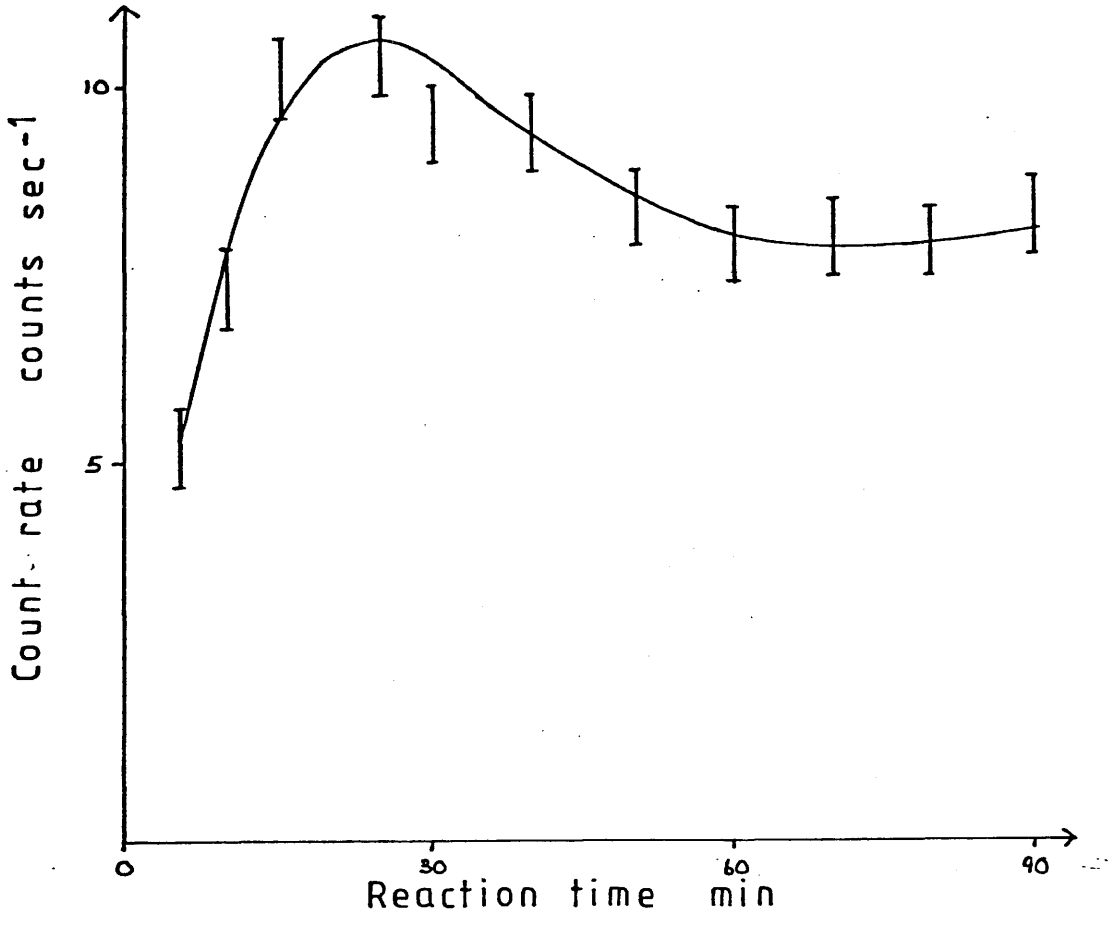

Initial pressure = 25 Torr

Figure 5·9

Reaction of $^{35}SF_4$ with NbF_5

Solid count rate vs reaction time

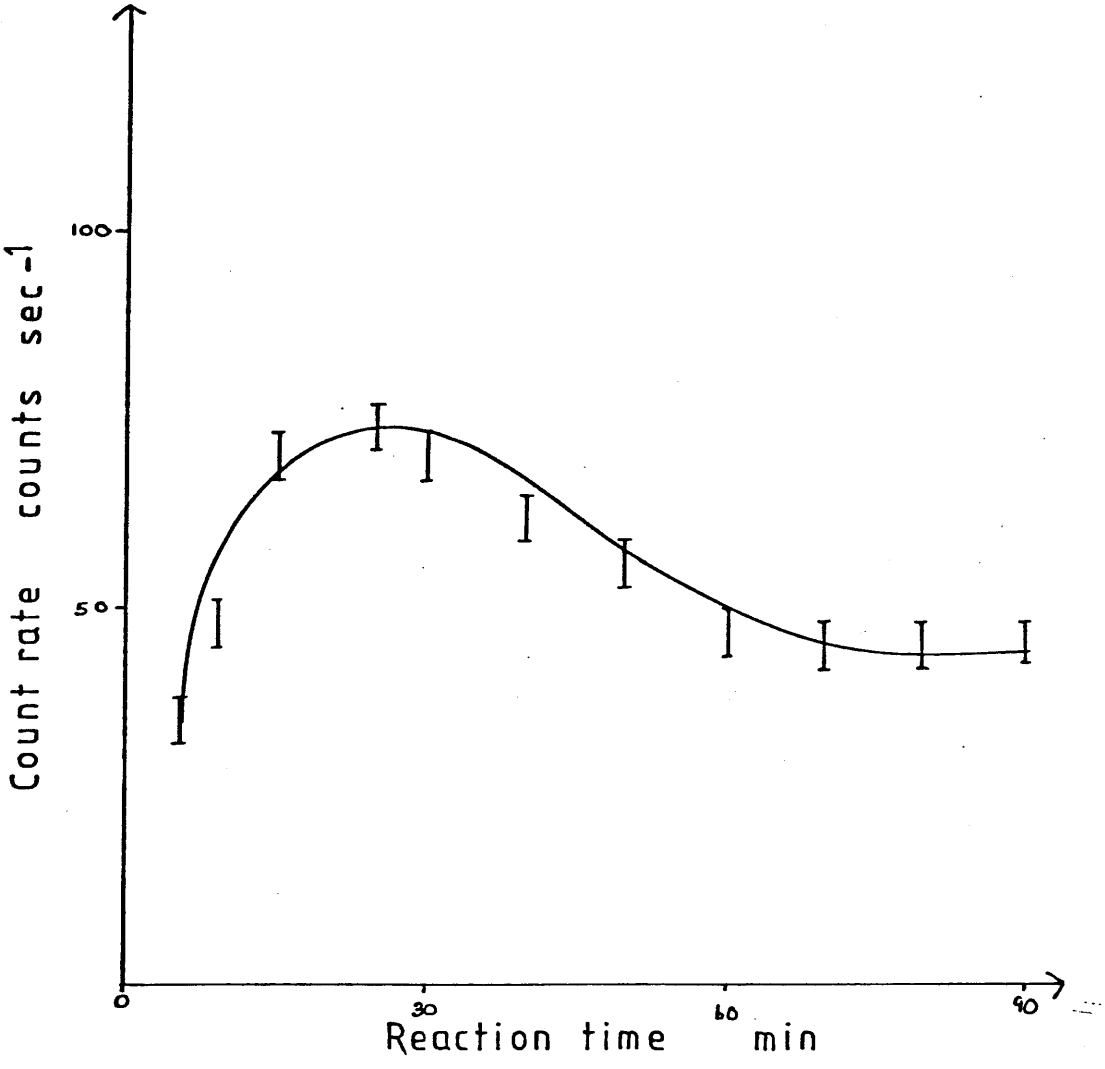

Initial pressure = 125 Torr

Figure 5·10

Reaction of SF_4 with NbF_5

Solid count rate vs reaction time

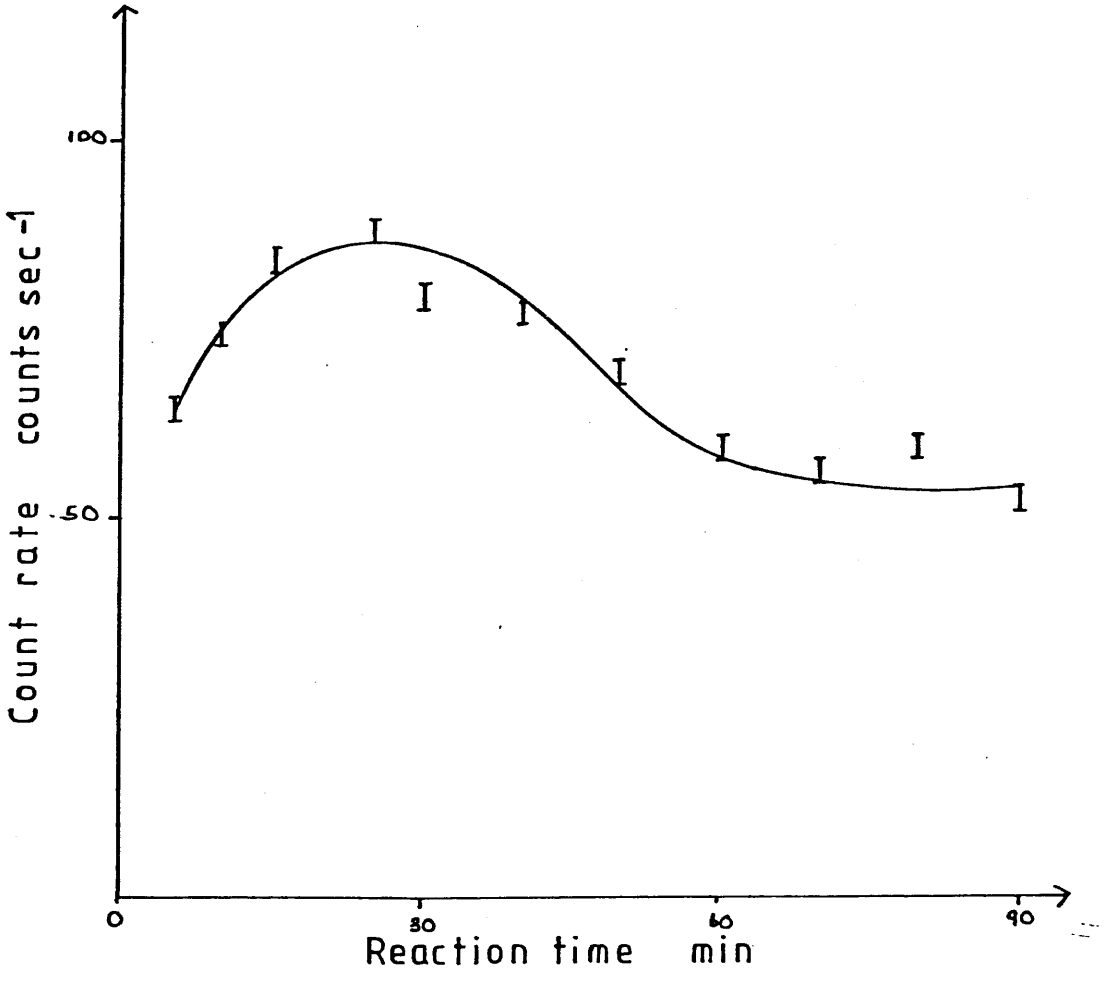

Initial pressure = 305 Torr

The admission of a further sample of $^{35}SF_4$ to the counting vessel results in a slight increase in the count rate which remains after removal of the gas. The surface count rate increases from 0.16 counts sec^{-1} to 0.26 counts sec^{-1}.

5.4 DISCUSSION OF RESULTS

Due to its volatility at room temperature no surface area or manometric measurements were carried out on NbF_5. Its reaction with SF_4 was studied using radiotracer techniques alone.

100% ^{18}F exchange is observed in the reaction of $SF_3{}^{18}F$ with NbF_5. Complete ^{18}F exchange was also observed in a study of the reaction of $SF_3{}^{18}F$ with TaF_5 carried out in conjunction with the work reported in this thesis.[97]

The reaction of $^{35}SF_4$ with NbF_5 produces a rapid initial increase in surface count rate followed by a slow decrease. In addition to this the walls of the reaction vessel become coated with a white solid as the reaction progresses. The decrease in surface count rate is due to the formation of a volatile reaction product, hence the appearance of a white solid on the walls of the reaction vessel. When the gas is removed from the reaction vessel all of the surface activity is removed indicating that the surface species is weakly adsorbed. The transition from a weakly adsorbed species to a strongly adsorbed species must be very slow because longer reaction times ($t > 3$ hours) and repeated

addition of gas to the same sample result in barely detectable levels of permanently retained $^{35}SF_4$. Similar results were also obtained in the study of the reaction between SF_4 and TaF_5 using $^{35}SF_4$, with an increase followed by a fall in the surface count rate accompanied by the formation of a white coating on the walls of the reaction vessel.[97]

Infra red spectroscopy does not provide any clues to the identity of the adsorbed species. This is because the species is weakly adsorbed and only present if there is a pressure of SF_4 in the reaction vessel.

The adsorbed species can however be identified by comparison of the results reported in this chapter with the literature results of the reactions of SF_4 and SeF_4 with a range of Lewis acids.

SF_4 reacts with BF_3, PF_5, AsF_5, SbF_5 and GeF_4[22,24] to form compounds of the form $SF_3^+ MF_n^-$. In each case there is evidence for fluorine bridging between the ions.[128] The crystal structures of SF_3^+, BF_4^- [26] and $(SF_3^+)_2 GeF_6^{2-}$[22] have been determined and are shown in chapter 1 figures 1.2 and 1.8. Each structure shows evidence of fluorine bridging with each sulphur atom making close contact with one fluorine atom from each of three different anions.

SeF_4 is isostructural with SF_4 and has been shown to react in a similar manner[129,130,23] with Lewis acids forming

compounds containing the SeF_3^+ cation. Spectroscopic studies of these compounds indicate that they are best regarded as ionic compounds of the type $SeF_3^+ MF_n^-$ and that the ions are held together by relatively strong fluorine bridges.[23]

In 1970 Edwards and Jones published the results of the reaction between NbF_5 and SeF_4.[132] In this study the room temperature reaction of SeF_4 with NbF_5 resulted in the formation of the adduct $SeF_4\ 2NbF_5$ with $SeF_4\ NbF_5$ as a minor product. A crystal structure determination shows that the molecular geometry of the adduct is consistant with the ionic formulation $(SeF_3)^+ (Nb_2F_{11})^-$. The crystal structure is shown in figure 5.11. Although this ionic formulation gives a reasonable representation of the structure it does not completely describe the structure. The selenium atom is surrounded by three fluorine atoms at 1.66 ± 0.03 Å with F-Se-F angles 94.2 ± 0.4^o, giving the expected C_{3v} symmetry for the cation. In addition to these three fluorine atoms the three fluorine atoms from neighbouring $Nb_2F_{11}^-$ ions are almost equidistant from the selenium atom at 2.40, 2.42 and 2.47Å, and form cis bridges to niobium atoms. The large distances between the bridging atoms are compatible with the presence of the non bonding electron pair on selenium filling a seventh co-ordination position.

Edwards and Jones described the structure as being "derived largely from the ionic formulation $(SeF_3)^+$

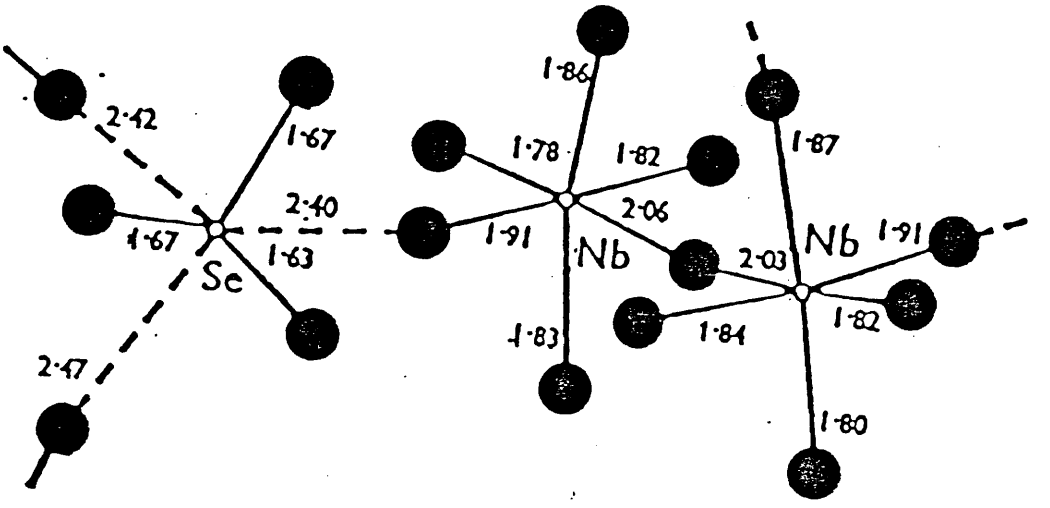

Figure 5·11 The structure of $SeF_3Nb_2F_{11}$

$(Nb_2F_{11})^-$ with some contribution from a covalently linked arrangement with $Nb_2F_{11}^-$ units cis bridged to distorted octahedral SeF_6 units." In view of the similarities in the reactions of SeF_4 and SF_4 with BF_3, PF_5, AsF_5 and SbF_5 it is reasonable to assume that the reaction of SF_4 with NbF_5 will result in the formation of $(SF_3)^+ (Nb_2F_{11})^-$ similar to the $(SeF_3)^+ (Nb_2F_{11})^-$ compound described by Edwards and Jones. The transfer of a fluoride ion from SF_4 to NbF_5 in the formation of the $(SF_3)^+ (Nb_2F_{11})^-$ compound provides an acceptable mechanism for ^{18}F exchange.

Although $(SF_3)^+ (Nb_2F_{11})^-$ is the most likely product, the possibility of the formation of $(SF_3)^+(MF_6)^-$ or of polymeric anions of the form $(Nb_n F_{5n+1})^-$ similar to those observed in antimony pentafluoride systems [133] cannot be ruled out.

The reaction of $SF_3{}^{18}F$ with AlF_3 results in 30% ^{18}F exchange. A similar result was obtained in a radiotracer study of the reaction of SF_4 with CrF_3 carried out in conjunction with the work reported in this thesis. [97] In this study 20% ^{18}F exchange was observed after 60 minutes and it was proposed that exchange occurred via a fluorine bridged donor-acceptor species between SF_3^+ and CrF_4^-. Similar fluorine bridged intermediates have been proposed in other reactions between Lewis acids and SF_4 as previously mentioned. It is therefore reasonable to assume that a similar species is involved in the reaction between SF_4 and AlF_3.

Studies using $^{35}SF_4$ indicate that the reaction between $^{35}SF_4$ and AlF_3 is complete in less than five minutes. The reaction must be limited to the surface of the AlF_3 since the overall drop in gas phase counts is equivalent to the increase in surface counts. The extent of surface adsorption is dependant on the initial pressure of $^{35}SF_4$, indicating that saturation coverage of the solid surface was not achieved within the pressure range studied. This is due to the large B.E.T. surface area of the AlF_3 ($22.3 \pm 2.6\ m^2\ g^{-1}$) which is much larger than that of the CsF used previously where surface saturation was observed at relatively low pressures. Removal of the gas from the counting vessel results in complete removal of the surface activity, so the surface species must be weakly adsorbed.

In the reaction of $^{35}SF_4$ with CrF_3, adsorption was limited to the surface of the solid and the equilibrium count rate was not reached until after 30 minutes. Removal of the gas resulted in complete removal of the surface count rate.

The results of a manometric study of the reaction between SF_4 and AlF_3 confirm that the reaction is dependant on initial pressure.

The formation of the SF_3^+ cation has been proposed in all of the reactions discussed in this chapter, however only 30% ^{18}F exchange was observed in the reaction of SF_3 ^{18}F

with AlF_3 and 20% in the reaction of $SF_3{}^{18}F$ with CrF_3 compared to 100% exchange in the $SF_3{}^{18}F/NbF_5$ and $SF_3{}^{18}F/TaF_5$ systems. The only difference observed between the two sets of reactions was the formation of a volatile reaction product in the reactions of NbF_5 and TaF_5. The volatility of the reaction product must therefore play a part in determining the amount of ^{18}F exchange observed. In other words ^{18}F exchange in the SF_4/AlF_3 and SF_4/CrF_3 systems is limited to the surface of the solid whereas ^{18}F exchange in the SF_4/NbF_5 and SF_4/TaF_5 systems occurs both on the surface of the solid and to a large extent in the gaseous phase.

The results described in this chapter show that simple molecular analogies are very useful in describing the surface reactions between a solid Lewis acid and a gaseous Lewis base.

ooOoo

CHAPTER SIX

CHAPTER 6

THE INTERACTION OF SF_4 WITH β-UF_5

INTRODUCTION

The room temperature reaction between SF_4 and β-UF_5 has previously been studied by D K Sanyal and J M Winfield[134] using both ^{18}F and ^{35}S labelled SF_4. Due to problems with the recording equipment, reliable results were not obtained for the ^{35}S experiments. The work reported in this chapter was undertaken in an attempt to fill this void. All ^{18}F results quoted are those of Sanyal and Winfield.

6.1 EXPERIMENTAL

β-UF_5 was prepared as described in chapter 2 section 2.2.12. The reaction between $^{35}SF_4$ and β-UF_5 was followed using the techniques and apparatus described briefly in chapter 4 section 4.1 and in detail in chapter 2.

6.2 RESULTS

The reaction between $^{35}SF_4$ and β-UF_5 was studied at ten different pressures between 23 and 398 Torr. Each reaction was followed for 1 hour before removal of the $^{35}SF_4$.

Representative results are given in tables 6.1 and 6.2 and in figures 6.1, 6.2 and 6.3. Figures 6.1, 6.2 and 6.3 are plots of solid count rate versus time at initial $^{35}SF_4$ pressures of 23, 150 and 398 Torr. These plots show that the reaction is complete within the five minutes before the first count is taken. The surface count rate is dependent on the initial pressure of $^{35}SF_4$ at all pressures below 200 Torr. Above 200 Torr the surface count rate is independant of the initial pressure. The maximum surface count rate of 26 ± 1 counts sec^{-1} corresponds to an uptake of 0.36 ± 0.01 m mol of $^{35}SF_4$. Surface count rates were accurately determined by extending the counting time to give total counts of 5×10^3 (See tables 6.1 and 6.2).

At each different pressure of $^{35}SF_4$ the drop in the overall gas count rate was approximately equal to the growth in the solid count rate. This shows that there is no bulk adsorption occurring with the reaction being limited to surface adsorption. Figure 6.4 shows a plot of the drop in gas count rate versus initial pressure and figure 6.5 shows a plot of surface count rate versus initial pressure.

When the $^{35}SF_4$ is removed from the counting vessel there is no change in the surface count rate. When $^{35}SF_4$ is readmitted to the counting vessel there is no increase in the surface count rate. Admission of non radioactive SF_4 does not affect the surface count rate.

TABLE 6.1

REACTION OF $^{35}SF_4$ WITH β-UF_5

TIME min	SOLID & GAS COUNTS COUNTS SEC^{-1}	GAS COUNTS COUNTS SEC^{-1}	SOLID COUNTS COUNTS SEC^{-1}
5	37.33	28.12	9.21
10	37.93	28.56	9.37
20	36.60	28.03	8.57
30	38.77	29.01	9.76
40	37.83	28.73	9.10
50	37.57	28.55	9.02
60	37.40	27.97	9.43
AVERAGE		28.42	9.21

Initial pressure of $^{35}SF_4$ = 56 Torr

Counting time = 200 seconds

Count rate of $^{35}SF_4$ before reaction = 38.04 counts sec^{-1}

Drop in count rate = 9.62 counts sec^{-1}

TABLE 6.2

REACTION OF $^{35}SF_4$ WITH β-UF_5

TIME MIN	SOLID + GAS COUNTS COUNTS SEC^{-1}	GAS COUNTS COUNTS SEC^{-1}	SOLID COUNTS COUNTS SEC^{-1}
5	208.14	179.79	28.35
10	207.34	178.35	28.99
20	208.78	179.95	28.38
30	207.61	178.99	28.62
40	208.84	179.33	29.51
50	208.43	179.89	28.54
60	207.37	179.49	27.88
AVERAGE		179.39	28.67

Initial pressure of $^{35}SF_4$ = 305 Torr

Count time = 100 seconds

Count rate of $^{35}SF_4$ before reaction = 208.69 counts sec^{-1}

Drop in count rate = 29.29 counts sec^{-1}

Figure 6·1

Reaction of $^{35}SF_4$ with β-UF_5

Solid count rate vs reaction time

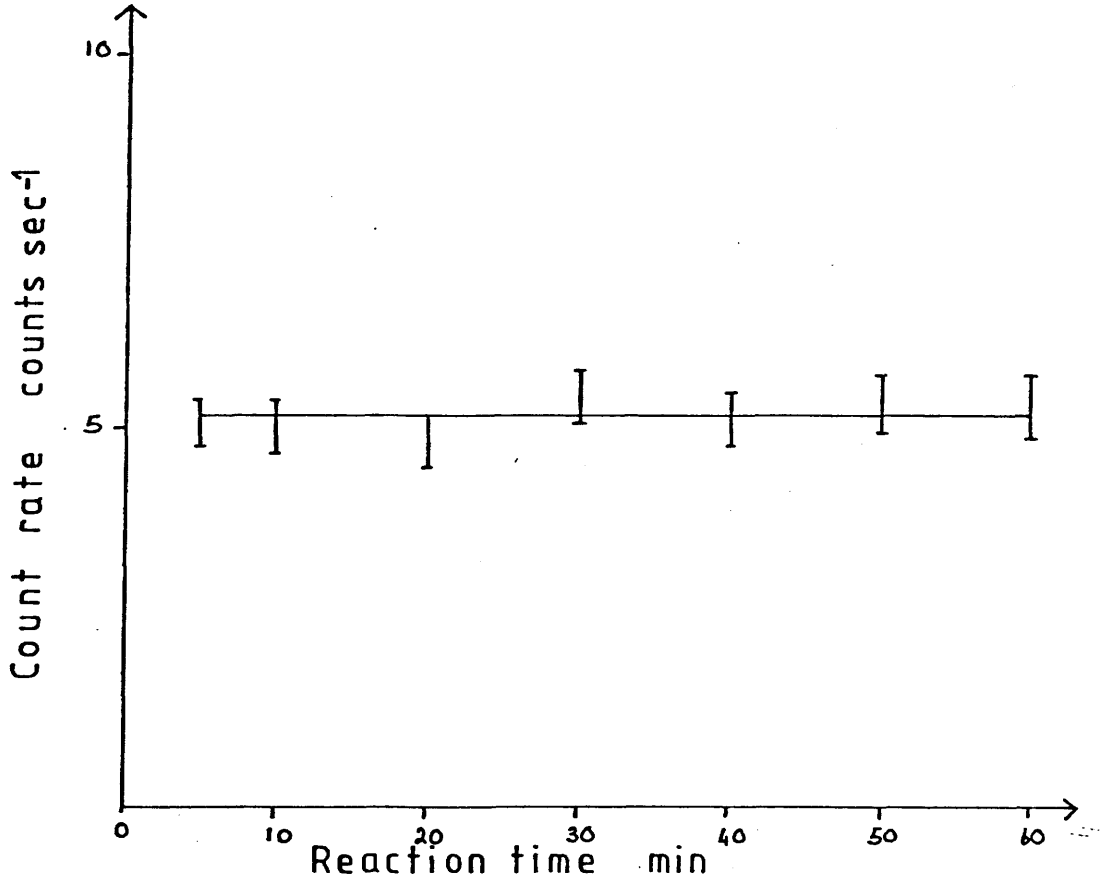

Initial pressure = 23 Torr

Figure 6·2

Reaction of $^{35}SF_4$ with β-UF_5

Solid count rate vs reaction time

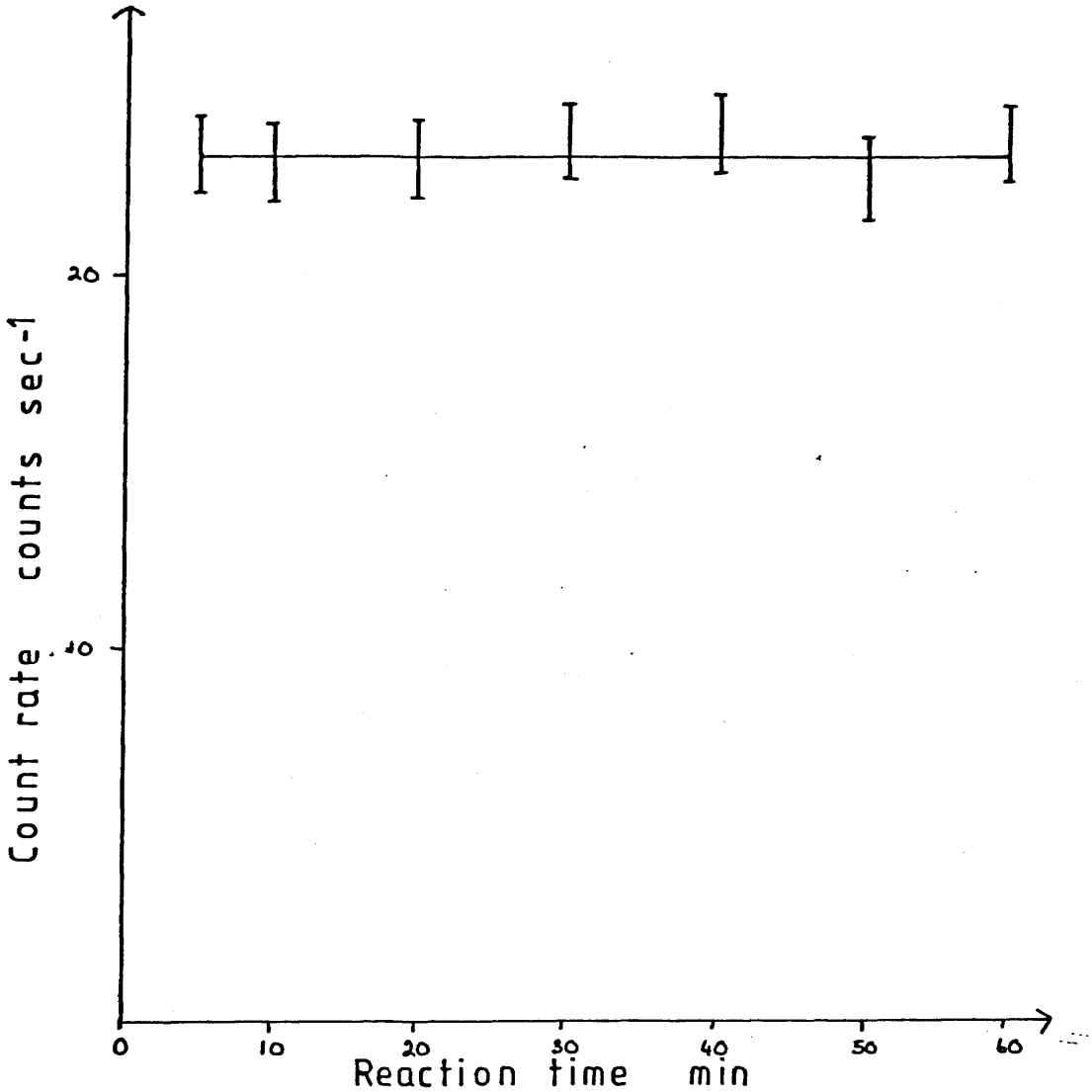

Initial pressure =150 Torr

Figure 6·3

Reaction of $^{35}SF_4$ with β-UF_5

Solid count rate vs reaction time

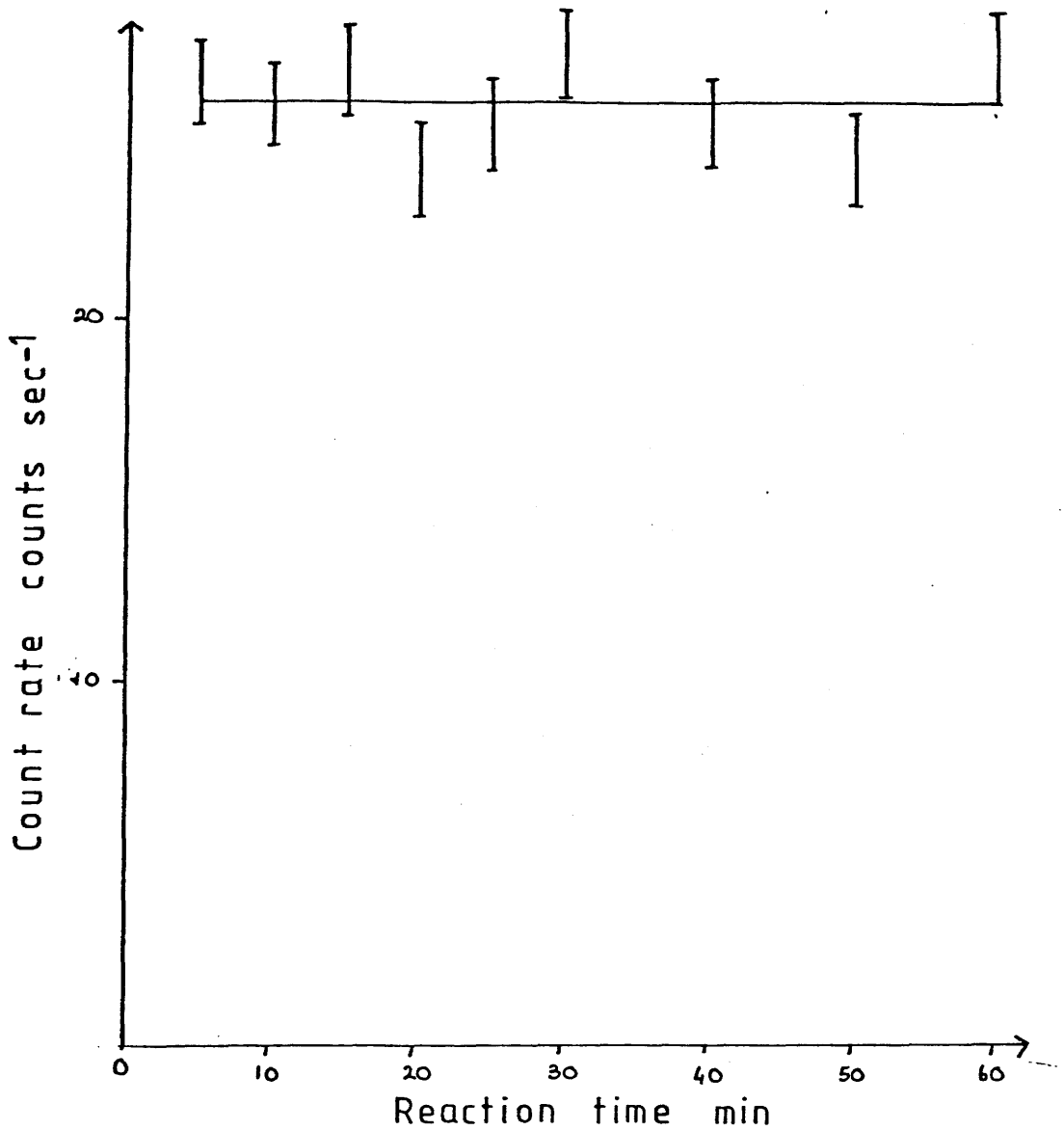

Initial pressure = 398 Torr

Figure 6·4 Reaction of $^{35}SF_4$ with β-UF_5

Drop in gas phase count rate vs initial pressure

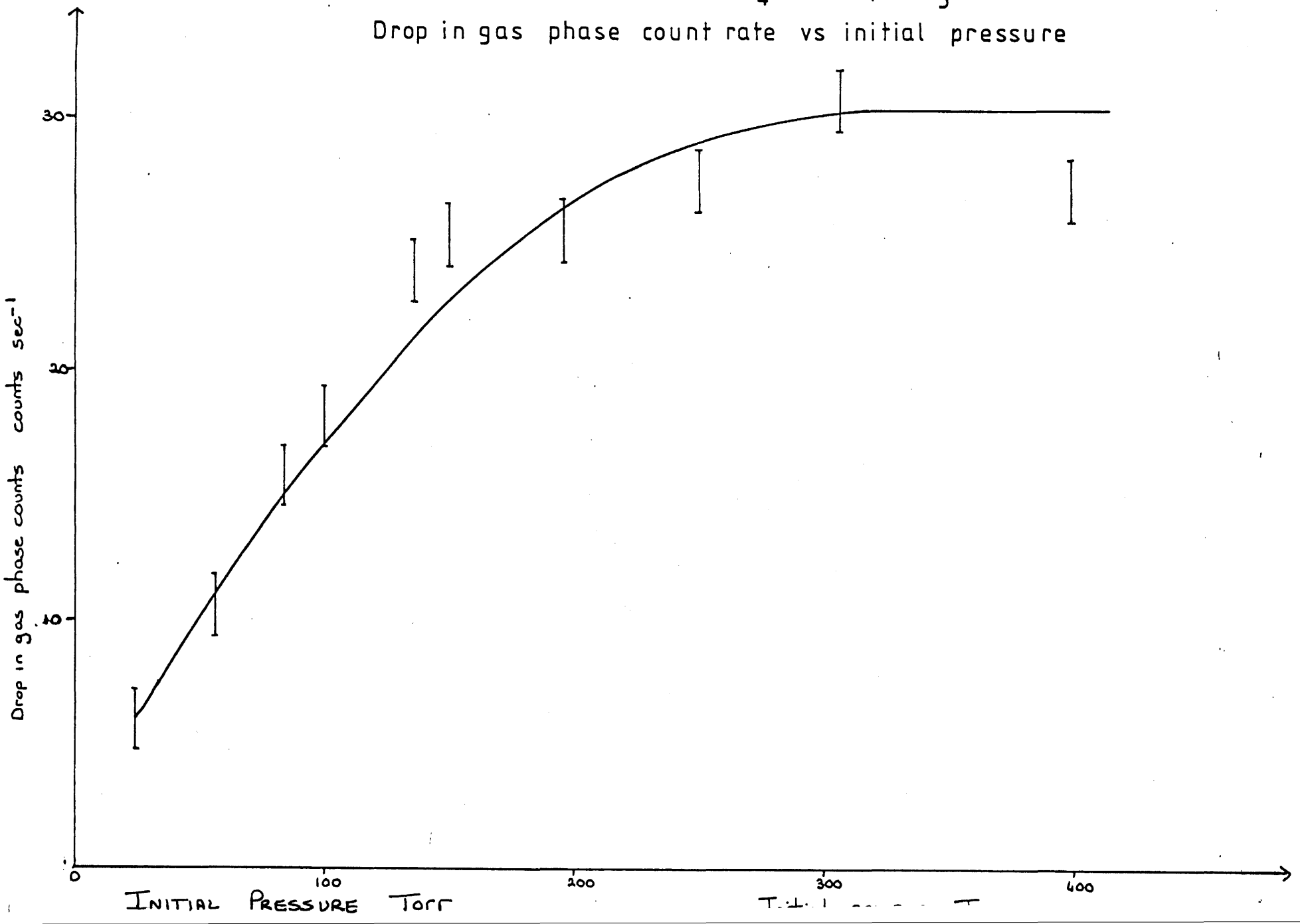

Figure 6·5 Reaction of SF_4 with β-UF_5

Surface count rate vs initial pressure

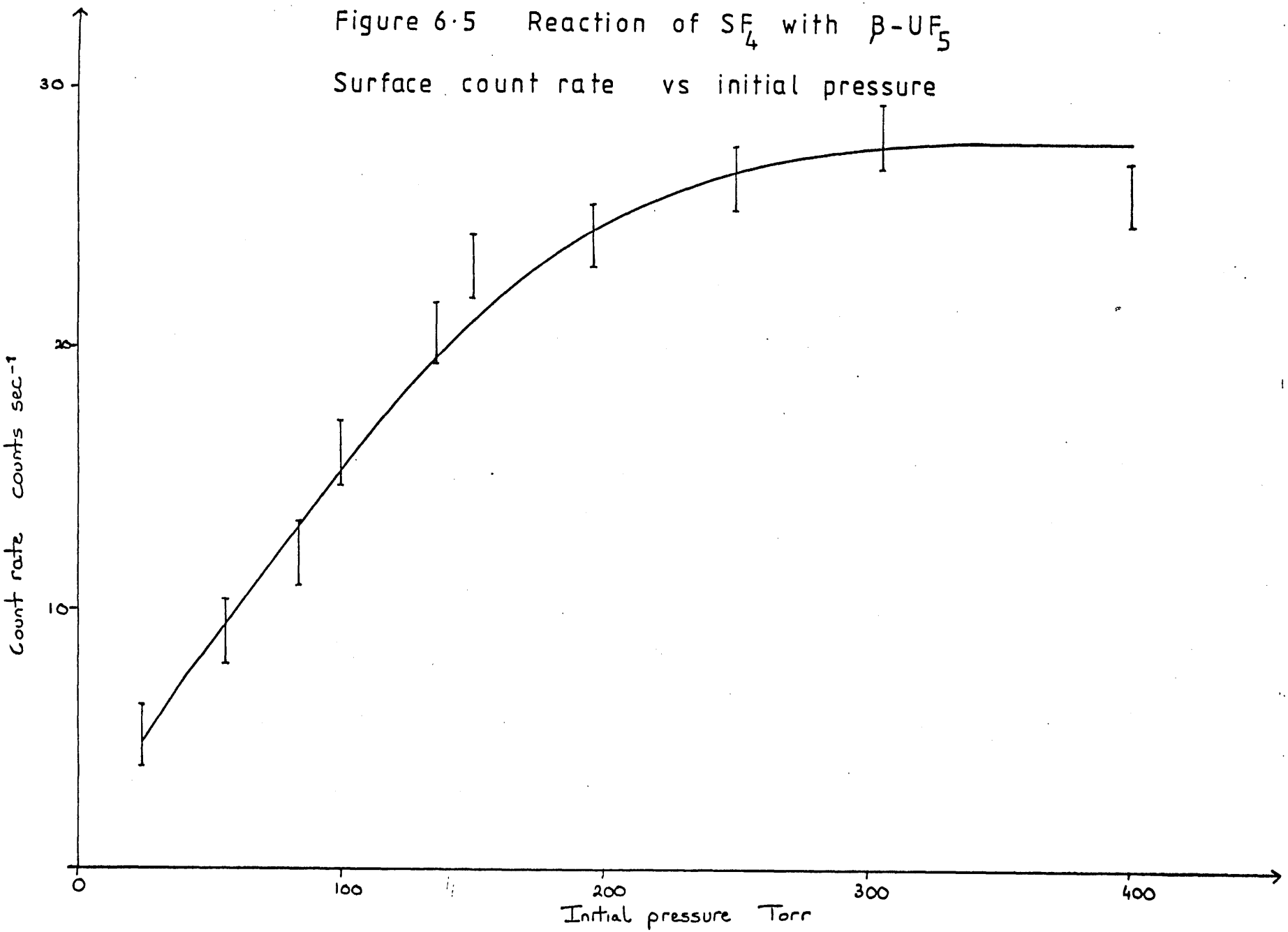

6.3 DISCUSSION OF RESULTS

Solid β-UF_5 is polymeric and contains eight co-ordinate uranium.[135] The symmetry of UF_5 as an isolated molecule[136] is not known but is believed to be C_{4v}.[137]

Uranium pentafluoride behaves as a Lewis acid with fluoride ion donors such as ammonium or alkali metal fluorides forming ionic derivatives $M^+ UF_6^-$ (M = NH_4, Li, Na, K, Rb and Cs).[138] With the strong Lewis acids SbF_5, AsF_5, NbF_5 and TaF_5 it forms fluorine bridged adducts in which ionic formulations play a minor part in the bonding.[139,140] Uranium pentafluoride can therefore behave as a Lewis acid or as a Lewis base.

There is some disagreement over the reaction of β-UF_5 with SF_4. In 1984 Sanyal and Winfield[134] published the results of a radiotracer study of the reactions of BF_3, PF_5 and SF_4 with β-UF_5. Fluorine - 18 exchange was observed in each case, together with retention of a small amount of the gas by the β-UF_5. In view of these similarities in the reactions of the three fluorides it was proposed that SF_4 was acting as a Lewis acid in the reaction with β-UF_5. Holloway and coworkers[140] published the results of the reaction of SF_4 with β-UF_5 in HF in the same year. Based on spectroscopic evidence they proposed that SF_4 was acting as a Lewis base. Since neither of these papers provides conclusive evidence it is necessary to look for

similarities between both papers and the work reported in this chapter before attempting to reach a conclusion.

The reaction between SF_4 and β-UF_5 is rapid and restricted to the surface of the solid. The adsorbed species is permanently adsorbed and is unaffected by removal of the $^{35}SF_4$.

Experiments carried out using $SF_3{}^{18}F$ show that approximately 70% ^{18}F exchange is observed after two hours (Table 6.3).

By comparison with the results of the reactions discussed in chapter 4, the formation of a permanently adsorbed species suggests that the SF_5^- anion has been formed. Further evidence for this comes from a radiotracer study of the reactions of β-UF_5 with SF_4 and the Lewis acids BF_3 and PF_5 by Sanyal and Winfield.[134] They showed that small amounts of the Lewis acids were retained by the β-UF_5. Since SF_4 was also retained they proposed that it must be acting as a Lewis acid. However, the ^{18}F experiments carried out in chapter 4 showed that no ^{18}F exchange was observed in systems where SF_5^- was formed. Sanyal and Winfield have demonstrated that 70% ^{18}F exchange is observed after two hours. The observation of ^{18}F exchange suggests that the adsorbed species is SF_3^+ by comparison with the results of the reactions between SF_4 and NbF_5 and AlF_3 discussed in chapter 5. The formation of the SF_3^+ cation was also proposed by Holloway and coworkers[140] who studied the reaction of SF_4

TABLE 6.3

RESULTS OF REACTION OF $SF_3{}^{18}F$ WITH $\beta UF_5{}^{134}$

AMOUNT OF β-UF_5 m mol	AMOUNT OF $SF_3{}^{18}F$ m mol	REACTION TIME min	FRACTION EXCHANGED
0.52	1.62	120	0.72
0.66	2.75	100	0.67

with β-UF_5 in HF. Their results indicated that an adduct of composition $3UF_5$. SF_4 was formed.

Raman and infra red studies of the adduct were carried out both in HF solution and in the solid state. The x-ray powder photograph of the adduct was also recorded. The x-ray powder photograph showed that the adduct was a well defined crystalline compound which did not contain UF_5.

Holloway and coworkers interpretation of the spectroscopic data was based on the formation of SF_3^+ and UF_6^- ions as shown in table 6.4. Table 6.5 lists the infra red spectrum of the SF_3^+ ion in four different compounds. Comparison of the two sets of data shows that SF_3^+ and UF_6^- are indeed the most likely products of this reaction. As this reaction was carried out in HF the results are not directly applicable to the heterogeneous reaction of SF_4 and β-UF_5 since SF_4 is known to be a weak base in HF,[128] ionizing to give SF_3^+ and HF_2^-. The infra red spectrum of Holloway and coworkers contains a number of additional bands, suggesting the presence of fluorine bridged species. Holloway and coworkers do in fact say that the reaction of SF_4 with β-UF_5 in HF yields "an adduct of composition $3UF_5.SF_4$ in which both ionic and fluorine bridged species are present."

As already mentioned SF_4 reacts with a number of Lewis acids to form fluorine bridged adducts which are essentially non ionic. It is therefore necessary to considerthe possibility that the heterogeneous reaction of SF_4 with β-UF_5 results in

TABLE 6.4

Spectroscopic data of Holloway and coworkers [140]

Solid		HF (soln)	Assignment	
I.r	Raman	Raman	$(SF_3)^+$	$(UF_6)^-$
962 m	962 w		)	
		952)	) $\nu_1(a_1)$	
		947) wbr	)	
		940)	)	
		934)	)	
907 m	906 m		) $\nu_3(e)$	
	894 m	892 s*	)	
885 m			)	
629 m	623 s	627 m		$\nu_1(a_1g)$
592 s				
566 s	556 vw			
542 sh		540 s*	)	
	535 vw	533)	) $\nu_2 a_1$	
	523 vw	530) s*	)	
		525)	)	
509 s				$\nu_3(f_1u)$
	470 w			ν_2 (eg)
		455 vw*		
	216 w			$\nu_3(f_2g)$

* - Bands assigned to SF_4

TABLE 6.5

VIBRATIONAL SPECTRUM OF THE SF_3^+ ION cm^{-1} [128]

$SF_3.BF_4$	$SF_3.PF_6$	$SF_3.AsF_5$	$SF_3.SbF_6$	Assignment
939	954	945	943	$\nu_1(A_1)$
529	531	530	529	$\nu_2(A)$
913	929	926	928	$\nu_3(E)$
414	408	411	411	$\nu_4(E)$

a non ionic fluorine bridged species. Adsorption of SF_4 to form two fluorine bridges, as shown in figure 6.6 would result in a seven co-ordinate sulphur species, with the lone pair occupying the seventh co-ordination position.

figure 6·6

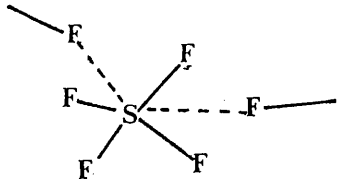

The structure of this species is similar to that of the SF_3^+ cation in $SF_3\ BF_4$ and $GeF_6\ (SF_3)_2$ (see figures 1.2 and 1.8) and the SeF_3^+ cation in $SeF_3\ Nb_2F_{11}$ (figure 5.11) In each case the S (or Se) forms three fluorine bridges to neighbouring anions to give seven co-ordinate sulphur. A species of this type would allow ^{18}F exchange and could be strongly adsorbed thus agreeing with the results of Sanyal and Winfield. In the presence of HF an ionic species as found by Holloway and coworkers would be more likely. It therefore seems most likely that the heterogeneous reaction of SF_4 with β-UF results in a fluorine bridged species, not an ionic species as previously proposed.

ooOoo

CHAPTER SEVEN

CHAPTER 7

CONCLUSIONS

Activation of CsF by treatment with hexafluoroacetone in MeCN causes a tenfold increase in its B.E.T. surface area. This large increase in surface area is due to the formation of a porous solid. CsF treated in this way is a useful synthetic reagent as it reacts readily at room temperature with a range of Lewis acids to form the Cs salt of the Lewis acid. Preparations of this type normally require solvents or high reaction temperatures and long reaction times.

Experiments carried out to determine the best conditions for labelling gaseous Lewis acid fluorides from reactor produced $Cs^{18}F$ show that considerable uptake of gas occurs. This suggests that the mechanism of ^{18}F exchange between $Cs^{18}F$ and gaseous Lewis acids involves more than one step. The first step is adsorption of the acid by the caesium fluoride followed by formation of the anion of the acid. Exchange then occurs between the anion and the Lewis acid rather than between the fluoride ion and the Lewis acid. Further evidence for this is provided by the effect of hexafluoroacetone pretreatment of the $Cs^{18}F$ before exchange. Pretreatment of the $Cs^{18}F$ results in increased uptake of gas and anion formation. Therefore the observation of increased ^{18}F exchange coupled with an increase in anion formation supports the view that exchange occurs between the anion of the Lewis acid and the Lewis acid itself.

Radiotracer studies of the reactions of gaseous Lewis acids with CsF and of solid Lewis acids with SF_4 have shown that surface adsorption always occurs, and in many systems additional bulk reactions occur.

The reactions of gaseous Lewis acids with activated CsF result in detectable bulk reaction but no ^{18}F exchange is observed except in the reaction of $F^{18}FCO$ with activated CsF. In the reactions of CO_2 and SF_4 with activated CsF two distinct surface species have been identified, one which is strongly adsorbed and one which is weakly adsorbed. The permanently adsorbed species are proposed to be CO_2F^- and SF_5^- respectively and in each case the weakly adsorbed species is proposed to be an adsorbed molecule of gas.

The reaction between F_2CO and activated CsF results in the observation of two distinct species, both on the surface and in the bulk of the solid. The two species are proposed to be the CF_3O^- anion and weakly adsorbed F_2CO. ^{18}F exchange is observed in this system. ^{18}F exchange is observed in the reactions of SF_4 with the solid Lewis acids AlF_3 and NbF_5. In experiments using $^{35}SF_4$ bulk reaction is observed, together with a single weakly adsorbed surface species which can be removed by pumping. This weakly adsorbed species is proposed to be SF_3^+.

The reaction of βUF_5 with SF_4 is restricted to the surface of the solid. ^{18}F exchange is observed and the surface species,

proposed to be F-bridged SF_4 molecules, is permanently adsorbed.

All of the reactions studied follow a general trend. The first step in all reactions is the formation of a surface adsorbed species which acts as a precursor for a Lewis acid base reaction. ^{18}F exchange is observed at room temperature when the species formed is co-ordinatively unsaturated. If a co-ordinatively saturated species is formed no fluorine exchange will be observed unless formation of complex ions containing bridging fluorines is possible.

Although the CF_3O^- anion is formed in the reaction of F_2CO with activated CsF, ^{18}F exchange is observed. In this case the reaction is complicated by the presence of both strongly and weakly adsorbed species on the surface and in the bulk of the solid.

By combining all of the aforementioned results it is possible to derive a general model to describe room temperature heterogeneous Lewis acid base reactions between binary fluorides as shown below.

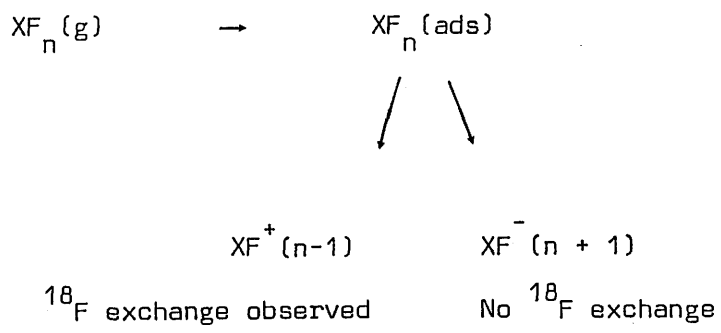

The work presented in this thesis shows that radiotracer techniques can produce results which are comparable to those obtained by conventional techniques such as manometry. It also demonstrates that identical results can be obtained from two different radioisotopes using two different counting techniques. This shows that the counting techniques and apparatus used in this study are valid for this type of work.

The original aim of this work was to investigate the usefulness of molecular analogies in describing the reactions which occur at metal halide surfaces. The results presented in this thesis show that molecular analogies are certainly very useful in describing the reactions which occur between binary fluorides, having given rise to a general model which can be used to describe these reactions.

In view of this it seems highly likely that molecular analogies could be similarly applied to all surface reactions of metal halides, not just those of binary fluorides.

ooOoo

APPENDIX

This appendix contains programme listings of all the computer programmes written specifically for this work. Each listing is accompanied by a brief explanation of the way in which the programme operates.

PROGRAMME 1 "B.E.T.S.A"

This programme was written for the BBC microcomputer and is used to calculate the B.E.T. surface areas of samples. The programme operates via a number of procedures (subroutines). The operation of each procedure is now explained.

PROC Background : Calculates the average background count.

PROC Input : Enters and stores experimental data

PROC Count : Corrects room temperature counts for background and calculates count rate in counts sec^{-1}.

PROC Temp : Converts ^{o}C to K

PROC Pressure : Converts count rate to equivalent pressure of ^{85}Kr using calibration data.

PROC Presstemp : Calculates T/P

PROC Linefit : Calculates best fitting straight line in a plot of volume versus T/P using linear regression. The calculated gradient and intercept are stored as C3 and M1 in line 180.

PROC Counts, PROC Temp, PROC Pressure, PROC Presstemp and PROC line fit are repeated in lines 190 - 230 for the 77K results.

The intercept and gradient are stored as C2 and M2 in line 240.

PROC Deltavol : Calculates the theoretical low temperature isotherm and then calculates the difference in volume between the theoretical and experimental isotherms at each point.

PROC Calc : Calculates $P/n\ (Po - P) \times 10^{18}$ and P/Po

PROC Linefit is then used to calculate the best fitting straight line in a plot of $P/n\ (Po - P) \times 10^{18}$ versus P/Po

PROC Calc SA : Calculate the surface area using the gradient and intercept calculated in PROC Calc.

PROC Results : Prints out the results

All variables are defined in chapter 3 section 3.1.4.

PROGRAMME 1 B.E.T.S.A.

```
 10REM KRYPTON SURFACE AREA PROGRAMME          JULY 85
 20CLS:PRINTTAB(10,1)"KRYPTON SURFACE AREA."
 30DIM V(8),V1(8),T(8),C(8),C1(8),CB(6),TP(12),TP1(12),P(12)
   P1(12),Y1(8),Y2(8),H(8),G(8),Y(8)
 40PRINT''"Calibration date 6/9/83"
 50 PRINT''"NEW CALIBRATION (Y/N)":A$=GET$
 60 IF A$="Y" THEN PROCRecal ELSE 90
 70END
 80FOR I=1 TO B%/2:V(I)=0:C(I)=0:T(I)=0:TP(I)=0:NEXT
 90 PROCBackground
100 PROCInput
110 PROCCounts
120 PROCTemp
130 PROCPressure
140 PROCPresstemp
150 PROCLinefit
160FOR I=1 TO B%/2:V(I)=0:C(I)=0:T(I)=0:TP(I)=0:NEXT
170 FOR I=1 TO B%/2:V(I)=V1(I):C(I)=C1(I):T(I)=T1(I):NEXT
180 C3=IT:M1=M:R1=R
190 PROCCounts
200 PROCTemp
210 PROCPressure
220 PROCPresstemp
230 PROCLinefit
240 C2=IT:M2=M:R2=R
250 PROCDeltavol
260 PROCCalc
270 VDU2
```

```
280 FOR I=1TO B%/2
290 PRINT G(I),H(I)
300 NEXT
310 VDU3
320 FOR I=1 TO B%/2:TP(I)=G(I):V(I)=H(I):NEXT
330 PROCLinefit
340 PROCCalcSA
350 PROCResults
360 END
370 DEFPROCBackground
380 CLS:INPUT''"NUMBER OF BACKGROUND COUNTS (MAX.OF 6)";A%
390 PRINT''"INPUT BACKGROUND READINGS"
400 B=0
410 FOR I=1 TO A%:INPUT CB(I)
420 B=CB(I)+B:NEXT
430 B=B/A%
440 PRINT "B=";B
450 ENDPROC
460 DEFPROCRecal
470 CLS:PRINT'"TO RECALIBRATE USE RECAL PROGRAMME TO ";
480 PRINT"OBTAIN GRADIENT(M) AND INTERCEPT(C) OF ";
490 PRINT"NEW CALIBRATION CURVE."
500 PRINT'"SUBSTITUTE THESE VALUES FOR THOSE STORED ";
510 PRINT"IN LINE 850."
520 PRINT'"CALIBRATION DATE IS STORED IN LINE 40."
530 PRINT'"AFTER CHANGING M,C AND DATE SAVE PROGRAMME ON TAPE."
540 ENDPROC
550 DEFPROCInput
```

```
560 CLS:INPUT''"NUMBER OF READINGS (MAX.OF 10)";B%
570 INPUT'"SAMPLE WEIGHT";W
580 INPUT'"COUNT TIME (SECONDS)";T%
590 INPUT'"D.S.T.VOLUME DIFFERENTIAL";VD
600 CLS:PRINTTAB(10,1)"ROOM TEMPERATURE RUN."
610 PRINT'"INPUT VOLUME,COUNTS,TEMPERATURE"
620 FOR I=1 TO B%/2:INPUT V(I),C(I),T(I):NEXT
630 PRINT'"ANY MISTAKES (Y/N)":A$=GET$
640 IF A$<>"Y" THEN 680
650 PRINT'"INPUT DATA NUMBER,V,C,T":INPUT I,V(I),C(I),T(I)
660 PRINT'"ANY MORE MISTAKES (Y/N)":A$=GET$
670 IF A$="Y" THEN 650 ELSE 680
680 CLS:PRINTTAB(10,1)"LOW TEMPERATURE RUN."
690 PRINT'"1NPUT VOLUME,COUNTS,TEMPERATURE"
700 FOR I=1 TO B%/2:INPUT V1(I),C1(I),T1(I):NEXT
710 PRINT'"ANY MISTAKES (Y/N)":A$=GET$
720 IF A$<>"Y" THEN 760
730 PRINT'"INPUT DATA NUMBER,V,C,T":INPUTI,V1(I),C1(I),T1(I)
740 PRINT'"ANY MORE MISTAKES (Y/N)":A$=GET$
750 IF A$="Y" THEN 730 ELSE 760
760 ENDPROC
770 DEFPROCCounts
780FOR I= 1 TO B%/2:C(I)=((C(I)-B)/T%):NEXT
790 ENDPROC
800 DEFPROCTemp
810 FOR I=1 TO B%/2:T(I)=T(I)+273:NEXT
820 ENDPROC
830 DEFPROCPressure
```

```
 840 LOCAL M,C
 850 C=7.1638E-3:M=3.1933E-3
 860 FOR I= 1 TO B%/2:P(I)=M*C(I)+C:NEXT
 870 ENDPROC
 880 DEFPROCPresstemp
 890 FOR I = 1 TO B%/2:TP(I)=T(I)/P(I):NEXT
 900 ENDPROC
 910 DEFPROCLinefit
 920 XX=0:YY=0:XY=0:sumX=0:sumY=0:sumXY=0:sumYY=0:sumXX=0
 930 LOCAL MEANX,MEANY
 940 M=0:C=0:IT=0
 950 FOR I=1 TO B%/2
 960 sumX=sumX+TP(I):sumY=sumY+V(I):NEXT
 970 MEANX=sumX/(B%/2):MEANY=sumY/(B%/2)
 980 FOR I=1 TO B%/2
 990 sumXX=sumXX+TP(I)*TP(I):sumYY=sumYY+V(I)*V(I)
1000 sumXY=sumXY+TP(I)*V(I)
1010 XX=XX+(TP(I)-MEANX)*(TP(I)-MEANX):YY=YY+(V(I)-MEANY)*(V(I)-MEANY):
     XY=XY+(TP(I)-MEANX)*(V(I)-MEANY)
1020 NEXT
1030 M=((B%/2)*sumXY-sumX*sumY)/((B%/2)*sumXX-sumX*sumX)
1040 IT=(sumY*sumXX-sumX*sumXY)/((B%/2)*sumXX-sumX*sumX)
1050 R=XY/SQR(XX*YY)
1060 ENDPROC
1070 DEFPROCDeltavol
1080 FOR I=1 TO B%/2
1090 C1=C3-VD
1100 Y1(I)=M1*TP(I)+C1
```

```
1110 Y2(I)=M2*TP(I)+C2
1120 Y(I)=Y1(I)-Y2(I)
1130 NEXT
1140 ENDPROC
1150 DEFPROCCalc
1160 FOR I=1 TO B%/2
1170 H(I)=P(I)/((Y(I)*P(I)*0.12468)*(2.49-P(I)))
1180 G(I)=P(I)/2.49
1190 NEXT
1200 ENDPROC
1210 DEFPROCCalcSA
1220 SA=1/M+IT
1230 SA=SA*0.195/W
1240 ENDPROC
1250 DEFPROCResults
1260 CLS:VDU2:PRINT'TAB(11,1)"ROOM TEMPERATURE RUN."
1270 @%=&2040C
1280 PRINT'"GRADIENT=";M1
1290 PRINT'"INTERCEPT=";C3
1300 PRINT'"CORRELATION COEFFICIENT=";R1
1310 VDU3
1320PRINT'''"PRESS 'C' TO CONTINUE":REPEAT UNTIL GET$="C"
1330 CLS:VDU2:PRINT'TAB(11,1)"LOW TEMPERATURE RUN."
1340 PRINT'"GRADIENT=";M2
1350 PRINT'"INTERCEPT=";C2
1360 PRINT'"CORRELATION COEFFICIENT=";R2
1370 VDU3
1380 PRINT'''"PRESS 'C' TO CONTINUE":REPEAT UNTIL GET$="C"
```

```
1390 CLS:VDU2:PRINTTAB(14,1)"SURFACE AREA."
1400 PRINT'"GRADIENT=";M
1410 PRINT'"INTERCEPT=";IT
1420PRINT'"CORRELATION COEFFICIENT=";R
1430 VDU3
1440 PRINT'''"PRESS 'C' TO CONTINUE":REPEAT UNTIL GET$="C"
1450 CLS:VDU2:PRINTTAB(8,4)"SURFACE AREA=";SA
1460 VDU3
1470 PRINTTAB(15,19)"'E' TO END":REPEAT UNTIL GET$="E"
1480 CLS:PRINTTAB(15,10)"END OF RUN"
1490 @%=&10
1500 ENDPROC
```

PROGRAMME 2 "F.18"

Written for the Dragon Microcomputer

This programme corrects for the decay of ^{18}F. Counts are corrected down to the latest time so that artificially high count rates are not produced.

The operation of the programme is as follows:

Lines 10-180	:	Input of data
Lines 200 - 260	:	Calculation based on equation 2.8
Lines 280 - 540	:	Print out of results both on screen and printer

PROGRAMME 2 F.18"

```
10 CLS:DIM A(20),B(20),C(20),D(20),T(20)
20 PRINT"FLUORINE 18 DECAY PROGRAMME"
30 PRINT
40 PRINT"INPUT NUMBER OF DATA PAIRS  (MAX OF 20 )
50 INPUT N
60 PRINT"AVERAGE NUMBER OF BACKGROUND COUNTS"
70 INPUT G
80 E=(LOG(2))/110
90 PRINT"INPUT A,T(MINUTES)
100 FOR I=1 TO N
110 INPUT A(I),T(I)
120 NEXT
130 PRINT
140 PRINT"ANY MISTAKES Y/N":INPUT C$
150 IF C$<>"Y" THEN 200
160 PRINT"DATA NO.,A,T":INPUT I,A(I),T(I)
170 PRINT"ANY MORE MISTAKES Y/N":INPUT D$
180 IF D$<>"Y" THEN 200
190 GOTO 160
200 FOR I=1 TO N
210 A(I)=A(I)-G
220 B(I)=T(I)*-E
230 C(I)=EXP(B(I))
240 D(I)=C(I)*A(I)
250 D(I)=INT(D(I)+0.5)
260 NEXT
270 CLS
```

```
290 IF N>10 GOTO 310
300 IF N<10 GOTO 410
310 FOR I=1 TO 10
320 PRINT D(I)
330 NEXT
340 PRINT"PRESS ENTER TO CONTINUE":INPUT A$
350 IF A$="K" THEN 520 360 CLS
360 CLS
370 FOR I=11 TO N
380 PRINT D(I)
390 NEXT
400 GOTO 440
410 FOR I=1 TO N
420 PRINT D(I)
430 NEXT
440 PRINT
450 PRINT#-2,"CORRECTED ACTIVITIES"
460 FOR I=1 TO N
470 PRINT#-2,D(I)
480 NEXT
490 PRINT"ANOTHER RUN Y/N":INPUT B$
500 IF B$="Y" THEN RUN ELSE 510
510 PRINT
520 PRINT"END OF CALCULATION"
530 END
```

PROGRAMME 3 "F.18 PLOT"

Written for the Dragon microcomputer

This programme corrects the observed counts for decay of ^{18}F and then produces a plot of solid counts versus reaction time on the monitor. The operation of the programme is as follows:

Lines 10 - 400	Correction of Gas + solid counts for decay, using method described for programme 2.
Lines 420 - 720	Correction of Gas phase counts for decay.
Lines 730 - 760	Calculation of corrected solid counts.
Lines 770 - 890	Print out of solid counts on screen only.
Lines 900 - 970	Input of adsorption times.
Lines 1040 - 1060	Scales points to fit computers graphic screen.
Lines 1070 - 1110	Converts experimental points to points on graphic screen.
Line 1130	Sets up graphic screen
Lines 1140 - 1220	Plots axes.
Lines 1230 - 1270	Plots points, drawing a circle round each point.
Lines 1280 - 1320	Joins points.

PROGRAMME 3 F.18.PLOT

```
10 DIM A(15),B(15),C(15),D(15),T(15)
20 DIM A1(15),B1(15),C1(15),D1(15,T1(15),X(15),Y(15)
30 CLS
40 PRINT"        F.18.PLOT"
50 PRINT''"NUMBER OF DATA PAIRS  (MAXIMUM OF 30)"
60 INPUT P
70 PRINT'"AV.NO.OF BACKGROUND COUNTS"
80 INPUT G
90 E=(LOG(2))/110
100 CLS
110 PRINT'"INPUT DECAY TIME(MINUTES),ACTIVITY(GAS+SOLID)"
120 FOR I=1 TO P/2
130 INPUT T(I),A(I)
140 NEXT I
150 PRINT"ANY MISTAKES Y/N":INPUT A$
160 IF A$<>"Y"THEN 200
170 PRINT"INPUT DATA NUMBER,TIME,ACTIVITY":INPUT I,T(I),A(I)
180 PRINT'"MORE MISTAKES Y/N":INPUTA$
190 IF A$<>"N" THEN 170
200 FOR I=1 TO P/2
210 A(I)=A(I)-G
220 B(I)=T(I)*-E
230 C(I)=EXP(B(I))
240 D(I)=C(I)*A(I)
250 D(I)=INT(D(I))
260 NEXT I
270 CLS
280 PRINT'"CORRECTED ACTIVITIES(GAS+SOLID)
```

```
290 FOR I=1 TO 10
300 PRINT D(I)
310 NEXT I
320 PRINT'"TYPE  C  TO CONTINUE"
330 A$=INKEY$
340 IF INKEY$<>"C" GOTO 340
350 FOR I= 11 TO P/2
360 PRINT D(I)
370 NEXT I
380 PRINT"TYPE   C  TO CONTINUE"
390 A$=INKEY$
400 IF INKEY$<>"C" GOTO 400
410 CLS
420 PRINT'"INPUT DECAY TIME(MINUTES),GAS PHASE COUNTS"
430 FOR I=1 TO P/2
440 INPUT T1(I),A1(I)
450 NEXT I
460 PRINT"ANY MISTAKES Y/N":INPUT A$
470 IF A$<>"Y" THEN 510
480 PRINT"INPUT DATA NUMBER,TIME,ACTIVITY":INPUT I,T1(I),A1(I)
490 PRINT"ANY MORE MISTAKES Y/N": INPUT A$
500 IF A$<>"N" THEN 480
510 FOR I=1 TO P/2
520 A1(I)=A1(I)-G
530 B1(I)=T1(I)*-E
540 C1(I)=EXP(B1(I))
550 D1(I)=C1(I)*A1(I)
560 D1(I)=INT(D1(I))
```

```
570 NEXT I
580 CLS
590 PRINT'"CORRECTED ACTIVITIES (GAS PHASE)"
600 FOR I= 1 TO 10
610 PRINT D1(I)
620 NEXT I
630 PRINT"TYPE C TO CONTINUE"
640 A$=INKEY$
650 IF INKEY$<>"C" GOTO 650
660 FOR I=11 TO P/2
670 PRINT D(I)
680 NEXT I
690 PRINT"TYPE C TO CONTINUE"
700 A$=INKEY$
710 IF INKEY$<>"C" GOTO 710
720 CLS
730 FOR A= 1 TO P/2
740 Y(A)=D(A)-D1(A)
750 NEXT A
760 PRINT'"CORRECTED SOLID COUNTS"
770 FOR A= 1 TO 10
780 PRINT Y(A)
790 NEXT A
800 PRINT"TYPE C TO CONTINUE"
810 A$=INKEY$
820 IF INKEY$<>"C" GOTO 820
830 FOR A= 11 TO P/2
840 PRINT Y(A)
```

```
850 NEXT A
860 PRINT"TYPE C TO CONTINUE"
870 A$=INKEY$
880 IF INKEY$<>"C" GOTO 880
890 CLS
900 PRINT'"INPUT ADS TIMES"
910 FOR A=1 TO P/2:INPUT X(A)
920 NEXT A
930 PRINT"ANY MISTAKES Y/N":INPUT A$
940 IF A$<>"Y" THEN 980
950 PRINT'"INPUT DATA NUMBER,TIME":INPUT A,X(A)
960 PRINT'"ANY MORE MISTAKES Y/N":INPUT A$
970 IF A$<>"N"THEN 950
980 REM**LINE GRAPH**
990 CLS
1000 PRINT''"PRESS E TO END PROGRAMME AFTER THE GRAPH IS DRAWN"
1010 A$=INKEY$
1020 PRINT'"TYPE C TO CONTINUE"
1030 IF INKEY$<>"C"THEN GOTO 1030
1040 REM**SCALE**
1050 S=S+1
1060 FOR A=1 TO P/2:IF Y(A)/S>148 THEN 1050 ELSE NEXT A
1070 REM**CONVERSION OF X&Y TO GRID COORDINATES**
1080 FOR D=1 TO P/2
1090 X(D)=(3*X(D))+20
1100 Y(D)=178-(Y(D)/S)
1110 NEXT D
1120 CLS
```

```
1130 PMODE 4,1:PCLS:SCREEN 1,0
1140 REM**DRAW AXES**
1150 LINE(20,10)-(20,178),PSET
1160 FOR F-10 TO 178 STEP 4
1170 LINE(15,F)-(20,F),PSET
1180 NEXT F
1190 LINE(20,178)-(245,178),PSET
1200 FOR G=20 TO 245 STEP 15
1210 LINE(G,183)-(G,178),PSET
1220 NEXT G
1230 REM**PLOT POINTS**
1240 FOR D= 1 TO P/2
1250 PSET(X(D),Y(D)),1
1260 CIRCLE(X(D),Y(D)),1
1270 NEXT D
1280 REM**JOIN POINTS**
1290 LINE(20,178)-(X(1),Y(1)),PSET
1300 FOR D=1 TO (P/2)-1
1310 LINE(X(D),Y(D))-(X(D+1),Y(D+1)),PSET
1320 NEXT D
1330 A$=INKEY$
1340 IF INKEY$<>"E" THEN GOTO 1340
1350 PRINT"ANOTHER RUN Y/N":INPUT A$
1360 IF A$="Y" THEN RUN ELSE 1370
1370 PRINT'"END OF PROGRAMME"
1380 END
```

PROGRAMME 4 "F.E.X."

Written for the Dragon microcomputer

This programme calculates the fraction of ^{18}F exchanged between a ^{18}F labelled gas and a solid metal fluoride using equations 2.4 and 2.5. The programme operates as follows:

Lines 40 - 100	Calculation of the number of m moles of gas.
Lines 140 - 210	Calculation of the number of m moles of solid.
Lines 230 - 360	Calculation of fractions exchanged
Lines 360 - 400	Print out of results on screen.

F1 is the fraction exchanged calculated using equation 2.5

F2 is the fraction exchanged calculated using equation 2.4

PROGRAMME 4 F.EX.

```
10 CLS
20 PRINT"PROGRAMME  TO  CALCULATE FRACTION EXCHANGED BETWEEN  F18 LABELL
   GAS AND A METAL FLUORIDE"
30 PRINT
40 PRINT"P(TORR),VOL,T":INPUT P,V,T
50 CLS
60 T=T+273
70 P=P/760
80 R=82.053
90 N=(P*V)/(R*T)
100 M2=N*1000
110 PRINT
120 PRINT M2;"MMOL OF GAS"
130 PRINT
140 PRINT"WEIGHT OF SOLID":INPUT W
150 CLS
160 PRINT
170 PRINT"MOL.WT.OF SOLID":INPUT MW
180 CLS
190 M1=(W/MW)*1000
200 PRINT
210 PRINT M1;"MMOL OF SOLID"
220 PRINT
230 PRINT"ACTIVITY OF GAS BEFORE REACTION ":INPUT AO
240 PRINT
250 PRINT"ACTIVITY OF GAS AFTER REACTION":INPUT AT
260 CLS
270 PRINT
```

```
280 PRINT"ACTIVITY OF SOLID AFTER REACTION":INPUT A1
290 PRINT
300 PRINT"NO.OF F ATOMS IN SOLID":INPUT N1
310 PRINT
320 PRINT"NO.OF F ATOMS IN GAS":INPUT N2
330 PRINT
340 F1=((A0-AT)*((N1*M1)+(N2*M2)))/(N1*M1*A0)
350 F2=(A1/(A1+AT))/(N1*M1/(N1*M1+N2*M2))
360 CLS
370 PRINT
380 PRINT"FRACTION EXCHANGED (F1)=";F1
390 PRINT"FRACTION EXCHANGED (F2)=";F2
400 PRINT"ANOTHER RUN Y/N":INPUT A$
410 IF A$="Y" THEN 430 ELSE RUN
420 PRINT
430 CLS:PRINT"END OF CALCULATION"
440 END
```

PROGRAMME 5 "D.T.C."

Written for the Dragon microcomputer

This programme is used to calculate the dead time of a GM tube. The method of obtaining the data required for this calculation is described in chapter 2 section 2.4.4.

The programme operates as follows:

Lines 10 - 110	Input of data
Lines 120 - 140	Calculation of dead time using equation 2.6.
Lines 150 - 180	Print out of dead time on printer

PROGRAMME 5 DTC

```
10 DIM C(20),CC(20)
20 CLS:PRINT"DEAD TIME CORRECTION PROGRAMME"
30 PRINT:INPUT"NUMBER OF BACKGROUND COUNTS";N
40 PRINT:PRINT"ENTER BACKGROUND COUNTS"
50 FOR I=1 TO N:INPUT B(I)
60 CB=CB+B(I):NEXT:CB=CB/N
70 PRINT:PRINT"ENTER NUMBER OF COUNTS":INPUT M
80 PRINT:PRINT"COUNT TIME":INPUT T
90 PRINT:PRINT"DEAD TIME":INPUT DT
100 PRINT "INPUT COUNTS"
110 FOR I=1 TOM:INPUT C(I)
120 NEXT
130 PRINT"ANY MISTAKES Y/N":INPUT A$
140 IF A$<>"Y" THEN 180
150 PRINT"ENTER COUNT NUMBER,COUNT":INPUT I,C(I)
160 PRINT"ANY MORE MISTAKES Y/N":INPUT A$
170 IF A$="Y" THEN 150
180 FOR I=1 TO M
190 C(I)=C(I)-CB:C(I)=C(I)/T
200 CC(I)=C(I)/(1-DT*C(I))
210 NEXT
220 CLS:PRINT:PRINT"ENTER TUBE CORRELATION FACTOR "
230 PRINT"ENTER 1 IF NOT REQUIRED"
240 INPUT CF
250 FOR I=1 TO M
260 CC(I)=CC(I)*CF
270 CC(I)=INT(CC(I)*100+0.5)/100
```

```
280 NEXT
290 PRINT -2"COUNTS","CORRECTED COUNTS"
300 FOR I=1 TO M
310 PRINT -2,C(1),CC(I)
320 NEXT
330 PRINT"ANOTHER RUN Y/N":INPUT B$
340 IF B$="Y" THEN RUN ELSE 350
350 CLS :PRINT"END OF CALCULATION"
360 END
```

PROGRAMME 6 "DT.CR."

Written for the BBC microcomputer

This programme is used to correct observed counts for the dead time of the Geiger Muller tubes and to take account of the correlation factor of the tubes. The programme operates as follows:

Lines 10 - 60	Calculation of average background count
Lines 70 - 170	Input of data
Lines 180 - 280	Calculation using equation 2.6
Lines 290 - 320	Print out of results on printer

PROGRAMME 6 DT.CR.

```
10 DIM T820),AO(20),AT(20)
20 CLS:PRINT"DEAD TIME CALCULATION PROGRAMME"
30 PRINT:INPUT"NUMBER OF DATA PAIRS";N
40 PRINT:PRINT"ENTER OBSERVED ACTIVITY,TRUE ACTIVITY"
50 FOR I=1 TO N
60 INPUT AO(I),AT(I):NEXT
70 PRINT"ANY MISTAKES Y/N":INPUT A$
80 IF A$<>"Y" THEN 120
90   PRINT:INPUT"ENTER   PAIR   NUMBER  ,OBSERVED  ACTIVITY,TRUE  ACTIVITY
";I,AO(I),AT(I)
100 PRINT"ANY MORE MISTAKES Y/N":INPUT A$
110 IF A$="Y" THEN 90
120 FOR I=1 TO N
130 T(I9=(AT(1)-AO(I))/(AT(I)*AO(I))
140 NEXT
150 VDU1:PRINT"DEAD TIME"
160 FOR I=1 TO N
170 PRINT"T=";T(I)
180 NEXT
190 PRINT"ANOTHER RUN Y/N":INPUT A$
200 IF A$="Y" THEN RUN ELSE 210
210 CLS:PRINT "END OF CALCULATION"
220 END
```

REFERENCES

1. S Arrhenius **Z.** Phys.Chem 1887, 1, 631

2. "Inorganic Chemistry" R B Heslop and K Jones Eds., Elsevier Scientific Publishing Company, Amsterdam, 1976

3. T M Lowry Chem. and Ind. 1923, 42, 43

4. J N Bronsted Rec. Trav. Chim. 1923, 42, 718

5. A F O Germann J. Am. Chem. Soc. 1925, 47, 2461

6. G N Lewis "Valence and Structures of Atoms and Molecules" Chemical Catalogue Co. Inc., New York, 1923

7. G N Lewis J Franklin Inst. 1938, 226, 293

8. R G Pearson J Chem Educ. 1968, 45, 581, 643

9. "Determination of Organic Structures by Physical Methods" Vol 1 F C Nachod and E A Braude, Eds, Academic Press, New York, 1955

10. "Survey of Progress in Chemistry "Vol 5, A F Scott, Ed. Academic Press, New York, 1969

11. D A McCaulay and A P Lien J Am. Chem. Soc. 1951, 73,2013
D A McCaulay, W S Highley and A P Lien, J Am. Chem. Soc, 1956, 78, 3009

12. A F Clifford, H C Beachell and W Jack, J Inorg, Nucl Chem. 1957, 5, 57
A F Clifford and S Kongpricha, J Inorg, Nucl Chem. 1961, 20, 147

13 M Kramar and L C Duncan Inorg Chem. 1971, 10, 647

14. S Brownstein Can. J. Chem 1969, 47, 605

15. "Negative Ions and the Magnetron" F M Page and G C Goode
Wiley Interscience, New York, 1969

16. T C Rhyne and J G Dillard, Inorg. Chem. 1971, 10, 730

17. J C Haartz and D H McDaniel, J Am Chem Soc., 1973, 95, 8562

18. A P J Altshuller J Am. Chem. Soc. 1955, 77, 6187

19. M K Murphy and J L Beachamp J Am. Chem. Soc 1977, 99, 4992

20. 'Halogen Chemistry' V Gutman Ed.
Academic Press, London, New York 1967, Vol 1, p 1

21. J Bills and F A Cotton J Phys. Chem. 1960, 64, 1477

22. T E Mallouk, G L Rosenthal, G Muller, R Brusasco and
N Bartlett
Inorg. Chem. 1984, 23, 3167

23. R J Gillespie and A Whitla Can.J. Chem 1970, 48, 657

24. N Bartlett and P L Robinson Chem Ind (London) 1956, 1351
N Bartlett and P L Robinson J. Chem. Soc 1961, 3417

25. J Weidlein and K Dehnicke Z. Anorg. Allg. Chem. 1965, 337, 113

26. D D Gibler, C J Adams, M Fischer, A Zalkin and N Bartlett
Inorg. Chem 1972, 11, 2325

27. M E Redwood and C J Willis Can J Chem. 1965, 43, 1893

28. K O Christe, E C Curtis and C J Schack
Spectrochim Acta 1975, 31A, 1035

29. W B Farnham, B E Smart, W J Middleton, J C Calabrese and D A Dixon J Am. Chem. Soc. 1985, 107, 4565

30. E Martineau and J B Milne, J Chem. Soc. Chem. Commun, 1971, 1327

31. L Lawlor and J Passmore Inorg. Chem. 1979, 18, 2923

32. S J David and B S Ault Inorg Chem 1985, 24, 1238

33. J A A Ketelaar Nature 1931, 128, 303
J A A Ketelaar Z Krist 1933, 85, 119

34. A J Edwards J Chem. Soc 1964, 3714

35. A Moerkerken, B Behr, MA Noordeloos - Mass and C Boelhouwer J Catalysis 1972, 24, 177

36. R E Dodd, L A Woodward and H L Roberts Trans Faraday Soc. 1956, 52, 1052

37. F A Cotton, J W George, J S Waugh J Chem. Phys 1958, 28, 994
W M Tolles and W D Gurinn J Chem. Phys 1961, 36, 1119

38. C W Tullock D D Coffman and E L Muetterties J Am. Chem. Soc 1964, 86, 357

39. R Tonder and B Siegel J Inorg. Nucl. Chem. 1963, 25, 1097

40. K O Christe, E C Curtis, C J Shack and D. Pilipovich Inorg. Chem. 1972, 11, 1679
L F Drullinger and J E Griffiths Spectrochem Acta, 1971, 27A, 1793

41. Organic Reactions 1974, 21, 1

42. G G Yakobsen and N E Akhmetova Synthesis 1983, 169

43. A N Nesmeyanov, K A Petherskaya and G Y Uretskaya
Izv Akad Nauk SSSR Ser Khim, 1948, 240

44. A L Logothetis and G N Sausen J Org. Chem 1966, 31, 3689

45. N N Vorozhtsov and G G Yakobsen Zh Obshch Khim 1958, 28, 40

46. H Yasuda, H Mikorikawa and S Aoyama
Sci Papers Inst Phys Chem Res Jpn 1959, 53, 19

48. L Rand, W Wagner, P O Warner and L R Kovac
J Org. Chem 1962, 27, 1034

49. W T Miller, W Frass, P R Resnick J Am Chem Soc 1961, 83, 1767

50 G Camaggi and F Gozzo J Chem Soc Chem Commun 1967, 236

51. D P Graham J Org Chem 1966, 31, 955

52. N L Madison British Patent 1141265, 1969

53. D E Gould, L R Anderson, D E Young and W B Fox
J Am Chem Soc. 1969, 91, 1310

54. F A Nohorst and J M Shreeve J Am Chem Soc 1967, 89, 1809

55. M Lustig, A R Pitochelli and J K Ruff, J Am Chem Soc.
1967, 89, 2841

56. F Nyman and H L Roberts J Chem Soc 1962, 3180

57. C J Schack, R D Wilson and M G Warner
J Chem Soc Chem Commun 1969, 1110

58. R C Kennedy and G H Cady J Fluorine Chem 1973/74, 3, 41

59. G A Kolta, G Webb and J M Winfield
Applied Catalysis 1982, 2, 257

60. J M Winfield J Fluorine Chem 1984, 25, 91

61. F S Fawcett, C W Tullock and D D Coffman J Am Chem Soc.
1962, 84, 4275

62.a C T Ratcliffe and J M Shreeve Inorg. Synth 1968, 11, 194
b C T Ratcliffe and J M Shreeve J Chem Soc Chem Commun, 1966, 674

63. G Kolta, G Webb and J M Winfield J Fluorine Chem 1981/82, 19, 89

64. J A Berry, A Prescott, D W A Sharp and J M Winfield
J Fluorine Chem 1977, 10, 247

65. F Joliot and I Curie Nature 1934, 133, 201

66. " Halogen Chemistry" V Gutman Ed.
Academic Press London, New York 1967, 1, 41

67. G T Seaborg Chem Rev 1940, 27, 199

68. H A C McKay Nature 1938, 142, 997

69. R M Adams, R B Bernstein and J J Katz
J Chem Phys 1954, 22, 13

70. C J W Fraser, D W A Sharp, G Webb and J M Winfield
J Chem Soc Dalton Trans 1972, 2226

71. J D Mahoney and S S Markowitz J Inorg Nucl Chem 1964,
26, 907

72. J P De Kleijn J Fluorine Chem 1977, 10, 341

73. G Friedlander, J W Kennedy, E S Macias and J M Miller
"Nuclear and Radiochemistry" 3rd Ed. 1981 Wiley Interscience
New York.

74. A S Al Ammar and G Webb J Chem Soc Faraday Trans I, 1978, 74, 195

75. B Swanson Inorg Chem 1970, 6, 1406

76. D M Byler and D F Schriver Inorg Chem 1974, 13, 441

77. D K Padma J Fluorine Chem 1974, 4, 441

78. J E Whitley Scottish Research and Reactor Centre Report No 26/28

79. C J W Fraser, D W A Sharp, G Webb and J M Winfield J Chem Soc Dalton 1974, 112

80. K O Christe, H Willner and W Sawodny Spectrochim Acta 1979, A35, 1347

81. Infra red Spectra of Inorganic and Co-ordination Compounds, 2nd Ed K Nakamoto, Wiley Interscience New York 1970

82. R A DeMarco, D A Couch and J M Shreeve J Org Chem 1972, 37, 3332

83. G A Kolta, G Webb and J M Winfield J Fluorine Chem 1979, 14, 331

84. M E Redwood and C J Willis Can J Chem 1967, 45, 389

85. D A C Compton J D Goddard S C Hsi W F Murphy and D M Rayner J Phys Chem 1984, 88, 356

86. A Azman and A Ocvirk Spectrochim Acta 1967, 23A, 1597

87. S Bhagavantum and T Verkatarayudu Proc. Indian Acad Sci, Sect A 1939, 9A, 224

88. D W Aylmore and W B Jepson J Sci Instruments, 1961, 38, 156

89. L M Smith Undergraduate Research Report
University of Glasgow 1984-85

90. T Takeuchi, D Myatani, Y Takada and K Okamoto
J Phys Chem 1972, 76, 2625

91. I Langmuir J Am Chem Soc 1916, 38, 2221

92. S Brunauer, P H Emmett and E Teller
J Am Chem Soc 1938, 60, 309

93. "Errors, Measurement and Results in Chemical Analysis", p 99
K Eckschlager, Van Nostrand Reinhold Company, London 1969

94. "Adsorption, Surface Area and Porosity" S J Gregg and K S W Sing 2nd Ed Academic Press, London 1982

95. M M Dubinin Zhur Phys Chem 1960, 34, 959
M M Dubinin Chem Rev 1960, 60, 235

96. S J Gregg, J F Langford Trans Faraday Soc 1969, 65, 1394

97. M F Ghorab MSc Thesis University of Glasgow 1985

98. R W G Wyckoff 'Crystal Structures', Interscience, New York
2nd Ed, Vol 1, p 86

99. S B H Bach and B S Ault Inorg Chem 1984 24, 4394

100. B S Ault J Phys Chem 1980, 84, 3448

101. J N Keith, I J Solomon, I Sheft and H Hyman
J Inorg Nucl Chem Hyman memorial issue 1976, 143

102 R J Gillespie, J S Hartman and M Parekh
Can J Chem 1968, 46, 1601

103 D W A Sharp Adv Fluor Chem 1960, 1, 81

104 J Goubeau and W Bues Z Anorg Allg Chem 1952, 268, 221

105 N N Greenwood J Chem Soc 1959, 3811

106 S Brownstein and J Paasivirta Can J Chem 1965, 43, 1645

107 J S Hartman and P Stilbs J Chem Soc Chem Commun 1975, 566

108a J J Harris Inorg Chem 1966, 5, 1627
b M G Thomas, C W Schultz and R W Parry Inorg Chem 1977, 16, 994

109 J Vanderryn J Chem Phys 1959, 30, 331

110 G M Begun and A C Rutenberg Inorg Chem 1967, 6, 2212

111 eg W Fink and M Schmeisser Angew Chem 1957, 69, 780
S F Seel and O Detmer Angew Chem 1958, 70, 163
N Bartlett and P L Robinson Proc Chem Soc 1957, 230

112 S Brownstein Can J Chem 1969, 47, 605

113 P A W Dean, R J Gillespie, R Hulme and D A Humphreys
J Chem Soc (A) 1971, 341

114 'Infra red Spectra of Inorganic and Co-ordination Compounds'
2nd Ed, p 119
K Nakamoto, Wiley Interscience New York 1970

115 B S Ault Inorg Chem 1982, 21, 756

116 J S Ogden, S J J Williams J Chem Soc Dalton Trans 1981, 456

117 D L Bernitt, K O Hartman and I C Hisatsune
J Chem Phys 1965, 42, 3553

118 C J W Fraser, D W A Sharp, R A Sule, G Webb and J M Winfield
J Chem Research (m) 1978, 0311

119 T B McMahon and C J Northcot
Can J Chem 1978, 56, 1069

120 R H Borgwardt and R D Harvey
Environ Sci Technol 1972, 6, 350

121 L C Hoskins and R C Lord J Chem Phys 1967, 46, 2402

122 A H Neilson J Chem Phys 1954, 22, 659

123 "Tables of physical and chemical constants"
Longman, Green and Company Limited London 1968 13th Ed, p 159

124 M Nakata, K Kohata, T Fukuyama, K Kuchitsu and C J Wilkins
J Mol Struct 1980, 68, 271

125 H Selig, A Reis and L Gasner J Inorg Nucl Chem 1968,
30, 2087

126 J C Fuggle PhD Thesis University of Glasgow 1971

128 M Azeem, M Brownstein and R J Gillespie Can J Chem
1969, 47, 4159

129 E E Aynsley, R D Peacock and P L Robinson J Chem Soc
1952, 1231

130 J A Evans and D A Long J Chem Soc (A) 1968, 1688

132 A J Edwards and G R Jones J Chem Soc (A) 1970,1491

133 R J Gillespie and K C Moss J Chem Soc (A) 1966, 1170

134 D K Sanyal and J M Winfield J Fluorine Chem 1984, 24, 75

135. R R Ryan, R A Penneman, L B Asprey and R T Paine
Acta Cryst, 1976, B32, 3311

136 R T Paine, R S McDowell, L B Asprey and L H Jones
J Chem Phys 1976, 64, 3081
K R Kunze, R H Hauge, D Hamill and J L Margrave
J Chem Phys 1976, 65, 2026

137 B J Krohn, W B Pearson and J Overand.
J Chem Phys 1976, 65, 969

138 R A Penneman, G D Sturgeon and L B Asprey
Inorg Chem 1964, 3, 126

139 R Bougon and P Charpin J Fluorine Chem 1979, 14. 235

140 J H Holloway, G M Staunton, K Rediess, R Bougon and D Brown
J Chem Soc Dalton Trans 1984, 2163

ooOoo